CODATA Recommended Values of the Fundamental Physical Constants: 2010

Cite as: J. Phys. Chem. Ref. Data **41**, 043109 (2012); https://doi.org/10.1063/1.4724320
Submitted: 21 March 2012 . Accepted: 17 May 2012 . Published Online: 28 December 2012

Peter J. Mohr, Barry N. Taylor, and David B. Newell

CODATA Recommended Values of the Fundamental Physical Constants: 2010*

Peter J. Mohr,[a] Barry N. Taylor,[b] and David B. Newell[c]

National Institute of Standards and Technology, Gaithersburg, Maryland 20899-8420, USA

(Received 21 March 2012; accepted 17 May 2012; published online 28 December 2012)

This paper gives the 2010 self-consistent set of values of the basic constants and conversion factors of physics and chemistry recommended by the Committee on Data for Science and Technology (CODATA) for international use. The 2010 adjustment takes into account the data considered in the 2006 adjustment as well as the data that became available from 1 January 2007, after the closing date of that adjustment, until 31 December 2010, the closing date of the new adjustment. Further, it describes in detail the adjustment of the values of the constants, including the selection of the final set of input data based on the results of least-squares analyses. The 2010 set replaces the previously recommended 2006 CODATA set and may also be found on the World Wide Web at physics.nist.gov/constants. [http://dx.doi.org/10.1063/1.4724320]

CONTENTS

* This report was prepared by the authors under the auspices of the CODATA Task Group on Fundamental Constants. The members of the task group are F. Cabiati, Istituto Nazionale di Ricerca Metrologica, Italy; J. Fischer, Physikalisch-Technische Bundesanstalt, Germany; J. Flowers, National Physical Laboratory, United Kingdom; K. Fujii, National Metrology Institute of Japan, Japan; S. G. Karshenboim, Pulkovo Observatory, Russian Federation; P. J. Mohr, National Institute of Standards and Technology, United States of America; D. B. Newell, National Institute of Standards and Technology, United States of America; F. Nez, Laboratoire Kastler-Brossel, France; K. Pachucki, University of Warsaw, Poland; T. J. Quinn, Bureau international des poids et mesures; B. N. Taylor, National Institute of Standards and Technology, United States of America; B. M. Wood, National Research Council, Canada; and Z. Zhang, National Institute of Metrology, People's Republic of China. This review is being published simultaneously by *Reviews of Modern Physics*; see Rev. Mod. Phys. **84**, 1527 (2012).

[a]mohr@nist.gov
[b]barry.taylor@nist.gov
[c]dnewell@nist.gov

List of Tables

List of Figures

1. Introduction

1.1. Background

This article reports work carried out under the auspices of the Committee on Data for Science and Technology (CODATA) Task Group on Fundamental Constants.[1] It describes in detail the CODATA 2010 least-squares adjustment of the values of the constants, for which the closing date for new data was 31 December 2010. Equally important, it gives the 2010 self-consistent set of over 300 CODATA recommended values of the fundamental physical constants based on the 2010 adjustment. The 2010 set, which replaces its immediate predecessor resulting from the CODATA 2006 adjustment (Mohr, Taylor, and Newell, 2008), first became available on 2 June 2011 at physics.nist.gov/constants, a Web site of the NIST Fundamental Constants Data Center (FCDC).

The World Wide Web has engendered a sea change in expectations regarding the availability of timely information. Further, in recent years new data that influence our knowledge of the values of the constants seem to appear almost continuously. As a consequence, the Task Group decided at the time of the 1998 CODATA adjustment to take advantage of the extensive computerization that had been incorporated in that effort to issue a new set of recommended values every 4 years; in the era of the Web, the 12–13 years between the first CODATA set of 1973 (Cohen and Taylor, 1973) and the second CODATA set of 1986 (Cohen and Taylor, 1987), and between this second set and the third set of 1998 (Mohr and Taylor, 2000), could no longer be tolerated. Thus, if the 1998 set is counted as the first of the new 4-year cycle, the 2010 set is the 4th of that cycle.

Throughout this article we refer to the detailed reports describing the 1998, 2002, and 2006 adjustments as CODATA-98, CODATA-02, and CODATA-06, respectively (Mohr and Taylor, 2000, 2005; Mohr, Taylor, and Newell, 2008). To keep the paper to a reasonable length, our data review focuses on the new results that became available between the 31 December 2006 and 31 December 2010 closing dates of the 2006 and 2010 adjustments; the reader should consult these past reports for detailed discussions of the older data. These past reports should also be consulted for discussions of motivation, philosophy, the treatment of numerical calculations and uncertainties, etc. A rather complete list of acronyms and symbols can be found in the list of symbols and abbreviations near the end of the paper.

To further achieve a reduction in the length of this report compared to the lengths of its three most recent predecessors, it has been decided to omit extensive descriptions of new experiments and calculations and to comment only on their most pertinent features; the original references should be consulted for details. For the same reason, sometimes the older data used in the 2010 adjustment are not given in the portion of the paper that discusses the data by category, but are given in the portion of the paper devoted to data analysis. For example, the actual values of the 16 older items of input data recalled in Sec. 8 are given only in Sec. 13, rather than in both sections as done in previous adjustment reports.

As in all previous CODATA adjustments, as a working principle, the validity of the physical theory underlying the 2010 adjustment is assumed. This includes special relativity, quantum mechanics, quantum electrodynamics (QED), the standard model of particle physics, including *CPT* invariance, and the exactness (for all practical purposes, see Sec. 8) of the relationships between the Josephson and von Klitzing constants K_J and R_K and the elementary charge e and Planck constant h, namely, $K_J = 2e/h$ and $R_K = h/e^2$.

Although the possible time variation of the constants continues to be an active field of both experimental and theoretical research, there is no observed variation relevant to the data on which the 2010 recommended values are based; see, for example, the recent reviews by Chiba (2011) and Uzan (2011). Other references can be found in the FCDC bibliographic database at physics.nist.gov/constantsbib using, for example, the keywords "time variation" or "constants."

With regard to the 31 December closing date for new data, a datum was considered to have met this date if the Task Group received a preprint describing the work by that date and the preprint had already been, or shortly would be, submitted for publication. Although results are identified by the year in which they were published in an archival journal, it can be safely assumed that any input datum labeled with an "11" or "12" identifier was in fact available by the closing date. However, the 31 December 2010 closing date does not

[1]CODATA was established in 1966 as an interdisciplinary committee of the International Council for Science. The Task Group was founded 3 years later.

apply to clarifying information requested from authors; indeed, such information was received up to shortly before 2 June 2011, the date the new values were posted on the FCDC Web site. This is the reason that some private communications have 2011 dates.

1.2. Brief overview of CODATA 2010 adjustment

The 2010 set of recommended values is the result of applying the same procedures as in previous adjustments and is based on a least-squares adjustment with, in this case, $N = 160$ items of input data, $M = 83$ variables called *adjusted constants*, and $\nu = N - M = 77$ degrees of freedom. The statistic "chi squared" is $\chi^2 = 59.1$ with probability $p(\chi^2|\nu) = 0.94$ and Birge ratio $R_B = 0.88$.

A significant number of new results became available for consideration, both experimental and theoretical, from 1 January 2007, after the closing date of the 2006 adjustment, to 31 December 2010, the closing date of the current adjustment. Data that affect the determination of the fine-structure constant α, Planck constant h, molar gas constant R, Newtonian constant of gravitation G, Rydberg constant R_∞, and rms proton charge radius r_p are the focus of this brief overview, because of their inherent importance and, in the case of α, h, and R, their impact on the determination of the values of many other constants. (Constants that are not among the directly adjusted constants are calculated from appropriate combinations of those that are directly adjusted.)

1.2.1. Fine-structure constant α

An improved measurement of the electron magnetic-moment anomaly a_e, the discovery and correction of an error in its theoretical expression, and an improved measurement of the quotient $h/m(^{87}\mathrm{Rb})$ have led to a 2010 value of α with a relative standard uncertainty of 3.2×10^{-10} compared to 6.8×10^{-10} for the 2006 value. Of more significance, because of the correction of the error in the theory, the 2010 value of α shifted significantly and now is larger than the 2006 value by 6.5 times the uncertainty of that value. This change has rather profound consequences, because many constants depend on α, for example, the molar Planck constant $N_A h$.

1.2.2. Planck constant h

A new value of the Avogadro constant N_A with a relative uncertainty of 3.0×10^{-8} obtained from highly enriched silicon with amount of substance fraction $x(^{28}\mathrm{Si}) \approx 0.999\,96$ replaces the 2006 value based on natural silicon and provides an inferred value of h with essentially the same uncertainty. This uncertainty is somewhat smaller than 3.6×10^{-8}, the uncertainty of the most accurate directly measured watt-balance value of h. Because the two values disagree, the uncertainties used for them in the adjustment were increased by a factor of 2 to reduce the inconsistency to an acceptable level; hence the relative uncertainties of the recommended values of h and N_A are 4.4×10^{-8}, only slightly smaller than the uncertainties of the corresponding 2006 values. The 2010 value of h is larger than the 2006 value by the fractional amount 9.2×10^{-8} while the 2010 value of N_A is smaller than the 2006 value by the fractional amount 8.3×10^{-8}. A number of other constants depend on h, for example, the first radiation constant c_1, and consequently the 2010 recommended values of these constants reflect the change in h.

1.2.3. Molar gas constant R

Four consistent new values of the molar gas constant together with the two previous consistent values, with which the new values also agree, have led to a new 2010 recommended value of R with an uncertainty of 9.1×10^{-7} compared to 1.7×10^{-6} for the 2006 value. The 2010 value is smaller than the 2006 value by the fractional amount 1.2×10^{-6} and the relative uncertainty of the 2010 value is a little over half that of the 2006 value. This shift and uncertainty reduction is reflected in a number of constants that depend on R, for example, the Boltzmann constant k and the Stefan-Boltzmann constant σ.

1.2.4. Newtonian constant of gravitation G

Two new values of G resulting from two new experiments each with comparatively small uncertainties but in disagreement with each other and with earlier measurements with comparable uncertainties led to an even larger expansion of the *a priori* assigned uncertainties of the data for G than was used in 2006. In both cases the expansion reduced the inconsistencies to an acceptable level. This increase has resulted in a 20% increase in uncertainty of the 2010 recommended value compared to that of the 2006 value: 12 parts in 10^5 vs 10 parts in 10^5. Furthermore, the 2010 recommended value of G is smaller than the 2006 value by the fractional amount 6.6×10^{-5}.

1.2.5. Rydberg constant R_∞ and proton radius r_p

New experimental and theoretical results that have become available in the past 4 years have led to the reduction in the relative uncertainty of the recommended value of the Rydberg constant from 6.6×10^{-12} to 5.0×10^{-12}, and the reduction in uncertainty of the proton rms charge radius from 0.0069 fm to 0.0051 fm based on spectroscopic and scattering data but not muonic hydrogen data. Data from muonic hydrogen, with the assumption that the muon and electron interact with the proton at short distances in exactly the same way, are so inconsistent with the other data that they have not been included in the determination of r_p and thus do not have an influence on R_∞. The 2010 value of R_∞ exceeds the 2006 value by the fractional amount 1.1×10^{-12} and the 2010 value of r_p exceeds the 2006 value by 0.0007 fm.

1.3. Outline of the paper

Section 2 briefly recalls some constants that have exact values in the International System of Units (SI) (BIPM, 2006),

the unit system used in all CODATA adjustments. Sections 3–12 discuss the input data with a strong focus on those results that became available between the 31 December 2006 and 31 December 2010 closing dates of the 2006 and 2010 adjustments. It should be recalled (see especially Appendix E of CODATA-98) that in a least-squares analysis of the constants, both the experimental and theoretical numerical data, also called observational data or input data, are expressed as functions of a set of independent variables called directly adjusted constants (or sometimes simply adjusted constants). The functions themselves are called observational equations, and the least-squares procedure provides best estimates, in the least-squares sense, of the adjusted constants. In essence, the procedure determines the best estimate of a particular adjusted constant by automatically taking into account all possible ways of determining its value from the input data. The recommended values of those constants not directly adjusted are calculated from the adjusted constants.

Section 13 describes the analysis of the data. The analysis includes comparison of measured values of the same quantity, measured values of different quantities through inferred values of another quantity such as α or h, and by the method of least squares. The final input data used to determine the adjusted constants, and hence the entire 2010 CODATA set of recommended values, are based on these investigations.

Section 14 provides, in several tables, the set of over 300 recommended values of the basic constants and conversion factors of physics and chemistry, including the covariance matrix of a selected group of constants. Section 15 concludes the report with a comparison of a small representative subset of 2010 recommended values with their 2006 counterparts, comments on some of the more important implications of the 2010 adjustment for metrology and physics, and suggestions for future experimental and theoretical work that will improve our knowledge of the values of the constants. Also touched upon is the potential importance of this work and that of the next CODATA constants adjustment (expected 31 December 2014 closing date) for the redefinition of the kilogram, ampere, kelvin, and mole currently under discussion internationally (Mills *et al.*, 2011).

2. Special Quantities and Units

As a consequence of the SI definitions of the meter, the ampere, and the mole, c, μ_0, and ϵ_0, and $M(^{12}\mathrm{C})$ and M_u, have exact values; see Table 1. Since the relative atomic mass $A_\mathrm{r}(X)$ of an entity X is defined by $A_\mathrm{r}(X) = m(X)/m_\mathrm{u}$, where $m(X)$ is the mass of X, and the (unified) atomic mass constant m_u is defined according to $m_\mathrm{u} = m(^{12}\mathrm{C})/12$, $A_\mathrm{r}(^{12}\mathrm{C}) = 12$ exactly, as shown in the table. Since the number of specified entities in 1 mol is equal to the numerical value of the Avogadro constant $N_\mathrm{A} \approx 6.022 \times 10^{23}/\mathrm{mol}$, it follows that the molar mass of an entity X, $M(X)$, is given by $M(X) = N_\mathrm{A} m(X) = A_\mathrm{r}(X) M_\mathrm{u}$ and $M_\mathrm{u} = N_\mathrm{A} m_\mathrm{u}$. The (unified) atomic mass unit u (also called the dalton, Da) is defined as $1\ \mathrm{u} = m_\mathrm{u} \approx 1.66 \times 10^{-27}$ kg. The last two entries in Table 1, $K_{\mathrm{J}-90}$ and $R_{\mathrm{K}-90}$, are the conventional values of the Josephson and von Klitzing constants introduced on 1 January 1990 by the International Committee for Weights and Measures (CIPM) to foster worldwide uniformity in the measurement of electrical quantities. In this paper, those electrical quantities measured in terms of the Josephson and quantum Hall effects with the assumption that K_J and R_K have these conventional values are labeled with a subscript 90.

Measurements of the quantity $K_\mathrm{J}^2 R_\mathrm{K} = 4/h$ using a moving coil watt balance (see Sec. 8) require the determination of the local acceleration of free fall g at the site of the balance with a relative uncertainty of a few parts in 10^9. That currently available absolute gravimeters can achieve such an uncertainty if properly used has been demonstrated by comparing different instruments at essentially the same location. An important example is the periodic international comparison of absolute gravimeters (ICAG) carried out at the International Bureau of Weights and Measures (BIPM), Sèvres, France (Jiang *et al.*, 2011). The good agreement obtained between a commercial optical interferometer-based gravimeter that is in wide use and a cold atom, atomic interferometer-based instrument also provides evidence that the claimed uncertainties of determinations of g are realistic (Merlet *et al.*, 2010). However, not all gravimeter comparisons have obtained such satisfactory results (Louchet-Chauvet *et al.*, 2011). Additional work in this area may be needed when the relative uncertainties of watt-balance experiments reach the level of 1 part in 10^8.

3. Relative Atomic Masses

The directly adjusted constants include the relative atomic masses $A_\mathrm{r}(X)$ of a number of particles, atoms, and ions. Further, values of $A_\mathrm{r}(X)$ of various atoms enter the calculations of several potential input data. The following sections and Tables 2–4 summarize the relevant information.

TABLE 1. Some exact quantities relevant to the 2010 adjustment.

Quantity	Symbol	Value
Speed of light in vacuum	c, c_0	$299\,792\,458\ \mathrm{m\,s^{-1}}$
Magnetic constant	μ_0	$4\pi \times 10^{-7}\ \mathrm{N\,A^{-2}} = 12.566\,370\,614\ldots \times 10^{-7}\ \mathrm{N\,A^{-2}}$
Electric constant	ϵ_0	$(\mu_0 c^2)^{-1} = 8.854\,187\,817\ldots \times 10^{-12}\ \mathrm{F\,m^{-1}}$
Molar mass of ^{12}C	$M(^{12}\mathrm{C})$	$12 \times 10^{-3}\ \mathrm{kg\,mol^{-1}}$
Molar mass constant	M_u	$10^{-3}\ \mathrm{kg\,mol^{-1}}$
Relative atomic mass of ^{12}C	$A_\mathrm{r}(^{12}\mathrm{C})$	12
Conventional value of Josephson constant	$K_{\mathrm{J}-90}$	$483\,597.9\ \mathrm{GHz\,V^{-1}}$
Conventional value of von Klitzing constant	$R_{\mathrm{K}-90}$	$25\,812.807\ \Omega$

TABLE 2. Values of the relative atomic masses of the neutron and various atoms as given in the 2003 atomic mass evaluation together with the defined value for ^{12}C.

Atom	Relative atomic mass $A_r(X)$	Relative standard uncertainty u_r
n	1.008 664 915 74(56)	5.6×10^{-10}
^{1}H	1.007 825 032 07(10)	1.0×10^{-10}
^{2}H	2.014 101 777 85(36)	1.8×10^{-10}
^{3}H	3.016 049 2777(25)	8.2×10^{-10}
^{3}He	3.016 029 3191(26)	8.6×10^{-10}
^{4}He	4.002 603 254 153(63)	1.6×10^{-11}
^{12}C	12	Exact
^{16}O	15.994 914 619 56(16)	1.0×10^{-11}
^{28}Si	27.976 926 5325(19)	6.9×10^{-11}
^{29}Si	28.976 494 700(22)	7.6×10^{-10}
^{30}Si	29.973 770 171(32)	1.1×10^{-9}
^{36}Ar	35.967 545 105(28)	7.8×10^{-10}
^{38}Ar	37.962 732 39(36)	9.5×10^{-9}
^{40}Ar	39.962 383 1225(29)	7.2×10^{-11}
^{87}Rb	86.909 180 526(12)	1.4×10^{-10}
^{107}Ag	106.905 0968(46)	4.3×10^{-8}
^{109}Ag	108.904 7523(31)	2.9×10^{-8}
^{133}Cs	132.905 451 932(24)	1.8×10^{-10}

3.1. Relative atomic masses of atoms

Table 2, which is identical to Table II in CODATA-06, gives values of $A_r(X)$ taken from the 2003 atomic mass evaluation (AME2003) carried out by the Atomic Mass Data Center (AMDC), Centre de Spectrométrie Nucléaire et de Spectrométrie de Masse, Orsay, France (Audi, Wapstra, and Thibault, 2003; Wapstra, Audi, and Thibault, 2003; AMDC, 2006). However, not all of these values are actually used in the adjustment; some are given for comparison purposes only. Although these values are correlated to a certain extent, the only correlation that needs to be taken into account in the current adjustment is that between $A_r(^1\text{H})$ and $A_r(^2\text{H})$; their correlation coefficient is 0.0735 (AMDC, 2003).

Table 3 lists seven values of $A_r(X)$ relevant to the 2010 adjustment obtained since the publication of AME2003. It is the updated version of Table IV in CODATA-06. The changes made are the deletion of the ^{3}H and ^{3}He values obtained by the SMILETRAP group at Stockholm University (StockU), Sweden; and the inclusion of values for ^{28}Si, ^{87}Rb, and ^{133}Cs obtained by the group at Florida State University (FSU), Tallahassee, FL, USA (Redshaw, McDaniel, and Myers, 2008; Mount, Redshaw, and Myers, 2010). This group uses the method initially developed at the Massachusetts Institute of Technology (MIT), Cambridge, MA, USA (Rainville *et al.*, 2005). In the MIT approach, which eliminates or reduces a number of systematic effects and their associated uncertainties, mass ratios are determined by directly comparing the cyclotron frequencies of two different ions simultaneously confined in a Penning trap. [The value of $A_r(^{29}\text{Si})$ in Table 3 is given in the supplementary information of the last cited reference.]

TABLE 3. Values of the relative atomic masses of various atoms that have become available since the 2003 atomic mass evaluation.

Atom	Relative atomic mass $A_r(X)$	Relative standard uncertainty u_r
^{2}H	2.014 101 778 040(80)	4.0×10^{-11}
^{4}He	4.002 603 254 131(62)	1.5×10^{-11}
^{16}O	15.994 914 619 57(18)	1.1×10^{-11}
^{28}Si	27.976 926 534 96(62)	2.2×10^{-11}
^{29}Si	28.976 494 6625(20)	6.9×10^{-11}
^{87}Rb	86.909 180 535(10)	1.2×10^{-10}
^{133}Cs	132.905 451 963(13)	9.8×10^{-11}

TABLE 4. The variances, covariances, and correlation coefficients of the University of Washington values of the relative atomic masses of deuterium, helium 4, and oxygen 16. The numbers in bold above the main diagonal are 10^{20} times the numerical values of the covariances; the numbers in bold on the main diagonal are 10^{20} times the numerical values of the variances; and the numbers in italics below the main diagonal are the correlation coefficients.

	$A_r(^2\text{H})$	$A_r(^4\text{He})$	$A_r(^{16}\text{O})$
$A_r(^2\text{H})$	**0.6400**	**0.0631**	**0.1276**
$A_r(^4\text{He})$	*0.1271*	**0.3844**	**0.2023**
$A_r(^{16}\text{O})$	*0.0886*	*0.1813*	**3.2400**

The deleted SMILETRAP results are not discarded but are included in the adjustment in a more fundamental way, as described in Sec. 3.3. The values of $A_r(^2\text{H})$, $A_r(^4\text{He})$, and $A_r(^{16}\text{O})$ in Table 3 were obtained by the University of Washington (UWash) group, Seattle, WA, USA, and were used in the 2006 adjustment. The three values are correlated and their variances, covariances, and correlation coefficients are given in Table 4, which is identical to Table VI in CODATA-06.

The values of $A_r(X)$ from Table 2 initially used as input data for the 2010 adjustment are $A_r(^1\text{H})$, $A_r(^2\text{H})$, $A_r(^{87}\text{Rb})$, and $A_r(^{133}\text{Cs})$; and from Table 3, $A_r(^2\text{H})$, $A_r(^4\text{He})$, $A_r(^{16}\text{O})$, $A_r(^{87}\text{Rb})$, and $A_r(^{133}\text{Cs})$. These values are items *B*1, *B*2.1, *B*2.2, and *B*7–*B*10.2 in Table 20, Sec. 13. As in the 2006 adjustment, the AME2003 values for $A_r(^3\text{H})$, and $A_r(^3\text{He})$ in Table 2 are not used because they were influenced by an earlier ^{3}He result of the UWash group that disagrees with their newer, more accurate result (Van Dyck, 2010). Although not yet published, it can be said that it agrees well with the value from the SMILETRAP group; see Sec. 3.3.

Also as in the 2006 adjustment, the UWash group's values for $A_r(^4\text{He})$ and $A_r(^{16}\text{O})$ in Table 3 are used in place of the corresponding AME2003 values in Table 2 because the latter are based on a preliminary analysis of the data while those in Table 3 are based on a thorough reanalysis of the data (Van Dyck, *et al.*, 2006).

Finally, we note that the $A_r(^2\text{H})$ value of the UWash group in Table 3 is the same as used in the 2006 adjustment. As discussed in CODATA-06, it is a near-final result with a

conservatively assigned uncertainty based on the analysis of 10 runs taken over a 4-year period privately communicated to the Task Group in 2006 by R. S. Van Dyck. A final result completely consistent with it based on the analysis of 11 runs but with an uncertainty of about half that given in the table should be published in due course together with the final result for $A_r(^3\mathrm{He})$ (Van Dyck, 2010).

3.2. Relative atomic masses of ions and nuclei

For a neutral atom X, $A_r(X)$ can be expressed in terms of A_r of an ion of the atom formed by the removal of n electrons according to

$$A_r(X) = A_r(X^{n+}) + nA_r(e) - \frac{E_b(X) - E_b(X^{n+})}{m_u c^2}. \quad (1)$$

In this expression, $E_b(X)/m_u c^2$ is the relative-atomic-mass equivalent of the total binding energy of the Z electrons of the atom and Z is the atom's atomic number (proton number). Similarly, $E_b(X^{n+})/m_u c^2$ is the relative-atomic-mass equivalent of the binding energy of the $Z - n$ electrons of the X^{n+} ion. For an ion that is fully stripped $n = Z$ and X^{Z+} is simply N, the nucleus of the atom. In this case $E_b(X^{Z+})/m_u c^2 = 0$ and Eq. (1) becomes of the form of the first two equations of Table 33, Sec. 13.

The binding energies E_b employed in the 2010 adjustment are the same as those used in that of 2002 and 2006; see Table IV of CODATA-02. However, the binding energy for tritium, ^{3}H, is not included in that table. We employ the value used in the 2006 adjustment, $1.097\,185\,439 \times 10^7$ m^{-1}, due to Kotochigova (2006). For our purposes here, the uncertainties of the binding energies are negligible.

3.3. Relative atomic masses of the proton, triton, and helion

The focus of this section is the cyclotron frequency ratio measurements of the SMILETRAP group that lead to values of A_r(p), A_r(t), and A_r(h), where the triton t and helion h are the nuclei of ^{3}H and ^{3}He. The reported values of Nagy *et al.* (2006) for $A_r(^3\mathrm{H})$ and $A_r(^3\mathrm{He})$ were used as input data in the 2006 adjustment but are not used in this adjustment. Instead, the actual cyclotron frequency ratio results underlying those values are used as input data. This more fundamental way of handling the SMILETRAP group's results is motivated by the similar but more recent work of the group related to the proton, which we discuss before considering the earlier work.

Solders *et al.* (2008) used the Penning-trap mass spectrometer SMILETRAP, described in detail by Bergström *et al.* (2002), to measure the ratio of the cyclotron frequency f_c of the $H_2{}^{+*}$ molecular ion to that of the deuteron d, the nucleus of the ^{2}H atom. (The cyclotron frequency of an ion of charge q and mass m in a magnetic flux density B is given by $f_c = qB/2\pi m$.) Here the asterisk indicates that the singly ionized H_2 molecules are in excited vibrational states as a result of the 3.4 keV electrons used to bombard neutral H_2 molecules in their vibrational ground state in order to ionize them. The reported result is

$$\frac{f_c(H_2^{+*})}{f_c(d)} = 0.999\,231\,659\,33(17) \quad [1.7 \times 10^{-10}]. \quad (2)$$

This value was obtained using a two-pulse Ramsey technique to excite the cyclotron frequencies, thereby enabling a more precise determination of the cyclotron resonance frequency line center than was possible with the one-pulse excitation used in earlier work (George *et al.*, 2007; Suhonen *et al.*, 2007). The uncertainty is essentially all statistical; components of uncertainty from systematic effects such as "q/A asymmetry" (difference of charge-to-mass ratio of the two ions), time variation of the 4.7 T applied magnetic flux density, relativistic mass increase, and ion-ion interactions were deemed negligible by comparison.

The frequency ratio $f_c(H_2{}^{+*})/f_c(d)$ can be expressed in terms of adjusted constants and ionization and binding energies that have negligible uncertainties in this context. Based on Sec. 3.2 we can write

$$A_r(H_2) = 2A_r(H) - E_B(H_2)/m_u c^2, \quad (3)$$

$$A_r(H) = A_r(p) + A_r(e) - E_I(H)/m_u c^2, \quad (4)$$

$$A_r(H_2) = A_r(H_2^+) + A_r(e) - E_I(H_2)/m_u c^2, \quad (5)$$

$$A_r(H_2^{+*}) = A_r(H_2^+) + E_{av}/m_u c^2, \quad (6)$$

which yields

$$A_r(H_2^{+*}) = 2A_r(p) + A_r(e) - E_B(H_2^{+*})/m_u c^2, \quad (7)$$

where

$$E_B(H_2^{+*}) = 2E_I(H) + E_B(H_2) - E_I(H_2) - E_{av} \quad (8)$$

is the binding energy of the H_2^{+*} excited molecule. Here $E_I(H)$ is the ionization energy of hydrogen, $E_B(H_2)$ is the disassociation energy of the H_2 molecule, $E_I(H_2)$ is the single electron ionization energy of H_2, and E_{av} is the average vibrational excitation energy of an H_2^+ molecule as a result of the ionization of H_2 by 3.4 keV electron impact.

The observational equation for the frequency ratio is thus

$$\frac{f_c(H_2^{+*})}{f_c(d)} = \frac{A_r(d)}{2A_r(p) + A_r(e) - E_B(H_2^{+*})/m_u c^2}. \quad (9)$$

We treat E_{av} as an adjusted constant in addition to A_r(e), A_r(p), and A_r(d) in order to take its uncertainty into account in a consistent way, especially since it enters into the observational equations for the frequency ratios to be discussed below.

The required ionization and binding energies as well as E_{av} that we use are as given by Solders *et al.* (2008) and except for E_{av}, have negligible uncertainties:

$$E_I(H) = 13.5984 \text{ eV} = 14.5985 \times 10^{-9} m_u c^2, \quad (10)$$

$$E_B(H_2) = 4.4781\ \text{eV} = 4.8074 \times 10^{-9} m_u c^2, \quad (11)$$

$$E_I(H_2) = 15.4258\ \text{eV} = 16.5602 \times 10^{-9} m_u c^2, \quad (12)$$

$$E_{av} = 0.740(74)\ \text{eV} = 0.794(79) \times 10^{-9} m_u c^2. \quad (13)$$

We now consider the SMILETRAP results of Nagy *et al.* (2006) for the ratio of the cyclotron frequency of the triton t and of the $^3He^+$ ion to that of the H_2^{+*} molecular ion. They report for the triton

$$\frac{f_c(t)}{f_c(H_2^{+*})} = 0.668\,247\,726\,86(55) \quad [8.2 \times 10^{-10}] \quad (14)$$

and for the $^3He^+$ ion

$$\frac{f_c(^3He^+)}{f_c(H_2^{+*})} = 0.668\,252\,146\,82(55) \quad [8.2 \times 10^{-10}]. \quad (15)$$

The relative uncertainty of the triton ratio consists of the following uncertainty components in parts in 10^9: 0.22 statistical, and 0.1, 0.1, 0.77, and 0.1 due to relativistic mass shift, ion number dependence, q/A asymmetry, and contaminant ions, respectively. The components for the $^3He^+$ ion ratio are the same except the statistical uncertainty is 0.24. All of these components are independent except the 0.77×10^{-9} component due to q/A asymmetry; it leads to a correlation coefficient between the two frequency ratios of 0.876.

Observational equations for these frequency ratios are

$$\frac{f_c(t)}{f_c(H_2^{+*})} = \frac{2A_r(p) + A_r(e) - E_B(H_2^{+*})/m_u c^2}{A_r(t)} \quad (16)$$

and

$$\frac{f_c(^3He^+)}{f_c(H_2^{+*})} = \frac{2A_r(p) + A_r(e) - E_B(H_2^{+*})/m_u c^2}{A_r(h) + A_r(e) - E_I(^3He^+)/m_u c^2,} \quad (17)$$

where

$$A_r(^3He^+) = A_r(h) + A_r(e) - E_I(^3He^+)/m_u c^2 \quad (18)$$

and

$$E_I(^3He^+) = 51.4153\ \text{eV} = 58.4173 \times 10^{-9} m_u c^2 \quad (19)$$

is the ionization energy of the $^3He^+$ ion, based on Table IV of CODATA-02.

The energy E_{av} and the three frequency ratios given in Eqs. (2), (14), and (15), are items *B*3 to *B*6 in Table 20.

3.4. Cyclotron resonance measurement of the electron relative atomic mass

As in the 2002 and 2006 CODATA adjustments, we take as an input datum the Penning-trap result for the electron relative atomic mass $A_r(e)$ obtained by the University of Washington group (Farnham, Van Dyck, Jr., and Schwinberg, 1995):

$$A_r(e) = 0.000\,548\,579\,9111(12) \quad [2.1 \times 10^{-9}]. \quad (20)$$

This is item *B*11 of Table 20.

4. Atomic Transition Frequencies

Measurements and theory of transition frequencies in hydrogen, deuterium, antiprotonic helium, and muonic hydrogen provide information on the Rydberg constant, the proton and deuteron charge radii, and the relative atomic mass of the electron. These topics as well as hyperfine and fine-structure splittings are considered in this section.

4.1. Hydrogen and deuterium transition frequencies, the Rydberg constant R_∞, and the proton and deuteron charge radii r_p, r_d

Transition frequencies between states a and b in hydrogen and deuterium are given by

$$\nu_{ab} = \frac{E_b - E_a}{h}, \quad (21)$$

where E_a and E_b are the energy levels of the states. The energy levels divided by h are given by

$$\frac{E_a}{h} = -\frac{\alpha^2 m_e c^2}{2 n_a^2 h}(1 + \delta_a) = -\frac{R_\infty c}{n_a^2}(1 + \delta_a), \quad (22)$$

where $R_\infty c$ is the Rydberg constant in frequency units, n_a is the principal quantum number of state a, and δ_a is a small correction factor ($|\delta_a| \ll 1$) that contains the details of the theory of the energy level, including the effect of the finite size of the nucleus as a function of the rms charge radius r_p for hydrogen or r_d for deuterium. In the following summary, corrections are given in terms of the contribution to the energy level, but in the numerical evaluation for the least-squares adjustment, R_∞ is factored out of the expressions and is an adjusted constant.

4.1.1. Theory of hydrogen and deuterium energy levels

Here we provide the information necessary to determine theoretical values of the relevant energy levels, with the emphasis of the discussion on results that have become available since the 2006 adjustment. For brevity, most references to earlier work, which can be found in Eides, Grotch, and Shelyuto (2001b, 2007), for example, are not included here.

Theoretical values of the energy levels of different states are highly correlated. In particular, uncalculated terms for S states are primarily of the form of an unknown common constant divided by n^3. We take this fact into account by calculating covariances between energy levels in addition to the uncertainties of the individual levels (see Sec. 4.1.1.12). The

correlated uncertainties are denoted by u_0, while the uncorrelated uncertainties are denoted by u_n.

4.1.1.1. Dirac eigenvalue

The Dirac eigenvalue for an electron in a Coulomb field is

$$E_{\rm D} = f(n,j)m_{\rm e}c^2, \tag{23}$$

where

$$f(n,j) = \left[1 + \frac{(Z\alpha)^2}{(n-\delta)^2}\right]^{-1/2}, \tag{24}$$

n and j are the principal quantum number and total angular momentum of the state, respectively, and

$$\delta = j + \frac{1}{2} - \left[\left(j+\frac{1}{2}\right)^2 - (Z\alpha)^2\right]^{1/2}. \tag{25}$$

In Eqs. (24) and (25), Z is the charge number of the nucleus, which for hydrogen and deuterium is 1. However, we shall retain Z as a parameter to classify the various contributions.

Equation (23) is valid only for an infinitely heavy nucleus. For a nucleus with a finite mass $m_{\rm N}$ that expression is replaced by (Barker and Glover, 1955; Sapirstein and Yennie, 1990):

$$E_M({\rm H}) = Mc^2 + [f(n,j)-1]m_{\rm r}c^2 - [f(n,j)-1]^2\frac{m_{\rm r}^2c^2}{2M} + \frac{1-\delta_{\ell 0}}{\kappa(2\ell+1)}\frac{(Z\alpha)^4 m_{\rm r}^3c^2}{2n^3m_{\rm N}^2} + \cdots \tag{26}$$

for hydrogen or by (Pachucki and Karshenboim, 1995)

$$E_M({\rm D}) = Mc^2 + [f(n,j)-1]m_{\rm r}c^2 - [f(n,j)-1]^2\frac{m_{\rm r}^2c^2}{2M} + \frac{1}{\kappa(2\ell+1)}\frac{(Z\alpha)^4 m_{\rm r}^3c^2}{2n^3m_{\rm N}^2} + \cdots \tag{27}$$

for deuterium. In Eqs. (26) and (27) ℓ is the nonrelativistic orbital angular momentum quantum number, $\kappa = (-1)^{j-\ell+1/2}(j+\frac{1}{2})$ is the angular-momentum-parity quantum number, $M = m_{\rm e} + m_{\rm N}$, and $m_{\rm r} = m_{\rm e}m_{\rm N}/(m_{\rm e}+m_{\rm N})$ is the reduced mass.

Equations (26) and (27) differ in that the Darwin-Foldy term proportional to $\delta_{\ell 0}$ is absent in Eq. (27), because it does not occur for a spin-one nucleus such as the deuteron (Pachucki and Karshenboim, 1995). In the three previous adjustments, Eq. (26) was used for both hydrogen and deuterium and the absence of the Darwin-Foldy term in the case of deuterium was accounted for by defining an effective deuteron radius given by Eq. (A56) of CODATA-98 and using it to calculate the finite nuclear-size correction given by Eq. (A43) and the related equations in that paper. The extra term in the size correction canceled the Darwin-Foldy term in Eq. (26); see also Sec. 4.1.1.8.

4.1.1.2. Relativistic recoil

The leading relativistic-recoil correction, to lowest order in $Z\alpha$ and all orders in $m_{\rm e}/m_{\rm N}$, is (Erickson, 1977; Sapirstein and Yennie, 1990)

$$E_{\rm S} = \frac{m_{\rm r}^3}{m_{\rm e}^2 m_{\rm N}}\frac{(Z\alpha)^5}{\pi n^3}m_{\rm e}c^2\left\{\frac{1}{3}\delta_{\ell 0}\ln(Z\alpha)^{-2} - \frac{8}{3}\ln k_0(n,\ell) - \frac{1}{9}\delta_{\ell 0} - \frac{7}{3}a_n - \frac{2}{m_{\rm N}^2 - m_{\rm e}^2}\delta_{\ell 0} \times\left[m_{\rm N}^2\ln\left(\frac{m_{\rm e}}{m_{\rm r}}\right) - m_{\rm e}^2\ln\left(\frac{m_{\rm N}}{m_{\rm r}}\right)\right]\right\}, \tag{28}$$

where

$$a_n = -2\left[\ln\left(\frac{2}{n}\right) + \sum_{i=1}^{n}\frac{1}{i} + 1 - \frac{1}{2n}\right]\delta_{\ell 0} + \frac{1-\delta_{\ell 0}}{\ell(\ell+1)(2\ell+1)}. \tag{29}$$

To lowest order in the mass ratio, the next two orders in $Z\alpha$ are

$$E_{\rm R} = \frac{m_{\rm e}}{m_{\rm N}}\frac{(Z\alpha)^6}{n^3}m_{\rm e}c^2[D_{60} + D_{72}Z\alpha\ln^2(Z\alpha)^{-2} + \cdots], \tag{30}$$

where for $n{\rm S}_{1/2}$ states (Pachucki and Grotch, 1995; Eides and Grotch, 1997c; Melnikov and Yelkhovsky, 1999; Pachucki and Karshenboim, 1999)

$$D_{60} = 4\ln 2 - \frac{7}{2}, \tag{31}$$

$$D_{72} = -\frac{11}{60\pi}, \tag{32}$$

and for states with $\ell \geq 1$ (Golosov *et al.*, 1995; Elkhovskiĭ, 1996; Jentschura and Pachucki, 1996)

$$D_{60} = \left[3 - \frac{\ell(\ell+1)}{n^2}\right]\frac{2}{(4\ell^2-1)(2\ell+3)}. \tag{33}$$

Based on the general pattern of the magnitudes of higher-order coefficients, the uncertainty for S states is taken to be 10% of Eq. (30), and for states with $\ell \geq 1$, it is taken to be 1%. Numerical values for Eq. (30) to all orders in $Z\alpha$ have been obtained by Shabaev *et al.* (1998), and although they disagree somewhat with the analytic result, they are consistent within the uncertainty assigned here. We employ the analytic equations in the adjustment. The covariances of the theoretical values are calculated by assuming that the uncertainties are predominately due to uncalculated terms proportional to $(m_{\rm e}/m_{\rm N})/n^3$.

4.1.1.3. Nuclear polarizability

For hydrogen, we use the result (Khriplovich and Sen'kov, 2000)

$$E_{\rm P}({\rm H}) = -0.070(13)h\frac{\delta_{\ell 0}}{n^3}\ {\rm kHz}. \tag{34}$$

More recent results are a model calculation by Nevado and Pineda (2008) and a slightly different result than Eq. (34) calculated by Martynenko (2006).

For deuterium, the sum of the proton polarizability, the neutron polarizibility (Khriplovich and Sen'kov, 1998), and the dominant nuclear structure polarizibility (Friar and Payne, 1997a), gives

$$E_{\rm P}({\rm D}) = -21.37(8)h\frac{\delta_{\ell 0}}{n^3}\ {\rm kHz}. \tag{35}$$

Presumably the polarization effect is negligible for states of higher ℓ in either hydrogen or deuterium.

4.1.1.4. Self energy

The one-photon self energy of the bound electron is

$$E^{(2)}_{\rm SE} = \frac{\alpha}{\pi}\frac{(Z\alpha)^4}{n^3}F(Z\alpha)m_{\rm e}c^2, \tag{36}$$

where

$$\begin{aligned} F(Z\alpha) = {} & {\rm A}_{41}\ln(Z\alpha)^{-2} + A_{40} + A_{50}(Z\alpha) \\ & + A_{62}(Z\alpha)^2\ln^2(Z\alpha)^{-2} + A_{61}(Z\alpha)^2\ln(Z\alpha)^{-2} \\ & + G_{\rm SE}(Z\alpha)(Z\alpha)^2. \end{aligned} \tag{37}$$

From Erickson and Yennie (1965) and earlier papers cited therein,

$$\begin{aligned} A_{41} &= \frac{4}{3}\delta_{\ell 0}, \\ A_{40} &= -\frac{4}{3}\ln k_0(n,\ell) + \frac{10}{9}\delta_{\ell 0} - \frac{1}{2\kappa(2\ell+1)}(1-\delta_{\ell 0}), \\ A_{50} &= \left(\frac{139}{32} - 2\ln 2\right)\pi\delta_{\ell 0}, \\ A_{62} &= -\delta_{\ell 0}, \\ A_{61} &= \left[4\left(1+\frac{1}{2}+\cdots+\frac{1}{n}\right) + \frac{28}{3}\ln 2 - 4\ln n - \frac{601}{180} \right. \\ &\quad \left. - \frac{77}{45n^2}\right]\delta_{\ell 0} + \left(1-\frac{1}{n^2}\right)\left(\frac{2}{15}+\frac{1}{3}\delta_{j\frac{1}{2}}\right)\delta_{\ell 1} \\ &\quad + \frac{[96n^2 - 32\ell(\ell+1)](1-\delta_{\ell 0})}{3n^2(2\ell-1)(2\ell)(2\ell+1)(2\ell+2)(2\ell+3)}. \end{aligned} \tag{38}$$

TABLE 5. Relevant values of the Bethe logarithms $\ln k_0(n,l)$.

n	S	P	D
1	2.984 128 556		
2	2.811 769 893	−0.030 016 709	
3	2.767 663 612		
4	2.749 811 840	−0.041 954 895	−0.006 740 939
6	2.735 664 207		−0.008 147 204
8	2.730 267 261		−0.008 785 043
12			−0.009 342 954

The Bethe logarithms $\ln k_0(n,\ell)$ in Eq. (38) are given in Table 5 (Drake and Swainson, 1990).

For S and P states with $n \le 4$, the values we use here for $G_{\rm SE}(Z\alpha)$ in Eq. (37) are listed in Table 6 and are based on direct numerical evaluations by Jentschura, Mohr, and Soff (1999, 2001) and Jentschura and Mohr (2004, 2005). The values of $G_{\rm SE}(\alpha)$ for the 6S and 8S states are based on the low-Z limit $G_{\rm SE}(0) = A_{60}$ (Jentschura, Czarnecki, and Pachucki, 2005) together with extrapolations of the results of complete numerical calculations of $F(Z\alpha)$ in Eq. (36) at higher Z (Kotochigova and Mohr, 2006). A calculation of the constant A_{60} for various D states, including 12D states, has been done by Wundt and Jentschura (2008). In CODATA-06 this constant was obtained by extrapolation from lower-n states. The more recent calculated values are

$$A_{60}(12{\rm D}_{3/2}) = 0.008\,909\,60(5), \tag{39}$$

$$A_{60}(12{\rm D}_{5/2}) = 0.034\,896\,67(5). \tag{40}$$

To estimate the corresponding value of $G_{\rm SE}(\alpha)$, we use the data from Jentschura *et al.* (2005) given in Table 7. It is evident from the table that

$$G_{\rm SE}(\alpha) - A_{60} \approx 0.000\,22 \tag{41}$$

for the $n{\rm D}_{3/2}$ and $n{\rm D}_{5/2}$ states for $n = 4, 5, 6, 7, 8$, so we make the approximation

$$G_{\rm SE}(\alpha) = A_{60} + 0.000\,22, \tag{42}$$

with an uncertainty given by 0.000 09 and 0.000 22 for the $12{\rm D}_{3/2}$ and $12{\rm D}_{5/2}$ states, respectively. This yields

$$G_{\rm SE}(\alpha) = 0.000\,130(90) \quad \text{for } 12{\rm D}_{3/2}, \tag{43}$$

$$G_{\rm SE}(\alpha) = 0.035\,12(22) \quad \text{for } 12{\rm D}_{5/2}. \tag{44}$$

TABLE 6. Values of the function $G_{\rm SE}(\alpha)$.

n	$S_{1/2}$	$P_{1/2}$	$P_{3/2}$	$D_{3/2}$	$D_{5/2}$
1	−30.290 240(20)				
2	−31.185 150(90)	−0.973 50(20)	−0.486 50(20)		
3	−31.047 70(90)				
4	−30.9120(40)	−1.1640(20)	−0.6090(20)		0.031 63(22)
6	−30.711(47)				0.034 17(26)
8	−30.606(47)			0.007 940(90)	0.034 84(22)
12				0.009 130(90)	0.035 12(22)

TABLE 7. Data from Jentschura *et al.* (2005) and the deduced values of $G_{SE}(\alpha)$ for $n = 12$.

	A_{60}		$G_{SE}(\alpha)$		$G_{SE}(\alpha) - A_{60}$	
n	$D_{3/2}$	$D_{5/2}$	$D_{3/2}$	$D_{5/2}$	$D_{3/2}$	$D_{5/2}$
3	0.005 551 575(1)	0.027 609 989(1)	0.005 73(15)	0.027 79(18)	0.000 18(15)	0.000 18(18)
4	0.005 585 985(1)	0.031 411 862(1)	0.005 80(9)	0.031 63(22)	0.000 21(9)	0.000 22(22)
5	0.006 152 175(1)	0.033 077 571(1)	0.006 37(9)	0.033 32(25)	0.000 22(9)	0.000 24(25)
6	0.006 749 745(1)	0.033 908 493(1)	0.006 97(9)	0.034 17(26)	0.000 22(9)	0.000 26(26)
7	0.007 277 403(1)	0.034 355 926(1)	0.007 50(9)	0.034 57(22)	0.000 22(9)	0.000 21(22)
8	0.007 723 850(1)	0.034 607 492(1)	0.007 94(9)	0.034 84(22)	0.000 22(9)	0.000 23(22)
12	0.008 909 60(5)	0.034 896 67(5)	0.009 13(9)	0.035 12(22)	0.000 22(9)	0.000 22(22)

All values for $G_{SE}(\alpha)$ that we use here are listed in Table 6. The uncertainty of the self-energy contribution to a given level arises entirely from the uncertainty of $G_{SE}(\alpha)$ listed in that table and is taken to be type u_n.

The dominant effect of the finite mass of the nucleus on the self-energy correction is taken into account by multiplying each term of $F(Z\alpha)$ by the reduced-mass factor $(m_r/m_e)^3$, except that the magnetic-moment term $-1/[2\kappa(2\ell+1)]$ in A_{40} is instead multiplied by the factor $(m_r/m_e)^2$. In addition, the argument $(Z\alpha)^{-2}$ of the logarithms is replaced by $(m_e/m_r)(Z\alpha)^{-2}$ (Sapirstein and Yennie, 1990).

4.1.1.5. Vacuum polarization

The second-order vacuum-polarization level shift is

$$E^{(2)}_{VP} = \frac{\alpha}{\pi}\frac{(Z\alpha)^4}{n^3} H(Z\alpha) m_e c^2, \tag{45}$$

where the function $H(Z\alpha)$ consists of the Uehling potential contribution $H^{(1)}(Z\alpha)$ and a higher-order remainder $H^{(R)}(Z\alpha)$:

$$H^{(1)}(Z\alpha) = V_{40} + V_{50}(Z\alpha) + V_{61}(Z\alpha)^2 \ln (Z\alpha)^{-2} + G^{(1)}_{VP}(Z\alpha)(Z\alpha)^2, \tag{46}$$

$$H^{(R)}(Z\alpha) = G^{(R)}_{VP}(Z\alpha)(Z\alpha)^2, \tag{47}$$

with

$$V_{40} = -\frac{4}{15}\delta_{\ell 0}, \quad V_{50} = \frac{5}{48}\pi\delta_{\ell 0}, \quad V_{61} = -\frac{2}{15}\delta_{\ell 0}. \tag{48}$$

Values of $G^{(1)}_{VP}(Z\alpha)$ are given in Table 8 (Mohr, 1982; Kotochigova, Mohr, and Taylor, 2002). The Wichmann-Kroll contribution $G^{(R)}_{VP}(Z\alpha)$ has the leading powers in $Z\alpha$ given by (Wichmann and Kroll, 1956; Mohr, 1975, 1983)

$$G^{(R)}_{VP}(Z\alpha) = \left(\frac{19}{45} - \frac{\pi^2}{27}\right)\delta_{\ell 0} + \left(\frac{1}{16} - \frac{31\pi^2}{2880}\right)\pi(Z\alpha)\delta_{\ell 0} + \cdots. \tag{49}$$

Higher-order terms are negligible.

The finite mass of the nucleus is taken into account by multiplying Eq. (45) by $(m_r/m_e)^3$ and including a factor of (m_e/m_r) in the argument of the logarithm in Eq. (46).

Vacuum polarization from $\mu^+\mu^-$ pairs is (Eides and Shelyuto, 1995; Karshenboim, 1995)

$$E^{(2)}_{\mu VP} = \frac{\alpha}{\pi}\frac{(Z\alpha)^4}{n^3}\left(-\frac{4}{15}\delta_{\ell 0}\right)\left(\frac{m_e}{m_\mu}\right)^2\left(\frac{m_r}{m_e}\right)^3 m_e c^2, \tag{50}$$

and the effect of $\tau^+\tau^-$ pairs is negligible.

Hadronic vacuum polarization gives (Friar, Martorell, and Sprung, 1999)

$$E^{(2)}_{had\,VP} = 0.671(15) E^{(2)}_{\mu\,VP}, \tag{51}$$

where the uncertainty is of type u_0.

The muonic and hadronic vacuum-polarization contributions are negligible for higher-ℓ states.

TABLE 8. Values of the function $G^{(1)}_{VP}(\alpha)$. (The minus signs on the zeros in the last two columns indicate that the values are nonzero negative numbers smaller than the digits shown.)

n	$S_{1/2}$	$P_{1/2}$	$P_{3/2}$	$D_{3/2}$	$D_{5/2}$
1	−0.618 724				
2	−0.808 872	−0.064 006	−0.014 132		
3	−0.814 530				
4	−0.806 579	−0.080 007	−0.017 666		−0.000 000
6	−0.791 450				−0.000 000
8	−0.781 197			−0.000 000	−0.000 000
12				−0.000 000	−0.000 000

4.1.1.6. Two-photon corrections

The two-photon correction, in powers of $Z\alpha$, is

$$E^{(4)} = \left(\frac{\alpha}{\pi}\right)^2 \frac{(Z\alpha)^4}{n^3} m_e c^2 F^{(4)}(Z\alpha), \tag{52}$$

where

$$F^{(4)}(Z\alpha) = B_{40} + B_{50}(Z\alpha) + B_{63}(Z\alpha)^2 \ln^3(Z\alpha)^{-2} + B_{62}(Z\alpha)^2 \ln^2(Z\alpha)^{-2} + B_{61}(Z\alpha)^2 \ln(Z\alpha)^{-2} + B_{60}(Z\alpha)^2 + \cdots. \tag{53}$$

The leading term B_{40} is

$$B_{40} = \left[\frac{3\pi^2}{2}\ln 2 - \frac{10\pi^2}{27} - \frac{2179}{648} - \frac{9}{4}\zeta(3)\right]\delta_{\ell 0} + \left[\frac{\pi^2 \ln 2}{2} - \frac{\pi^2}{12} - \frac{197}{144} - \frac{3\zeta(3)}{4}\right]\frac{1-\delta_{\ell 0}}{\kappa(2\ell+1)}, \tag{54}$$

where ζ is the Riemann zeta function (Olver *et al.*, 2010), and the next term is (Pachucki, 1993a, 1994; Eides and Shelyuto, 1995; Eides, Grotch, and Shelyuto, 1997; Dowling *et al.*, 2010)

$$B_{50} = -21.554\,47(13)\delta_{\ell 0}. \tag{55}$$

The leading sixth-order coefficient is (Karshenboĭm, 1993; Manohar and Stewart, 2000; Yerokhin, 2000; Pachucki, 2001)

$$B_{63} = -\frac{8}{27}\delta_{\ell 0}. \tag{56}$$

For S states B_{62} is (Karshenboim, 1996; Pachucki, 2001)

$$B_{62} = \frac{16}{9}\left[\frac{71}{60} - \ln 2 + \gamma + \psi(n) - \ln n - \frac{1}{n} + \frac{1}{4n^2}\right], \tag{57}$$

where $\gamma = 0.577\ldots$ is Euler's constant and ψ is the psi function (Olver *et al.*, 2010). For P states (Karshenboim, 1996; Jentschura and Nándori, 2002)

$$B_{62} = \frac{4}{27}\frac{n^2-1}{n^2}, \tag{58}$$

and $B_{62} = 0$ for $\ell \geq 2$.

For S states B_{61} is (Pachucki, 2001; Jentschura, Czarnecki, and Pachucki, 2005)

$$B_{61} = \frac{413\,581}{64\,800} + \frac{4N(n\mathrm{S})}{3} + \frac{2027\pi^2}{864} - \frac{616\ln 2}{135} - \frac{2\pi^2 \ln 2}{3} + \frac{40\ln^2 2}{9} + \zeta(3) + \left(\frac{304}{135} - \frac{32\ln 2}{9}\right) \times \left[\frac{3}{4} + \gamma + \psi(n) - \ln n - \frac{1}{n} + \frac{1}{4n^2}\right]. \tag{59}$$

For P states (Jentschura, 2003; Jentschura, Czarnecki, and Pachucki, 2005)

$$B_{61}(n\mathrm{P}_{1/2}) = \frac{4}{3}N(n\mathrm{P}) + \frac{n^2-1}{n^2}\left(\frac{166}{405} - \frac{8}{27}\ln 2\right), \tag{60}$$

$$B_{61}(n\mathrm{P}_{3/2}) = \frac{4}{3}N(n\mathrm{P}) + \frac{n^2-1}{n^2}\left(\frac{31}{405} - \frac{8}{27}\ln 2\right), \tag{61}$$

and $B_{61} = 0$ for $\ell \geq 2$. Values for B_{61} used in the adjustment are listed in Table 9.

For the 1S state, the result of a perturbation theory estimate for the term B_{60} is (Pachucki, 2001; Pachucki and Jentschura, 2003)

$$B_{60}(1\mathrm{S}) = -61.6(9.2). \tag{62}$$

All-order numerical calculations of the two-photon correction have also been carried out. The diagrams with closed electron loops have been evaluated by Yerokhin, Indelicato, and Shabaev (2008). They obtained results for the 1S, 2S, and 2P states at $Z = 1$ and higher Z, and obtained a value for the contribution of the terms of order $(Z\alpha)^6$ and higher. The remaining contributions to B_{60} are from the self-energy diagrams. These have been evaluated by Yerokhin, Indelicato, and Shabaev (2003, 2005a, 2005b, 2007) for the 1S state for $Z = 10$ and higher Z, and more recently, Yerokhin (2010) has done an all-order calculation of the 1S-state no-electron-loop two-loop self-energy correction for $Z \geq 10$. His extrapolation of the higher-Z values to obtain a value for $Z = 1$ yields a contribution to B_{60}, including higher-order terms, given by $-86(15)$. This result combined with the result for the electron-loop two-photon diagrams, reported by Yerokhin, Indelicato, and Shabaev (2008), gives a total of $B_{60} + \cdots = -101(15)$, where the dots represent the contribution of the higher-order terms. This may be compared to the earlier evaluation which gave

TABLE 9. Values of B_{61} used in the 2010 adjustment.

n	$B_{61}(n\mathrm{S}_{1/2})$	$B_{61}(n\mathrm{P}_{1/2})$	$B_{61}(n\mathrm{P}_{3/2})$	$B_{61}(n\mathrm{D}_{3/2})$	$B_{61}(n\mathrm{D}_{5/2})$
1	48.958 590 24(1)				
2	41.062 164 31(1)	0.004 400 847(1)	0.004 400 847(1)		
3	38.904 222(1)				
4	37.909 514(1)	−0.000 525 776 (1)	−0.000 525 776 (1)		0.0(0)
6	36.963 391(1)				0.0(0)
8	36.504 940(1)			0.0(0)	0.0(0)
12				0.0(0)	0.0(0)

TABLE 10. Values of B_{60}, $\bar{B}_{60}$, or ΔB_{71} used in the 2010 adjustment.

n	$B_{60}(n\mathrm{S}_{1/2})$	$\bar{B}_{60}(n\mathrm{P}_{1/2})$	$\bar{B}_{60}(n\mathrm{P}_{3/2})$	$\bar{B}_{60}(n\mathrm{D}_{3/2})$	$\bar{B}_{60}(n\mathrm{D}_{5/2})$	$\Delta B_{71}(n\mathrm{S}_{1/2})$
1	−81.3(0.3)(19.7)					
2	−66.2(0.3)(19.7)	−1.6(3)	−1.7(3)			16(8)
3	−63.0(0.6)(19.7)					22(11)
4	−61.3(0.8)(19.7)	−2.1(3)	−2.2(3)		−0.005(2)	25(12)
6	−59.3(0.8)(19.7)				−0.008(4)	28(14)
8	−58.3(2.0)(19.7)			0.015(5)	−0.009(5)	29(15)
12				0.014(7)	−0.010(7)	

−127(39) (Yerokhin, Indelicato, and Shabaev, 2003, 2005a, 2005b, 2007). The new value also differs somewhat from the result in Eq. (62). In view of this difference between the two calculations, to estimate B_{60} for the 2010 adjustment, we use the average of the analytic value of B_{60} and the numerical result for B_{60} with higher-order terms included, with an uncertainty that is half the difference. The higher-order contribution is small compared to the difference between the results of the two methods of calculation. The average result is

$$B_{60}(1\mathrm{S}) = -81.3(0.3)(19.7). \tag{63}$$

In Eq. (63), the first number in parentheses is the state-dependent uncertainty $u_n(B_{60})$ associated with the two-loop Bethe logarithm, and the second number in parentheses is the state-independent uncertainty $u_0(B_{60})$ that is common to all S-state values of B_{60}. Two-loop Bethe logarithms needed to evaluate $B_{60}(n\mathrm{S})$ have been given for $n = 1$ to 6 (Pachucki and Jentschura, 2003; Jentschura, 2004), and a value at $n = 8$ may be obtained by a simple extrapolation from the calculated values [see Eq. (43) of CODATA-06]. The complete state dependence of $B_{60}(n\mathrm{S})$ in terms of the two-loop Bethe logarithms has been calculated by Czarnecki, Jentschura, and Pachucki (2005) and Jentschura, Czarnecki, and Pachucki (2005). Values of B_{60} for all relevant S states are given in Table 10.

For higher-ℓ states, an additional consideration is necessary. The radiative level shift includes contributions associated with decay to lower levels. At the one-loop level, this is the imaginary part of the level shift corresponding to the resonance scattering width of the level. At the two-loop level there is an imaginary contribution corresponding to two-photon decays and radiative corrections to the one-photon decays, but in addition there is a real contribution from the square of the one-photon decay width. This can be thought of as the second-order term that arises in the expansion of the resonance denominator for scattering of photons from the atom in its ground state in powers of the level width (Jentschura *et al.*, 2002). As such, this term should not be included in the calculation of the resonant line-center shift of the scattering cross section, which is the quantity of interest for the least-squares adjustment. The leading contribution of the square of the one-photon width is of order $\alpha(Z\alpha)^6 m_e c^2/\hbar$. This correction vanishes for the 1S and 2S states, because the 1S level has no width and the 2S level can only decay with transition rates that are higher order in α and/or $Z\alpha$. The higher-n S states have a contribution from the square of the one-photon width from decays to lower P states, but for the 3S and 4S states for which it has been separately identified, this correction is negligible compared to the uncertainty in B_{60} (Jentschura, 2004, 2006). We assume the correction for higher S states is also negligible compared to the numerical uncertainty in B_{60}. However, the correction is taken into account in the 2010 adjustment for P and D states for which it is relatively larger (Jentschura *et al.*, 2002; Jentschura, 2006).

Calculations of B_{60} for higher-ℓ states have been made by Jentschura (2006). The results can be expressed as

$$B_{60}(nL_j) = a(nL_j) + b_{\mathrm{L}}(nL), \tag{64}$$

where $a(nL_j)$ is a precisely calculated term that depends on j, and the two-loop Bethe logarithm $b_{\mathrm{L}}(nL)$ has a larger numerical uncertainty but does not depend on j. Jentschura (2006) gives semianalytic formulas for $a(nL_j)$ that include numerically calculated terms. The information needed for the 2010 adjustment is in Eqs. (22a), (22b), (23a), and (23b), Tables 7–10 of Jentschura (2006) and Eq. (17) of Jentschura (2003). Two corrections to Eq. (22b) are

$$-\frac{73\,321}{103\,680}+\frac{185}{1152n}+\frac{8111}{25\,920n^2} \to -\frac{14\,405}{20\,736}+\frac{185}{1152n}+\frac{1579}{5184n^2} \tag{65}$$

on the first line and

$$-\frac{3187}{3600n^2} \to +\frac{3187}{3600n^2} \tag{66}$$

on the fourth line (Jentschura, 2011a).

Values of the two-photon Bethe logarithm $b_{\mathrm{L}}(nL)$ may be divided into a contribution of the "squared level width" term $\delta^2 B_{60}$ and the rest $\bar{b}_{\mathrm{L}}(nL)$, so that

$$b_{\mathrm{L}}(nL) = \delta^2 B_{60} + \bar{b}_{\mathrm{L}}(nL). \tag{67}$$

The corresponding value $\bar{B}_{60}$ that represents the shift of the level center is given by

$$\bar{B}_{60}(nL_j) = a(nL_j) + \bar{b}_{\mathrm{L}}(nL). \tag{68}$$

Here we give the numerical values for $\bar{B}(nL_j)$ in Table 10 and refer the reader to Jentschura (2006) for the separate values for $a(nL_j)$ and $\bar{b}_{\mathrm{L}}(nL)$. The D-state values for $n = 6$, 8 are extrapolated from the corresponding values at $n = 5$, 6 with a function of the form $a + b/n$. The values in Table 10 for S states may be regarded as being either B_{60} or $\bar{B}_{60}$, since the difference is expected to be smaller than the uncertainty. The uncertainties listed for the P- and D-state values of $\bar{B}(nL_j)$ in that table are predominately from the two-photon Bethe

logarithm which depends on n and L, but not on j for a given n, L. Therefore there is a large covariance between the corresponding two values of $\bar{B}(nL_j)$. However, we do not take this into consideration when calculating the uncertainty in the fine-structure splitting, because the uncertainty of higher-order coefficients dominates over any improvement in accuracy the covariance would provide. We assume that the uncertainties in the two-photon Bethe logarithms are sufficiently large to account for higher-order P- and D-state two-photon uncertainties as well.

For S states, higher-order terms have been estimated by Jentschura, Czarnecki, and Pachucki (2005) with an effective potential model. They find that the next term has a coefficient of B_{72} and is state independent. We thus assume that the uncertainty $u_0[B_{60}(n\mathrm{S})]$ is sufficient to account for the uncertainty due to omitting such a term and higher-order state-independent terms. In addition, they find an estimate for the state dependence of the next term, given by

$$\begin{aligned}\Delta B_{71}(n\mathrm{S}) &= B_{71}(n\mathrm{S}) - B_{71}(1\mathrm{S}) \\ &= \pi\left(\frac{427}{36} - \frac{16}{3}\ln 2\right) \\ &\quad \times \left[\frac{3}{4} - \frac{1}{n} + \frac{1}{4n^2} + \gamma + \psi(n) - \ln n\right],\end{aligned} \tag{69}$$

with a relative uncertainty of 50%. We include this additional term, which is listed in Table 10, along with the estimated uncertainty $u_n(B_{71}) = B_{71}/2$.

4.1.1.7. Three-photon corrections

The three-photon contribution in powers of $Z\alpha$ is

$$E^{(6)} = \left(\frac{\alpha}{\pi}\right)^3 \frac{(Z\alpha)^4}{n^3} m_e c^2 [C_{40} + C_{50}(Z\alpha) + \cdots]. \tag{70}$$

The leading term C_{40} is (Baikov and Broadhurst, 1995; Eides and Grotch, 1995a; Laporta and Remiddi, 1996; Melnikov and van Ritbergen, 2000)

$$\begin{aligned}C_{40} = &\left[-\frac{568\mathrm{a}_4}{9} + \frac{85\zeta(5)}{24} - \frac{121\pi^2\zeta(3)}{72} - \frac{84\,071\zeta(3)}{2304}\right. \\ &- \frac{71\ln^4 2}{27} - \frac{239\pi^2\ln^2 2}{135} + \frac{4787\pi^2\ln 2}{108} + \frac{1591\pi^4}{3240} \\ &\left. - \frac{252\,251\pi^2}{9720} + \frac{679\,441}{93\,312}\right]\delta_{\ell 0} + \left[-\frac{100\mathrm{a}_4}{3} + \frac{215\zeta(5)}{24}\right. \\ &- \frac{83\pi^2\zeta(3)}{72} - \frac{139\zeta(3)}{18} - \frac{25\ln^4 2}{18} + \frac{25\pi^2\ln^2 2}{18} \\ &\left. + \frac{298\pi^2\ln 2}{9} + \frac{239\pi^4}{2160} - \frac{17\,101\pi^2}{810} - \frac{28\,259}{5184}\right] \\ &\times \frac{1-\delta_{\ell 0}}{\kappa(2\ell+1)},\end{aligned} \tag{71}$$

where $\mathrm{a}_4 = \sum_{n=1}^{\infty} 1/(2^n n^4) = 0.517\,479\,061\ldots$. Partial results for C_{50} have been calculated by Eides and Shelyuto (2004, 2007). The uncertainty is taken to be $u_0(C_{50}) = 30\delta_{\ell 0}$ and $u_n(C_{63}) = 1$, where C_{63} would be the coefficient of $(Z\alpha)^2\ln^3(Z\alpha)^{-2}$ in the square brackets in Eq. (70). The dominant effect of the finite mass of the nucleus is taken into account by multiplying the term proportional to $\delta_{\ell 0}$ by the reduced-mass factor $(m_r/m_e)^3$ and the term proportional to $1/\kappa(2\ell+1)$, the magnetic-moment term, by the factor $(m_r/m_e)^2$.

The contribution from four photons would be of order

$$\left(\frac{\alpha}{\pi}\right)^4 \frac{(Z\alpha)^4}{n^3} m_e c^2, \tag{72}$$

which is about 10 Hz for the 1S state and is negligible at the level of uncertainty of current interest.

4.1.1.8. Finite nuclear size

In the nonrelativistic limit, the level shift due to the finite size of the nucleus is

$$E^{(0)}_{\mathrm{NS}} = \mathcal{E}_{\mathrm{NS}}\delta_{\ell 0}, \tag{73}$$

where

$$\mathcal{E}_{\mathrm{NS}} = \frac{2}{3}\left(\frac{m_r}{m_e}\right)^3 \frac{(Z\alpha)^2}{n^3} m_e c^2 \left(\frac{Z\alpha r_N}{\lambda\!\!\!^{-}_C}\right)^2, \tag{74}$$

r_N is the bound-state root-mean-square (rms) charge radius of the nucleus, and $\lambda\!\!\!^{-}_C$ is the Compton wavelength of the electron divided by 2π.

Higher-order contributions have been examined by Friar (1979b), Friar and Payne (1997b), and Karshenboim (1997) [see also Borisoglebsky and Trofimenko (1979) and Mohr (1983)]. For S states the leading- and next-order corrections are given by

$$\begin{aligned}E_{\mathrm{NS}} = \mathcal{E}_{\mathrm{NS}}\left\{1 - C_\eta \frac{m_r}{m_e}\frac{r_N}{\lambda\!\!\!^{-}_C} Z\alpha - \left[\ln\left(\frac{m_r}{m_e}\frac{r_N}{\lambda\!\!\!^{-}_C}\frac{Z\alpha}{n}\right)\right.\right. \\ \left.\left. + \psi(n) + \gamma - \frac{(5n+9)(n-1)}{4n^2} - C_\theta\right](Z\alpha)^2\right\},\end{aligned} \tag{75}$$

where C_η and C_θ are constants that depend on the charge distribution in the nucleus with values $C_\eta = 1.7(1)$ and $C_\theta = 0.47(4)$ for hydrogen or $C_\eta = 2.0(1)$ and $C_\theta = 0.38(4)$ for deuterium.

For the $\mathrm{P}_{1/2}$ states in hydrogen the leading term is

$$E_{\mathrm{NS}} = \mathcal{E}_{\mathrm{NS}} \frac{(Z\alpha)^2(n^2-1)}{4n^2}. \tag{76}$$

For $\mathrm{P}_{3/2}$ states and higher-ℓ states the nuclear-size contribution is negligible.

As mentioned in Sec. 4.1.1.1, in the 2010 adjustment, we do not use an effective radius for the deuteron, but rather simply r_d which is defined by Eq. (74). In CODATA-02, and CODATA-

06, the adjustment code used r_d as an adjusted variable and that value was reported for the rms radius, rather than the value for R_d defined by Eq. (A56) of CODATA-98, which differs from r_d by less than 0.1%.

4.1.1.9. Nuclear-size correction to self energy and vacuum polarization

There is a correction from the finite size of the nucleus to the self energy (Pachucki, 1993b; Eides and Grotch, 1997b; Milstein, Sushkov, and Terekhov, 2002, 2003b),

$$E_{\mathrm{NSE}} = \left(4\ln 2 - \frac{23}{4}\right)\alpha(Z\alpha)\mathcal{E}_{\mathrm{NS}}\delta_{\ell 0}, \tag{77}$$

and to the vacuum polarization (Friar, 1979a; Hylton, 1985; Eides and Grotch, 1997b),

$$E_{\mathrm{NVP}} = \frac{3}{4}\alpha(Z\alpha)\mathcal{E}_{\mathrm{NS}}\delta_{\ell 0}. \tag{78}$$

For the self energy, higher-order size corrections have been calculated for S states by Milstein, Sushkov, and Terekhov (2002) and for P states by Jentschura (2003), Milstein, Sushkov, and Terekhov (2003b, 2004). Yerokhin (2011) calculated the finite nuclear-size corrections to the self energy and vacuum polarization nonperturbatively in $Z\alpha$ and has extrapolated the values for the 1S state to $Z = 1$. The results are consistent with the higher-order analytic results. Pachucki, in a private communication quoted by Yerokhin (2011), notes that the coefficients of the leading log terms are the same for the nuclear-size correction to the self energy as they are for the self-energy correction to the hyperfine splitting. The latter terms have been calculated by Jentschura and Yerokhin (2010). However, these higher-order terms are negligible at the level of accuracy under consideration. Corrections for higher-ℓ states are also expected to be negligible.

4.1.1.10. Radiative-recoil corrections

Corrections to the self energy and vacuum polarization for the finite mass of the nucleus, beyond the reduced-mass corrections already included, are radiative-recoil effects given by Eides and Grotch (1995b), Pachucki (1995), Melnikov and Yelkhovsky (1999), Pachucki and Karshenboim (1999), Czarnecki and Melnikov (2001), and Eides, Grotch, and Shelyuto (2001a):

$$E_{\mathrm{RR}} = \frac{m_r^3}{m_e^2 m_N}\frac{\alpha(Z\alpha)^5}{\pi^2 n^3} m_e c^2 \delta_{\ell 0}\left[6\zeta(3) - 2\pi^2\ln 2 + \frac{35\pi^2}{36} - \frac{448}{27} + \frac{2}{3}\pi(Z\alpha)\ln^2(Z\alpha)^{-2} + \cdots\right]. \tag{79}$$

The uncertainty is taken to be the term $(Z\alpha)\ln(Z\alpha)^{-2}$ relative to the square brackets with numerical coefficients 10 for u_0 and 1 for u_n. Corrections for higher-ℓ states are expected to be negligible.

4.1.1.11. Nucleus self energy

A correction due to the self energy of the nucleus is (Pachucki, 1995; Eides, Grotch, and Shelyuto, 2001b)

$$E_{\mathrm{SEN}} = \frac{4Z^2\alpha(Z\alpha)^4}{3\pi n^3}\frac{m_r^3}{m_N^2}c^2\left[\ln\left(\frac{m_N}{m_r(Z\alpha)^2}\right)\delta_{\ell 0} - \ln k_0(n,\ell)\right]. \tag{80}$$

For the uncertainty, we assign a value to u_0 corresponding to an additive constant of 0.5 in the square brackets in Eq. (80) for S states. For higher-ℓ states, the correction is not included.

4.1.1.12. Total energy and uncertainty

The energy $E_X(n\mathrm{L}_j)$ of a level (where $\mathrm{L} = \mathrm{S}, \mathrm{P}, \ldots$ and $X = \mathrm{H}$, D) is the sum of the various contributions listed in the preceding sections plus an additive correction $\delta_X(n\mathrm{L}_j)$ that is zero with an uncertainty that is the rms sum of the uncertainties of the individual contributions:

$$u^2[\delta_X(n\mathrm{L}_j)] = \sum_i \frac{u_{0i}^2(X\mathrm{L}_j) + u_{ni}^2(X\mathrm{L}_j)}{n^6}, \tag{81}$$

where $u_{0i}(X\mathrm{L}_j)/n^3$ and $u_{ni}(X\mathrm{L}_j)/n^3$ are the components of uncertainty u_0 and u_n of contribution i. Uncertainties from the fundamental constants are not explicitly included here, because they are taken into account through the least-squares adjustment.

The covariance of any two δ's follows from Eq. (F7) of Appendix F of CODATA-98. For a given isotope

$$u[\delta_X(n_1\mathrm{L}_j), \delta_X(n_2\mathrm{L}_j)] = \sum_i \frac{u_{0i}^2(X\mathrm{L}_j)}{(n_1 n_2)^3}, \tag{82}$$

which follows from the fact that $u(u_{0i}, u_{ni}) = 0$ and $u(u_{n_1 i}, u_{n_2 i}) = 0$ for $n_1 \neq n_2$. We also assume that

$$u[\delta_X(n_1\mathrm{L}_{1j_1}), \delta_X(n_2\mathrm{L}_{2j_2})] = 0 \tag{83}$$

if $\mathrm{L}_1 \neq \mathrm{L}_2$ or $j_1 \neq j_2$.

For covariances between δ's for hydrogen and deuterium, we have for states of the same n

$$u[\delta_{\mathrm{H}}(n\mathrm{L}_j), \delta_{\mathrm{D}}(n\mathrm{L}_j)] = \sum_{i=i_c} \frac{u_{0i}(\mathrm{HL}_j)u_{0i}(\mathrm{DL}_j) + u_{ni}(\mathrm{HL}_j)u_{ni}(\mathrm{DL}_j)}{n^6}, \tag{84}$$

and for $n_1 \neq n_2$

$$u[\delta_{\mathrm{H}}(n_1\mathrm{L}_j), \delta_{\mathrm{D}}(n_2\mathrm{L}_j)] = \sum_{i=i_c} \frac{u_{0i}(\mathrm{HL}_j)u_{0i}(\mathrm{DL}_j)}{(n_1 n_2)^3}, \tag{85}$$

where the summation is over the uncertainties common to hydrogen and deuterium. We assume

$$u[\delta_{\mathrm{H}}(n_1\mathrm{L}_{1j_1}), \delta_{\mathrm{D}}(n_2\mathrm{L}_{2j_2})] = 0 \tag{86}$$

if $\mathrm{L}_1 \neq \mathrm{L}_2$ or $j_1 \neq j_2$.

The values of $u[\delta_X(nL_j)]$ of interest for the 2010 adjustment are given in Table 18 of Sec. 13, and the non-negligible covariances of the δ's are given as correlation coefficients in Table 19 of that section. These coefficients are as large as 0.9999.

4.1.1.13. Transition frequencies between levels with $n = 2$ and the fine-structure constant α

To test the QED predictions, we calculate the values of the transition frequencies between levels with $n = 2$ in hydrogen. This is done by running the least-squares adjustment with the hydrogen and deuterium spectroscopic data included, but excluding experimental values for the transitions being calculated (items *A*39, *A*40.1, and *A*40.2 in Table 18). The necessary constants $A_r(e)$, $A_r(p)$, $A_r(d)$, and α are assigned their 2010 adjusted values. The results are

$$\begin{aligned}
\nu_H(2P_{1/2} - 2S_{1/2}) &= 1\,057\,844.4(1.8)\ \text{kHz} \quad [1.7 \times 10^{-6}],\\
\nu_H(2S_{1/2} - 2P_{3/2}) &= 9\,911\,197.1(1.8)\ \text{kHz} \quad [1.8 \times 10^{-7}],\\
\nu_H(2P_{1/2} - 2P_{3/2}) &= 10\ 969\ 041.571(41)\ \text{kHz} \quad [3.7 \times 10^{-9}],
\end{aligned} \tag{87}$$

which are consistent with the relevant experimental results given in Table 18. There is a significant reduction in uncertainty in these frequencies compared to the corresponding 2006 theoretical values.

We obtain a value for the fine-structure constant α from the data on the hydrogen and deuterium transitions. This is done by running a variation of the 2010 least-squares adjustment that includes all the transition-frequency data in Table 18 and the 2010 adjusted values of $A_r(e)$, $A_r(p)$, and $A_r(d)$. This yields

$$\alpha^{-1} = 137.036\,003(41) \quad [3.0 \times 10^{-7}], \tag{88}$$

which is in excellent agreement with, but substantially less accurate than, the 2010 recommended value, and is included in Table 25.

4.1.1.14. Isotope shift and the deuteron-proton radius difference

A new experimental result for the hydrogen-deuterium isotope shift is included in Table 11 (Parthey *et al.*, 2010; Jentschura *et al.*, 2011). In Jentschura *et al.* (2011) there is a discussion of the theory of the isotope shift, with the objective of extracting the difference of the squares of the charge radii for the deuteron and proton. The analysis in Jentschura *et al.* (2011) is in general agreement with the review given in the preceding sections of the present work, with a few differences in the estimates of uncertainties.

TABLE 11. Summary of measured transition frequencies ν considered in the present work for the determination of the Rydberg constant R_∞ (H is hydrogen and D is deuterium).

Authors	Laboratory[a]	Frequency interval(s)	Reported value ν (kHz)	Rel. stand. uncert. u_r
(Fischer *et al.*, 2004)	MPQ	$\nu_H(1S_{1/2} - 2S_{1/2})$	2 466 061 413 187.080(34)	1.4×10^{-14}
(Weitz *et al.*, 1995)	MPQ	$\nu_H(2S_{1/2} - 4S_{1/2}) - \frac{1}{4}\nu_H(1S_{1/2} - 2S_{1/2})$	4 797 338(10)	2.1×10^{-6}
		$\nu_H(2S_{1/2} - 4D_{5/2}) - \frac{1}{4}\nu_H(1S_{1/2} - 2S_{1/2})$	6 490 144(24)	3.7×10^{-6}
		$\nu_D(2S_{1/2} - 4S_{1/2}) - \frac{1}{4}\nu_D(1S_{1/2} - 2S_{1/2})$	4 801 693(20)	4.2×10^{-6}
		$\nu_D(2S_{1/2} - 4D_{5/2}) - \frac{1}{4}\nu_D(1S_{1/2} - 2S_{1/2})$	6 494 841(41)	6.3×10^{-6}
(Parthey *et al.*, 2010)	MPQ	$\nu_D(1S_{1/2} - 2S_{1/2}) - \nu_H(1S_{1/2} - 2S_{1/2})$	670 994 334.606(15)	2.2×10^{-11}
(de Beauvoir *et al.*, 1997)	LKB/SYRTE	$\nu_H(2S_{1/2} - 8S_{1/2})$	770 649 350 012.0(8.6)	1.1×10^{-11}
		$\nu_H(2S_{1/2} - 8D_{3/2})$	770 649 504 450.0(8.3)	1.1×10^{-11}
		$\nu_H(2S_{1/2} - 8D_{5/2})$	770 649 561 584.2(6.4)	8.3×10^{-12}
		$\nu_D(2S_{1/2} - 8S_{1/2})$	770 859 041 245.7(6.9)	8.9×10^{-12}
		$\nu_D(2S_{1/2} - 8D_{3/2})$	770 859 195 701.8(6.3)	8.2×10^{-12}
		$\nu_D(2S_{1/2} - 8D_{5/2})$	770 859 252 849.5(5.9)	7.7×10^{-12}
(Schwob *et al.*, 1999)	LKB/SYRTE	$\nu_H(2S_{1/2} - 12D_{3/2})$	799 191 710 472.7(9.4)	1.2×10^{-11}
		$\nu_H(2S_{1/2} - 12D_{5/2})$	799 191 727 403.7(7.0)	8.7×10^{-12}
		$\nu_D(2S_{1/2} - 12D_{3/2})$	799 409 168 038.0(8.6)	1.1×10^{-11}
		$\nu_D(2S_{1/2} - 12D_{5/2})$	799 409 184 966.8(6.8)	8.5×10^{-12}
(Arnoult *et al.*, 2010)	LKB	$\nu_H(1S_{1/2} - 3S_{1/2})$	2 922 743 278 678(13)	4.4×10^{-12}
(Bourzeix *et al.*, 1996)	LKB	$\nu_H(2S_{1/2} - 6S_{1/2}) - \frac{1}{4}\nu_H(1S_{1/2} - 3S_{1/2})$	4 197 604(21)	4.9×10^{-6}
		$\nu_H(2S_{1/2} - 6D_{5/2}) - \frac{1}{4}\nu_H(1S_{1/2} - 3S_{1/2})$	4 699 099(10)	2.2×10^{-6}
(Berkeland, Hinds, and Boshier, 1995)	Yale	$\nu_H(2S_{1/2} - 4P_{1/2}) - \frac{1}{4}\nu_H(1S_{1/2} - 2S_{1/2})$	4 664 269(15)	3.2×10^{-6}
		$\nu_H(2S_{1/2} - 4P_{3/2}) - \frac{1}{4}\nu_H(1S_{1/2} - 2S_{1/2})$	6 035 373(10)	1.7×10^{-6}
(Hagley and Pipkin, 1994)	Harvard	$\nu_H(2S_{1/2} - 2P_{3/2})$	9 911 200(12)	1.2×10^{-6}
(Lundeen and Pipkin, 1986)	Harvard	$\nu_H(2P_{1/2} - 2S_{1/2})$	1 057 845.0(9.0)	8.5×10^{-6}
(Newton, Andrews, and Unsworth, 1979)	U. Sussex	$\nu_H(2P_{1/2} - 2S_{1/2})$	1 057 862(20)	1.9×10^{-5}

[a]MPQ: Max-Planck-Institut für Quantenoptik, Garching. LKB: Laboratoire Kastler-Brossel, Paris. SYRTE: Systèmes de référence Temps Espace, Paris, formerly Laboratoire Primaire du Temps et des Fréquences (LPTF).

As pointed out by Jentschura *et al.* (2011), the isotope shift is roughly given by

$$\Delta f_{1S-2S,d} - \Delta f_{1S-2S,p} \approx -\frac{3}{4} R_\infty c \left(\frac{m_e}{m_d} - \frac{m_e}{m_p} \right) = \frac{3}{4} R_\infty c \frac{m_e (m_d - m_p)}{m_d m_p}, \quad (89)$$

and from a comparison of experiment and theory, they obtain

$$r_d^2 - r_p^2 = 3.820\,07(65)\ \text{fm}^2 \quad (90)$$

for the difference of the squares of the radii. This can be compared to the result given by the 2010 adjustment:

$$r_d^2 - r_p^2 = 3.819\,89(42)\ \text{fm}^2, \quad (91)$$

which is in good agreement. (The difference of the squares of the quoted 2010 recommended values of the radii gives 87 in the last two digits of the difference, rather than 89, due to rounding.) The uncertainty follows from Eqs. (F11) and (F12) of CODATA-98. Here there is a significant reduction in the uncertainty compared to the uncertainties of the individual radii because of the large correlation coefficient (physics.nist.gov/constants)

$$r(r_d, r_p) = 0.9989. \quad (92)$$

Part of the reduction in uncertainty in Eq. (91) compared to Eq. (90) is due to the fact that the correlation coefficient takes into account the covariance of the electron-nucleon mass ratios in Eq. (89).

4.1.2. Experiments on hydrogen and deuterium

The hydrogen and deuterium transition frequencies used in the 2010 adjustment for the determination of the Rydberg constant R_∞ are given in Table 11. These are items *A*26 to *A*48 in Table 18, Sec. 13. There are only three differences between Table 11 in this report and the corresponding Table XII in CODATA-06.

First, the last two digits of the $1S_{1/2}-2S_{1/2}$ transition frequency obtained by the group at the Max-Planck-Institute für Quantenoptik (MPQ), Garching, Germany have changed from 74 to 80 as a result of the group's improved measurement of the 2S hydrogen hyperfine splitting frequency (HFS). Their result is (Kolachevsky *et al.*, 2009)

$$\nu_{HFS}(H; 2S) = 177\,556\,834.3(6.7)\ \text{Hz} \quad [3.8 \times 10^{-8}]. \quad (93)$$

The reduction in the uncertainty of their previous value for this frequency (Kolachevsky *et al.*, 2004) by a factor of 2.4 was mainly due to the use of a new ultrastable optical reference (Alnis *et al.*, 2008) and a reanalysis of the shift with pressure of the 2S HFS frequency that showed it was negligible in their apparatus. The 2S HFS enters the determination of the $1S_{1/2}-2S_{1/2}$ transition frequency because the transition actually measured is $(1S, F = 1, m_F = \pm 1) \rightarrow (2S, F' = 1, m'_F = \pm 1)$ and the well-known 1S HFS (Ramsey, 1990) and the 2S HFS are required to convert the measured frequency to the frequency of the hyperfine centroid.

For completeness, we note that the MPQ group has very recently reported a new value for the $1S_{1/2}-2S_{1/2}$ transition frequency that has an uncertainty of 10 Hz, corresponding to a relative standard uncertainty of 4.2×10^{-15}, or about 30% of the uncertainty of the value in the table (Parthey *et al.*, 2011).

Second, the previous MPQ value (Huber *et al.*, 1998) for the hydrogen-deuterium 1S–2S isotope shift, that is, the frequency difference $\nu_D(1S_{1/2}-2S_{1/2}) - \nu_H(1S_{1/2}-2S_{1/2})$, has been replaced by their recent, much more accurate value (Parthey *et al.*, 2010); its uncertainty of 15 Hz, corresponding to a relative uncertainty of 2.2×10^{-11}, is a factor of 10 smaller than the uncertainty of their previous result. Many experimental advances enabled this significant uncertainty reduction, not the least of which was the use of a fiber frequency comb referenced to an active hydrogen maser steered by the Global Positioning System (GPS) to measure laser frequencies. The principal uncertainty components in the measurement are 11 Hz due to density effects in the atomic beam, 6 Hz from second-order Doppler shift, and 5.1 Hz statistical.

Third, Table 11 includes a new result from the group at the Laboratoire Kastler-Brossel (LKB), École Normale Supérieure et Université Pierre et Marie Curie, Paris, France. These researchers have extended their previous work and determined the $1S_{1/2}-3S_{1/2}$ transition frequency in hydrogen using Doppler-free two-photon spectroscopy with a relative uncertainty of 4.4×10^{-12} (Arnoult *et al.*, 2010), the second smallest uncertainty for a hydrogen or deuterium optical transition frequency ever obtained. The transition occurs at a wavelength of 205 nm, and light at this wavelength was obtained by twice doubling the frequency of light emitted by a titanium-sapphire laser of wavelength 820 nm whose frequency was measured using an optical frequency comb.

A significant problem in the experiment was the second-order Doppler effect due to the velocity v of the 1S atomic beam which causes an apparent shift of the transition frequency. The velocity was measured by having the beam pass through a transverse magnetic field, thereby inducing a motional electric field and hence a quadratic Stark shift that varies as v^2. The variation of this Stark shift with field was used to determine v and thus the correction for the second-order Doppler effect. The dominant 12.0 kHz uncertainty component in the LKB experiment is statistical, corresponding to a relative uncertainty of 4.1×10^{-12}; the remaining components together contribute an additional uncertainty of only 4.8 kHz.

As discussed in CODATA-98, some of the transition frequencies measured in the same laboratory are correlated. Table 19, Sec. 13, gives the relevant correlation coefficients.

4.1.3. Nuclear radii

Transition frequencies in hydrogen and deuterium depend on the rms charge radius of the nucleus, denoted by r_p and r_d, respectively. The main difference between energy levels for a

point charge nucleus and for a nucleus with a finite charge radius is given by Eq. (74). These radii are treated as adjusted constants, so the H and D experimental transition-frequency input data, together with theory, provide adjusted values for them.

4.1.3.1. Electron scattering

The radii can also be determined from elastic electron-proton (e-p) scattering data in the case of r_p, and from elastic electron-deuteron (e-d) scattering data in the case of r_d. These independently determined values are used as additional input data which, together with the H and D spectroscopic data and the theory, determine the 2010 recommended values of the radii. The experimental electron-scattering values of r_p and r_d that we take as input data in the 2010 adjustment are

$$r_p = 0.895(18)\ \text{fm}, \tag{94}$$

$$r_p = 0.8791(79)\ \text{fm}, \tag{95}$$

$$r_d = 2.130(10)\ \text{fm}. \tag{96}$$

The first result for r_p, which was also used in the 2002 and 2006 adjustments, is due to Sick (2003, 2007, 2008) and is based on a reanalysis of the world e-p cross section and polarization transfer data. The value in Eq. (94) is consistent with the more accurate result $r_p = 0.894(8)$ fm reported after the closing date of the 2010 adjustment by Sick (2011) using an improved method to treat the proton's charge density at large radii. It is also consistent with the very recent result $r_p = 0.886(8)$ fm calculated by Sick (2012) that extends this method and is based in part on the data obtained by Bernauer *et al.* (2010) in the experiment that yields the second result for r_p, which we now discuss. [Note that the recent paper of Sick (2012) gives an overview of the problems associated with determining a reliable value of r_p from e-p scattering data. Indeed, Adamuscin, Dubnicka, and Dubnickova (2012) find $r_p = 0.849(7)$ fm based on a reanalysis of selected nucleon form-factor data; see also Arrington, Melnitchouk, and Tjon (2007).]

The value of r_p given in Eq. (95) was obtained at the Mainz University, Germany, with the Mainz linear electron accelerator MAMI. About 1400 elastic e-p scattering cross sections were measured at six beam energies from 180 MeV to 855 MeV, covering the range of four-momentum transfers squared from $Q^2 = 0.004\ (\text{GeV}/c)^2$ to $1\ (\text{GeV}/c)^2$. The value of r_p was extracted from the data using spline fits or polynomial fits, and because the reason for the comparatively small difference between the resulting values could not be identified, Bernauer *et al.* (2010) give as their final result the average of the two values with an added uncertainty equal to half the difference. [Note that the value in Eq. (95) contains extra digits provided by Bernauer (2010); see also Arrington (2011) and Bernauer *et al.* (2011).]

The result for r_d is that given by Sick (2008) and is based on an analysis of the world data on e-d scattering similar to that used to determine the value of r_p in Eq. (94).

For completeness we note the recent e-p scattering result for r_p based in part on new data obtained in the range $Q^2 = 0.3\ (\text{GeV}/c)^2$ to $0.7\ (\text{GeV}/c)^2$ at the Thomas Jefferson National Accelerator Facility, Newport News, Virginia, USA, often referred to as simply JLab. The new data, acquired using a technique called polarization transfer or recoil polarimetry, were combined with previous cross section and polarization measurements to produce the result $r_p = 0.875(10)$ fm from an updated global fit in this range of Q^2 (Ron *et al.*, 2011; Zhan *et al.*, 2011). It is independent of and agrees with the Mainz result in Eq. (95), and it also agrees with the result in Eq. (94) but the two are not independent since the data used to obtain the latter result were included in the JLab fit. This result became available after the 31 December 2010 closing date of the 2010 adjustment.

4.1.3.2. Muonic hydrogen

A muonic hydrogen atom, μ^-p, consists of a negative muon and a proton. Since $m_\mu/m_e \approx 207$, the Bohr radius of the muon is about 200 times smaller than the electron Bohr radius, so the muon is more sensitive to the size of the nucleus. Indeed, the finite-size effect for the 2S state in μ^-p is about 2% of the total Lamb shift, that is, the energy difference between the 2S and 2P states, which should make it an ideal system for measuring the size of the proton. (Because of the large electron vacuum-polarization effect in muonic hydrogen, the $2S_{1/2}$ level is well below both the $2P_{3/2}$ and $2P_{1/2}$ levels.)

In a seminal experiment carried out using pulsed laser spectroscopy at a specially built muon beam line at the proton accelerator of the Paul Scherrer Institute (PSI), Villigen, Switzerland, Pohl *et al.* (2010, 2011) measured the 206 meV (50 THz or 6 μm) μ^-p Lamb shift, in particular, the $2S_{1/2}(F = 1) - 2P_{3/2}(F = 2)$ transition, with an impressive relative standard uncertainty of 15 parts in 10^6. The result, when combined with the theoretical expression for the transition, leads to (Jentschura, 2011b)

$$r_p = 0.841\,69(66)\ \text{fm}. \tag{97}$$

The value given in Eq. (97) is based on a review and reanalysis of the theory by Jentschura (2011b, 2011c) but is not significantly different from the value first given by Pohl *et al.* (2010). Because the muonic hydrogen value of r_p differs markedly from the 2006 CODATA recommended value given in CODATA-06, its publication in 2010 has led to a significant number of papers that reexamine various aspects of the theory or propose possible reasons for the disagreement; see, for example, the recent review of Borie (2012). If Eq. (97) is compared to the 2010 recommended value of 0.8775(51) fm, the disagreement is 7σ. If it is compared to the value 0.8758(77) fm based on only H and D spectroscopic data (see Table 38), the disagreement is 4.4σ. (Throughout the paper, σ as used here is the standard uncertainty u_{diff} of the difference between two values.)

The impact of including Eq. (97) on the 2010 adjustment and the reasons the Task Group decided not to include it are discussed in Sec. 13.2.2. We also note the following fact.

If the least-squares adjustment that leads to the value of α given in Eq. (88) is carried out with the value in Eq. (97) added as an input datum, the result is $\alpha^{-1} = 137.035\,881(35)$ $[2.6 \times 10^{-7}]$, which differs from the 2010 recommended value by 3.4σ. The value of R_∞ from this adjustment is $10\,973\,731.568\,016(49)$ m^{-1}.

4.2. Antiprotonic helium transition frequencies and A_r(e)

Consisting of a ^{4}He or a ^{3}He nucleus, an antiproton, and an electron, the antiprotonic helium atom is a three-body system denoted by $\bar{p}He^+$. Because it is assumed that *CPT* is a valid symmetry, determination of the antiproton-electron mass ratio from antiprotonic helium experiments can be interpreted as determination of the proton-electron mass ratio. Further, because the relative atomic mass of the proton A_r(p) is known with a significantly smaller relative uncertainty from other data than is A_r(e), a value of the antiproton-electron mass ratio with a sufficiently small uncertainty can provide a competitive value of A_r(e).

Theoretical and experimental values of frequencies corresponding to transitions between atomic levels of the antiprotons with large principal quantum number n and angular momentum quantum number l, such that $n \approx l + 1 \approx 38$, were used to obtain a value of A_r(e) in the 2006 adjustment. Table 12 summarizes the relevant experimental and theoretical data. The first column indicates the mass number of the helium nucleus of the antiprotonic atom and the principal and angular momentum quantum numbers of the energy levels involved in the transitions. The second column gives the experimentally measured values of the transition frequencies while the third gives the theoretically calculated values. The last two columns give the values in the unit $2cR_\infty$ of quantities a and b used in the observational equations that relate the experimental values of the transition frequencies to their calculated values and relevant adjusted constants, as discussed in the next section. Besides a few comparatively minor changes in some of the calculated frequencies and their uncertainties, the only significant difference between Table 12 in this report and the corresponding Table XIII in CODATA-06 is the addition of recently acquired data on three two-photon transitions: $(33, 32) \rightarrow (31, 30)$ and $(36, 34) \rightarrow (34, 32)$ for $\bar{p}^4He^+$, and $(35, 33) \rightarrow (33, 31)$ for $\bar{p}^3He^+$.

It is noteworthy that Hori *et al.* (2011), who determined the experimental values of these three frequencies (discussed further in Sec. 4.2.2), have used the new experimental and theoretical data to obtain an important new limit. With the aid of the long-known result that the absolute value of the charge-to-mass ratio of p and $\bar{p}$ are the same within at least 9 parts in 10^{11} (Gabrielse, 2006), they showed that the charge and mass of p and $\bar{p}$ are the same within 7 parts in 10^{10} at the 90% confidence level.

4.2.1. Theory relevant to antiprotonic helium

The calculated transition frequencies in Table 12 are due to Korobov (2008, 2010) and are based on the 2002 recommended values of the required fundamental constants with no uncertainties. Korobov's publication updates some of the values and uncertainties of the calculated transition frequencies used in the 2006 adjustment that he provided directly to the Task Group (Korobov, 2006), but it also includes results for the $\bar{p}^4He^+$ and $\bar{p}^3He^+$ two-photon transition frequencies $(36, 34) \rightarrow (34, 32)$ and $(35, 33) \rightarrow (33, 31)$. The calculated value for the $\bar{p}^4He^+$ two-photon frequency

TABLE 12. Summary of data related to the determination of A_r(e) from measurements of antiprotonic helium. The uncertainties of the 15 calculated values are the root sum square (rss) of the following 15 pairs of uncertainty components in MHz, where the first component reflects the possible size of uncalculated terms of order $R_\infty\alpha^5 \ln\alpha$ and higher, and the second component reflects the uncertainty of the numerical calculations: (0.8, 0.2); (1.0, 0.3); (1.1, 0.3); (1.1, 0.3); (1.1, 0.4); (1.0, 0.8); (1.8, 0.4); (1.6, 0.3); (2.1, 0.3); (0.9, 0.1); (1.1, 0.2); (1.1, 0.4); (1.1, 0.3); (1.8, 0.3); (2.2, 0.2).

Transition $(n, l) \rightarrow (n', l')$	Experimental value (MHz)	Calculated value (MHz)	a $(2cR_\infty)$	b $(2cR_\infty)$
$\bar{p}^4He^+$: $(32, 31) \rightarrow (31, 30)$	1 132 609 209(15)	1 132 609 223.50(82)	0.2179	0.0437
$\bar{p}^4He^+$: $(35, 33) \rightarrow (34, 32)$	804 633 059.0(8.2)	804 633 058.0(1.0)	0.1792	0.0360
$\bar{p}^4He^+$: $(36, 34) \rightarrow (35, 33)$	717 474 004(10)	717 474 001.1(1.1)	0.1691	0.0340
$\bar{p}^4He^+$: $(37, 34) \rightarrow (36, 33)$	636 878 139.4(7.7)	636 878 151.7(1.1)	0.1581	0.0317
$\bar{p}^4He^+$: $(39, 35) \rightarrow (38, 34)$	501 948 751.6(4.4)	501 948 755.6(1.2)	0.1376	0.0276
$\bar{p}^4He^+$: $(40, 35) \rightarrow (39, 34)$	445 608 557.6(6.3)	445 608 569.3(1.3)	0.1261	0.0253
$\bar{p}^4He^+$: $(37, 35) \rightarrow (38, 34)$	412 885 132.2(3.9)	412 885 132.8(1.8)	−0.1640	−0.0329
$\bar{p}^4He^+$: $(33, 32) \rightarrow (31, 30)$	2 145 054 858.2(5.1)	2 145 054 857.9(1.6)	0.4213	0.0846
$\bar{p}^4He^+$: $(36, 34) \rightarrow (34, 32)$	1 522 107 061.8(3.5)	1 522 107 058.9(2.1)	0.3483	0.0699
$\bar{p}^3He^+$: $(32, 31) \rightarrow (31, 30)$	1 043 128 608(13)	1 043 128 579.70(91)	0.2098	0.0524
$\bar{p}^3He^+$: $(34, 32) \rightarrow (33, 31)$	822 809 190(12)	822 809 170.9(1.1)	0.1841	0.0460
$\bar{p}^3He^+$: $(36, 33) \rightarrow (35, 32)$	646 180 434(12)	646 180 408.2(1.2)	0.1618	0.0405
$\bar{p}^3He^+$: $(38, 34) \rightarrow (37, 33)$	505 222 295.7(8.2)	505 222 280.9(1.1)	0.1398	0.0350
$\bar{p}^3He^+$: $(36, 34) \rightarrow (37, 33)$	414 147 507.8(4.0)	414 147 507.8(1.8)	−0.1664	−0.0416
$\bar{p}^3He^+$: $(35, 33) \rightarrow (33, 31)$	1 553 643 099.6(7.1)	1 553 643 100.7(2.2)	0.3575	0.0894

$(33, 32) \rightarrow (31, 30)$ was again provided directly to the Task Group by Korobov (2010), as were slightly updated values for the two other two-photon frequencies. The same calculated values of the three two-photon frequencies are also given by Hori *et al.* (2011).

The quantities $a \equiv a_{\bar{p}\mathrm{He}}(n, l : n', l')$ and $b \equiv b_{\bar{p}\mathrm{He}}(n, l : n', l')$ in Table 12, also directly provided to the Task Group by Korobov (2006, 2010), are actually the numerical values of derivatives defined and used as follows (in these and other similar expressions in this section, He is either ^{3}He or ^{4}He).

The theoretical values of the transition frequencies are functions of the mass ratios $A_r(\bar{p})/A_r(e)$ and $A_r(N)/A_r(\bar{p})$, where N is either $^4He^{2+}$ or $^3He^{2+}$, that is, the alpha particle α or helion h. If the transition frequencies as a function of these mass ratios are denoted by $\nu_{\bar{p}\mathrm{He}}(n, l : n', l')$, and the calculated values in Table 12 by $\nu^{(0)}_{\bar{p}\mathrm{He}}(n, l : n', l')$, we have

$$a_{\bar{p}\mathrm{He}}(n, l : n', l') = \left(\frac{A_r(\bar{p})}{A_r(e)}\right)^{(0)} \frac{\partial \Delta\nu_{\bar{p}\mathrm{He}}(n, l : n', l')}{\partial\left(\dfrac{A_r(\bar{p})}{A_r(e)}\right)}, \quad (98)$$

$$b_{\bar{p}\mathrm{He}}(n, l : n', l') = \left(\frac{A_r(N)}{A_r(\bar{p})}\right)^{(0)} \frac{\partial \Delta\nu_{\bar{p}\mathrm{He}}(n, l : n', l')}{\partial\left(\dfrac{A_r(N)}{A_r(\bar{p})}\right)}, \quad (99)$$

where

$$\Delta\nu_{\bar{p}\mathrm{He}}(n, l : n', l') = \nu_{\bar{p}\mathrm{He}}(n, l : n', l') - \nu^{(0)}_{\bar{p}\mathrm{He}}(n, l : n', l') \quad (100)$$

and the superscript (0) denotes the fact that the 2002 CODATA values of the relative-atomic-mass ratios were used by Korobov in his calculations. The zero-order frequencies, mass ratios, and the derivatives a and b provide a first-order approximation to the transition frequencies as a function of changes in the mass ratios:

$$\begin{aligned}\nu_{\bar{p}\mathrm{He}}(n, l : n', l') = {} & \nu^{(0)}_{\bar{p}\mathrm{He}}(n, l : n', l') + a_{\bar{p}\mathrm{He}}(n, l : n', l') \\ & \times \left[\left(\frac{A_r(e)}{A_r(\bar{p})}\right)^{(0)} \left(\frac{A_r(\bar{p})}{A_r(e)}\right) - 1\right] \\ & + b_{\bar{p}\mathrm{He}}(n, l : n', l') \\ & \times \left[\left(\frac{A_r(\bar{p})}{A_r(N)}\right)^{(0)} \left(\frac{A_r(N)}{A_r(\bar{p})}\right) - 1\right] + \cdots .\end{aligned} \quad (101)$$

This expression is the basis for the observational equations for the measured and calculated transition frequencies as a function of the mass ratios in the least-squares adjustment; see Table 35, Sec. 13. Although $A_r(e)$, $A_r(p)$, and $A_r(N)$ are adjusted constants, the principal effect of including the antiprotonic helium transition frequencies in the adjustment is to provide information about $A_r(e)$. This is because independent data in the adjustment provide values of $A_r(p)$ and $A_r(N)$ with significantly smaller relative uncertainties than the uncertainty of $A_r(e)$.

The uncertainties of the calculated transition frequencies are taken into account by including an additive constant $\delta_{\bar{p}\mathrm{He}}(n, l : n', l')$ in the observational equation for each measured frequency; see Tables 34 and 35 in Sec. 13. The additive constants are adjusted constants and their assigned values are zero with the uncertainties of the theoretical values. They are data items $C1$–$C15$ in Table 22. Moreover, the input data for the additive constants are correlated; their correlation coefficients, calculated from information provided by Korobov (2010), are given in Table 23. (In the 2006 adjustment, the correlations between the ^{4}He and ^{3}He calculated frequencies were omitted.)

4.2.2. Experiments on antiprotonic helium

Recent reviews of the experimental work, which is carried out at the European Center for Nuclear Research (CERN), Geneva, Switzerland, have been given by Hori (2011) and by Hayano (2010). The first seven ^{4}He and the first five ^{3}He experimental transition frequencies in Table 12, obtained by Hori *et al.* (2006), were used in the 2006 adjustment and are discussed in CODATA-06. The measurements were carried out with antiprotons from the CERN antiproton decelerator and employed the technique of single-photon precision laser spectroscopy. The transition frequencies and their uncertainties include an extra digit beyond those reported by Hori *et al.* (2006) that were provided to the Task Group by Hori (2006) to reduce rounding errors.

During the past four years the CERN group has been able to improve their experiment and, as noted above, Hori *et al.* (2011) have recently reported results for three transitions based on two-photon laser spectroscopy. In this work $\bar{p}^4He^+$ or $\bar{p}^3He^+$ atoms are irradiated by two counterpropagating laser beams that excite deep ultraviolet, nonlinear, two-photon transitions of the type $(n, l) \rightarrow (n - 2, l - 2)$. This technique reduces thermal Doppler broadening of the resonances of the antiprotonic atoms, thereby producing narrower spectral lines and reducing the uncertainties of the measured transition frequencies.

In normal two-photon spectroscopy the frequencies of the two counterpropagating laser beams are the same and equal to one-half the resonance frequency. In consequence, to first order in the atom's velocity, Doppler broadening is reduced to zero. However, normal two-photon spectroscopy is difficult to do in antiprotonic helium because of the small transition probabilities of the nonlinear two-photon transitions. The CERN group was able to mitigate this problem by using the fact that the probability can be increased some 5 orders of magnitude if the two beams have different frequencies ν_1 and ν_2 such that the virtual state of the two-photon transition is within approximately 10 GHz of a real state with quantum numbers $(n - 1, l - 1)$ (Hori and Korobov, 2010). In this case the first-order Doppler width of the resonance is reduced by the factor $|\nu_1 - \nu_2|/(\nu_1 + \nu_2)$.

As for the earlier data, an extra digit, provided to the Task Group by Hori (2010), has been added to the three new two-photon frequencies and their uncertainties. Further, as for the one-photon transitions used in 2006, Hori (2010) has provided the Task Group with a detailed uncertainty budget for each of the new frequencies so that their correlation coefficients could be properly evaluated. (There are no correlations between the 12 older one-photon frequencies and the 3 new two-photon frequencies.) As for the one-photon frequencies, the dominant uncertainty component for the two-photon frequencies is statistical; it varies from 3.0 MHz to 6.6 MHz compared to 3.2 MHz to 13.8 MHz for the one-photon frequencies. The 15 transition frequencies are data items $C16-C30$ in Table 22; all relevant correlation coefficients are given in Table 23.

4.2.3. Inferred value of A_r(e) from antiprotonic helium

Use of the 2010 recommended values of $A_r(p)$, $A_r(\alpha)$, and $A_r(h)$, the experimental and theoretical values of the 15 transition frequencies in Table 12, the correlation coefficients in Table 23, and the observational equations in Table 35 derived as discussed above, yields the following inferred value of the electron relative atomic mass:

$$A_r(e) = 0.000\ 548\ 579\ 909\ 14(75) \quad [1.4 \times 10^{-9}]. \tag{102}$$

The $\bar{p}^3$He data alone give a value of $A_r(e)$ that has an uncertainty that is 1.7 times as large as the uncertainty of the value in Eq. (102); and it is smaller by a factor 1.2 times its uncertainty. The combined result is consistent and competitive with other values, as discussed in Sec. 13.

4.3. Hyperfine structure and fine structure

During the past four years two highly accurate values of the fine-structure constant α from dramatically different experiments have become available, one from the electron magnetic-moment anomaly a_e and the other from $h/m(^{87}\mathrm{Rb})$ obtained by atom recoil. They are consistent and have relative standard uncertainties of 3.7×10^{-10} and 6.6×10^{-10}, respectively; see Table 25. These uncertainties imply that for another value of α to be competitive, its relative uncertainty should be no more than about a factor of 10 larger.

By equating the experimentally measured ground-state hyperfine transition frequency of a simple atom such as hydrogen, muonium Mu (μ^+e^- atom), or positronium (e^+e^- atom) to its theoretical expression, one could in principle obtain a value of α, since this frequency is proportional to $\alpha^2 R_\infty c$. Muonium is, however, still the only atom for which both the measured value of the hyperfine frequency and its theoretical expression have sufficiently small uncertainties to be of possible interest, and even for this atom with a structureless nucleus the resulting value of α is no longer competitive; instead, muonium provides the most accurate value of the electron-muon mass ratio, as discussed in Sec. 6.2.

Also proportional to $\alpha^2 R_\infty c$ are fine-structure transition frequencies, and thus in principal these could provide a useful value of α. However, even the most accurate measurements of such frequencies in the relatively simple one-electron atoms hydrogen and deuterium do not provide a competitive value; see Table 11 and Sec. 4.1.1.13, especially Eq. (88). Rather, the experimental hydrogen fine-structure transition frequencies given in that table are included in the 2010 adjustment, as in past adjustments, because of their influence on the adjusted constant R_∞.

The large natural linewidths of the 2P levels in H and D limit the accuracy with which the fine-structure frequencies in these atoms can be measured. By comparison, the 2^3P_J states of ^{4}He are narrow (1.6 MHz vs 100 MHz) because they cannot decay to the ground 1^1S_0 state by allowed electric dipole transitions. Since the energy differences between the three 2^3P levels and the corresponding transition frequencies can be calculated and measured with reasonably small uncertainties, it has long been hoped that the fine structure of ^{4}He could one day provide a competitive value of α. Although the past four years has seen considerable progress toward this goal, it has not yet been reached.

The fine structure of the 2^3P_J triplet state of ^{4}He consists of three levels; they are, from highest to lowest, 2^3P_0, 2^3P_1, and 2^3P_2. The three transition frequencies of interest are $\nu_{01} \approx 29.6$ GHz, $\nu_{12} \approx 2.29$ GHz, and $\nu_{02} \approx 31.9$ GHz. In a series of papers Pachucki (2006), and Pachucki and Yerokhin (2009, 2010, 2011a, 2011b), but see also Pachucki and Sapirstein (2010) and Sapirstein (2010), have significantly advanced the theory of these transitions in both helium and light helium-like ions. Based on this work, the theory is now complete to orders $m\alpha^7$ and $m(m/M)\alpha^6$ (m the electron mass and m/M the electron-alpha particle mass ratio), previous disagreements among calculations have been resolved, and an estimate of uncertainty due to the uncalculated $m\alpha^8$ term has been made. Indeed, the uncertainty of the theoretical expression for the ν_{02} transition, which is the most accurately known both theoretically and experimentally, is estimated to be 1.7 kHz, corresponding to a relative uncertainty of 5.3×10^{-8} or 2.7×10^{-8} for α. Nevertheless, even if an experimental value of ν_{02} with an uncertainty of just a few hertz were available, the uncertainty in the value of α from the helium fine structure would still be too large to be included in the 2010 adjustment.

In fact, the most accurate experimental value of ν_{02} is that measured by Smiciklas and Shiner (2010) with an uncertainty of 300 Hz, corresponding to a relative uncertainty of 9.4×10^{-9} or 4.7×10^{-9} for α. As given by Pachucki and Yerokhin (2011b), the value of α obtained by equating this experimental result and the theoretical result is $\alpha^{-1} = 137.035\ 9996(37)\ [2.7 \times 10^{-8}]$, which agrees well with the two most accurate values mentioned at the start of this section but is not competitive with them.

Another issue is that the agreement among different experimental values of the various helium fine-structure transitions and their agreement with theory is not completely satisfactory. Besides the result of Smiciklas and Shiner (2010) for ν_{02}, there

is the measurement of ν_{12} by Borbely *et al.* (2009), all three frequencies by Zelevinsky, Farkas, and Gabrielse (2005), ν_{01} by Giusfredi *et al.* (2005), ν_{01} by George, Lombardi, and Hessels (2001), ν_{12} by Castillega *et al.* (2000), and ν_{02} by Shiner and Dixson (1995). Graphical comparisons of these data among themselves and with theory may be found in the paper by Smiciklas and Shiner (2010).

In summary, no ^{4}He fine-structure datum is included in the 2010 adjustment, because the resulting value of α has too large an uncertainty compared to the uncertainties of the values from a_e and $h/m(^{87}\mathrm{Rb})$.

5. Magnetic-Moment Anomalies and *g*-Factors

As discussed in CODATA-06, the magnetic moment of any of the three charged leptons $\ell = e, \mu, \tau$ is

$$\boldsymbol{\mu}_\ell = g_\ell \frac{e}{2m_\ell}\boldsymbol{s}, \tag{103}$$

where g_ℓ is the g-factor of the particle, m_ℓ is its mass, and $\boldsymbol{s}$ is its spin. In Eq. (103), e is the (positive) elementary charge. For the negatively charged leptons ℓ^-, g_ℓ is negative. These leptons have eigenvalues of spin projection $s_z = \pm\hbar/2$, so that

$$\mu_\ell = \frac{g_\ell}{2}\frac{e\hbar}{2m_\ell}, \tag{104}$$

and for the electron $\hbar/2m_e = \mu_B$, the Bohr magneton. The magnetic-moment anomaly a_ℓ is defined by

$$|g_\ell| = 2(1 + a_\ell), \tag{105}$$

where the free-electron Dirac equation gives $a_\ell = 0$. In fact, the anomaly is not zero, but is given by

$$a_\ell(\mathrm{th}) = a_\ell(\mathrm{QED}) + a_\ell(\mathrm{weak}) + a_\ell(\mathrm{had}), \tag{106}$$

where the terms denoted by QED, weak, and had account for the purely quantum electrodynamic, predominantly electroweak, and predominantly hadronic (that is, strong interaction) contributions to a_ℓ, respectively.

For a comprehensive review of the theory of a_e, but particularly of a_μ, see Jegerlehner and Nyffeler (2009). It has long been recognized that the comparison of experimental and theoretical values of the electron and muon g-factors can test our description of nature, in particular, the standard model of particle physics, which is the theory of the electromagnetic, weak, and strong interactions. Nevertheless, our main purpose here is not to test physical theory critically, but to obtain "best" values of the fundamental constants.

5.1. Electron magnetic-moment anomaly a_e and the fine-structure constant α

Comparison of theory and experiment for the electron magnetic-moment anomaly gives the value for the fine-structure constant α with the smallest estimated uncertainty in the 2010 adjustment.

5.1.1. Theory of a_e

The QED contribution for the electron may be written as (Kinoshita, Nizic, and Okamoto, 1990)

$$a_e(\mathrm{QED}) = A_1 + A_2(m_e/m_\mu) + A_2(m_e/m_\tau) + A_3(m_e/m_\mu, m_e/m_\tau). \tag{107}$$

The leading term A_1 is mass independent and the masses in the denominators of the ratios in A_2 and A_3 correspond to particles in vacuum-polarization loops.

Each of the four terms on the right-hand side of Eq. (107) is expressed as a power series in the fine-structure constant α:

$$A_i = A_i^{(2)}\left(\frac{\alpha}{\pi}\right) + A_i^{(4)}\left(\frac{\alpha}{\pi}\right)^2 + A_i^{(6)}\left(\frac{\alpha}{\pi}\right)^3 + A_i^{(8)}\left(\frac{\alpha}{\pi}\right)^4 + A_i^{(10)}\left(\frac{\alpha}{\pi}\right)^5 + \cdots, \tag{108}$$

where $A_2^{(2)} = A_3^{(2)} = A_3^{(4)} = 0$. Coefficients proportional to $(\alpha/\pi)^n$ are of order e^{2n} and are referred to as $2n$th-order coefficients. For $i = 1$, the second-order coefficient is known exactly, and the fourth- and sixth-order coefficients are known analytically in terms of readily evaluated functions:

$$A_1^{(2)} = \frac{1}{2}, \tag{109}$$

$$A_1^{(4)} = -0.328\,478\,965\,579\ldots, \tag{110}$$

$$A_1^{(6)} = 1.181\,241\,456\ldots. \tag{111}$$

The eighth-order coefficient $A_1^{(8)}$ arises from 891 Feynman diagrams of which only a few are known analytically. Evaluation of this coefficient numerically by Kinoshita and co-workers has been underway for many years (Kinoshita, 2010). The value used in the 2006 adjustment is $A_1^{(8)} = -1.7283(35)$ as reported by Kinoshita and Nio (2006). However, and as discussed in CODATA-06, well after the 31 December 2006 closing date of the 2006 adjustment, as well as the date when the 2006 CODATA recommended values of the constants were made public, it was discovered by Aoyama *et al.* (2007) that a significant error had been made in the calculation. In particular, 2 of the 47 integrals representing 518 diagrams that had not been confirmed independently required a corrected treatment of infrared divergences. The error was identified by using FORTRAN code generated by an automatic code generator. The new value is (Aoyama *et al.*, 2007)

$$A_1^{(8)} = -1.9144(35); \tag{112}$$

details of the calculation are given by Aoyama *et al.* (2008). In view of the extensive effort made by these workers to ensure that the result in Eq. (112) is reliable, the Task Group adopts both its value and quoted uncertainty for use in the 2010 adjustment.

Independent work is in progress on analytic calculations of eighth-order integrals; see, for example, Laporta (2001, 2008), Mastrolia and Remiddi (2001), and Laporta, Mastrolia, and

Remiddi (2004). Work is also in progress on numerical calculations of the 12 672 Feynman diagrams for the tenth-order coefficient; see Aoyama *et al.* (2011) and references cited therein.

The evaluation of the contribution to the uncertainty of a_e(th) from the fact that $A_1^{(10)}$ is unknown follows the procedure in CODATA-98 and yields $A_1^{(10)} = 0.0(4.6)$, which contributes a standard uncertainty component to a_e(th) of $2.7 \times 10^{-10} a_e$. This uncertainty is larger than the uncertainty attributed to $A_1^{(10)}$ in CODATA-06, because the absolute value of $A_1^{(8)}$ has increased. All higher-order coefficients are assumed to be negligible.

The mass-dependent coefficients for the electron based on the 2010 recommended values of the mass ratios are

$$A_2^{(4)}(m_e/m_\mu) = 5.197\,386\,68(26) \times 10^{-7} \rightarrow 24.182 \times 10^{-10} a_e, \tag{113}$$

$$A_2^{(4)}(m_e/m_\tau) = 1.837\,98(33) \times 10^{-9} \rightarrow 0.086 \times 10^{-10} a_e, \tag{114}$$

$$A_2^{(6)}(m_e/m_\mu) = -7.373\,941\,62(27) \times 10^{-6} \rightarrow -0.797 \times 10^{-10} a_e, \tag{115}$$

$$A_2^{(6)}(m_e/m_\tau) = -6.5830(11) \times 10^{-8} \rightarrow -0.007 \times 10^{-10} a_e, \tag{116}$$

where the standard uncertainties of the coefficients are due to the uncertainties of the mass ratios and are negligible. The contributions from $A_3^{(6)}(m_e/m_\mu, m_e/m_\tau)$ and all higher-order mass-dependent terms are also negligible.

The dependence on α of any contribution other than a_e(QED) is negligible, hence the anomaly as a function of α is given by combining QED terms that have like powers of α/π:

$$a_e(\text{QED}) = C_e^{(2)}\left(\frac{\alpha}{\pi}\right) + C_e^{(4)}\left(\frac{\alpha}{\pi}\right)^2 + C_e^{(6)}\left(\frac{\alpha}{\pi}\right)^3 + C_e^{(8)}\left(\frac{\alpha}{\pi}\right)^4 + C_e^{(10)}\left(\frac{\alpha}{\pi}\right)^5 + \cdots, \tag{117}$$

with

$$\begin{aligned} C_e^{(2)} &= 0.5, \\ C_e^{(4)} &= -0.328\,478\,444\,00, \\ C_e^{(6)} &= 1.181\,234\,017, \\ C_e^{(8)} &= -1.9144(35), \\ C_e^{(10)} &= 0.0(4.6). \end{aligned} \tag{118}$$

The electroweak contribution, calculated as in CODATA-98 but with the 2010 values of G_F and $\sin^2\theta_W$, is

$$a_e(\text{weak}) = 0.029\,73(52) \times 10^{-12} = 0.2564(45) \times 10^{-10} a_e. \tag{119}$$

The hadronic contribution can be written as

$$a_e(\text{had}) = a_e^{(4)}(\text{had}) + a_e^{(6a)}(\text{had}) + a_e^{(\gamma\gamma)}(\text{had}) + \cdots, \tag{120}$$

where $a_e^{(4)}$(had) and $a_e^{(6a)}$(had) are due to hadronic vacuum polarization and are of order $(\alpha/\pi)^2$ and $(\alpha/\pi)^3$, respectively; also of order $(\alpha/\pi)^3$ is $a_\mu^{(\gamma\gamma)}$, which is due to light-by-light vacuum polarization. The total value

$$a_e(\text{had}) = 1.685(22) \times 10^{-12} = 1.453(19) \times 10^{-9} a_e \tag{121}$$

is the sum of the following three contributions: $a_e^{(4)}(\text{had}) = 1.875(18) \times 10^{-12}$ obtained by Davier and Höcker (1998); $a_e^{(6a)}(\text{had}) = -0.225(5) \times 10^{-12}$ given by Krause (1997); and $a_e^{(\gamma\gamma)}(\text{had}) = 0.035(10) \times 10^{-12}$ as given by Prades, de Rafael, and Vainshtein (2010). In past adjustments this contribution was calculated by assuming that $a_e^{(\gamma\gamma)} = (m_e/m_\mu)^2 a_\mu^{(\gamma\gamma)}(\text{had})$. However, Prades, de Rafael, and Vainshtein (2010) have shown that such scaling is not adequate for the neutral pion exchange contribution to $a_\mu^{(\gamma\gamma)}$(had) and have taken this into account in obtaining their above result for $a_e^{(\gamma\gamma)}$(had) from their muon value $a_\mu^{(\gamma\gamma)}(\text{had}) = 105(26) \times 10^{-11}$.

The theoretical prediction is

$$a_e(\text{th}) = a_e(\text{QED}) + a_e(\text{weak}) + a_e(\text{had}). \tag{122}$$

The various contributions can be put into context by comparing them to the most accurate experimental value of a_e currently available, which has an uncertainty of $2.8 \times 10^{-10} a_e$; see Eq. (126).

The standard uncertainty of a_e(th) from the uncertainties of the terms listed above is

$$u[a_e(\text{th})] = 0.33 \times 10^{-12} = 2.8 \times 10^{-10} a_e \tag{123}$$

and is dominated by the uncertainty of the coefficient $C_e^{(10)}$.

For the purpose of the least-squares calculations carried out in Sec. 13, we include an additive correction δ_e to a_e(th) to account for the uncertainty of a_e(th) other than that due to α, and hence the complete theoretical expression in the observational equation for the electron anomaly ($B13$ in Table 33) is

$$a_e(\alpha, \delta_e) = a_e(\text{th}) + \delta_e. \tag{124}$$

The input datum for δ_e is zero with standard uncertainty $u[a_e(\text{th})]$, or $0.00(33) \times 10^{-12}$, which is data item $B12$ in Table 20.

5.1.2. Measurements of a_e

5.1.2.1. University of Washington

The classic series of measurements of the electron and positron anomalies carried out at the University of Washington by Van Dyck, Jr., Schwinberg, and Dehmelt (1987) yield the value

$$a_e = 1.159\ 652\ 1883(42) \times 10^{-3} \quad [3.7 \times 10^{-9}], \tag{125}$$

as discussed in CODATA-98. This result, which assumes that *CPT* invariance holds for the electron-positron system, is data item *B*13.1 in Table 20.

5.1.2.2. Harvard University

In both the University of Washington and Harvard University, Cambridge, MA, USA experiments, the electron magnetic-moment anomaly is essentially determined from the relation $a_e = f_a/f_c$ by measuring in the same magnetic flux density $B \approx 5$ T the anomaly difference frequency $f_a = f_s - f_c$ and cyclotron frequency $f_c = eB/2\pi m_e$, where $f_s = |g_e|\mu_B B/h$ is the electron spin-flip (or precession) frequency.

Because of its small relative standard uncertainty of 7.6×10^{-10}, the then new result for a_e obtained by Odom *et al.* (2006) at Harvard using a cylindrical rather than a hyperbolic Penning trap played the dominant role in determining the 2006 recommended value of α. This work continued with a number of significant improvements and a new value of a_e consistent with the earlier one but with an uncertainty nearly a factor of 3 smaller was reported by Hanneke, Fogwell, and Gabrielse (2008):

$$a_e = 1.159\,652\,180\,73(28) \times 10^{-3}. \tag{126}$$

A paper that describes this measurement in detail was subsequently published by Hanneke, Fogwell Hoogerheide, and Gabrielse (2011) [see also the review by Gabrielse (2010)]. As discussed by Hanneke, Fogwell Hoogerheide, and Gabrielse (2011), the improvement that contributed most to the reduction in uncertainty is a better understanding of the Penning-trap cavity frequency shifts of the radiation used to measure f_c. A smaller reduction resulted from narrower linewidths of the anomaly and cyclotron resonant frequencies. Consequently, Hanneke, Fogwell Hoogerheide, and Gabrielse (2011) state that their 2008 result should be viewed as superseding the earlier Harvard result. Therefore, only the value of a_e in Eq. (126) is included as an input datum in the 2010 adjustment; it is data item *B*13.2 in Table 20.

5.1.3. Values of α inferred from a_e

Equating the theoretical expression with the two experimental values of a_e given in Eqs. (125) and (126) yields

$$\alpha^{-1}(a_e) = 137.035\,998\,19(50) \quad [3.7 \times 10^{-9}] \tag{127}$$

from the University of Washington result and

$$\alpha^{-1}(a_e) = 137.035\,999\,084(51) \quad [3.7 \times 10^{-10}] \tag{128}$$

from the Harvard University result. The contribution of the uncertainty in a_e(th) to the relative uncertainty of either of these results is 2.8×10^{-10}. The value in Eq. (128) has the smallest uncertainty of any value of alpha currently available. The fact that the next most accurate value of α, which has a relative standard uncertainty of 6.6×10^{-10} and is obtained from the quotient $h/m(^{87}\mathrm{Rb})$ measured by atom recoil, is consistent with this value suggests that the theory of a_e is well in hand; see Sec. 13.

5.2. Muon magnetic-moment anomaly a_μ

The 2006 adjustment included data that provided both an experimental value and a theoretical value for a_μ. Because of problems with the theory, the uncertainty assigned to the theoretical value was over 3 times larger than that of the experimental value. Nevertheless, the theoretical value with its increased uncertainty was included in the adjustment, even if with a comparatively small weight.

For the 2010 adjustment, the Task Group decided not to include the theoretical value for a_μ, with the result that the 2010 recommended value is based mainly on experiment. This is consistent with the fact that the value of a_μ recommended by the Particle Data Group in their biennial 2010 *Review of Particle Physics* (Nakamura *et al.*, 2010) is the experimental value. The current situation is briefly summarized in the following sections.

5.2.1. Theory of a_μ

The mass-independent coefficients $A_1^{(n)}$ for the muon are the same as for the electron. Based on the 2010 recommended values of the mass ratios, the relevant mass-dependent terms are

$$A_2^{(4)}(m_\mu/m_e) = 1.094\,258\,3118(81) \rightarrow 506\,386.4620(38) \times 10^{-8} a_\mu, \tag{129}$$

$$A_2^{(4)}(m_\mu/m_\tau) = 0.000\,078\,079(14) \rightarrow 36.1325(65) \times 10^{-8} a_\mu, \tag{130}$$

$$A_2^{(6)}(m_\mu/m_e) = 22.868\,380\,04(19) \rightarrow 24\,581.766\,56(20) \times 10^{-8} a_\mu, \tag{131}$$

$$A_2^{(6)}(m_\mu/m_\tau) = 0.000\,360\,63(11) \rightarrow 0.387\,65(12) \times 10^{-8} a_\mu, \tag{132}$$

$$A_2^{(8)}(m_\mu/m_e) = 132.6823(72) \rightarrow 331.288(18) \times 10^{-8} a_\mu, \quad (133)$$

$$A_2^{(10)}(m_\mu/m_e) = 663(20) \rightarrow 3.85(12) \times 10^{-8} a_\mu, \quad (134)$$

$$A_3^{(6)}(m_\mu/m_e, m_\mu/m_\tau) = 0.000\,527\,762(94) \rightarrow 0.567\,30(10) \times 10^{-8} a_\mu, \quad (135)$$

$$A_3^{(8)}(m_\mu/m_e, m_\mu/m_\tau) = 0.037\,594(83) \rightarrow 0.093\,87(21) \times 10^{-8} a_\mu. \quad (136)$$

The QED contribution to the theory of a_μ, where terms that have like powers of α/π are combined, is

$$a_\mu(\mathrm{QED}) = C_\mu^{(2)}\left(\frac{\alpha}{\pi}\right) + C_\mu^{(4)}\left(\frac{\alpha}{\pi}\right)^2 + C_\mu^{(6)}\left(\frac{\alpha}{\pi}\right)^3 + C_\mu^{(8)}\left(\frac{\alpha}{\pi}\right)^4 + C_\mu^{(10)}\left(\frac{\alpha}{\pi}\right)^5 + \cdots, \quad (137)$$

with

$$C_\mu^{(2)} = 0.5,$$
$$C_\mu^{(4)} = 0.765\,857\,426(16),$$
$$C_\mu^{(6)} = 24.050\,509\,88(28),$$
$$C_\mu^{(8)} = 130.8055(80),$$
$$C_\mu^{(10)} = 663(21), \quad (138)$$

which yields, using the 2010 recommended value of α,

$$a_\mu(\mathrm{QED}) = 0.001\,165\,847\,1810(15) \quad [1.3 \times 10^{-9}]. \quad (139)$$

In absolute terms, the uncertainty in $a_\mu(\mathrm{QED})$ is 0.15×10^{-11}.

The current theoretical expression for the muon anomaly is of the same form as for the electron:

$$a_\mu(\mathrm{th}) = a_\mu(\mathrm{QED}) + a_\mu(\mathrm{weak}) + a_\mu(\mathrm{had}). \quad (140)$$

The electroweak contribution, calculated by Czarnecki *et al.* (2003), is $a_\mu(\mathrm{weak}) = 154(2) \times 10^{-11}$. In contrast to the case of the electron, $a_\mu(\mathrm{weak})$ is a significant contribution compared to $a_\mu(\mathrm{QED})$.

In a manner similar to that for the electron, the hadronic contribution can be written as

$$a_\mu(\mathrm{had}) = a_\mu^{(4)}(\mathrm{had}) + a_\mu^{(6a)}(\mathrm{had}) + a_\mu^{(\gamma\gamma)}(\mathrm{had}) + \cdots. \quad (141)$$

It is also of much greater importance for the muon than for the electron. Indeed, $a_\mu(\mathrm{had})$ is roughly $7000(50) \times 10^{-11}$, which should be compared with the 63×10^{-11} uncertainty of the experimental value $a_\mu(\mathrm{exp})$ discussed in the next section.

For well over a decade a great deal of effort has been devoted by many researchers to the improved evaluation of $a_\mu(\mathrm{had})$. The standard method of calculating $a_\mu^{(4)}(\mathrm{had})$ and $a_\mu^{(6a)}(\mathrm{had})$ is to evaluate dispersion integrals over experimentally measured cross sections for the scattering of e^+e^- into hadrons. However, in some calculations data on decays of the τ into hadrons are used to replace the e^+e^- data in certain energy regions. The results of three evaluations which include the most recent data can be concisely summarized as follows.

Davier *et al.* (2011) find that $a_\mu(\mathrm{exp})$ exceeds their theoretically predicted value $a_\mu(\mathrm{th})$ by 3.6 times the combined standard uncertainty of the difference, or 3.6σ, using only e^+e^- data, and by 2.4σ if τ data are included. On the other hand, Jegerlehner and Szafron (2011) find that by correcting the τ data for the effect they term ρ–γ mixing, the values of $a_\mu^{(4)}(\mathrm{had})$ obtained from only e^+e^- data, and from e^+e^- and τ data together, are nearly identical and that the difference between experiment and theory is 3.3σ. And Hagiwara *et al.* (2011) find the same 3.3σ difference using e^+e^- data alone. Finally, we note that in a very recent paper, Benayoun *et al.* (2012) obtain a difference in the range 4.07σ to 4.65σ, depending on the assumptions made, using a "hidden local symmetry" model.

The disagreement between experiment and theory has long been known and numerous theoretical papers have been published that attempt to explain the discrepancy in terms of new physics; see Stöckinger (2010). Although a contribution to $a_\mu(\mathrm{th})$ large enough to bring it into agreement with $a_\mu(\mathrm{exp})$ from physics beyond the standard model is possible, no outside experimental evidence currently exists for such physics. Thus, because of the persistence of the discrepancy and its confirmation by the most recent calculations, and because no known physics has yet been able to eliminate it, the Task Group has decided to omit the theory of a_μ from the 2010 adjustment.

5.2.2. Measurement of a_μ: Brookhaven

Experiment E821 at Brookhaven National Laboratory (BNL), Upton, New York, USA, has been discussed in the past three CODATA reports. It involves the direct measurement of the anomaly difference frequency $f_a = f_s - f_c$, where $f_s = |g_\mu|(e\hbar/2m_\mu)B/h$ is the muon spin-flip (or precession) frequency in the applied magnetic flux density B and $f_c = eB/2\pi m_\mu$ is the corresponding muon cyclotron frequency. However, in contrast to the case of the electron where both f_a and f_c are measured directly and the electron anomaly is calculated from $a_e = f_a/f_c$, for the muon B is eliminated by determining its value from proton nuclear magnetic resonance (NMR) measurements. This means that the muon anomaly is calculated from

$$a_\mu(\mathrm{exp}) = \frac{\bar{R}}{|\mu_\mu/\mu_p| - \bar{R}}, \quad (142)$$

where $\bar{R} = f_a/\bar{f}_p$ and $\bar{f}_p$ is the free proton NMR frequency corresponding to the average flux density B seen by the muons in their orbits in the muon storage ring.

The final value of $\bar{R}$ obtained in the E821 experiment is (Bennett *et al.*, 2006)

$$\bar{R} = 0.003\,707\,2063(20), \tag{143}$$

which is used as an input datum in the 2010 adjustment and is data item $B14$ in Table 20. [The last digit of this value is 1 less than that of the value used in 2006, because the 2006 value was taken from Eq. (57) in the paper by Bennett *et al.* (2006) but the correct value is that given in Table 15 (Roberts, 2009).] Based on this value of $\bar{R}$, Eq. (142), and the 2010 recommended value of μ_μ/μ_p, whose uncertainty is negligible in this context, the experimental value of the muon anomaly is

$$a_\mu(\text{exp}) = 1.165\,920\,91(63) \times 10^{-3}. \tag{144}$$

Further, with the aid of Eq. (230), the equation for $\bar{R}$ can be written as

$$\bar{R} = -\frac{a_\mu}{1 + a_e(\alpha, \delta_e)}\frac{m_e}{m_\mu}\frac{\mu_{e^-}}{\mu_p}, \tag{145}$$

where use has been made of the relations $g_e = -2(1 + a_e)$, $g_\mu = -2(1 + a_\mu)$, and a_e is replaced by the theoretical expression $a_e(\alpha, \delta_e)$ given in Eq. (106). However, since the theory of a_μ is omitted from the 2010 adjustment, a_μ is not replaced in Eq. (145) by a theoretical expression, rather it is made to be an adjusted constant.

5.3. Bound-electron *g*-factor in $^{12}C^{5+}$ and in $^{16}O^{7+}$ and $A_r(e)$

Competitive values of $A_r(e)$ can be obtained from precise measurements and theoretical calculations of the g-factor of the electron in hydrogenic ^{12}C and ^{16}O.

For a ground-state hydrogenic ion $^AX^{(Z-1)+}$ with mass number A, atomic number (proton number) Z, nuclear spin quantum number $i = 0$, and g-factor $g_{e^-}(^AX^{(Z-1)+})$ in an applied magnetic flux density B, the ratio of the electron's spin-flip (or precession) frequency $f_s = |g_{e^-}(^AX^{(Z-1)+})|(e\hbar/2m_e)B/h$ to the cyclotron frequency of the ion $f_c = (Z-1)eB/2\pi\, m(^AX^{(Z-1)+})$ in the same magnetic flux density is

$$\frac{f_s(^AX^{(Z-1)+})}{f_c(^AX^{(Z-1)+})} = -\frac{g_{e^-}(^AX^{(Z-1)+})}{2(Z-1)}\frac{A_r(^AX^{(Z-1)+})}{A_r(e)}, \tag{146}$$

where $A_r(X)$ is the relative atomic mass of particle X.

This expression can be used to obtain a competitive result for $A_r(e)$ if for a particular ion the quotient f_s/f_c, its bound-state g-factor, and the relative atomic mass of the ion can be obtained with sufficiently small uncertainties. In fact, work underway since the mid-1990s has been so successful that Eq. (146) now provides the most accurate values of $A_r(e)$. Measurements of f_s/f_c for $^{12}C^{5+}$ and $^{16}O^{7+}$, performed at the Gesellschaft für Schwerionenforschung, Darmstadt, Germany (GSI) by GSI and University of Mainz researchers, are discussed in CODATA-06 and the results were included in the 2006 adjustment. These data are recalled in Sec. 5.3.2, and the present status of the theoretical expressions for the bound-state g-factors of the two ions are discussed in the following section.

For completeness, we note that well after the closing date of the 2010 adjustment Sturm *et al.* (2011) reported a value of f_s/f_c for the hydrogenic ion $^{28}Si^{13+}$. Using the 2006 recommended value of $A_r(e)$ and the applicable version of Eq. (146), they found good agreement between the theoretical and experimental values of the g-factor of this ion, thereby strengthening confidence in our understanding of bound-state QED theory.

5.3.1. Theory of the bound electron *g*-factor

The energy of a free electron with spin projection s_z in a magnetic flux density B in the z direction is

$$E = -\boldsymbol{\mu}\cdot\boldsymbol{B} = -g_{e^-}\frac{e}{2m_e}s_z B, \tag{147}$$

and hence the spin-flip energy difference is

$$\Delta E = -g_{e^-}\mu_B B. \tag{148}$$

(In keeping with the definition of the g-factor in Sec. 5, the quantity g_{e^-} is negative.) The analogous expression for ions with no nuclear spin is

$$\Delta E_b(X) = -g_{e^-}(X)\mu_B B, \tag{149}$$

which defines the bound-state electron g-factor, and where X is either $^{12}C^{5+}$ or $^{16}O^{7+}$.

The theoretical expression for $g_{e^-}(X)$ is written as

$$g_{e^-}(X) = g_D + \Delta g_{rad} + \Delta g_{rec} + \Delta g_{ns} + \cdots, \tag{150}$$

where the individual terms are the Dirac value, the radiative corrections, the recoil corrections, and the nuclear-size corrections, respectively. Numerical results are summarized in Tables 13 and 14.

TABLE 13. Theoretical contributions and total for the g-factor of the electron in hydrogenic carbon 12 based on the 2010 recommended values of the constants.

Contribution	Value	Source
Dirac g_D	−1.998 721 354 390 9(8)	Eq. (151)
$\Delta g_{SE}^{(2)}$	−0.002 323 672 436(4)	Eq. (159)
$\Delta g_{VP}^{(2)}$	0.000 000 008 512(1)	Eq. (162)
$\Delta g^{(4)}$	0.000 003 545 677(25)	Eq. (166)
$\Delta g^{(6)}$	−0.000 000 029 618	Eq. (168)
$\Delta g^{(8)}$	0.000 000 000 111	Eq. (169)
$\Delta g^{(10)}$	0.000 000 000 000(1)	Eq. (170)
Δg_{rec}	−0.000 000 087 629	Eqs. (171)–(173)
Δg_{ns}	−0.000 000 000 408(1)	Eq. (175)
$g_{e^-}(^{12}C^{5+})$	−2.001 041 590 181(26)	Eq. (176)

TABLE 14. Theoretical contributions and total for the g-factor of the electron in hydrogenic oxygen 16 based on the 2010 recommended values of the constants.

Contribution	Value	Source
Dirac g_D	−1.997 726 003 06	Eq. (151)
$\Delta g^{(2)}_{SE}$	−0.002 324 442 14(1)	Eq. (159)
$\Delta g^{(2)}_{VP}$	0.000 000 026 38	Eq. (162)
$\Delta g^{(4)}$	0.000 003 546 54(11)	Eq. (166)
$\Delta g^{(6)}$	−0.000 000 029 63	Eq. (168)
$\Delta g^{(8)}$	0.000 000 000 11	Eq. (169)
$\Delta g^{(10)}$	0.000 000 000 00	Eq. (170)
Δg_{rec}	−0.000 000 117 00	Eqs. (171)–(173)
Δg_{ns}	−0.000 000 001 56(1)	Eq. (175)
$g_{e^-}(^{16}O^{7+})$	−2.000 047 020 35(11)	Eq. (176)

Breit (1928) obtained the exact value

$$g_D = -\frac{2}{3}\left[1 + 2\sqrt{1-(Z\alpha)^2}\right] = -2\left[1 - \frac{1}{3}(Z\alpha)^2 - \frac{1}{12}(Z\alpha)^4 - \frac{1}{24}(Z\alpha)^6 + \cdots\right] \tag{151}$$

from the Dirac equation for an electron in the field of a fixed point charge of magnitude Ze, where the only uncertainty is that due to the uncertainty in α.

For the radiative corrections we have

$$\Delta g_{rad} = -2\left[C_e^{(2)}(Z\alpha)\left(\frac{\alpha}{\pi}\right) + C_e^{(4)}(Z\alpha)\left(\frac{\alpha}{\pi}\right)^2 + \cdots\right], \tag{152}$$

where

$$\lim_{Z\alpha\to 0} C_e^{(2n)}(Z\alpha) = C_e^{(2n)}, \tag{153}$$

and where the $C_e^{(2n)}$ are given in Eq. (118).

For the coefficient $C_e^{(2)}(Z\alpha)$, we have (Faustov, 1970; Grotch, 1970; Close and Osborn, 1971; Pachucki *et al.*, 2004, 2005)

$$C^{(2)}_{e,SE}(Z\alpha) = \frac{1}{2}\left\{1 + \frac{(Z\alpha)^2}{6} + (Z\alpha)^4\left[\frac{32}{9}\ln(Z\alpha)^{-2} + \frac{247}{216} - \frac{8}{9}\ln k_0 - \frac{8}{3}\ln k_3\right] + (Z\alpha)^5 R_{SE}(Z\alpha)\right\}, \tag{154}$$

where

$$\ln k_0 = 2.984\,128\,556, \tag{155}$$

$$\ln k_3 = 3.272\,806\,545, \tag{156}$$

$$R_{SE}(6\alpha) = 22.160(10), \tag{157}$$

$$R_{SE}(8\alpha) = 21.859(4). \tag{158}$$

The quantity $\ln k_0$ is the Bethe logarithm for the 1S state (see Table 5), $\ln k_3$ is a generalization of the Bethe logarithm, and $R_{SE}(Z\alpha)$ was obtained by extrapolation of the results of numerical calculations at higher Z (Yerokhin, Indelicato, and Shabaev, 2002; Pachucki *et al.*, 2004). Equation (154) yields

$$C^{(2)}_{e,SE}(6\alpha) = 0.500\,183\,606\,65(80),$$
$$C^{(2)}_{e,SE}(8\alpha) = 0.500\,349\,2887(14). \tag{159}$$

The one-loop self energy has been calculated directly at $Z = 6$ and $Z = 8$ by Yerokhin and Jentschura (2008, 2010). The results are in agreement with, but less accurate than the extrapolation from higher Z.

The lowest-order vacuum-polarization correction consists of a wave-function correction and a potential correction, each of which can be separated into a lowest-order Uehling potential contribution and a Wichmann-Kroll higher contribution. The wave-function correction is (Beier *et al.*, 2000; Karshenboim, 2000; Karshenboim, Ivanov, and Shabaev, 2001a, 2001b)

$$C^{(2)}_{e,VPwf}(6\alpha) = -0.000\,001\,840\,3431(43),$$
$$C^{(2)}_{e,VPwf}(8\alpha) = -0.000\,005\,712\,028(26). \tag{160}$$

For the potential correction, we have (Beier, 2000; Beier *et al.*, 2000; Karshenboim and Milstein, 2002; Lee *et al.*, 2005; Mohr and Taylor, 2005)

$$C^{(2)}_{e,VPp}(6\alpha) = 0.000\,000\,008\,08(12),$$
$$C^{(2)}_{e,VPp}(8\alpha) = 0.000\,000\,033\,73(50), \tag{161}$$

which is the unweighted average of two slightly inconsistent results with an uncertainty of half their difference. The total one-photon vacuum-polarization coefficients are given by the sum of Eqs. (160) and (161):

$$C^{(2)}_{e,VP}(6\alpha) = C^{(2)}_{e,VPwf}(6\alpha) + C^{(2)}_{e,VPp}(6\alpha) = -0.000\,001\,832\,26(12),$$
$$C^{(2)}_{e,VP}(8\alpha) = C^{(2)}_{e,VPwf}(8\alpha) + C^{(2)}_{e,VPp}(8\alpha) = -0.000\,005\,678\,30(50). \tag{162}$$

The total one-photon coefficient is the sum of Eqs. (159) and (162):

$$C^{(2)}_{e}(6\alpha) = C^{(2)}_{e,SE}(6\alpha) + C^{(2)}_{e,VP}(6\alpha) = 0.500\,181\,774\,39(81),$$
$$C^{(2)}_{e}(8\alpha) = C^{(2)}_{e,SE}(8\alpha) + C^{(2)}_{e,VP}(8\alpha) = 0.500\,343\,6104(14), \tag{163}$$

and the total one-photon contribution is

$$\Delta g^{(2)} = -2C^{(2)}_e(Z\alpha)\left(\frac{\alpha}{\pi}\right) = -0.002\,323\,663\,924(4) \quad \text{for } Z = 6$$
$$= -0.002\,324\,415\,756(7) \quad \text{for } Z = 8. \tag{164}$$

Separate one-photon self energy and vacuum-polarization contributions to the g-factor are given in Tables 13 and 14.

The leading binding correction to the higher-order coefficients is (Eides and Grotch, 1997a; Czarnecki, Melnikov, and Yelkhovsky, 2000)

$$C_e^{(2n)}(Z\alpha) = C_e^{(2n)}\left(1 + \frac{(Z\alpha)^2}{6} + \cdots\right). \tag{165}$$

The two-loop contribution of relative order $(Z\alpha)^4$ for the ground S state is (Pachucki *et al.*, 2005; Jentschura *et al.*, 2006)

$$\begin{aligned} C_e^{(4)}(Z\alpha) &= C_e^{(4)}\left(1 + \frac{(Z\alpha)^2}{6}\right) + (Z\alpha)^4\left[\frac{14}{9}\ln(Z\alpha)^{-2}\right. \\ &\quad + \frac{991\,343}{155\,520} - \frac{2}{9}\ln k_0 - \frac{4}{3}\ln k_3 + \frac{679\pi^2}{12\,960} \\ &\quad \left. - \frac{1441\pi^2}{720}\ln 2 + \frac{1441}{480}\zeta(3)\right] + \mathcal{O}(Z\alpha)^5 \\ &= -0.328\,5778(23) \quad \text{for } Z = 6 \\ &= -0.328\,6578(97) \quad \text{for } Z = 8, \end{aligned} \tag{166}$$

where $\ln k_0$ and $\ln k_3$ are given in Eqs. (155) and (156). As in CODATA-06, the uncertainty due to uncalculated terms is taken to be (Pachucki *et al.*, 2005)

$$u\left[C_e^{(4)}(Z\alpha)\right] = 2|(Z\alpha)^5 C_e^{(4)} R_{SE}(Z\alpha)|. \tag{167}$$

Jentschura (2009) has calculated a two-loop gauge-invariant set of vacuum-polarization diagrams to obtain a contribution of the same order in $Z\alpha$ as the above uncertainty. However, in general we do not include partial results of a given order. Jentschura also speculates that the complete term of that order could be somewhat larger than our uncertainty.

The three- and four-photon terms are calculated with the leading binding correction included:

$$\begin{aligned} C_e^{(6)}(Z\alpha) &= C_e^{(6)}\left(1 + \frac{(Z\alpha)^2}{6} + \cdots\right) \\ &= 1.181\,611\ldots \quad \text{for } Z = 6 \\ &= 1.181\,905\ldots \quad \text{for } Z = 8, \end{aligned} \tag{168}$$

where $C_e^{(6)} = 1.181\,234\ldots$, and

$$\begin{aligned} C_e^{(8)}(Z\alpha) &= C_e^{(8)}\left(1 + \frac{(Z\alpha)^2}{6} + \cdots\right) \\ &= -1.9150(35)\ldots \quad \text{for } Z = 6 \\ &= -1.9155(35)\ldots \quad \text{for } Z = 8, \end{aligned} \tag{169}$$

where $C_e^{(8)} = -1.9144(35)$. An uncertainty estimate

$$C_e^{(10)}(Z\alpha) \approx C_e^{(10)} = 0.0(4.6) \tag{170}$$

is included for the five-loop correction.

The recoil correction to the bound-state g-factor is $\Delta g_{rec} = \Delta g_{rec}^{(0)} + \Delta g_{rec}^{(2)} + \cdots$ where the terms on the right are zero order and first order in α/π, respectively. We have

$$\begin{aligned} \Delta g_{rec}^{(0)} &= \left\{-(Z\alpha)^2 + \frac{(Z\alpha)^4}{3[1+\sqrt{1-(Z\alpha)^2}]^2}\right. \\ &\quad \left. -(Z\alpha)^5 P(Z\alpha)\right\}\frac{m_e}{m_N} + \mathcal{O}\left(\frac{m_e}{m_N}\right)^2 \\ &= -0.000\,000\,087\,70\ldots \quad \text{for } Z = 6 \\ &= -0.000\,000\,117\,09\ldots \quad \text{for } Z = 8, \end{aligned} \tag{171}$$

where m_N is the mass of the nucleus. The mass ratios, obtained from the 2010 adjustment, are $m_e/m(^{12}C^{6+}) = 0.000\,045\,727\,5\ldots$ and $m_e/m(^{16}O^{8+}) = 0.000\,034\,306\,5\ldots$. The recoil terms are the same as in CODATA-02 and references to the original calculations are given there. An additional term of the order of the mass ratio squared (Eides and Grotch, 1997a; Eides, 2002)

$$(1+Z)(Z\alpha)^2\left(\frac{m_e}{m_N}\right)^2 \tag{172}$$

should also be included in the theory. The validity of this term for a nucleus of any spin has been reconfirmed by Pachucki (2008), Eides and Martin (2010), and Eides and Martin (2011).

For $\Delta g_{rec}^{(2)}$, we have

$$\begin{aligned} \Delta g_{rec}^{(2)} &= \frac{\alpha}{\pi}\frac{(Z\alpha)^2}{3}\frac{m_e}{m_N} + \cdots \\ &= 0.000\,000\,000\,06\ldots \quad \text{for } Z = 6 \\ &= 0.000\,000\,000\,09\ldots \quad \text{for } Z = 8. \end{aligned} \tag{173}$$

There is a small correction to the bound-state g-factor due to the finite size of the nucleus, of order (Karshenboim, 2000)

$$\Delta g_{ns} = -\frac{8}{3}(Z\alpha)^4\left(\frac{R_N}{\lambda\!\!\!^{-}_C}\right)^2 + \cdots, \tag{174}$$

where R_N is the bound-state nuclear rms charge radius and $\lambda\!\!\!^{-}_C$ is the Compton wavelength of the electron divided by 2π. This term is calculated by scaling the results of Glazov and Shabaev (2002) with the squares of updated values for the nuclear radii $R_N = 2.4703(22)$ fm and $R_N = 2.7013(55)$ fm from the compilation of Angeli (2004) for ^{12}C and ^{16}O, respectively. This yields the correction

$$\begin{aligned} \Delta g_{ns} &= -0.000\,000\,000\,408(1) \quad \text{for } ^{12}C, \\ \Delta g_{ns} &= -0.000\,000\,001\,56(1) \quad \text{for } ^{16}O. \end{aligned} \tag{175}$$

The theoretical value for the g-factor of the electron in hydrogenic carbon 12 or oxygen 16 is the sum of the individual contributions discussed above and summarized in Tables 13 and 14:

$$\begin{aligned} g_{e^-}(^{12}C^{5+}) &= -2.001\,041\,590\,181(26), \\ g_{e^-}(^{16}O^{7+}) &= -2.000\,047\,020\,35(11). \end{aligned} \tag{176}$$

For the purpose of the least-squares calculations carried out in Sec. 13, we define $g_C(\text{th})$ to be the sum of g_D as given in

Eq. (151), the term $-2(\alpha/\pi)C_e^{(2)}$, and the numerical values of the remaining terms in Eq. (150) as given in Table 13, where the standard uncertainty of these latter terms is

$$u[g_C(\text{th})] = 0.3 \times 10^{-10} = 1.3 \times 10^{-11}|g_C(\text{th})|. \quad (177)$$

The uncertainty in g_C(th) due to the uncertainty in α enters the adjustment primarily through the functional dependence of g_D and the term $-2(\alpha/\pi)C_e^{(2)}$ on α. Therefore this particular component of uncertainty is not explicitly included in $u[g_C(\text{th})]$. To take the uncertainty $u[g_C(\text{th})]$ into account we employ as the theoretical expression for the g-factor ($B17$ in Table 33)

$$g_C(\alpha, \delta_C) = g_C(\text{th}) + \delta_C, \quad (178)$$

where the input value of the additive correction δ_C is taken to be zero with standard uncertainty $u[g_C(\text{th})]$, or $0.00(26) \times 10^{-10}$, which is data item $B15$ in Table 20. Analogous considerations apply for the g-factor in oxygen, where

$$u[g_O(\text{th})] = 1.1 \times 10^{-10} = 5.3 \times 10^{-11}|g_O(\text{th})| \quad (179)$$

and ($B18$ in Table 33)

$$g_O(\alpha, \delta_O) = g_O(\text{th}) + \delta_O. \quad (180)$$

The input value for δ_O is $0.0(1.1) \times 10^{-10}$, which is data item $B16$ in Table 20.

The covariance of the quantities δ_C and δ_O is

$$u(\delta_C, \delta_O) = 27 \times 10^{-22}, \quad (181)$$

which corresponds to a correlation coefficient of $r(\delta_C, \delta_O) = 0.994$.

The theoretical value of the ratio of the two g-factors is

$$\frac{g_{e^-}(^{12}C^{5+})}{g_{e^-}(^{16}O^{7+})} = 1.000\,497\,273\,224(40), \quad (182)$$

where the covariance of the two values is taken into account.

5.3.2. Measurements of $g_e(^{12}C^{5+})$ and $g_e(^{16}O^{7+})$

The experimental values of f_s/f_c for $^{12}C^{5+}$ and $^{16}O^{7+}$ obtained at GSI using the double Penning-trap method are discussed in CODATA-02 and the slightly updated result for the oxygen ion is discussed in CODATA-06. For $^{12}C^{5+}$ we have (Beier *et al.*, 2001; Häffner *et al.*, 2003; Werth, 2003)

$$\frac{f_s(^{12}C^{5+})}{f_c(^{12}C^{5+})} = 4376.210\,4989(23), \quad (183)$$

while for $^{16}O^{7+}$ we have (Tomaselli *et al.*, 2002; Verdú *et al.*, 2004; Verdú, 2006)

$$\frac{f_s(^{16}O^{7+})}{f_c(^{16}O^{7+})} = 4164.376\,1837(32). \quad (184)$$

The correlation coefficient of these two frequency ratios, which are data items $B17$ and $B18$ in Table 20, is 0.082.

Equations (1) and (146) together yield

$$\frac{f_s(^{12}C^{5+})}{f_c(^{12}C^{5+})} = -\frac{g_{e^-}(^{12}C^{5+})}{10A_r(e)}\left[12 - 5A_r(e) + \frac{E_b(^{12}C) - E_b(^{12}C^{5+})}{m_u c^2}\right], \quad (185)$$

which is the basis of the observational equation for the $^{12}C^{5+}$ frequency ratio input datum, Eq. (183); see $B17$ in Table 33. In a similar manner we may write

$$\frac{f_s(^{16}O^{7+})}{f_c(^{16}O^{7+})} = -\frac{g_{e^-}(^{16}O^{7+})}{14A_r(e)}A_r(^{16}O^{7+}), \quad (186)$$

with

$$A_r(^{16}O) = A_r(^{16}O^{7+}) + 7A_r(e) - \frac{E_b(^{16}O) - E_b(^{16}O^{7+})}{m_u c^2}, \quad (187)$$

which are the basis for the observational equations for the oxygen frequency ratio and $A_r(^{16}O)$, respectively; see $B18$ and $B8$ in Table 33.

Evaluation of Eq. (185) using the result for the carbon frequency ratio in Eq. (183), the theoretical result for $g_{e^-}(^{12}C^{5+})$ in Table 13 of this report, and the relevant binding energies in Table IV of CODATA-02, yields

$$A_r(e) = 0.000\,548\,579\,909\,32(29) \quad [5.2 \times 10^{-10}]. \quad (188)$$

A similar calculation for oxygen using the value of $A_r(^{16}O)$ in Table 3 yields

$$A_r(e) = 0.000\,548\,579\,909\,57(42) \quad [7.6 \times 10^{-10}]. \quad (189)$$

These values of $A_r(e)$ are consistent with each other.

Finally, as a further consistency test, the experimental and theoretical values of the ratio of $g_{e^-}(^{12}C^{5+})$ to $g_{e^-}(^{16}O^{7+})$ can be compared (Karshenboim and Ivanov, 2002). The theoretical value of the ratio is given in Eq. (182) and the experimental value is

$$\frac{g_{e^-}(^{12}C^{5+})}{g_{e^-}(^{16}O^{7+})} = 1.000\,497\,273\,68(89) \quad [8.9 \times 10^{-10}], \quad (190)$$

in agreement with the theoretical value.

6. Magnetic-moment Ratios and the Muon-electron Mass Ratio

Magnetic-moment ratios and the muon-electron mass ratio are determined by experiments on bound states of the relevant particles and must be corrected to determine the free-particle moments.

For nucleons or nuclei with spin $\boldsymbol{I}$, the magnetic moment can be written as

$$\boldsymbol{\mu} = g\frac{e}{2m_\mathrm{p}}\boldsymbol{I}, \tag{191}$$

or

$$\mu = g\mu_\mathrm{N} i. \tag{192}$$

In Eq. (192), $\mu_\mathrm{N} = e\hbar/2m_\mathrm{p}$ is the nuclear magneton, defined in analogy with the Bohr magneton, and i is the spin quantum number of the nucleus defined by $\boldsymbol{I}^2 = i(i+1)\hbar^2$ and $I_z = -i\hbar, \ldots, (\mathrm{i}-1)\hbar, i\hbar$, where I_z is the spin projection.

Bound-state g-factors for atoms with a nonzero nuclear spin are defined by considering their interactions in an applied magnetic flux density $\boldsymbol{B}$. For hydrogen, in the Pauli approximation, we have

$$\begin{aligned}\mathcal{H} &= \beta(\mathrm{H})\boldsymbol{\mu}_{\mathrm{e}^-}\cdot\boldsymbol{\mu}_\mathrm{p} - \boldsymbol{\mu}_{\mathrm{e}^-}(\mathrm{H})\cdot\boldsymbol{B} - \boldsymbol{\mu}_\mathrm{p}(\mathrm{H})\cdot\boldsymbol{B}\\ &= \frac{2\pi}{\hbar}\Delta\nu_\mathrm{H}\boldsymbol{s}\cdot\boldsymbol{I} - g_{\mathrm{e}^-}(\mathrm{H})\frac{\mu_\mathrm{B}}{\hbar}\boldsymbol{s}\cdot\boldsymbol{B} - g_\mathrm{p}(\mathrm{H})\frac{\mu_\mathrm{N}}{\hbar}\boldsymbol{I}\cdot\boldsymbol{B},\end{aligned} \tag{193}$$

where $\beta(\mathrm{H})$ characterizes the strength of the hyperfine interaction, $\Delta\nu_\mathrm{H}$ is the ground-state hyperfine frequency, $\boldsymbol{s}$ is the spin of the electron, and $\boldsymbol{I}$ is the spin of the nucleus. Equation (193) defines the corresponding bound-state g-factors $g_{\mathrm{e}^-}(\mathrm{H})$ and $g_\mathrm{p}(\mathrm{H})$.

6.1. Magnetic-moment ratios

Theoretical binding corrections relate g-factors measured in the bound state to the corresponding free-particle g-factors. The corrections are sufficiently small that the adjusted constants used to calculate them are taken as exactly known. These corrections and the references for the relevant calculations are discussed in CODATA-98 and CODATA-02.

6.1.1. Theoretical ratios of atomic bound-particle to free-particle *g*-factors

For the electron in hydrogen, we have

$$\begin{aligned}\frac{g_{\mathrm{e}^-}(\mathrm{H})}{g_{\mathrm{e}^-}} &= 1 - \frac{1}{3}(Z\alpha)^2 - \frac{1}{12}(Z\alpha)^4 + \frac{1}{4}(Z\alpha)^2\left(\frac{\alpha}{\pi}\right)\\ &\quad + \frac{1}{2}(Z\alpha)^2\frac{m_\mathrm{e}}{m_\mathrm{p}} + \frac{1}{2}\left(A_1^{(4)} - \frac{1}{4}\right)(Z\alpha)^2\left(\frac{\alpha}{\pi}\right)^2\\ &\quad - \frac{5}{12}(Z\alpha)^2\left(\frac{\alpha}{\pi}\right)\frac{m_\mathrm{e}}{m_\mathrm{p}} + \cdots,\end{aligned} \tag{194}$$

where $A_1^{(4)}$ is given in Eq. (110). For the proton in hydrogen, we have

$$\begin{aligned}\frac{g_\mathrm{p}(\mathrm{H})}{g_\mathrm{p}} &= 1 - \frac{1}{3}\alpha(Z\alpha) - \frac{97}{108}\alpha(Z\alpha)^3\\ &\quad + \frac{1}{6}\alpha(Z\alpha)\frac{m_\mathrm{e}}{m_\mathrm{p}}\frac{3+4a_\mathrm{p}}{1+a_\mathrm{p}} + \cdots,\end{aligned} \tag{195}$$

where the proton magnetic-moment anomaly a_p is defined by

$$a_\mathrm{p} = \frac{\mu_\mathrm{p}}{e\hbar/2m_\mathrm{p}} - 1 \approx 1.793. \tag{196}$$

For deuterium, similar expressions apply for the electron

$$\begin{aligned}\frac{g_{\mathrm{e}^-}(\mathrm{D})}{g_{\mathrm{e}^-}} &= 1 - \frac{1}{3}(Z\alpha)^2 - \frac{1}{12}(Z\alpha)^4 + \frac{1}{4}(Z\alpha)^2\left(\frac{\alpha}{\pi}\right)\\ &\quad + \frac{1}{2}(Z\alpha)^2\frac{m_\mathrm{e}}{m_\mathrm{d}} + \frac{1}{2}\left(A_1^{(4)} - \frac{1}{4}\right)(Z\alpha)^2\left(\frac{\alpha}{\pi}\right)^2\\ &\quad - \frac{5}{12}(Z\alpha)^2\left(\frac{\alpha}{\pi}\right)\frac{m_\mathrm{e}}{m_\mathrm{d}} + \cdots\end{aligned} \tag{197}$$

and deuteron

$$\begin{aligned}\frac{g_\mathrm{d}(\mathrm{D})}{g_\mathrm{d}} &= 1 - \frac{1}{3}\alpha(Z\alpha) - \frac{97}{108}\alpha(Z\alpha)^3\\ &\quad + \frac{1}{6}\alpha(Z\alpha)\frac{m_\mathrm{e}}{m_\mathrm{d}}\frac{3+4a_\mathrm{d}}{1+a_\mathrm{d}} + \cdots,\end{aligned} \tag{198}$$

where the deuteron magnetic-moment anomaly a_d is defined by

$$a_\mathrm{d} = \frac{\mu_\mathrm{d}}{e\hbar/m_\mathrm{d}} - 1 \approx -0.143. \tag{199}$$

In the case of muonium Mu, some additional higher-order terms are included. For the electron in muonium, we have

$$\begin{aligned}\frac{g_{\mathrm{e}^-}(\mathrm{Mu})}{g_{\mathrm{e}^-}} &= 1 - \frac{1}{3}(Z\alpha)^2 - \frac{1}{12}(Z\alpha)^4 + \frac{1}{4}(Z\alpha)^2\left(\frac{\alpha}{\pi}\right)\\ &\quad + \frac{1}{2}(Z\alpha)^2\frac{m_\mathrm{e}}{m_\mu} + \frac{1}{2}\left(A_1^{(4)} - \frac{1}{4}\right)(Z\alpha)^2\left(\frac{\alpha}{\pi}\right)^2\\ &\quad - \frac{5}{12}(Z\alpha)^2\left(\frac{\alpha}{\pi}\right)\frac{m_\mathrm{e}}{m_\mu} - \frac{1}{2}(1+Z)(Z\alpha)^2\\ &\quad \times\left(\frac{m_\mathrm{e}}{m_\mu}\right)^2 + \cdots,\end{aligned} \tag{200}$$

and for the muon in muonium, the ratio is

$$\begin{aligned}\frac{g_{\mu^+}(\mathrm{Mu})}{g_{\mu^+}} &= 1 - \frac{1}{3}\alpha(Z\alpha) - \frac{97}{108}\alpha(Z\alpha)^3 + \frac{1}{2}\alpha(Z\alpha)\frac{m_\mathrm{e}}{m_\mu}\\ &\quad + \frac{1}{12}\alpha(Z\alpha)\left(\frac{\alpha}{\pi}\right)\frac{m_\mathrm{e}}{m_\mu} - \frac{1}{2}(1+Z)\alpha(Z\alpha)\\ &\quad \times\left(\frac{m_\mathrm{e}}{m_\mu}\right)^2 + \cdots.\end{aligned} \tag{201}$$

The numerical values of the corrections in Eqs. (194)–(201), based on the 2010 adjusted values of the relevant constants, are listed in Table 15; uncertainties are negligible here. An additional term of order $\alpha(Z\alpha)^5$ relevant to Eqs. (195), (198), and (201) has been calculated by Ivanov, Karshenboim, and Lee (2009), but it is negligible at the present level of uncertainty.

TABLE 15. Theoretical values for various bound-particle to free-particle g-factor ratios relevant to the 2010 adjustment based on the 2010 recommended values of the constants.

Ratio	Value
$g_{e^-}(\mathrm{H})/g_{e^-}$	$1-17.7054\times10^{-6}$
$g_p(\mathrm{H})/g_p$	$1-17.7354\times10^{-6}$
$g_{e^-}(\mathrm{D})/g_{e^-}$	$1-17.7126\times10^{-6}$
$g_d(\mathrm{D})/g_d$	$1-17.7461\times10^{-6}$
$g_{e^-}(\mathrm{Mu})/g_{e^-}$	$1-17.5926\times10^{-6}$
$g_{\mu^+}(\mathrm{Mu})/g_{\mu^+}$	$1-17.6254\times10^{-6}$

6.1.2. Bound helion to free helion magnetic-moment ratio μ'_h/μ_h

The bound helion to free helion magnetic-moment ratio correction σ_h, defined by

$$\frac{\mu'_h}{\mu_h} = 1 - \sigma_h, \tag{202}$$

has been calculated by Rudziński, Puchalski, and Pachucki (2009), who obtain

$$\sigma_h = 59.967\,43(10)\times10^{-6} \quad [1.7\times10^{-6}]. \tag{203}$$

This provides a recommended value for the unshielded helion magnetic moment, along with other related quantities.

6.1.3. Ratio measurements

Since all of the experimental bound-state magnetic-moment ratios of interest for the 2010 adjustment are discussed in one or more of the previous three CODATA reports, only minimal information is given here. The relevant input data are items $B19-B27$ of Table 20 and their respective observational equations are $B19-B27$ in Table 33. The adjusted constants in those equations may be identified using Table 32, and theoretical bound-particle to free-particle g-factor ratios, which are taken to be exact, are given in Table 15. The symbol μ'_p denotes the magnetic moment of a proton in a spherical sample of pure H_2O at 25 °C surrounded by vacuum; and the symbol μ'_h denotes the magnetic moment of a helion bound in a ^{3}He atom. Although the exact shape and temperature of the gaseous ^{3}He sample is unimportant, we assume that it is spherical, at 25 °C, and surrounded by vacuum.

Item $B19$, labeled MIT-72, is the ratio $\mu_{e^-}(\mathrm{H})/\mu_p(\mathrm{H})$ in the 1S state of hydrogen obtained at MIT by Winkler *et al.* (1972) and Kleppner (1997); and $B20$, labeled MIT-84, is the ratio $\mu_d(\mathrm{D})/\mu_{e^-}(\mathrm{D})$ in the 1S state of deuterium also obtained at MIT (Phillips, Kleppner, and Walther, 1984).

Item $B21$ with identification StPtrsb-03 is the magnetic-moment ratio $\mu_p(\mathrm{HD})/\mu_d(\mathrm{HD})$, and $B23$ with the same identification is the ratio $\mu_t(\mathrm{HT})/\mu_p(\mathrm{HT})$, both of which were determined from NMR measurements on the HD and HT molecules (bound state of hydrogen and deuterium and of hydrogen and tritium, respectively) by researchers working at institutes in St. Petersburg, Russian Federation (Neronov and Karshenboim, 2003; Karshenboim *et al.*, 2005). Here $\mu_p(\mathrm{HD})$ and $\mu_d(\mathrm{HD})$ are the proton and the deuteron magnetic moments in HD, and $\mu_t(\mathrm{HT})$ and $\mu_p(\mathrm{HT})$ are the triton and the proton magnetic moments in HT. Items $B22$ and $B24$, also with the identifications StPtrsb-03 and due to Neronov and Karshenboim (2003) and Karshenboim *et al.* (2005), are defined according to $\sigma_{dp} \equiv \sigma_d(\mathrm{HD}) - \sigma_p(\mathrm{HD})$ and $\sigma_{tp} \equiv \sigma_t(\mathrm{HT}) - \sigma_p(\mathrm{HT})$, where $\sigma_p(\mathrm{HD})$, $\sigma_d(\mathrm{HD})$, $\sigma_t(\mathrm{HT})$, and $\sigma_p(\mathrm{HT})$ are the corresponding nuclear magnetic shielding corrections, which are small: $\mu(\mathrm{bound}) = (1-\sigma)\mu(\mathrm{free})$.

We note that after the 31 December 2010 closing date of the 2010 adjustment, Neronov and Aleksandrov (2011) reported a result for the ratio $\mu_t(\mathrm{HT})/\mu_p(\mathrm{HT})$ with a relative standard uncertainty of 7×10^{-10} and which is consistent with data item $B23$.

Item $B25$, labeled MIT-77, is the ratio $\mu_{e^-}(\mathrm{H})/\mu'_p$ obtained at MIT by Phillips, Cooke, and Kleppner (1977), where the electron is in the 1S state of hydrogen. The results of Petley and Donaldson (1984) are used to correct the measured value of the ratio based on a spherical H_2O NMR sample at 34.7 °C to the reference temperature 25 °C.

Item $B26$ with identification NPL-93 is the ratio μ'_h/μ'_p determined at the National Physical Laboratory (NPL), Teddington, UK, by Flowers, Petley, and Richards (1993). And $B27$, labeled ILL-79, is the neutron to shielded proton magnetic-moment ratio μ_n/μ'_p determined at the Institut Max von Laue-Paul Langevin (ILL) in Grenoble, France (Greene *et al.*, 1977, 1979).

6.2. Muonium transition frequencies, the muon-proton magnetic-moment ratio μ_μ/μ_p, and muon-electron mass ratio m_μ/m_e

Experimental frequencies for transitions between Zeeman energy levels in muonium Mu provide measured values of μ_μ/μ_p and the muonium ground-state hyperfine splitting $\Delta\nu_{Mu}$ that depend only on the commonly used Breit-Rabi equation (Breit and Rabi, 1931).

The theoretical expression for the hyperfine splitting $\Delta\nu_{Mu}(\mathrm{th})$ is discussed in the following section and may be written as

$$\begin{aligned}\Delta\nu_{Mu}(\mathrm{th}) &= \frac{16}{3}cR_\infty\alpha^2\frac{m_e}{m_\mu}\left(1+\frac{m_e}{m_\mu}\right)^{-3}\mathcal{F}(\alpha, m_e/m_\mu)\\ &= \Delta\nu_F\mathcal{F}(\alpha, m_e/m_\mu),\end{aligned} \tag{204}$$

where the function $\mathcal{F}$ depends weakly on α and m_e/m_μ.

6.2.1. Theory of the muonium ground-state hyperfine splitting

Presented here is a brief summary of the present theory of $\Delta\nu_{Mu}$. Complete results of the relevant calculations are given along with references to new work; references to the original literature included in earlier CODATA reports are not repeated.

The hyperfine splitting is given mainly by the Fermi formula:

$$\Delta\nu_{\rm F} = \frac{16}{3} cR_\infty Z^3\alpha^2 \frac{m_{\rm e}}{m_\mu}\left[1+\frac{m_{\rm e}}{m_\mu}\right]^{-3}. \quad (205)$$

In order to identify the source of the terms, some of the theoretical expressions are for a muon with charge Ze rather than e.

The general expression for the hyperfine splitting is

$$\Delta\nu_{\rm Mu}({\rm th}) = \Delta\nu_{\rm D} + \Delta\nu_{\rm rad} + \Delta\nu_{\rm rec} + \Delta\nu_{\rm r-r} + \Delta\nu_{\rm weak} + \Delta\nu_{\rm had}, \quad (206)$$

where the terms labeled D, rad, rec, r-r, weak, and had account for the Dirac, radiative, recoil, radiative-recoil, electroweak, and hadronic contributions to the hyperfine splitting, respectively.

The Dirac equation yields

$$\Delta\nu_{\rm D} = \Delta\nu_{\rm F}(1+a_\mu)\left[1+\frac{3}{2}(Z\alpha)^2+\frac{17}{8}(Z\alpha)^4+\cdots\right], \quad (207)$$

where a_μ is the muon magnetic-moment anomaly.

The radiative corrections are

$$\Delta\nu_{\rm rad} = \Delta\nu_{\rm F}(1+a_\mu)\left[D^{(2)}(Z\alpha)\left(\frac{\alpha}{\pi}\right)+D^{(4)}(Z\alpha)\left(\frac{\alpha}{\pi}\right)^2 + D^{(6)}(Z\alpha)\left(\frac{\alpha}{\pi}\right)^3+\cdots\right], \quad (208)$$

where the functions $D^{(2n)}(Z\alpha)$ are contributions from n virtual photons. The leading term is

$$D^{(2)}(Z\alpha) = A_1^{(2)} + \left(\ln 2-\frac{5}{2}\right)\pi Z\alpha + \left[-\frac{2}{3}\ln^2(Z\alpha)^{-2} + \left(\frac{281}{360}-\frac{8}{3}\ln 2\right)\ln(Z\alpha)^{-2} + 16.9037\ldots\right](Z\alpha)^2 + \left[\left(\frac{5}{2}\ln 2-\frac{547}{96}\right)\ln(Z\alpha)^{-2}\right]\pi(Z\alpha)^3 + G(Z\alpha)(Z\alpha)^3, \quad (209)$$

where $A_1^{(2)} = \frac{1}{2}$, as in Eq. (109). The function $G(Z\alpha)$ accounts for all higher-order contributions in powers of $Z\alpha$; it can be divided into self energy and vacuum-polarization contributions, $G(Z\alpha) = G_{\rm SE}(Z\alpha) + G_{\rm VP}(Z\alpha)$. Yerokhin and Jentschura (2008, 2010) have calculated the one-loop self energy for the muonium HFS with the result

$$G_{\rm SE}(\alpha) = -13.8308(43) \quad (210)$$

which agrees with the value $G_{\rm SE}(\alpha) = -13.8(3)$ from an earlier calculation by Yerokhin *et al.* (2005), as well as with other previous estimates. The vacuum-polarization part is

$$G_{\rm VP}(\alpha) = 7.227(9). \quad (211)$$

For $D^{(4)}(Z\alpha)$, we have

$$D^{(4)}(Z\alpha) = A_1^{(4)} + 0.770\,99(2)\pi Z\alpha + \left[-\frac{1}{3}\ln^2(Z\alpha)^{-2} - 0.6390\ldots\times\ln(Z\alpha)^{-2} + 10(2.5)\right](Z\alpha)^2+\cdots, \quad (212)$$

where $A_1^{(4)}$ is given in Eq. (110). Calculation of the coefficient of $\pi Z\alpha$ is summarized in CODATA-98; the quoted value with a slightly smaller uncertainty is given by Mondéjar, Piclum, and Czarnecki (2010).

The next term is

$$D^{(6)}(Z\alpha) = A_1^{(6)}+\cdots, \quad (213)$$

where the leading contribution $A_1^{(6)}$ is given in Eq. (111), but only partial results of relative order $Z\alpha$ have been calculated (Eides and Shelyuto, 2007). Higher-order functions $D^{(2n)}(Z\alpha)$ with $n>3$ are expected to be negligible.

The recoil contribution is

$$\Delta\nu_{\rm rec} = \Delta\nu_{\rm F}\frac{m_{\rm e}}{m_\mu}\left(-\frac{3}{1-(m_{\rm e}/m_\mu)^2}\ln\left(\frac{m_\mu}{m_{\rm e}}\right)\frac{Z\alpha}{\pi}+\frac{1}{(1+m_{\rm e}/m_\mu)^2}\times\left\{\ln(Z\alpha)^{-2}-8\ln 2+\frac{65}{18}+\left[\frac{9}{2\pi^2}\ln^2\left(\frac{m_\mu}{m_{\rm e}}\right)+\left(\frac{27}{2\pi^2}-1\right)\ln\left(\frac{m_\mu}{m_{\rm e}}\right)+\frac{93}{4\pi^2}+\frac{33\zeta(3)}{\pi^2}-\frac{13}{12}-12\ln 2\right]\frac{m_{\rm e}}{m_\mu}\right\}(Z\alpha)^2+\left\{-\frac{3}{2}\ln\left(\frac{m_\mu}{m_{\rm e}}\right)\ln(Z\alpha)^{-2}-\frac{1}{6}\ln^2(Z\alpha)^{-2}+\left(\frac{101}{18}-10\ln 2\right)\ln(Z\alpha)^{-2}+40(10)\right\}\frac{(Z\alpha)^3}{\pi}\right)+\cdots, \quad (214)$$

as discussed in CODATA-02.

The radiative-recoil contribution is

$$\Delta\nu_{\rm r-r} = \Delta\nu_{\rm F}\left(\frac{\alpha}{\pi}\right)^2\frac{m_{\rm e}}{m_\mu}\left\{\left[-2\ln^2\left(\frac{m_\mu}{m_{\rm e}}\right)+\frac{13}{12}\ln\left(\frac{m_\mu}{m_{\rm e}}\right)+\frac{21}{2}\zeta(3)+\frac{\pi^2}{6}+\frac{35}{9}\right]+\left[\frac{4}{3}\ln^2\alpha^{-2}+\left(\frac{16}{3}\ln 2-\frac{341}{180}\right)\ln\alpha^{-2}-40(10)\right]\pi\alpha+\left[-\frac{4}{3}\ln^3\left(\frac{m_\mu}{m_{\rm e}}\right)+\frac{4}{3}\ln^2\left(\frac{m_\mu}{m_{\rm e}}\right)\right]\frac{\alpha}{\pi}\right\} - \nu_{\rm F}\alpha^2\left(\frac{m_{\rm e}}{m_\mu}\right)^2\left(6\ln 2+\frac{13}{6}\right)+\cdots, \quad (215)$$

where, for simplicity, the explicit dependence on Z is not shown. Partial radiative-recoil results are given by Eides and Shelyuto (2009a, 2009b, 2010), and are summarized as

$$\Delta\nu_{\rm ES} = \Delta\nu_{\rm F}\left(\frac{\alpha}{\pi}\right)^3 \frac{m_{\rm e}}{m_\mu}\left\{ \left[3\zeta(3) - 6\pi^2 \ln 2 + \pi^2 - 8\right] \times \ln\frac{m_\mu}{m_{\rm e}} + 63.127(2)\right\} = -34.7 \text{ Hz}. \quad (216)$$

The electroweak contribution due to the exchange of a Z^0 boson is (Eides, 1996)

$$\Delta\nu_{\rm weak} = -65 \text{ Hz}, \quad (217)$$

while for the hadronic vacuum-polarization contribution we have (Eidelman, Karshenboim, and Shelyuto, 2002)

$$\Delta\nu_{\rm had} = 236(4) \text{ Hz}, \quad (218)$$

as in CODATA-06. A negligible contribution (≈ 0.0065 Hz) from the hadronic light-by-light correction has been given by Karshenboim, Shelyuto, and Vainshtein (2008). Tau vacuum polarization contributes 3 Hz, which is also negligible at the present level of uncertainty (Sapirstein, Terray, and Yennie, 1984).

The four principal sources of uncertainty in $\Delta\nu_{\rm Mu}$(th) are $\Delta\nu_{\rm rad}$, $\Delta\nu_{\rm rec}$, $\Delta\nu_{\rm r-r}$, and $\Delta\nu_{\rm had}$ in Eq. (206). Based on the discussion in CODATA-02, CODATA-06, and the new results above, the current uncertainties from these contributions are 7 Hz, 74 Hz, 63 Hz, and 4 Hz, respectively, for a total of 98 Hz. Since this is only 3% less than the value 101 Hz used in the 2006 adjustment, and in view of the incomplete nature of the calculations, the Task Group has retained the 101 Hz standard uncertainty of that adjustment:

$$u[\Delta\nu_{\rm Mu}(\text{th})] = 101 \text{ Hz} \quad [2.3 \times 10^{-8}]. \quad (219)$$

For the least-squares calculations, we use as the theoretical expression for the hyperfine splitting

$$\Delta\nu_{\rm Mu}(R_\infty, \alpha, m_{\rm e}/m_\mu, \delta_\mu, \delta_{\rm Mu}) = \Delta\nu_{\rm Mu}(\text{th}) + \delta_{\rm Mu}, \quad (220)$$

where the input datum for the additive correction $\delta_{\rm Mu}$, which accounts for the uncertainty of the theoretical expression and is data item $B28$ in Table 20, is 0(101) Hz.

The above theory yields

$$\Delta\nu_{\rm Mu} = 4\,463\,302\,891(272) \text{ Hz} \quad [6.1 \times 10^{-8}] \quad (221)$$

using values of the constants obtained from the 2010 adjustment without the two LAMPF measured values of $\Delta\nu_{\rm Mu}$ discussed in the following section. The main source of uncertainty in this value is the mass ratio $m_{\rm e}/m_\mu$.

6.2.2. Measurements of muonium transition frequencies and values of $\mu_\mu/\mu_{\rm p}$ and $m_\mu/m_{\rm e}$

The two most precise determinations of muonium Zeeman transition frequencies were carried out at the Clinton P. Anderson Meson Physics Facility at Los Alamos (LAMPF), USA, and were reviewed in detail in CODATA-98. The results are as follows.

Data reported in 1982 by Mariam (1981) and Mariam *et al.* (1982) are

$$\Delta\nu_{\rm Mu} = 4\,463\,302.88(16) \text{ kHz} \quad [3.6 \times 10^{-8}], \quad (222)$$

$$\nu(f_{\rm p}) = 627\,994.77(14) \text{ kHz} \quad [2.2 \times 10^{-7}], \quad (223)$$

$$r[\Delta\nu_{\rm Mu}, \nu(f_{\rm p})] = 0.227, \quad (224)$$

where $f_{\rm p}$ is 57.972 993 MHz, corresponding to the magnetic flux density of about 1.3616 T used in the experiment, and $r[\Delta\nu_{\rm Mu}, \nu(f_{\rm p})]$ is the correlation coefficient of $\Delta\nu_{\rm Mu}$ and $\nu(f_{\rm p})$. The data reported in 1999 by Liu *et al.* (1999) are

$$\Delta\nu_{\rm Mu} = 4\,463\,302\,765(53) \text{ Hz} \quad [1.2 \times 10^{-8}], \quad (225)$$

$$\nu(f_{\rm p}) = 668\,223\,166(57) \text{ Hz} \quad [8.6 \times 10^{-8}], \quad (226)$$

$$r[\Delta\nu_{\rm Mu}, \nu(f_{\rm p})] = 0.195, \quad (227)$$

where $f_{\rm p}$ is 72.320 000 MHz, corresponding to the flux density of approximately 1.7 T used in the experiment. The data in Eqs. (222), (223), (225), and (226) are data items $B29.1$, $B30$, $B29.2$, and $B31$, respectively, in Table 20.

The expression for the magnetic-moment ratio is

$$\frac{\mu_{\mu^+}}{\mu_{\rm p}} = \frac{\Delta\nu_{\rm Mu}^2 - \nu^2(f_{\rm p}) + 2s_{\rm e}f_{\rm p}\nu(f_{\rm p})}{4s_{\rm e}f_{\rm p}^2 - 2f_{\rm p}\nu(f_{\rm p})}\left(\frac{g_{\mu^+}(\text{Mu})}{g_{\mu^+}}\right)^{-1}, \quad (228)$$

where $\Delta\nu_{\rm Mu}$ and $\nu(f_{\rm p})$ are the sum and difference of two measured transition frequencies, $f_{\rm p}$ is the free proton NMR reference frequency corresponding to the flux density used in the experiment, $g_{\mu^+}(\text{Mu})/g_{\mu^+}$ is the bound-state correction for the muon in muonium given in Table 15, and

$$s_{\rm e} = \frac{\mu_{\rm e^-}}{\mu_{\rm p}}\frac{g_{\rm e^-}(\text{Mu})}{g_{\rm e^-}}, \quad (229)$$

where $g_{\rm e^-}(\text{Mu})/g_{\rm e^-}$ is the bound-state correction for the electron in muonium given in the same table.

The muon to electron mass ratio $m_\mu/m_{\rm e}$ and the muon to proton magnetic-moment ratio $\mu_\mu/\mu_{\rm p}$ are related by

$$\frac{m_\mu}{m_{\rm e}} = \left(\frac{\mu_{\rm e}}{\mu_{\rm p}}\right)\left(\frac{\mu_\mu}{\mu_{\rm p}}\right)^{-1}\left(\frac{g_\mu}{g_{\rm e}}\right). \quad (230)$$

A least-squares adjustment using the LAMPF data, the 2010 recommended values of R_∞, $\mu_{\rm e}/\mu_{\rm p}$, $g_{\rm e}$, and g_μ, together with Eq. (204) and Eqs. (228)–(230), yields

$$\frac{\mu_{\mu^+}}{\mu_{\rm p}} = 3.183\,345\,24(37) \quad [1.2 \times 10^{-7}], \quad (231)$$

$$\frac{m_\mu}{m_e} = 206.768\,276(24) \quad [1.2 \times 10^{-7}], \tag{232}$$

$$\alpha^{-1} = 137.036\,0018(80) \quad [5.8 \times 10^{-8}], \tag{233}$$

where this value of α^{-1} is denoted as $\alpha^{-1}(\Delta\nu_{Mu})$.

The uncertainty of m_μ/m_e in Eq. (232) is nearly 5 times the uncertainty of the 2010 recommended value. In Eq. (232), the value follows from Eqs. (228)–(230) with almost the same uncertainty as the moment ratio in Eq. (231). Taken together, the experimental value of and theoretical expression for the hyperfine splitting essentially determine the value of the product $\alpha^2 m_e/m_\mu$, as is evident from Eq. (204), with an uncertainty dominated by the 2.3×10^{-8} relative uncertainty in the theory, and in this limited least-squares adjustment α is otherwise unconstrained. However, in the full adjustment the value of α is determined by other data which in turn determines the value of m_μ/m_e with a significantly smaller uncertainty than that of Eq. (232).

7. Quotient of Planck Constant and Particle Mass $h/m(X)$ and α

Measurements of $h/m(X)$ are of potential importance because the relation $R_\infty = \alpha^2 m_e c/2h$ implies

$$\alpha = \left[\frac{2R_\infty}{c}\frac{A_r(X)}{A_r(e)}\frac{h}{m(X)}\right]^{1/2}, \tag{234}$$

where $A_r(X)$ is the relative atomic mass of particle X with mass $m(X)$ and $A_r(e)$ is the relative atomic mass of the electron. Because c is exactly known, the relative standard uncertainties of R_∞ and $A_r(e)$ are 5.0×10^{-12} and 4.0×10^{-10}, respectively, and the uncertainty of $A_r(X)$ for many particles and atoms is less than that of $A_r(e)$, Eq. (234) can provide a competitive value of α if $h/m(X)$ is determined with a sufficiently small uncertainty. This section discusses measurements of $h/m(^{133}Cs)$ and $h/m(^{87}Rb)$.

7.1. Quotient $h/m(^{133}Cs)$

Wicht *et al.* (2002) determined $h/m(^{133}Cs)$ by measuring the atomic recoil frequency shift of photons absorbed and emitted by ^{133}Cs atoms using atom interferometry. Carried out at Stanford University, Stanford, California, USA, the experiment is discussed in CODATA-06 and CODATA-02. Consequently, only the final result is given here:

$$\frac{h}{m(^{133}Cs)} = 3.002\,369\,432(46) \times 10^{-9}\ \text{m}^2\,\text{s}^{-1} \quad [1.5 \times 10^{-8}]. \tag{235}$$

The observational equation for this datum is, from Eq. (234),

$$\frac{h}{m(^{133}Cs)} = \frac{A_r(e)}{A_r(^{133}Cs)}\frac{c\alpha^2}{2R_\infty}. \tag{236}$$

The value of α inferred from this expression and Eq. (235) is given in Table 25, Sec. 13.

The Stanford result for $h/m(^{133}Cs)$ was not included as an input datum in the final adjustment on which the 2006 recommended values are based because of its low weight, and is omitted from the 2010 final adjustment for the same reason. Nevertheless, it is included as an initial input datum to provide a complete picture of the available data that provide values of α.

7.2. Quotient $h/m(^{87}Rb)$

A value of $h/m(^{87}Rb)$ with a relative standard uncertainty of 1.3×10^{-8} obtained at LKB in Paris was taken as an input datum in the 2006 adjustment and its uncertainty was sufficiently small for it to be included in the 2006 final adjustment. Reported by Cladé *et al.* (2006) and discussed in CODATA-06, $h/m(^{87}Rb)$ was determined by measuring the rubidium recoil velocity $v_r = \hbar k/m(^{87}Rb)$ when a rubidium atom absorbs or emits a photon of wave vector $k = 2\pi/\lambda$, where λ is the wavelength of the photon and $\nu = c/\lambda$ is its frequency. The measurements were based on Bloch oscillations in a moving standing wave.

A value of $h/m(^{87}Rb)$ with a relative uncertainty of 9.2×10^{-9} and in agreement with the earlier result, obtained from a new LKB experiment using combined Bloch oscillations and atom interferometry, was subsequently reported by Cadoret *et al.* (2008a). In this approach Bloch oscillations are employed to transfer a large number of photon momenta to rubidium atoms and an atom interferometer is used to accurately determine the resulting variation in the velocity of the atoms. Significant improvements incorporated into this version of the experiment have now provided a newer value of $h/m(^{87}Rb)$ that not only agrees with the two previous values, but has an uncertainty over 10 and 7 times smaller, respectively. As given by Bouchendira *et al.* (2011), the new LKB result is

$$\frac{h}{m(^{87}Rb)} = 4.591\,359\,2729(57) \times 10^{-9}\ \text{m}^2\,\text{s}^{-1} \quad [1.2 \times 10^{-9}]. \tag{237}$$

Because the LKB researchers informed the Task Group that this result should be viewed as superseding the two earlier results (Biraben, 2011), it is the only value of $h/m(^{87}Rb)$ included as an input datum in the 2010 adjustment. The observational equation for this datum is, from Eq. (234),

$$\frac{h}{m(^{87}Rb)} = \frac{A_r(e)}{A_r(^{87}Rb)}\frac{c\alpha^2}{2R_\infty}. \tag{238}$$

The value of α inferred from this expression and Eq. (237) is given in Table 25, Sec. 13.

The experiment of the LKB group from which the result given in Eq. (237) was obtained is described in the paper by Bouchendira *et al.* (2011) and the references cited therein; see also Cadoret *et al.* (2008b, 2009, 2011), and Cladé *et al.*

(2010). It is worth noting, however, that the reduction in uncertainty of the 2008 result by over a factor of 7 was achieved by reducing the uncertainties of a number of individual components, especially those due to the alignment of beams, wave front curvature and Gouy phase, and the second-order Zeeman effect. The total fractional correction for systematic effects is $-53(12) \times 10^{-10}$ and the statistical or type A uncertainty is 4 parts in 10^{10}.

7.3. Other data

A result for the quotient $h/m_n d_{220}$(W04) with a relative standard uncertainty of 4.1×10^{-8}, where m_n is the neutron mass and d_{220}(W04) is the {220} lattice spacing of the crystal WASO 04, was included in the past three CODATA adjustments, although its uncertainty was increased by the multiplicative factor 1.5 in the 2006 final adjustment. It was obtained by Physikalisch-Technische Bundesanstalt (PTB), Braunschweig, Germany, researchers working at the ILL high-neutron-flux reactor in Grenoble (Krüger, Nistler, and Weirauch, 1999).

Since the result has a relative uncertainty of 4.1×10^{-8}, the value of α that can be inferred from it, even assuming that d_{220}(W04) is exactly known, has an uncertainty of about 2×10^{-8}. This is over 50 times larger than that of α from a_e and is not competitive. Further, the inferred value disagrees with the a_e value.

On the other hand, the very small uncertainty of the a_e value of α means that the PTB result for $h/m_n d_{220}$(W04) can provide an inferred value of d_{220}(W04) with the competitive relative uncertainty of about 4 parts in 10^8. However, this inferred lattice-spacing value, reflecting the disagreement of the inferred value of alpha, is inconsistent with the directly determined x-ray and optical interferometer (XROI) value. This discrepancy could well be the result of the different effective lattice parameters for the different experiments. In the PTB measurement of $h/m_n d_{220}$(W04), the de Broglie wavelength, $\lambda \approx 0.25$ nm, of slow neutrons was determined using back reflection from the surface of a silicon crystal. As pointed out to the Task Group by Peter Becker (2011) of the PTB, the lattice spacings near the surface of the crystal, which play a more critical role than in the XROI measurements carried out using x-ray transmission, may be strained and not the same as the spacings in the bulk of the crystal.

For these reasons, the Task Group decided not to consider this result for inclusion in the 2010 adjustment.

8. Electrical Measurements

This section focuses on 18 input data resulting from high-accuracy electrical measurements, 16 of which were also available for the 2006 adjustment. The remaining two became available in the intervening 4 years. Of the 16, 13 were not included in the final adjustment on which the 2006 recommended values are based because of their low weight. These same data and one of the two new values are omitted in the final 2010 adjustment for the same reason. Nevertheless, all are initially included as input data because of their usefulness in providing an overall picture of the consistency of the data and in testing the exactness of the Josephson and quantum-Hall-effect relations $K_J = 2e/h$ and $R_K = h/e^2$. As an aid, we begin with a concise overview of the seven different types of electrical quantities of which the 18 input data are particular examples.

8.1. Types of electrical quantities

If microwave radiation of frequency f is applied to a Josephson effect device, quantized voltages $U_J(n) = nf/K_J$ are induced across the device, where n, an integer, is the step number of the voltage and $K_J = 2e/h$ is the Josephson constant. Similarly, the quantized Hall resistance of the ith resistance plateau of a quantum-Hall-effect device carrying a current and in a magnetic field, i an integer, is given by $R_H(i) = R_K/i$, where $R_K = h/e^2 = \mu_0 c/2\alpha$ is the von Klitzing constant. Thus, measurement of K_J in its SI unit Hz/V determines the quotient $2e/h$, and since in the SI c and μ_0 are exactly known constants, measurement of R_K in its SI unit Ω determines α. Further, since $K_J^2 R_K = 4/h$, a measurement of this product in its SI unit $(\mathrm{J\,s})^{-1}$ determines h.

The gyromagnetic ratio γ_x of a bound particle x of spin quantum number i and magnetic moment μ_x is given by

$$\gamma_x = \frac{2\pi f}{B} = \frac{\omega}{B} = \frac{|\mu_x|}{i\hbar}, \tag{239}$$

where f is the spin-flip (or precession) frequency and ω is the angular precession frequency of the particle in the magnetic flux density B. For a bound and shielded proton p and helion h Eq. (239) gives

$$\gamma'_p = \frac{2\mu'_p}{\hbar}, \quad \gamma'_h = \frac{2\mu'_h}{\hbar}, \tag{240}$$

where the protons are in a spherical sample of pure H_2O at 25 °C surrounded by vacuum; and the helions are in a spherical sample of low-pressure, pure ^{3}He gas at 25 °C surrounded by vacuum.

The shielded gyromagnetic ratio of a particle can be determined by two methods but the quantities actually measured are different: the low-field method determines $\gamma'_x/K_J R_K$ while the high-field method determines $\gamma'_x K_J R_K$. In both cases an electric current I is measured using the Josephson and quantum Hall effects with the conventional values of the Josephson and von Klitzing constants. We have for the two methods

$$\gamma'_x = \Gamma'_{x-90}(\mathrm{lo}) \frac{K_J R_K}{K_{J-90} R_{K-90}}, \tag{241}$$

$$\gamma'_x = \Gamma'_{x-90}(\mathrm{hi}) \frac{K_{J-90} R_{K-90}}{K_J R_K}, \tag{242}$$

where Γ'_{x-90}(lo) and Γ'_{x-90}(hi) are the experimental values of γ'_x in SI units that would result from low- and hi-field experiments, respectively, if K_J and R_K had the exactly known conventional values K_{J-90} and R_{K-90}. The actual input data

used in the adjustment are $\Gamma'_{x-90}(\text{lo})$ and $\Gamma'_{x-90}(\text{hi})$ since these are the quantities actually measured in the experiments, but their observational equations (see Table 33) account for the fact that $K_{J-90} \neq K_J$ and $R_{K-90} \neq R_K$.

Finally, for the Faraday constant F we have

$$F = \mathcal{F}_{90} \frac{K_{J-90} R_{K-90}}{K_J R_K}, \tag{243}$$

where $\mathcal{F}_{90}$ is the actual quantity experimentally measured. Equation (243) is similar to Eq. (242) because $\mathcal{F}_{90}$ depends on current in the same way as $\Gamma'_{x-90}(\text{hi})$, and the same comments apply.

8.2. Electrical data

The 18 electrical input data are data items $B32.1-B38$ in Table 20, Sec. 13. Data items $B37.4$ and $B37.5$, the two new input data mentioned above and which, like the other three data in this category, are moving-coil watt-balance results for the product $K_J^2 R_K$, are discussed in the next two sections. Since the other 16 input data have been discussed in one or more of the three previous CODATA reports, we provide only limited information here.

$B32.1$ and $B32.2$, labeled NIST-89 and NIM-95, are values of $\Gamma'_{p-90}(\text{lo})$ obtained at the National Institute of Standards and Technology (NIST), Gaithersburg, MD, USA (Williams *et al.*, 1989), and at the National Institute of Metrology (NIM), Beijing, PRC (Liu *et al.*, 1995), respectively. $B33$, identified as KR/VN-98, is a similar value of $\Gamma'_{h-90}(\text{lo})$ obtained at the Korea Research Institute of Standards and Science (KRISS), Taedok Science Town, Republic of Korea, in a collaborative effort with researchers from the Mendeleyev All-Russian Research Institute for Metrology (VNIIM), St. Petersburg, Russian Federation (Shifrin, Khorev *et al.*, 1998; Shifrin, Park *et al.*, 1998; Shifrin *et al.*, 1999; Park *et al.*, 1999). $B34.1$ and $B34.2$ are values of $\Gamma'_{p-90}(\text{hi})$ from NIM (Liu *et al.*, 1995) and NPL (Kibble and Hunt, 1979), respectively, with identifications NIM-95 and NPL-79.

$B35.1-B35.5$ are five calculable-capacitor determinations of R_K from NIST (Jeffery *et al.*, 1997, 1998), the National Metrology Institute (NMI), Lindfield, Australia (Small *et al.*, 1997), NPL (Hartland, Jones, and Legg, 1988), NIM (Zhang *et al.*, 1995), and Laboratoire national de métrologie et d'essais (LNE), Trappes, France (Trapon *et al.*, 2001, 2003), respectively, and are labeled NIST-97, NMI-97, NPL-88, NIM-95, and LNE-01.

$B36.1$ with identification NMI-89 is the mercury electrometer result for K_J from NMI (Clothier *et al.*, 1989); and $B36.2$, labeled PTB-91, is the capacitor voltage balance result for K_J from the PTB (Sienknecht and Funck, 1985, 1986; Funck and Sienknecht, 1991).

$B37.1-B37.3$, with identifications NPL-90, NIST-98, and NIST-07, respectively, are moving-coil watt-balance results for $K_J^2 R_K$ from NPL (Kibble, Robinson, and Belliss, 1990) and from NIST (Williams *et al.*, 1998; Steiner *et al.*, 2007).

The last electrical input datum, $B38$ and labeled NIST-80, is the silver dissolution coulometer result for $\mathcal{F}_{90}$ from NIST (Bower and Davis, 1980).

The correlation coefficients of these data, as appropriate, are given in Table 21, Sec. 13; the observational equations for the seven different types of electrical data of which the 18 input data are particular examples are given in Table 33 in the same section and are $B32-B38$. Recalling that the relative standard uncertainties of R_∞, α, μ_{e^-}/μ'_p, μ'_h/μ'_p, and $A_r(e)$ are significantly smaller that those of the electrical input data, inspection of these equations shows that measured values of $\Gamma'_{p-90}(\text{lo})$, $\Gamma'_{h-90}(\text{lo})$, $\Gamma'_{p-90}(\text{hi})$, R_K, K_J, $K_J^2 R_K$, and $\mathcal{F}_{90}$ principally determine α, α, h, α, h, h, and h, respectively.

8.2.1. $K_J^2 R_K$ and h: NPL watt balance

We consider here and in the following section the two new watt-balance measurements of $K_J^2 R_K = 4/h$. For reviews of such experiments, see, for example, Eichenberger, Genevès, and Gournay (2009), Stock (2011), and Li *et al.* (2012). The basic idea is to compare electrical power measured in terms of the Josephson and quantum Hall effects to the equivalent mechanical power measured in the SI unit $\text{W} = \text{m}^2\,\text{kg}\,\text{s}^{-3}$. The comparison employs an apparatus now called a moving-coil watt balance, or simply a watt balance, first proposed by Kibble (1975) at NPL. A watt-balance experiment can be described by the simple equation $m_s g v = UI$, where I is the current in a circular coil in a radial magnetic flux density B and the force on the coil due to I and B is balanced by the weight $m_s g$ of a standard of mass m_s; and U is the voltage induced across the terminals of the coil when it is moved vertically with a velocity v in the same flux density B. Thus, a watt balance is operated in two different modes: the weighing mode and the velocity mode.

The NPL Mark II watt balance and its early history were briefly discussed in CODATA-06, including the initial result obtained with it by Robinson and Kibble (2007). Based on measurements carried out from October 2006 to March 2007 and having a relative standard uncertainty of 66 parts in 10^9, this result became available only after the closing date of the 2006 adjustment. Moreover, the NPL value of $K_J^2 R_K$ was 308 parts in 10^9 smaller than the NIST-07 value with a relative uncertainty of 36 parts in 10^9.

Significant modifications were subsequently made to the NPL apparatus in order to identify previously unknown sources of error as well as to reduce previously identified sources. The modifications were completed in November 2008, the apparatus was realigned in December 2008, and measurements and error investigations were continued until June 2009. From then to August 2009 the apparatus was dismantled, packed, and shipped to the National Research Council (NRC), Ottawa, Canada. A lengthy, highly detailed preprint reporting the final Mark II result was provided to the Task Group by I. A. Robinson of NPL prior to the 31 December 2010 closing date of the 2010 adjustment. This paper has

now been published and the reported value is (Robinson, 2012)

$$h = 6.626\,07123(133) \times 10^{-34}\ \text{J s} \quad [2.0 \times 10^{-7}]. \quad (244)$$

This corresponds to

$$K_J^2 R_K = 6.036\,7597(12) \times 10^{33}\ \text{J}^{-1}\,\text{s}^{-1} \quad [2.0 \times 10^{-7}] \quad (245)$$

identified as NPL-12 and which is included as an input datum in the current adjustment, data item $B37.4$.

The NPL final result is based on the initial data obtained from October 2006 to March 2007, data obtained during the first half of 2008, and data obtained during the first half of 2009, the final period. Many variables were investigated to determine their possible influence on the measured values of $K_J^2 R_K$. For example, several mass standards with different masses and fabricated from different materials were used during the course of the data taking. A comparison of the uncertainty budgets for the 2007 data and the 2009 data shows significant reductions in all categories, with the exception of the calibration of the mass standards, resulting in the reduction of the overall uncertainty from 66 parts in 10^9 to 36 parts in 10^9.

Nevertheless, during the week before the balance was to be dismantled, two previously unrecognized possible systematic errors in the weighing mode of the experiment came to light. Although there was insufficient time to derive a correction for the effects, Robinson obtained an uncertainty estimate for them. This additional uncertainty component, 197 parts in 10^9, when combined with the initially estimated overall uncertainty, leads to the 200 parts in 10^9 final uncertainty in Eqs. (244) and (245). Since the same component applies to the initial Mark II result, its uncertainty is increased from 66 parts in 10^9 to 208 parts in 10^9.

Finally, there is a slight correlation between the final Mark II value of $K_J^2 R_K$, NPL-12, item $B37.4$ in Table 20, and its 1990 predecessor, NPL-90, item $B37.1$ in the same table. Based on the paper by Robinson (2012), the correlation coefficient is 0.0025.

8.2.2. $K_J^2 R_K$ and h: METAS watt balance

The watt-balance experiment at the Federal Office of Metrology (METAS), Bern-Wabern, Switzerland, was initiated in 1997, and progress reports describing more than a decade of improvements and investigations of possible systematic errors have been published and presented at conferences (Beer *et al.*, 1999, 2001, 2003). A detailed preprint giving the final result of this effort, which is being continued with a new apparatus, was provided to the Task Group by A. Eichenberger of METAS prior to the 31 December 2010 closing date of the 2010 adjustment, and was subsequently published by Eichenberger *et al.* (2011). The METAS value for h and the corresponding value for $K_J^2 R_K$, identified as METAS-11, input datum $B37.5$, are

$$h = 6.626\,0691(20) \times 10^{-34}\ \text{J s} \quad [2.9 \times 10^{-7}], \quad (246)$$

and

$$K_J^2 R_K = 6.036\,7617(18) \times 10^{33}\ \text{J}^{-1}\,\text{s}^{-1} \quad [2.9 \times 10^{-7}]. \quad (247)$$

The METAS watt balance differs in a number of respects from those of NIST and NPL. For example, the METAS apparatus was designed to use a 100 g mass standard and a commercial mass comparator rather than a 1 kg standard and a specially designed and constructed balance in order to reduce the size and complexity of the apparatus. Also, the velocity mode was designed to be completely independent of the weighing mode. The use of two separated measuring systems for the two modes in the same apparatus make it possible to optimize each, but does require the transfer of the coil between the two systems during the course of the measurements. Improvements in the apparatus over the last several years of its operation focused on alignment, control of the coil position, and reducing magnet hysteresis.

The METAS result is based on six sets of data acquired in 2010, each containing at least 500 individual measurements which together represent over 3400 hours of operation of the apparatus. The 7×10^{-8} relative standard uncertainty of the mean of the means of the six data sets is considered by Eichenberger *et al.* (2011) to be a measure of the reproducibility of the apparatus. The uncertainty budget from which the 29×10^{-8} relative uncertainty of the METAS value of $K_J^2 R_K$ is obtained contains nine components, but the dominant contributions, totaling 20 parts in 10^8, are associated with the alignment of the apparatus. Eichenberger *et al.* (2011) point out that because of the mechanical design of the current METAS watt balance, it is not possible to reduce this source of uncertainty in a significant way.

8.2.3. Inferred value of K_J

As indicated in CODATA-06, a value of K_J with an uncertainty significantly smaller than those of the two directly measured values $B36.1$ and $B36.2$ can be obtained without assuming the validity of the relations $K_J = 2e/h$ and $R_K = h/e^2$. Dividing the weighted mean of the five directly measured watt-balance values of $K_J^2 R_K$, $B37.1$–$B37.5$, by the weighted mean of the five directly measured calculable-capacitor values of R_K, $B35.1$–$B35.5$, we have

$$K_J = K_{J-90}[1 - 3.0(1.9) \times 10^{-8}]$$
$$= 483\,597.8853(92)\ \text{GHz/V} \quad [1.9 \times 10^{-8}]. \quad (248)$$

This result is consistent with the two directly measured values but has an uncertainty that is smaller by more than an order of magnitude.

8.3. Josephson and quantum-Hall-effect relations

The theoretical and experimental evidence accumulated over the past 50 years for the Josephson effect and 30 years for the quantum Hall effect that supports the exactness of the

relations $K_J = 2e/h$ and $R_K = h/e^2$ has been discussed in the three previous CODATA reports and references cited therein. The vast majority of the experimental evidence for both effects over the years comes from tests of the universality of these relations; that is, their invariance with experimental variables such as the material of which the Josephson effect and quantum-Hall-effect devices are fabricated. However, in both the 2002 and 2006 adjustments, the input data were used to test these relations experimentally in an "absolute" sense, that is by comparing the values of $2e/h$ and $h/e^2 = \mu_0 c/2\alpha$ implied by the data assuming the relations are exact with those implied by the data under the assumption that they are not exact. Indeed, such an analysis is given in this report in Sec. 13.2.3. Also briefly discussed there is the "metrology triangle." Here we discuss other developments of interest that have occurred between the closing dates of the 2006 and 2010 adjustments.

Noteworthy for the Josephson effect is the publication by Wood and Solve (2009) of "A review of Josephson comparison results." They examined a vast number of Josephson junction voltage comparisons conducted over the past 30 years involving many different laboratories, junction materials, types of junctions, operating frequencies, step numbers, number of junctions in series, voltage level, and operating temperature with some comparisons achieving a precision of a few parts in 10^{11}. They find no evidence that the relation $K_J = 2e/h$ is not universal.

There are three noteworthy developments for the quantum Hall effect. First is the recent publication of a *C. R. Physique* special issue on the quantum Hall effect and metrology with a number of theoretical as well as experimental papers that support the exactness of the relation $R_K = h/e^2$; see the Foreword to this issue by Glattli (2011) and the papers contained therein, as well as the recent review article by Weis and von Klitzing (2011).

The second is the agreement found between the value of R_K in a normal GaAs/AlGaAs heterostructure quantum-Hall-effect device and a graphene (two-dimensional graphite) device to within the 8.6 parts in 10^{11} uncertainty of the experiment (Janssen *et al.*, 2011, 2012). This is an extremely important result in support of the universality of the above relation, because of the significant difference in the charge carriers in graphene and the usual two dimensional semiconductor systems; see Kramer *et al.* (2010), Peres (2010), and Goerbig (2011).

The third is the theoretical paper by Penin (2009). Penin's calculations appear to show that the relation $R_K = h/e^2$ is not exact but should be written as $R_K = (h/e^2)[1 + C]$, where the correction C is due to vacuum polarization and is given by $C = -(2/45)(\alpha/\pi)(B/B_0)^2$. Here B is the magnetic flux density applied to the quantum-Hall-effect device and $B_0 = 2\pi c^2 m_e^2/he \approx 4.4 \times 10^9$ T. However, since B is generally no larger than 20 T, the correction, approximately -2×10^{-21}, is vanishingly small and can be completely ignored. Further, Penin (2009) argues that because of the topological nature of the quantum Hall effect, there can be no other type of correction including finite-size effects.

9. Measurements Involving Silicon Crystals

Experimental results obtained using nearly perfect single crystals of natural silicon are discussed here, along with a new result for N_A with a relative standard uncertainty of 3.0×10^{-8} obtained using highly enriched silicon. For this material, $x(^{28}\mathrm{Si}) \approx 0.999\,96$, compared to $x(^{28}\mathrm{Si}) \approx 0.92$ for natural silicon, where $x(^{A}\mathrm{Si})$ is the amount-of-substance fraction of the indicated isotope.

The new N_A result (see Sec. 9.6) as well as much of the natural silicon data used in the current and previous CODATA adjustments were obtained as part of an extensive international effort under way since the early 1990s to determine N_A with the smallest possible uncertainty. This worldwide enterprise, which has many participating laboratories and is called the International Avogadro Coordination (IAC), carries out its work under the auspices of the Consultative Committee for Mass and Related Quantities (CCM) of the CIPM.

The eight natural silicon crystal samples of interest here are denoted WASO 4.2a, WASO 04, WASO 17, NRLM3, NRLM4, MO*, ILL, and N, and the {220} crystal lattice spacing of each, $d_{220}(X)$, is taken as an adjusted constant. For simplicity the shortened forms W4.2a, W04, W17, NR3, and NR4 are used in quantity symbols for the first five crystals. Note also that crystal labels actually denote the single crystal ingot from which the crystal samples are taken, since no distinction is made between different samples taken from the same ingot.

Silicon is a cubic crystal with $n = 8$ atoms per face-centered cubic unit cell of edge length (or lattice parameter) $a \approx 543$ pm with {220} crystal lattice spacing $d_{220} = a/\sqrt{8} \approx 192$ pm. For practical purposes, it can be assumed that a, and thus d_{220}, of an impurity free, crystallographically perfect or "ideal" silicon crystal at specified conditions of temperature t, pressure p, and isotopic composition is an invariant of nature. The currently adopted reference conditions for natural silicon are $t_{90} = 22.5\,^{\circ}\mathrm{C}$ and $p = 0$ (vacuum), where t_{90} is Celsius temperature on the International Temperature Scale of 1990 (ITS-90). Reference values for $x(^{A}\mathrm{Si})$ have not been adopted, because any variation of $d_{220}(X)$ with the typical isotopic composition variation observed for the natural silicon crystals used is deemed negligible. To convert the lattice spacing $d_{220}(X)$ of a real crystal to the lattice spacing d_{220} of an ideal crystal requires the application of corrections for impurities, mainly carbon, oxygen, and nitrogen.

Typical variation in the lattice spacing of different samples from the same ingot is taken into account by including an additional relative standard uncertainty component of $\sqrt{2} \times 10^{-8}$ for each crystal in the uncertainty budget of any measurement result involving one or more silicon lattice spacings. However, the component is $(3/2)\sqrt{2} \times 10^{-8}$ in the case of crystal MO* because it is known to contain a comparatively large amount of carbon. For simplicity, we do not explicitly mention the inclusion of such components in the following discussion.

9.1. Measurements of $d_{220}(X)$ of natural silicon

Measurements of $d_{220}(X)$ are performed using a combined XROI. The interferometer has three lamenae from a single crystal, one of which can be displaced and is called the analyzer; see CODATA-98. Also discussed there is the measurement at PTB using an XROI with WASO 4.2a (Becker *et al.*, 1981) This result, which was taken as an input datum in the past three adjustments, is also used in the current adjustment; its value is

$$d_{220}(\text{W4.2a}) = 192\,015.563(12)\ \text{fm} \quad [6.2 \times 10^{-8}], \quad (249)$$

which is data item *B*41.1, labeled PTB-81, in Table 20.

The three other {220} natural silicon lattice spacings taken as input data in the 2010 adjustment, determined at the Istituto Nazionale di Ricerca Metrologica, (INRIM) Torino, Italy, using XROIs fabricated from MO*, WASO 04, and WASO 4.2a, are much more recent results. Ferroglio, Mana, and Massa (2008) report

$$d_{220}(\text{MO}^*) = 192\,015.5508(42)\ \text{fm} \quad [2.2 \times 10^{-8}], \quad (250)$$

which is data item *B*39, labeled INRIM-08; Massa *et al.* (2009) find

$$d_{220}(\text{WO4}) = 192\,015.5702(29)\ \text{fm} \quad [1.5 \times 10^{-8}], \quad (251)$$

which is data item *B*40, labeled INRIM-09; and Massa, Mana, and Kuetgens (2009) give

$$d_{220}(\text{W4.2a}) = 192\,015.5691(29)\ \text{fm} \quad [1.5 \times 10^{-8}], \quad (252)$$

which is data item *B*41.2, labeled INRIM-09.

The XROI used to obtain these three results is a new design with many special features. The most significant advance over previous designs is the capability to displace the analyzer by up to 5 cm. In the new apparatus, laser interferometers and capacitive transducers sense crystal displacement, parasitic rotations, and transverse motions, and feedback loops provide positioning with picometer resolution, alignment with nanometer resolution, and movement of the analyzer with nanometer straightness. A number of fractional corrections for different effects, such as laser wavelength, laser beam diffraction, laser beam alignment, and temperature of the crystal, are applied in each determination; the total correction for each of the three results, in parts in 10^9, is 6.5, −4.0, and 3.7, respectively. The relative standard uncertainties of the three lattice-spacing measurements without the additional uncertainty component for possible variation in the lattice spacing of different samples from the same ingot, again in parts in 10^9, are 6.1, 5.2, and 5.2.

The three INRIM lattice-spacing values are correlated with one another, as well as with the enriched silicon value of N_A discussed in Sec. 9.6. The latter correlation arises because the {220} lattice spacing of the enriched silicon was determined at INRIM by Massa, Mana, Kuetgens, and Ferroglio (2011) using the same XROI apparatus (relative standard uncertainty of 3.5 parts in 10^9 achieved). The relevant correlation coefficients for these data are given in Table 21 and are calculated using information provided to the Task Group by Mana (2011).

The many successful cross-checks of the performance of the new INRIM combined x-ray and optical interferometer lend support to the reliability of the results obtained with it. Indeed, Massa *et al.* (2011) describe a highly successful test based on the comparison of the lattice spacings of enriched and natural silicon determined using the new XROI. Consequently, the IAC (Mana, 2011) and the Task Group view the new INRIM values for $d_{220}(\text{MO}^*)$ and $d_{220}(\text{W04})$ as superseding the earlier INRIM values of these lattice spacings used in the 2006 adjustment.

9.2. d_{220} difference measurements of natural silicon crystals

Measurements of the fractional difference $[d_{220}(X) - d_{220}(\text{ref})]/d_{220}(\text{ref})$ of the {220} lattice spacing of a sample of a single crystal ingot X and that of a reference crystal "ref" enable the lattice spacings of crystals used in various experiments to be related to one another. Both NIST and PTB have carried out such measurements, and the fractional differences from these two laboratories that we take as input data in the 2010 adjustment are data items *B*42−*B*53 in Table 20, labeled NIST-97, NIST-99, NIST-06, PTB-98, and PTB-03. Their relevant correlation coefficients can be found in Table 21. For details concerning the NIST and PTB difference measurements, see the three previous CODATA reports. A discussion of item *B*53, the fractional difference between the {220} lattice spacing of an ideal natural silicon crystal d_{220} and $d_{220}(\text{W04})$, is given in CODATA-06 following Eq. (312).

9.3. Gamma-ray determination of the neutron relative atomic mass $A_r(n)$

The value of $A_r(n)$ listed in Table 2 from AME2003 is not used in the 2010 adjustment. Rather, $A_r(n)$ is obtained as described here so that the 2010 recommended value is consistent with the current data on the {220} lattice spacing of silicon.

The value of $A_r(n)$ is obtained from measurement of the wavelength of the 2.2 MeV γ ray in the reaction $n + p \rightarrow d + \gamma$. The result obtained from Bragg-angle measurements carried out at the high-flux reactor of ILL in a NIST and ILL collaboration is (Kessler, Jr., *et al.*, 1999)

$$\frac{\lambda_{\text{meas}}}{d_{220}(\text{ILL})} = 0.002\,904\,302\,46(50) \quad [1.7 \times 10^{-7}]. \quad (253)$$

Here $d_{220}(\text{ILL})$ is the {220} lattice spacing of the silicon crystals of the ILL GAMS4 spectrometer at $t_{90} = 22.5\,^{\circ}\text{C}$ and $p = 0$ used in the measurements. Relativistic kinematics of the reaction yields the observational equation (see CODATA-98)

$$\frac{\lambda_{\text{meas}}}{d_{220}(\text{ILL})} = \frac{\alpha^2 A_r(e)}{R_\infty d_{220}(\text{ILL})} \frac{A_r(n) + A_r(p)}{[A_r(n) + A_r(p)]^2 - A_r^2(d)}, \quad (254)$$

where the quantities on the right-hand side are adjusted constants.

9.4. Historic x-ray units

Units used in the past to express the wavelengths of x-ray lines are the copper $K\alpha_1$ x unit, symbol xu(CuKα_1), the molybdenum $K\alpha_1$ x unit, symbol xu(MoKα_1), and the ångstrom star, symbol Å*. They are defined by assigning an exact, conventional value to the wavelength of the CuKα_1, MoKα_1, and WKα_1 x-ray lines when each is expressed in its corresponding unit:

$$\lambda(\mathrm{CuK}\alpha_1) = 1\,537.400\ \mathrm{xu(CuK}\alpha_1), \tag{255}$$

$$\lambda(\mathrm{MoK}\alpha_1) = 707.831\ \mathrm{xu(MoK}\alpha_1), \tag{256}$$

$$\lambda(\mathrm{WK}\alpha_1) = 0.209\,010\,0\ \text{Å}^*. \tag{257}$$

The data relevant to these units are (see CODATA-98)

$$\frac{\lambda(\mathrm{CuK}\alpha_1)}{d_{220}(\mathrm{W4.2a})} = 0.802\,327\,11(24) \quad [3.0 \times 10^{-7}], \tag{258}$$

$$\frac{\lambda(\mathrm{WK}\alpha_1)}{d_{220}(\mathrm{N})} = 0.108\,852\,175(98) \quad [9.0 \times 10^{-7}], \tag{259}$$

$$\frac{\lambda(\mathrm{MoK}\alpha_1)}{d_{220}(\mathrm{N})} = 0.369\,406\,04(19) \quad [5.3 \times 10^{-7}], \tag{260}$$

$$\frac{\lambda(\mathrm{CuK}\alpha_1)}{d_{220}(\mathrm{N})} = 0.802\,328\,04(77) \quad [9.6 \times 10^{-7}], \tag{261}$$

where d_{220}(W4.2a) and d_{220}(N) denote the {220} lattice spacings, at the standard reference conditions $p = 0$ and $t_{90} = 22.5\,^{\circ}\mathrm{C}$, of particular silicon crystals used in the measurements. The result in Eq. (258) is from a collaboration between researchers from Friedrich-Schiller University (FSUJ), Jena, Germany, and the PTB (Härtwig *et al.*, 1991).

To obtain recommended values for xu(CuKα_1), xu(MoKα_1), and Å*, we take these units to be adjusted constants. The observational equations for the data of Eqs. (258)–(261) are

$$\frac{\lambda(\mathrm{CuK}\alpha_1)}{d_{220}(\mathrm{W4.2a})} = \frac{1\,537.400\ \mathrm{xu(CuK}\alpha_1)}{d_{220}(\mathrm{W4.2a})}, \tag{262}$$

$$\frac{\lambda(\mathrm{WK}\alpha_1)}{d_{220}(\mathrm{N})} = \frac{0.209\,010\,0\ \text{Å}^*}{d_{220}(\mathrm{N})}, \tag{263}$$

$$\frac{\lambda(\mathrm{MoK}\alpha_1)}{d_{220}(\mathrm{N})} = \frac{707.831\ \mathrm{xu(MoK}\alpha_1)}{d_{220}(\mathrm{N})}, \tag{264}$$

$$\frac{\lambda(\mathrm{CuK}\alpha_1)}{d_{220}(\mathrm{N})} = \frac{1\,537.400\ \mathrm{xu(CuK}\alpha_1)}{d_{220}(\mathrm{N})}, \tag{265}$$

where d_{220}(N) is taken to be an adjusted constant and d_{220}(W17) and d_{220}(W4.2a) are adjusted constants as well.

9.5. Other data involving natural silicon crystals

Two input data used in the 2006 adjustment but not used in the 2010 adjustment at the request of the IAC (Fujii, 2010) are discussed in this section.

The first is the {220} lattice spacing d_{220}(NR3) from the National Metrology Institute of Japan (NMIJ), Tsukuba, Japan, reported by Cavagnero *et al.* (2004). The IAC formally requested that the Task Group not consider this result for the 2010 adjustment, because of its questionable reliability due to the problems discussed in Sec. VIII.A.1.b of CODATA-06.

The second is the molar volume of natural silicon V_m(Si) from which N_A can be determined. The value used in the 2006 adjustment is (Fujii *et al.*, 2005) $12.058\,8254(34) \times 10^{-6}\ \mathrm{m^3\,mol^{-1}}$ $[2.8 \times 10^{-7}]$. The IAC requested that the Task Group no longer consider this result, because of problems uncovered with the molar mass measurements of natural silicon M(Si) at the Institute for Reference Materials and Measurements (IRMM), Geel, Belgium.

One problem is associated with the experimental determination of the calibration factors of the mass spectrometer used to measure the amount-of-substance ratios (see the following section) of the silicon isotopes ^{28}Si, ^{29}Si, and ^{30}Si in various silicon crystals, as discussed by Valkiers *et al.* (2011). The factors are critical, because molar masses are calculated from these ratios and the comparatively well-known relative atomic masses of the isotopes. Another problem is the unexplained large scatter of ± 7 parts in 10^7 in molar mass values among crystals taken from the same ingot, as discussed by Fujii *et al.* (2005) in connection with their result for V_m(Si) given above.

More specifically, from 1994 to 2005 IRMM measured the molar masses of natural silicon in terms of the molar mass of WASO17.2, which was determined using the now suspect calibration factors (Valkiers *et al.*, 2011). Based on a new determination of the calibration factors, Valkiers *et al.* (2011) report a value for the molar mass of WASO17.2 that has a relative standard uncertainty of 2.4×10^{-7}, compared to the 1.3×10^{-7} uncertainty of the value used since 1994, and which is fractionally larger by 1.34×10^{-6} than the earlier value. [The recent paper by Yi *et al.* (2012) also points to a correction of the same general magnitude.] This new result and the data and calculations in Fujii *et al.* (2005) yield the following revised value for the molar volume of natural silicon:

$$V_m(\mathrm{Si}) = 12.058\,8416(45) \times 10^{-6}\,\mathrm{m^3\,mol^{-1}} \quad [3.7 \times 10^{-7}]. \tag{266}$$

Although the IAC does not consider this result to be sufficiently reliable for the Task Group to consider it for inclusion in the 2010 adjustment, we note that based on the 2010 recommended values of d_{220} and the molar Planck

constant $N_A h$, Eq. (266) implies

$$N_A = 6.022\,1456(23) \times 10^{23}\ \text{mol}^{-1} \quad [3.8 \times 10^{-7}],$$
$$h = 6.626\,0649(25) \times 10^{-34}\ \text{J s} \quad [3.8 \times 10^{-7}]. \qquad (267)$$

The difference between this value of N_A and the value with relative standard uncertainty 3.0×10^{-8} obtained from enriched silicon discussed in the next section is 7.9(3.8) parts in 10^7, while the difference between the NIST 2007 watt-balance value of h with uncertainty 3.6×10^{-8} and this value of h is 6.1(3.8) parts in 10^7.

9.6. Determination of N_A with enriched silicon

The IAC project to determine N_A using the x ray crystal density (XRCD) method and silicon crystals highly enriched with ^{28}Si was formally initiated in 2004, but its origin dates back two decades earlier. Its initial result is discussed in detail in a *Metrologia* special issue; see the Foreword by Massa and Nicolaus (2011), the 14 technical papers in the issue, and the references cited therein. The first paper, by Andreas *et al.* (2011a), provides an extensive overview of the entire project. The value of the Avogadro constant obtained from this unique international collaborative effort, identified as IAC-11, input datum *B*54, is (Andreas *et al.*, 2011a)

$$N_A = 6.022\,140\,82(18) \times 10^{23}\ \text{mol}^{-1} \quad [3.0 \times 10^{-8}]. \qquad (268)$$

Note that this result differs slightly from the somewhat earlier result reported by Andreas *et al.* (2011b) but is the preferred value (Bettin, 2011).

The basic equation for the XRCD determination of N_A has been discussed in previous CODATA reports. In brief,

$$N_A = \frac{A_r(\text{Si}) M_u}{\sqrt{8} d_{220}^3 \rho(\text{Si})}, \qquad (269)$$

which would apply to an impurity free, crystallographically perfect, ideal silicon crystal. Here A_r(Si) is the mean relative atomic mass of the silicon atoms in such a crystal, and ρ(Si) is the crystal's macroscopic mass density. (In this section, these quantities, as well as d_{220}, are for isotopically enriched silicon.) Thus, to determine N_A from Eq. (269) requires determining the density ρ(Si), the {220} lattice spacing d_{220}, and the amount-of-substance ratios $R_{29/28} = n(^{29}\text{Si})/n(^{28}\text{Si})$ and $R_{30/28} = n(^{30}\text{Si})/n(^{28}\text{Si})$ so that A_r(Si) can be calculated using the well-known values of $A_r(^A\text{Si})$. Equally important is the characterization of the material properties of the crystals used, for example, impurity content, nonimpurity point defects, dislocations, and microscopic voids must be considered.

The international effort to determine the Avogadro constant, as described in the *Metrologia* special issue, involved many tasks including the following: enrichment and polycrystal growth of silicon in the Russian Federation; growth and purification of a 5 kg single silicon crystal ingot in Germany; measurement of the isotopic composition of the crystals at PTB; measurement of the lattice spacing with the newly developed XROI described above at INRIM; grinding and polishing of two spheres cut from the ingot to nearly perfect spherical shape at NMI; optical interferometric measurement of the diameters of the spheres at PTB and NMIJ; measurement of the masses of the spheres in vacuum at PTB, NMIJ, and BIPM; and characterization of and correction for the effect of the contaminants on the surfaces of the spheres at various laboratories.

The uncertainty budget for the IAC value of N_A is dominated by components associated with determining the volumes and the surface properties of the spheres, followed by those related to measuring their lattice spacings and their molar masses. These four components, in parts in 10^9, are 29, 15, 11, and 8 for the sphere designated AVO28-S5.

How this result compares with other data and its role in the 2010 adjustment is discussed in Sec. 13.

10. Thermal Physical Quantities

Table 16 summarizes the eight results for the thermal physical quantities R, k, and k/h, the molar gas constant, the Boltzmann constant, and the quotient of the Boltzmann and Planck constants, respectively, that are taken as input data in the 2010 adjustment. They are data items *B*58.1−*B*60 in

TABLE 16. Summary of thermal physical measurements relevant to the 2010 adjustment (see text for details). AGT: acoustisc gas thermometry; RIGT: refractive index gas thermometry; JNT: Johnson noise thermometry; cylindrical, spherical, quasispherical: shape of resonator used; JE and QHE: Josephson effect voltage and quantum-Hall-effect resistance standards.

Source	Identification[a]	Quantity	Method	Value	Rel. stand. uncert. u_r
Colclough *et al.* (1979)	NPL-79	R	AGT, cylindrical, argon	8.314 504(70) J mol^{-1} K^{-1}	8.4×10^{-6}
Moldover *et al.* (1988)	NIST-88	R	AGT, spherical, argon	8.314 471(15) J mol^{-1} K^{-1}	1.8×10^{-6}
Pitre *et al.* (2009)	LNE-09	R	AGT, quasispherical, helium	8.314 467(22) J mol^{-1} K^{-1}	2.7×10^{-6}
Sutton *et al.* (2010)	NPL-10	R	AGT, quasispherical, argon	8.314 468(26) J mol^{-1} K^{-1}	3.1×10^{-6}
Gavioso *et al.* (2010)	INRIM-10	R	AGT, spherical, helium	8.314 412(63) J mol^{-1} K^{-1}	7.5×10^{-6}
Pitre *et al.* (2011)	LNE-11	R	AGT, quasispherical, argon	8.314 456(10) J mol^{-1} K^{-1}	1.2×10^{-6}
Schmidt *et al.* (2007)	NIST-07	k	RIGT, quasispherical, helium	$1.380\,653(13) \times 10^{-23}$ J K^{-1}	9.1×10^{-6}
Benz *et al.* (2011)	NIST-11	k/h	JNT, JE and QHE	$2.083\,666(25) \times 10^{10}$ Hz K^{-1}	1.2×10^{-5}

[a]NPL: National Physical Laboratory, Teddington, UK; NIST: National Institute of Standards and Technology, Gaithersburg, MD, and Boulder, CO, USA; LNE: Laboratoire commun de métrologie (LCM), Saint-Denis, France, of the Laboratoire national de métrologie et d'essais (LNE); INRIM: Istituto Nazionale di Ricerca Metrologica, Torino, Italy.

Table 20 with correlation coefficients as given in Table 21 and observational equations as given in Table 33. Values of k that can be inferred from these data are given in Table 27 and are graphically compared in Fig. 4. The first two results, the NPL 1979 and NIST 1988 values of R, were included in the three previous CODATA adjustments, but the other six became available during the four years between the closing dates of the 2006 and 2010 adjustments. (Note that not every result in Table 16 appears in the cited reference. For some, additional digits have been provided to the Task Group to reduce rounding errors; for others, the value of R or k actually determined in the experiment is recovered from the reported result using the relation $R = kN_A$ and the value of N_A used by the researchers to obtain that result.)

10.1. Acoustic gas thermometry

As discussed in CODATA-98 and the references cited therein, measurement of R by the method of acoustic gas thermometry (AGT) is based on the following expressions for the square of the speed of sound in a real gas of atoms or molecules in thermal equilibrium at thermodynamic temperature T and pressure p and occupying a volume V:

$$c_a^2(T,p) = A_0(T) + A_1(T)p + A_2(T)p^2 + A_3(T)p^3 + \cdots. \quad (270)$$

Here $A_1(T)$ is the first acoustic virial coefficient, $A_2(T)$ is the second, etc., In the limit $p \to 0$, this becomes

$$c_a^2(T,0) = A_0(T) = \frac{\gamma_0 RT}{A_r(X)M_u}, \quad (271)$$

where $\gamma_0 = c_p/c_V$ is the ratio of the specific heat capacity of the gas at constant pressure to that at constant volume and is $5/3$ for an ideal monotonic gas. The basic experimental approach to determining the speed of sound of a gas, usually argon or helium, is to measure the acoustic resonant frequencies of a cavity at or near the triple point of water, $T_{TPW} = 273.16$ K, and at various pressures and extrapolating to $p = 0$. The cavities are cylindrical of either fixed or variable length, or spherical, but most commonly quasispherical in the form of a triaxial ellipsoid. This shape removes the degeneracy of the microwave resonances used to measure the volume of the resonator in order to calculate $c_a^2(T,p)$ from the measured acoustic frequencies and the corresponding acoustic resonator eigenvalues known from theory. The cavities are formed by carefully joining quasihemispherical cavities.

In practice, the determination of R by AGT with a relative standard uncertainty of order 1 part in 10^6 is complex; the application of numerous corrections is required as well as the investigation of many possible sources of error. For a review of the advances made in AGT in the past 20 years, see Moldover (2009).

10.1.1. NPL 1979 and NIST 1988 values of *R*

Both the NPL and NIST experiments are discussed in detail in CODATA-98. We only note here that the NPL measurement used argon in a vertical, variable-path-length, 30 mm inner diameter cylindrical acoustic resonator operated at a fixed frequency, and the displacement of the acoustic reflector that formed the top of the resonator was measured using optical interferometry. The NIST experiment also used argon, and the volume of the stainless steel spherical acoustic resonator, of approximate inside diameter 180 mm, was determined from the mass of mercury of known density required to fill it. The 1986 CODATA recommended value of R is the NPL result while the 1998, 2002, and 2006 CODATA recommended values are the weighted means of the NPL and NIST results.

10.1.2. LNE 2009 and 2011 values of *R*

Pitre *et al.* (2009) and Pitre (2011) obtained the LNE 2009 result using a copper quasisphere of about 100 mm inner diameter and helium gas. The principal advantage of helium is that its thermophysical properties are well known based on *ab initio* theoretical calculations; the principal disadvantage is that because of its comparatively low mass, impurities have a larger effect on the speed of sound. This problem is mitigated by passing the helium gas through a liquid helium trap and having a continuous flow of helium through the resonator, thereby reducing the effect of outgassing from the walls of the resonator. In calculating the molar mass of the helium Pitre *et al.* (2009) assumed that the only remaining impurity is ^{3}He and that the ratio of ^{3}He to ^{4}He is less than 1.3×10^{-6}.

The critically important volume of the resonator was determined from measurements of its electromagnetic (EM) resonances together with relevant theory of the eigenvalues. The dimensions of the quasihemispheres were also measured using a coordinate measuring machine (CMM). The volumes so obtained agreed, but the 17×10^{-6} relative standard uncertainty of the CMM determination far exceeded the 0.85×10^{-6} relative uncertainty of the EM determination. The principal uncertainty components that contribute to the 2.7 parts in 10^6 uncertainty of the final result are, in parts in 10^6, 1.8, 1.0, 1.5, and 0.8 due, respectively, to measurement of the volume of the quasisphere (including various corrections), its temperature relative to T_{TPW}, extrapolation of $c_a^2(T_{TPW},p)$ to $p = 0$, and the reproducibility of the result, based on two runs using different purities of helium and different acoustic transducers (Pitre, 2011).

The 2011 LNE result for R, which has the smallest uncertainty of any reported to date, is described in great detail by Pitre *et al.* (2011). It was obtained using the same quasispherical resonator employed in the 2009 experiment, but with argon in place of helium. The reduction in uncertainty by more than a factor of 2 was achieved by improving all aspects of the experiment (Pitre *et al.*, 2011). The volume of the resonator was again determined from measurements of its EM resonances and cross checked with CMM dimensional measurements of the quasispheres carried out at NPL (de Podesta *et al.*, 2010). As usual in AGT, the square of the speed of sound was determined from measurements of the quasisphere's acoustic resonant frequencies at different pressures (50 kPa to 700 kPa in this case) and extrapolation to $p = 0$. The isotopic

composition of the argon and its impurity content was determined at IRMM (Valkiers *et al.*, 2010).

The five uncertainty components of the final 1.24 parts in 10^6 uncertainty of the result, with each component itself being composed of a number of subcomponents, are, in parts in 10^6, the following: 0.30 from temperature measurements (the nominal temperature of the quasisphere was T_{TPW}), 0.57 from the EM measurement of the quasisphere's volume, 0.84 from the determination of $c_{\mathrm{a}}^2(T_{\mathrm{TPW}}, 0)$, 0.60 associated with the argon molar mass and its impurities, and 0.25 for experimental repeatability based on the results from two series of measurements carried out in May and July of 2009.

Because the LNE 2009 and 2011 results are from experiments in which some of the equipment and measuring techniques are the same or similar, they are correlated. Indeed, for the same reason, there are non-negligible correlations among the four recent AGT determinations of R, that is, LNE-09, NPL-10, INRIM-10, and LNE-11. These correlations are given in Table 21 and have been calculated using information provided to the Task Group by researchers involved in the experiments (Gavioso, de Podesta, and Pitre, 2011).

10.1.3. NPL 2010 value of *R*

This result was obtained at NPL by Sutton *et al.* (2010) and de Podesta (2011) at T_{TPW} using a thin-walled copper quasispherical resonator of about 100 mm inner diameter on loan from LNE and argon as the working gas. The internal surfaces of the quasihemispheres were machined using diamond turning techniques. The 5 mm wall thickness of the quasisphere, about one-half that of the usual AGT resonators, was specially chosen to allow improved study of the effect of resonator shell vibrations on acoustic resonances. The volume of the quasisphere was determined from measurements of EM resonances and checked with CMM dimensional measurements of the quasihemispheres before assembly (de Podesta *et al.*, 2010). Two series of measurements were carried out, each lasting several days: one with the quasisphere rigidly attached to a fixed stainless steel post and one with it freely suspended by three wires attached to its equator. Pressures ranged from 50 kPa to 650 kPa and were measured with commercial pressure meters. The isotopic composition of the argon and its impurity content were again determined at IRMM (Valkiers *et al.*, 2010).

The final result is the average of the value obtained from each run. The 3.78 parts in 10^6 difference between the molar mass of the argon used in the fixed and hanging quasisphere runs is to a large extent canceled by the -2.77 parts in 10^6 difference between the values of $c_{\mathrm{a}}^2(T_{\mathrm{TPW}}, 0)$ for the two runs, so the two values of R agree within 1.01 parts in 10^6. The largest uncertainty components in parts in 10^6 contributing to the final uncertainty of 3.1 parts in 10^6 are, respectively (de Podesta *et al.*, 2010; Sutton *et al.*, 2010), 2, 1.1, 0.9, 1, and 1.4 arising from the difference between the acoustic and microwave volumes of the resonator, temperature calibration, temperature measurement, argon gas impurities, and correction for the layer of gas near the wall of the resonator (thermal boundary layer correction).

10.1.4. INRIM 2010 value of *R*

The INRIM determination of R by Gavioso *et al.* (2010) and Gavioso (2011) employed a stainless steel spherical resonator of about 182 mm inner diameter and nonflowing helium gas. Although the measurements were performed with the resonator very near T_{TPW} as in the other AGT molar-gas-constant determinations, two important aspects of the INRIM experiment are quite different. First, the speed of sound was measured at only one pressure, namely, 410 kPa, and the extrapolation to $p = 0$ was implemented using the comparatively well-known theoretical values of the required ^{4}He equation-of-state and acoustic virial coefficients. Second, the radius of the resonator was determined using the theoretical value of the ^{4}He index of refraction together with eight measured EM resonance frequencies and the corresponding predicted eigenvalues. The speed of sound was then calculated from this value of the radius and measured acoustic resonant frequencies. Gavioso *et al.* (2010) calculated the molar mass of their He sample assuming the known atmospheric abundance of ^{3}He represents an upper limit.

The two uncertainty components that are by far the largest contributors to the 7.5 parts in 10^6 final uncertainty of the experiment are, in parts in 10^6, 4.2 from fitting the shape of the eight measured microwave modes and 4.8 from the scatter of the squared frequencies of the six measured radial acoustic modes used to determine $c_{\mathrm{a}}^2(T_{\mathrm{TPW}}, p = 410\ \mathrm{kPa})$.

10.2. Boltzmann constant *k* and quotient *k*/*h*

The following two sections discuss the two NIST experiments that have yielded the last two entries of Table 16.

10.2.1. NIST 2007 value of *k*

This result was obtained by Schmidt *et al.* (2007) using the technique of refractive index gas thermometry (RIGT), an approach similar to that of dielectric constant gas thermometry (DCGT) discussed in CODATA-98, and to a lesser extent in CODATA-02 and CODATA-06. The starting point of both DCGT and RIGT is the virial expansion of the equation of state for a real gas of amount of substance n in a volume V (Schmidt *et al.*, 2007),

$$p = \rho RT[1 + \rho b(T) + \rho^2 c(T) + \rho^3 d(T) + \cdots], \tag{272}$$

where $\rho = n/V$ is the amount-of-substance density of the gas at thermodynamic temperature T, and $b(T)$ is the first virial

coefficient, $c(T)$ is the second, etc.; and the Clausius-Mossotti equation

$$\frac{\epsilon_r - 1}{\epsilon_r + 2} = \rho A_\epsilon [1 + \rho B_\epsilon(T) + \rho^2 C_\epsilon(T) + \rho^3 D_\epsilon(T) + \cdots], \tag{273}$$

where $\epsilon_r = \epsilon/\epsilon_0$ is the relative dielectric constant (relative permittivity) of the gas, ϵ is its dielectric constant, ϵ_0 is the exactly known electric constant, A_ϵ is the molar polarizability of the atoms, and $B_\epsilon(T)$, $C_\epsilon(T)$, etc., are the dielectric virial coefficients. The static electric polarizability of a gas atom α_0, and A_ϵ, R, and k are related by $A_\epsilon/R = \alpha_0/3\epsilon_0 k$, which shows that if α_0 is known sufficiently well from theory, which it currently is for ^{4}He (Łach, Jeziorski, and Szalewicz, 2004; Jentschura, Puchalski, and Mohr, 2011; Puchalski, Jentschura, and Mohr, 2011), then a competitive value of k can be obtained if the quotient A_ϵ/R can be measured with a sufficiently small uncertainty.

In fact, by appropriately combining Eqs. (272) and (273), an expression is obtained from which A_ϵ/R can be experimentally determined by measuring ϵ_r at a known constant temperature such as T_{TPW} and at different pressures and extrapolating to zero pressure. This is done in practice by measuring the fractional change in capacitance of a specially constructed capacitor, first without helium gas and then with helium gas at a known pressure. This is the DCGT technique.

In the RIGT technique of Schmidt *et al.* (2007), A_ϵ/R is determined, and hence k, from measurements of $n^2(T,p) \equiv \epsilon_r \mu_r$ of a gas of helium, where $n(T,p)$ is the index of refraction of the gas, $\mu_r = \mu/\mu_0$ is the relative magnetic permeability of the gas, μ is its magnetic permeability, and μ_0 is the exactly known magnetic constant. Because ^{4}He is slightly diamagnetic, the quantity actually determined is $(A_\epsilon + A_\mu)/R$, where $A_\mu = 4\pi\chi_0/3$ and χ_0 is the diamagnetic susceptibility of a ^{4}He atom. The latter quantity is known from theory and the theoretical value of A_μ was used to obtain A_ϵ/R from the determined quantity.

Schmidt *et al.* (2007) obtained $n(T,p)$ by measuring the microwave resonant frequencies from 2.7 GHz to 7.6 GHz of a quasispherical copper plated resonator, either evacuated or filled with He at pressures of 0.1 MPa to 6.3 MPa. The temperature of the resonator was within a few millikelvin of T_{TPW}. A network analyzer was used to measure the resonant frequencies and a calibrated pressure balance to measure p. The extrapolation to $p = 0$ employed both theoretical and experimental values of the virial coefficients B, C, D, b, and c taken from the literature. The uncertainties of these coefficients and of the pressure and temperature measurements, and the uncertainty of the isothermal compressibility of the resonator, are the largest components in the uncertainty budget.

10.2.2. NIST 2011 value of k/h

As discussed in CODATA-98, the Nyquist theorem predicts, with a fractional error of less than 1 part in 10^6 at frequencies less than 10 MHz and temperatures greater than 250 K, that

$$\langle U^2 \rangle = 4kTR_s\Delta f. \tag{274}$$

Here $\langle U^2 \rangle$ is the mean square voltage, or Johnson noise voltage, in a measurement bandwidth of frequency Δf across the terminals of a resistor of resistance R_s in thermal equilibrium at thermodynamic temperature T. If $\langle U^2 \rangle$ is measured in terms of the Josephson constant $K_J = 2e/h$ and R_s in terms of the von Klitzing constant $R_K = h/e^2$, then this experiment yields a value of k/h.

Such an experiment has been carried out at NIST, yielding the result in Table 16; see the paper by Benz *et al.* (2011) and references therein. In that work, digitally synthesized pseudonoise voltages are generated by means of a pulse-biased Josephson junction array. These known voltages are compared to the unknown thermal-noise voltages generated by a specially designed 100 Ω resistor in a well regulated thermal cell at or near T_{TPW}. Since the spectral density of the noise voltage of a 100 Ω resistor at 273.16 K is only 1.23 nV$\sqrt{\text{Hz}}$, it is measured using a low-noise, two-channel, cross-correlation technique that enables the resistor signal to be extracted from uncorrelated amplifier noise of comparable amplitude and spectral density. The bandwidths range from 10 kHz to 650 kHz. The final result is based on two data runs, each of about 117 hour duration, separated in time by about three months.

The dominant uncertainty component of the 12.1 parts in 10^6 total uncertainty is the 12.0 parts in 10^6 component due to the measurement of the ratio $\langle V_R^2/V_Q^2 \rangle$, where V_R is the resistor noise voltage and V_Q is the synthesized voltage. The main uncertainty component contributing to the uncertainty of the ratio is 10.4 parts in 10^6 due to spectral aberrations, that is, effects that lead to variations of the ratio with bandwidth.

10.3. Other data

We note for completeness the following three results, each of which agrees with its corresponding 2010 recommended value. The first has a noncompetitive uncertainty but is of interest because it is obtained from a relatively new method that could yield a value with a competitive uncertainty in the future. The other two became available only after the 31 December 2010 closing date of the 2010 adjustment.

Lemarchand *et al.* (2011) find $R = 8.314\,80(42)$ J m^{-1} K^{-1} [50×10^{-6}] determined by the method of Doppler spectroscopy, in particular, by measuring near the ice point $T = 273.15$ K the absorption profile of a rovibrational line at $\nu = 30$ THz of ammonia molecules in an ammonium gas in thermal equilibrium. The width of the line is mainly determined by the Doppler width due to the velocity distribution of the NH_3 molecules along the direction of the incident laser beam. The relevant expression is

$$\frac{\Delta\omega_D}{\omega_0} = \left(\frac{2kT}{m(NH_3)c^2}\right)^{1/2} = \left(\frac{2RT}{A_r(NH_3)M_u c^2}\right)^{1/2}, \tag{275}$$

where $\Delta\omega_D$ is the e-fold angular frequency half-width of the Doppler profile of the ammonium line at temperature T, ω_0 is its angular frequency, and $m(NH_3)$ and $A_r(NH_3)$ are the mass and relative atomic mass of the ammonium molecule.

Zhang (2011) and Zhang *et al.* (2011) obtain $R = 8.314\,474(66)$ J mol^{-1} K^{-1} $[7.9 \times 10^{-6}]$ using acoustic gas thermometry with argon gas, more specifically, by measuring resonant frequencies of a fixed-path-length cylindrical acoustic resonator at T_{TPW}; its approximate 129 mm length is measured by two-color optical interferometry.

Fellmuth *et al.* (2011) and Gaiser and Fellmuth (2012) give $k = 1.380\,655(11) \times 10^{-23}$ J/K $[7.9 \times 10^{-6}]$ measured using dielectric gas thermometry (see Sec. 10.2.1) and helium gas at T_{TPW} and also at temperatures in the range 21 K to 27 K surrounding the triple point of neon at $T \approx 25$ K.

10.4. Stefan-Boltzmann constant σ

The Stefan-Boltzmann constant is related to c, h, and k by $\sigma = 2\pi^5 k^4/15h^3c^2$, which, with the aid of the relations $k = R/N_A$ and $N_A h = cA_r(e)M_u\alpha^2/2R_\infty$, can be expressed in terms of the molar gas constant and other adjusted constants as

$$\sigma = \frac{32\pi^5 h}{15c^6}\left(\frac{R_\infty R}{A_r(e)M_u\alpha^2}\right)^4. \qquad (276)$$

Since no competitive directly measured value of σ is available for the 2010 adjustment, the 2010 recommended value is obtained from this equation.

11. Newtonian Constant of Gravitation G

Table 17 summarizes the 11 values of the Newtonian constant of gravitation G of interest in the 2010 adjustment. Because they are independent of the other data relevant to the current adjustment, and because there is no known quantitative theoretical relationship between G and other fundamental constants, they contribute only to the determination of the 2010 recommended value of G. The calculation of this value is discussed in Sec. 13.2.1.

The inconsistencies between different measurements of G as discussed in the reports of previous CODATA adjustments demonstrate the historic difficulty of determining this most important constant. Unfortunately, this difficulty has been demonstrated anew with the publication of two new competitive results for G during the past four years. The first is an improved value from the group at the Huazhong University of Science and Technology (HUST), PRC, identified as HUST-09 (Luo *et al.*, 2009; Tu *et al.*, 2010); the second is a completely new value from researchers at JILA, Boulder, Colorado, USA, identified as JILA-10 (Parks and Faller, 2010).

The publication of the JILA value has led the Task Group to reexamine and modify two earlier results. The first is that obtained at NIST (then known as the National Bureau of Standards) by Luther and Towler (1982) in a NIST-University of Virginia (UVa) collaboration, labeled NIST-82. This value was the basis for the CODATA 1986 recommended value (Cohen and Taylor, 1987) and was taken into account in determining the CODATA 1998 value (Mohr and Taylor, 2000), but played no role in either the 2002 or 2006 adjustments. The second is the Los Alamos National Laboratory (LANL), Los Alamos, USA, result of Bagley and Luther (1997), labeled LANL-97; it was first included in the 1998 CODATA adjustment and in all subsequent adjustments. The 11 available values of G, which are data items $G1-G11$ in Table 24, Sec. 13, are the same as in 2006 with the exception of NIST-82, slightly modified LANL-97, and the two new values. Thus, in keeping with our approach in this report, there is no discussion of the other seven values since they have been covered in one or more of the previous reports.

TABLE 17. Summary of the results of measurements of the Newtonian constant of gravitation G relevant to the 2010 adjustment.

Source	Identification[a]	Method	Value (10^{-11} m^3 kg^{-1} s^{-2})	Rel. stand. uncert. u_r
Luther and Towler (1982)	NIST-82	Fiber torsion balance, dynamic mode	6.672 48(43)	6.4×10^{-5}
Karagioz and Izmailov (1996)	TR&D-96	Fiber torsion balance, dynamic mode	6.672 9(5)	7.5×10^{-5}
Bagley and Luther (1997)	LANL-97	Fiber torsion balance, dynamic mode	6.673 98(70)	1.0×10^{-4}
Gundlach and Merkowitz (2000, 2002)	UWash-00	Fiber torsion balance, dynamic compensation	6.674 255(92)	1.4×10^{-5}
Quinn *et al.* (2001)	BIPM-01	Strip torsion balance, compensation mode, static deflection	6.675 59(27)	4.0×10^{-5}
Kleinevoß (2002); Kleinvoß *et al.* (2002)	UWup-02	Suspended body, displacement	6.674 22(98)	1.5×10^{-4}
Armstrong and Fitzgerald (2003)	MSL-03	Strip torsion balance, compensation mode	6.673 87(27)	4.0×10^{-5}
Hu, Guo, and Luo (2005)	HUST-05	Fiber torsion balance, dynamic mode	6.672 28(87)	1.3×10^{-4}
Schlamminger *et al.* (2006)	UZur-06	Stationary body, weight change	6.674 25(12)	1.9×10^{-5}
Luo *et al.* (2009); Tu *et al.* (2010)	HUST-09	Fiber torsion balance, dynamic mode	6.673 49(18)	2.7×10^{-5}
Parks and Faller (2010)	JILA-10	Suspended body, displacement	6.672 34(14)	2.1×10^{-5}

[a]NIST: National Institute of Standards and Technology, Gaithersburg, MD, USA; TR&D: Tribotech Research and Development Company, Moscow, Russian Federation; LANL: Los Alamos National Laboratory, Los Alamos, New Mexico, USA; UWash: University of Washington, Seattle, Washington, USA; BIPM: International Bureau of Weights and Measures, Sèvres, France; UWup: University of Wuppertal, Wuppertal, Germany; MSL: Measurement Standards Laboratory, Lower Hutt, New Zealand; HUST: Huazhong University of Science and Technology, Wuhan, PRC; UZur: University of Zurich, Zurich, Switzerland; JILA: a joint institute of the University of Colorado and NIST, Boulder, Colorado, USA.

For simplicity we write G as a numerical factor multiplying G_0, where

$$G_0 = 10^{-11}\ \mathrm{m^3\,kg^{-1}\,s^{-2}}. \quad (277)$$

11.1. Updated values

11.1.1. National Institute of Standards and Technology and University of Virginia

As discussed in CODATA-98, the experiment of Luther and Towler (1982) used a fiber-based torsion balance operated in the dynamic mode and the time-of-swing method, thereby requiring measurement of a small change in the long oscillation period of the balance. Ideally, the torsional spring constant of the fiber should be independent of frequency at very low frequencies, for example, at 3 mHz.

Long after the publication of the NIST-UVa result, Kuroda (1995) [see also Matsumura *et al.* (1998) and Kuroda (1999)] pointed out that the anelasticity of such fibers is sufficiently large to cause the value of G determined in this way to be biased. If Q is the quality factor of the main torsional mode of the fiber and it is assumed that the damping of the torsion balance is solely due to the losses in the fiber, then the unbiased value of G is related to the experimentally observed value G(obs) by (Kuroda, 1995)

$$G = \frac{G(\mathrm{obs})}{1 + \pi Q}. \quad (278)$$

Although the exact value of the Q of the fiber used in the NIST-UVa experiment is unknown, Luther (2010) provided an estimate, based on data obtained during the course of the experiment, of no less than 10 000 and no greater than 30 000. Assuming a rectangular probability density function for Q with these lower and upper limits then leads to $Q = 2 \times 10^4$ with a relative standard uncertainty of 4.6×10^{-6}. Using these values, the result $G(\mathrm{obs}) = 6.672\,59(43)G_0$ $[64 \times 10^{-6}]$ (Luther and Towler, 1982; Luther, 1986), and Eq. (278) we obtain

$$G = 6.672\,48(43)G_0 \quad [6.4 \times 10^{-5}]. \quad (279)$$

In this case the correction $1/(1 + \pi Q)$ reduced G(obs) by the fractional amount $15.9(4.6) \times 10^{-6}$, but increased its 64×10^{-6} relative standard uncertainty by a negligible amount.

The Task Group decided to include the value given in Eq. (279) as an input datum in the 2010 adjustment even though it was not included in the 2002 and 2006 adjustments, because information provided by Luther (2010) allows the original result to be corrected for the Kuroda effect. Further, although there were plans to continue the NIST-UVa experiment (Luther and Towler, 1982), recent conversations with Luther (2010) made clear that the measurements on which the result is based were thorough and complete.

11.1.2. Los Alamos National Laboratory

The experiment of Bagley and Luther (1997), also described in detail in CODATA-98, is similar to the NIST-UVa experiment of Luther and Towler (1982), and in fact used some of the same components including the tungsten source masses. Its purpose was not only to determine G, but also to test the Kuroda hypothesis by using two different fibers, one with $Q = 950$ and the other with $Q = 490$. Because the value of G resulting from this experiment is correlated with the NIST-UVa value and both values are now being included in the adjustment, we evaluated the correlation coefficient of the two results. This was done with information from Bagley (2010) and Luther (2010) and Bagley (1996). We also recalculated the result of the experiment of Bagley and Luther (1997) by taking into account the uncertainties of the two Q values (2%) and the correlation coefficient of the two values of G obtained from the two fibers (0.147) when computing their weighted mean. The final value is

$$G = 6.673\,98(70)G_0 \quad [1.0 \times 10^{-4}], \quad (280)$$

which in fact is essentially the same as the value used in the 2002 and 2006 adjustments. The correlation coefficient of the NIST-UVa and LANL values of G is 0.351.

11.2. New values

11.2.1. Huazhong University of Science and Technology

The improved HUST-09 result for G was first reported by Luo *et al.* (2009) and subsequently described in detail by Tu *et al.* (2010); it represents a reduction in uncertainty, compared to the previous Huazhong University result HUST-05, of about a factor of 5. As pointed out by Tu *et al.* (2010), a number of changes in the earlier experiment contributed to this uncertainty reduction, including (i) replacement of the two stainless steel cylindrical source masses by spherical source masses with a more homogeneous density; (ii) use of a rectangular quartz block as the principal portion of the torsion balance's pendulum, thereby improving the stability of the period of the balance and reducing the uncertainty of the pendulum's moment of inertia; (iii) a single vacuum chamber for the source masses and pendulum leading to a reduction of the uncertainty of their relative positions; (iv) a remotely operated stepper motor to change the positions of the source masses, thereby reducing environmental changes; and (v) measurement of the anelasticity of the torsion fiber with the aid of a high-Q quartz fiber.

The final result is the average of two values of G that differ by 9 parts in 10^6 obtained from two partially correlated determinations using the same apparatus. The dominant components of uncertainty, in parts in 10^6, are 19 from the measurement of the fiber's anelasticity, 14 (statistical) from the measurement of the change in the square of the angular frequency of the pendulum when the source masses are in their

near and far positions, and 10 from the measured distance between the geometric centers of the source masses. Although the uncertainty of HUST-05 is 5 times larger than that of HUST-09, Luo (2010) and co-workers do not believe that HUST-09 supersedes HUST-05. Thus, both are considered for inclusion in the 2010 adjustment. Based on information provided to the Task Group by the researchers (Luo, 2010), their correlation coefficient is estimated to be 0.234 and is used in the calculations of Sec. 13. The extra digits for the value and uncertainty of HUST-05 were also provided by Luo (2011).

11.2.2. JILA

As can be seen from Table 17, the 21×10^{-6} relative standard uncertainty of the value of G identified as JILA-10 and obtained at JILA by Parks and Faller (2010) has the third smallest estimated uncertainty of the values listed and is the second smallest of those values. It differs from the value with the smallest uncertainty, identified as UWash-00, by 287(25) parts in 10^6, which is 11 times the standard uncertainty of their difference u_{diff}, or 11σ. This disagreement is an example of the "historic difficulty" referred to at the very beginning of this section. The data on which the JILA researchers based their result were taken in 2004, but being well aware of this inconsistency they hesitated to publish it until they checked and rechecked their work (Parks and Faller, 2010). With this done, they decided it was time to report their value for G.

The apparatus used in the JILA experiment of Parks and Faller (2010) consisted of two 780 g copper test masses (or "pendulum bobs") separated by 34 cm, each of which was suspended from a supporting bar by four wires and together they formed a Fabry-Perot cavity. When the four 120 kg cylindrical tungsten source masses, two pairs with each member of the pair on either side of the laser beam traversing the cavity, were periodically moved parallel to the laser beam from their inner and outer positions (they remained stationary for 80 s in each position), the separation between the bobs changed by about 90 nm. This change was observed as a 125 MHz beat frequency between the laser locked to the pendulum cavity and the laser locked to a reference cavity that was part of the supporting bar. The geometry of the experiment reduces the most difficult aspect of determining the gravitational field of the source masses to six one dimensional measurements: the distance between opposite source mass pairs in the inner and outer positions and the distances between adjacent source masses in the inner position. The most important relative standard uncertainty components contributing to the uncertainty of G are, in parts in 10^6 (Parks and Faller, 2010), the six critical dimension measurements, 14; all other dimension measurements and source mass density inhomogeneities, 8 each; pendulum spring constants, 7; and total mass measurement and interferometer misalignment, 6 each.

12. Electroweak Quantities

As in previous adjustments, there are a few cases in the 2010 adjustment where an inexact constant that is used in the analysis of input data is not treated as an adjusted quantity, because the adjustment has a negligible effect on its value. Three such constants, used in the calculation of the theoretical expression for the electron magnetic-moment anomaly a_e, are the mass of the tau lepton m_τ, the Fermi coupling constant G_F, and sine squared of the weak mixing angle $\sin^2\theta_W$; they are obtained from the most recent report of the Particle Data Group (Nakamura *et al.*, 2010):

$$m_\tau c^2 = 1776.82(16)\ \text{MeV} \quad [9.0 \times 10^{-5}], \tag{281}$$

$$G_F/(\hbar c)^3 = 1.166\,364(5) \times 10^{-5}\ \text{GeV}^{-2} \quad [4.3 \times 10^{-6}], \tag{282}$$

$$\sin^2\theta_W = 0.2223(21) \quad [9.5 \times 10^{-3}]. \tag{283}$$

The value for $G_F/(\hbar c)^3$ is from Nakamura *et al.* (2010), p. 127. We use the definition $\sin^2\theta_W = 1 - (m_W/m_Z)^2$, where m_W and m_Z are, respectively, the masses of the $W^\pm$ and Z^0 bosons, because it is employed in the calculation of the electroweak contributions to a_e (Czarnecki, Krause, and Marciano, 1996). The Particle Data Group's recommended value for the mass ratio of these bosons is $m_W/m_Z = 0.8819(12)$, which leads to the value of $\sin^2\theta_W$ given above.

13. Analysis of Data

We examine in this section the input data discussed in the previous sections and, based upon that examination, select the data to be used in the least-squares adjustment that determines the 2010 CODATA recommended values of the constants. Tables 18, 20, 22, and 24 give the input data, including the δ's, which are corrections added to theoretical expressions to account for the uncertainties of those expressions. The covariances of the data are given as correlation coefficients in Tables 19, 21, 23, and 24. There are 14 types of input data for which there are two or more experiments, and the data of the same type generally agree (values of G excepted).

13.1. Comparison of data through inferred values of α, h, k, and A_r(e)

Here the level of consistency of the data is shown by comparing values of α, h, k, and A_r(e) that can be inferred from different types of experiments. Note, however, that the inferred value is for comparison purposes only; the datum from which it is obtained, not the inferred value, is used as the input datum in the least-squares calculations.

Table 25 and Figs. 1 and 2 compare values of α obtained from the indicated input data. These values are calculated using the appropriate observational equation for each input datum as given in Table 33 and the 2010 recommended values of the constants other than α that enter that equation. (Some inferred values have also been given where the relevant datum is discussed.) Inspection of the table and figures shows that there is agreement among the vast majority of the various

TABLE 18. Summary of principal input data for the determination of the 2010 recommended value of the Rydberg constant R_∞.

Item No.	Input datum	Value	Relative standard uncertainty[a] u_r	Identification	Sec.
*A*1	$\delta_H(1S_{1/2})$	0.0(2.5) kHz	$[7.5 \times 10^{-13}]$	Theory	4.1.1.12
*A*2	$\delta_H(2S_{1/2})$	0.00(31) kHz	$[3.8 \times 10^{-13}]$	Theory	4.1.1.12
*A*3	$\delta_H(3S_{1/2})$	0.000(91) kHz	$[2.5 \times 10^{-13}]$	Theory	4.1.1.12
*A*4	$\delta_H(4S_{1/2})$	0.000(39) kHz	$[1.9 \times 10^{-13}]$	Theory	4.1.1.12
*A*5	$\delta_H(6S_{1/2})$	0.000(15) kHz	$[1.6 \times 10^{-13}]$	Theory	4.1.1.12
*A*6	$\delta_H(8S_{1/2})$	0.0000(63) kHz	$[1.2 \times 10^{-13}]$	Theory	4.1.1.12
*A*7	$\delta_H(2P_{1/2})$	0.000(28) kHz	$[3.5 \times 10^{-14}]$	Theory	4.1.1.12
*A*8	$\delta_H(4P_{1/2})$	0.0000(38) kHz	$[1.9 \times 10^{-14}]$	Theory	4.1.1.12
*A*9	$\delta_H(2P_{3/2})$	0.000(28) kHz	$[3.5 \times 10^{-14}]$	Theory	4.1.1.12
*A*10	$\delta_H(4P_{3/2})$	0.0000(38) kHz	$[1.9 \times 10^{-14}]$	Theory	4.1.1.12
*A*11	$\delta_H(8D_{3/2})$	0.000 00(44) kHz	$[8.5 \times 10^{-15}]$	Theory	4.1.1.12
*A*12	$\delta_H(12D_{3/2})$	0.000 00(13) kHz	$[5.7 \times 10^{-15}]$	Theory	4.1.1.12
*A*13	$\delta_H(4D_{5/2})$	0.0000(35) kHz	$[1.7 \times 10^{-14}]$	Theory	4.1.1.12
*A*14	$\delta_H(6D_{5/2})$	0.0000(10) kHz	$[1.1 \times 10^{-14}]$	Theory	4.1.1.12
*A*15	$\delta_H(8D_{5/2})$	0.000 00(44) kHz	$[8.5 \times 10^{-15}]$	Theory	4.1.1.12
*A*16	$\delta_H(12D_{5/2})$	0.000 00(13) kHz	$[5.7 \times 10^{-15}]$	Theory	4.1.1.12
*A*17	$\delta_D(1S_{1/2})$	0.0(2.3) kHz	$[6.9 \times 10^{-13}]$	Theory	4.1.1.12
*A*18	$\delta_D(2S_{1/2})$	0.00(29) kHz	$[3.5 \times 10^{-13}]$	Theory	4.1.1.12
*A*19	$\delta_D(4S_{1/2})$	0.000(36) kHz	$[1.7 \times 10^{-13}]$	Theory	4.1.1.12
*A*20	$\delta_D(8S_{1/2})$	0.0000(60) kHz	$[1.2 \times 10^{-13}]$	Theory	4.1.1.12
*A*21	$\delta_D(8D_{3/2})$	0.000 00(44) kHz	$[8.5 \times 10^{-15}]$	Theory	4.1.1.12
*A*22	$\delta_D(12D_{3/2})$	0.000 00(13) kHz	$[5.6 \times 10^{-15}]$	Theory	4.1.1.12
*A*23	$\delta_D(4D_{5/2})$	0.0000(35) kHz	$[1.7 \times 10^{-14}]$	Theory	4.1.1.12
*A*24	$\delta_D(8D_{5/2})$	0.000 00(44) kHz	$[8.5 \times 10^{-15}]$	Theory	4.1.1.12
*A*25	$\delta_D(12D_{5/2})$	0.000 00(13) kHz	$[5.7 \times 10^{-15}]$	Theory	4.1.1.12
*A*26	$\nu_H(1S_{1/2} - 2S_{1/2})$	2 466 061 413 187.080(34) kHz	1.4×10^{-14}	MPQ-04	4.1.2
*A*27	$\nu_H(1S_{1/2} - 3S_{1/2})$	2 922 743 278 678(13) kHz	4.4×10^{-12}	LKB-10	4.1.2
*A*28	$\nu_H(2S_{1/2} - 8S_{1/2})$	770 649 350 012.0(8.6) kHz	1.1×10^{-11}	LK/SY-97	4.1.2
*A*29	$\nu_H(2S_{1/2} - 8D_{3/2})$	770 649 504 450.0(8.3) kHz	1.1×10^{-11}	LK/SY-97	4.1.2
*A*30	$\nu_H(2S_{1/2} - 8D_{5/2})$	770 649 561 584.2(6.4) kHz	8.3×10^{-12}	LK/SY-97	4.1.2
*A*31	$\nu_H(2S_{1/2} - 12D_{3/2})$	799 191 710 472.7(9.4) kHz	1.2×10^{-11}	LK/SY-98	4.1.2
*A*32	$\nu_H(2S_{1/2} - 12D_{5/2})$	799 191 727 403.7(7.0) kHz	8.7×10^{-12}	LK/SY-98	4.1.2
*A*33	$\nu_H(2S_{1/2} - 4S_{1/2}) - \frac{1}{4}\nu_H(1S_{1/2} - 2S_{1/2})$	4 797 338(10) kHz	2.1×10^{-6}	MPQ-95	4.1.2
*A*34	$\nu_H(2S_{1/2} - 4D_{5/2}) - \frac{1}{4}\nu_H(1S_{1/2} - 2S_{1/2})$	6 490 144(24) kHz	3.7×10^{-6}	MPQ-95	4.1.2
*A*35	$\nu_H(2S_{1/2} - 6S_{1/2}) - \frac{1}{4}\nu_H(1S_{1/2} - 3S_{1/2})$	4 197 604(21) kHz	4.9×10^{-6}	LKB-96	4.1.2
*A*36	$\nu_H(2S_{1/2} - 6D_{5/2}) - \frac{1}{4}\nu_H(1S_{1/2} - 3S_{1/2})$	4 699 099(10) kHz	2.2×10^{-6}	LKB-96	4.1.2
*A*37	$\nu_H(2S_{1/2} - 4P_{1/2}) - \frac{1}{4}\nu_H(1S_{1/2} - 2S_{1/2})$	4 664 269(15) kHz	3.2×10^{-6}	YaleU-95	4.1.2
*A*38	$\nu_H(2S_{1/2} - 4P_{3/2}) - \frac{1}{4}\nu_H(1S_{1/2} - 2S_{1/2})$	6 035 373(10) kHz	1.7×10^{-6}	YaleU-95	4.1.2
*A*39	$\nu_H(2S_{1/2} - 2P_{3/2})$	9 911 200(12) kHz	1.2×10^{-6}	HarvU-94	4.1.2
*A*40.1	$\nu_H(2P_{1/2} - 2S_{1/2})$	1 057 845.0(9.0) kHz	8.5×10^{-6}	HarvU-86	4.1.2
*A*40.2	$\nu_H(2P_{1/2} - 2S_{1/2})$	1 057 862(20) kHz	1.9×10^{-5}	USus-79	4.1.2
*A*41	$\nu_D(2S_{1/2} - 8S_{1/2})$	770 859 041 245.7(6.9) kHz	8.9×10^{-12}	LK/SY-97	4.1.2
*A*42	$\nu_D(2S_{1/2} - 8D_{3/2})$	770 859 195 701.8(6.3) kHz	8.2×10^{-12}	LK/SY-97	4.1.2
*A*43	$\nu_D(2S_{1/2} - 8D_{5/2})$	770 859 252 849.5(5.9) kHz	7.7×10^{-12}	LK/SY-97	4.1.2
*A*44	$\nu_D(2S_{1/2} - 12D_{3/2})$	799 409 168 038.0(8.6) kHz	1.1×10^{-11}	LK/SY-98	4.1.2
*A*45	$\nu_D(2S_{1/2} - 12D_{5/2})$	799 409 184 966.8(6.8) kHz	8.5×10^{-12}	LK/SY-98	4.1.2
*A*46	$\nu_D(2S_{1/2} - 4S_{1/2}) - \frac{1}{4}\nu_D(1S_{1/2} - 2S_{1/2})$	4 801 693(20) kHz	4.2×10^{-6}	MPQ-95	4.1.2
*A*47	$\nu_D(2S_{1/2} - 4D_{5/2}) - \frac{1}{4}\nu_D(1S_{1/2} - 2S_{1/2})$	6 494 841(41) kHz	6.3×10^{-6}	MPQ-95	4.1.2
*A*48	$\nu_D(1S_{1/2} - 2S_{1/2}) - \nu_H(1S_{1/2} - 2S_{1/2})$	670 994 334.606(15) kHz	2.2×10^{-11}	MPQ-10	4.1.2
*A*49.1	r_p	0.895(18) fm	2.0×10^{-2}	rp-03	4.1.3
*A*49.2	r_p	0.8791(79) fm	9.0×10^{-3}	rp-10	4.1.3
*A*50	r_d	2.130(10) fm	4.7×10^{-3}	rd-98	4.1.3

[a]The values in brackets are relative to the frequency equivalent of the binding energy of the indicated level.

TABLE 19. Correlation coefficients $|r(x_i, x_j)| \geq 0.0001$ of the input data related to R_∞ in Table 18. For simplicity, the two items of data to which a particular correlation coefficient corresponds are identified by their item numbers in Table 18.

$r(A1, A2) = 0.9905$	$r(A6, A19) = 0.7404$	$r(A28, A29) = 0.3478$	$r(A31, A45) = 0.1136$
$r(A1, A3) = 0.9900$	$r(A6, A20) = 0.9851$	$r(A28, A30) = 0.4532$	$r(A32, A35) = 0.0278$
$r(A1, A4) = 0.9873$	$r(A7, A8) = 0.0237$	$r(A28, A31) = 0.0899$	$r(A32, A36) = 0.0553$
$r(A1, A5) = 0.7640$	$r(A9, A10) = 0.0237$	$r(A28, A32) = 0.1206$	$r(A32, A41) = 0.1512$
$r(A1, A6) = 0.7627$	$r(A11, A12) = 0.0006$	$r(A28, A35) = 0.0225$	$r(A32, A42) = 0.1647$
$r(A1, A17) = 0.9754$	$r(A11, A21) = 0.9999$	$r(A28, A36) = 0.0448$	$r(A32, A43) = 0.1750$
$r(A1, A18) = 0.9656$	$r(A11, A22) = 0.0003$	$r(A28, A41) = 0.1225$	$r(A32, A44) = 0.1209$
$r(A1, A19) = 0.9619$	$r(A12, A21) = 0.0003$	$r(A28, A42) = 0.1335$	$r(A32, A45) = 0.1524$
$r(A1, A20) = 0.7189$	$r(A12, A22) = 0.9999$	$r(A28, A43) = 0.1419$	$r(A33, A34) = 0.1049$
$r(A2, A3) = 0.9897$	$r(A13, A14) = 0.0006$	$r(A28, A44) = 0.0980$	$r(A33, A46) = 0.2095$
$r(A2, A4) = 0.9870$	$r(A13, A15) = 0.0006$	$r(A28, A45) = 0.1235$	$r(A33, A47) = 0.0404$
$r(A2, A5) = 0.7638$	$r(A13, A16) = 0.0006$	$r(A29, A30) = 0.4696$	$r(A34, A46) = 0.0271$
$r(A2, A6) = 0.7625$	$r(A13, A23) = 0.9999$	$r(A29, A31) = 0.0934$	$r(A34, A47) = 0.0467$
$r(A2, A17) = 0.9656$	$r(A13, A24) = 0.0003$	$r(A29, A32) = 0.1253$	$r(A35, A36) = 0.1412$
$r(A2, A18) = 0.9754$	$r(A13, A25) = 0.0003$	$r(A29, A35) = 0.0234$	$r(A35, A41) = 0.0282$
$r(A2, A19) = 0.9616$	$r(A14, A15) = 0.0006$	$r(A29, A36) = 0.0466$	$r(A35, A42) = 0.0307$
$r(A2, A20) = 0.7187$	$r(A14, A16) = 0.0006$	$r(A29, A41) = 0.1273$	$r(A35, A43) = 0.0327$
$r(A3, A4) = 0.9864$	$r(A14, A23) = 0.0003$	$r(A29, A42) = 0.1387$	$r(A35, A44) = 0.0226$
$r(A3, A5) = 0.7633$	$r(A14, A24) = 0.0003$	$r(A29, A43) = 0.1475$	$r(A35, A45) = 0.0284$
$r(A3, A6) = 0.7620$	$r(A14, A25) = 0.0003$	$r(A29, A44) = 0.1019$	$r(A36, A41) = 0.0561$
$r(A3, A17) = 0.9651$	$r(A15, A16) = 0.0006$	$r(A29, A45) = 0.1284$	$r(A36, A42) = 0.0612$
$r(A3, A18) = 0.9648$	$r(A15, A23) = 0.0003$	$r(A30, A31) = 0.1209$	$r(A36, A43) = 0.0650$
$r(A3, A19) = 0.9611$	$r(A15, A24) = 0.9999$	$r(A30, A32) = 0.1622$	$r(A36, A44) = 0.0449$
$r(A3, A20) = 0.7183$	$r(A15, A25) = 0.0003$	$r(A30, A35) = 0.0303$	$r(A36, A45) = 0.0566$
$r(A4, A5) = 0.7613$	$r(A16, A23) = 0.0003$	$r(A30, A36) = 0.0602$	$r(A37, A38) = 0.0834$
$r(A4, A6) = 0.7600$	$r(A16, A24) = 0.0003$	$r(A30, A41) = 0.1648$	$r(A41, A42) = 0.5699$
$r(A4, A17) = 0.9625$	$r(A16, A25) = 0.9999$	$r(A30, A42) = 0.1795$	$r(A41, A43) = 0.6117$
$r(A4, A18) = 0.9622$	$r(A17, A18) = 0.9897$	$r(A30, A43) = 0.1908$	$r(A41, A44) = 0.1229$
$r(A4, A19) = 0.9755$	$r(A17, A19) = 0.9859$	$r(A30, A44) = 0.1319$	$r(A41, A45) = 0.1548$
$r(A4, A20) = 0.7163$	$r(A17, A20) = 0.7368$	$r(A30, A45) = 0.1662$	$r(A42, A43) = 0.6667$
$r(A5, A6) = 0.5881$	$r(A18, A19) = 0.9856$	$r(A31, A32) = 0.4750$	$r(A42, A44) = 0.1339$
$r(A5, A17) = 0.7448$	$r(A18, A20) = 0.7366$	$r(A31, A35) = 0.0207$	$r(A42, A45) = 0.1687$
$r(A5, A18) = 0.7445$	$r(A19, A20) = 0.7338$	$r(A31, A36) = 0.0412$	$r(A43, A44) = 0.1423$
$r(A5, A19) = 0.7417$	$r(A21, A22) = 0.0002$	$r(A31, A41) = 0.1127$	$r(A43, A45) = 0.1793$
$r(A5, A20) = 0.5543$	$r(A23, A24) = 0.0001$	$r(A31, A42) = 0.1228$	$r(A44, A45) = 0.5224$
$r(A6, A17) = 0.7435$	$r(A23, A25) = 0.0001$	$r(A31, A43) = 0.1305$	$r(A46, A47) = 0.0110$
$r(A6, A18) = 0.7433$	$r(A24, A25) = 0.0002$	$r(A31, A44) = 0.0901$	

values of α, and hence the data from which they are obtained, to the extent that the difference between any two values of α is less than $2u_{\text{diff}}$, the standard uncertainty of the difference.

The two exceptions are the values of α from the NIST-89 result for $\Gamma'_{\text{p}-90}(\text{lo})$ and, to a lesser extent, the KR/VN-98 result for $\Gamma'_{\text{h}-90}(\text{lo})$; of the 91 differences, six involving α from NIST-89 and two involving α from KR/VN-98 are greater than $2u_{\text{diff}}$. The inconsistency of these data has in fact been discussed in previous CODATA reports but, as in 2006, because their self-sensitivity coefficients S_c (see Sec. 13.2) are less than 0.01, they are not included in the final adjustment on which the 2010 recommended values are based. Hence, their disagreement is not a serious issue. Examination of the table and figures also shows that even if all of the data from which these values of α have been inferred were to be included in the final adjustment, the recommended value of α would still be determined mainly by the HarvU-08 a_e and LKB-10 $h/m(^{87}\text{Rb})$ data. Indeed, the comparatively large uncertainties of some of the values of α means that the data from which they are obtained will have values of $S_c < 0.01$ and will not be included in the final adjustment.

Table 26 and Fig. 3 compare values of h obtained from the indicated input data. The various values of h, and hence the data from which they are calculated, agree to the extent that the 55 differences between any two values of h is less than $2u_{\text{diff}}$, except for the difference between the NIST-07 and IAC-11 values. In this case, the difference is $3.8u_{\text{diff}}$.

Because the uncertainties of these two values of h are comparable and are smaller than the other values of h, they play the dominant role in the determination of the recommended value of h. This discrepancy is dealt with before carrying out the final adjustment. The relatively large uncertainties of many of the other values of h means that the data from which they are calculated will not be included in the final adjustment.

Table 27 and Fig. 4 compare values of k obtained from the indicated input data. Although most of the source data are values of R, values of $k = R/N_A$ are compared, because that is the constant used to define the kelvin in the "new" SI; see, for

TABLE 20. Summary of principal input data for the determination of the 2010 recommended values of the fundamental constants (R_∞ and G excepted).

Item No.	Input datum	Value	Relative standard uncertainty[a] u_r	Identification	Sec. and Eq.
*B*1	$A_r(^1H)$	1.007 825 032 07(10)	1.0×10^{-10}	AMDC-03	3.1
*B*2.1	$A_r(^2H)$	2.014 101 777 85(36)	1.8×10^{-10}	AMDC-03	3.1
*B*2.2	$A_r(^2H)$	2.014 101 778 040(80)	4.0×10^{-11}	UWash-06	3.1
*B*3	$A_r(E_{av})$	0.794(79)	1.0×10^{-1}	StockU-08	3.3 (13)
*B*4	$f_c(H_2^{+*})/f_c(d)$	0.999 231 659 33(17)	1.7×10^{-10}	StockU-08	3.3 (2)
*B*5	$f_c(t)/f_c(H_2^{+*})$	0.668 247 726 86(55)	8.2×10^{-10}	StockU-06	3.3 (14)
*B*6	$f_c(^3He^+)/f_c(H_2^{+*})$	0.668 252 146 82(55)	8.2×10^{-10}	StockU-06	3.3 (15)
*B*7	$A_r(^4He)$	4.002 603 254 131(62)	1.5×10^{-11}	UWash-06	3.1
*B*8	$A_r(^{16}O)$	15.994 914 619 57(18)	1.1×10^{-11}	UWash-06	3.1
*B*9.1	$A_r(^{87}Rb)$	86.909 180 526(12)	1.4×10^{-10}	AMDC-03	3.1
*B*9.2	$A_r(^{87}Rb)$	86.909 180 535(10)	1.2×10^{-10}	FSU-10	3.1
*B*10.1[b]	$A_r(^{133}Cs)$	132.905 451 932(24)	1.8×10^{-10}	AMDC-03	3.1
*B*10.2[b]	$A_r(^{133}Cs)$	132.905 451 963(13)	9.8×10^{-11}	FSU-10	3.1
*B*11	$A_r(e)$	0.000 548 579 9111(12)	2.1×10^{-9}	UWash-95	3.4 (20)
*B*12	δ_e	$0.00(33) \times 10^{-12}$	$[2.8 \times 10^{-10}]$	theory	5.1.1
*B*13.1[b]	a_e	$1.159\,652\,1883(42) \times 10^{-13}$	3.7×10^{-9}	UWash-87	5.1.2.1 (125)
*B*13.2	a_e	$1.159\,652\,180\,73(28) \times 10^{-13}$	2.4×10^{-10}	HarvU-08	5.1.2.2 (126)
*B*14	$\bar{R}$	0.003 707 2063(20)	5.4×10^{-7}	BNL-06	5.2.2 (143)
*B*15	δ_C	$0.00(26) \times 10^{-10}$	$[1.3 \times 10^{-11}]$	theory	5.3.1
*B*16	δ_O	$0.0(1.1) \times 10^{-10}$	$[5.3 \times 10^{-11}]$	theory	5.3.1
*B*17	$f_s(^{12}C^{5+})/f_c(^{12}C^{5+})$	4376.210 4989(23)	5.2×10^{-10}	GSI-02	5.3.2 (183)
*B*18	$f_s(^{16}O^{7+})/f_c(^{16}O^{7+})$	4164.376 1837(32)	7.6×10^{-10}	GSI-04	5.3.2 (184)
*B*19	μ_e-(H)/μ_p(H)	−658.210 7058(66)	1.0×10^{-8}	MIT-72	6.1.3
*B*20	μ_d(D)/μ_e-(D)	$-4.664\,345\,392(50) \times 10^{-14}$	1.1×10^{-8}	MIT-84	6.1.3
*B*21	μ_p(HD)/μ_d(HD)	3.257 199 531(29)	8.9×10^{-9}	StPtrsb-03	6.1.3
*B*22	σ_{dp}	$15(2) \times 10^{-9}$		StPtrsb-03	6.1.3
*B*23	μ_t(HT)/μ_p(HT)	1.066 639 887(10)	9.4×10^{-9}	StPtrsb-03	6.1.3
*B*24	σ_{tp}	$20(3) \times 10^{-9}$		StPtrsb-03	6.1.3
*B*25	μ_e-(H)/μ'_p	−658.215 9430(72)	1.1×10^{-8}	MIT-77	6.1.3
*B*26	μ'_h/μ'_p	−0.761 786 1313(33)	4.3×10^{-9}	NPL-93	6.1.3
*B*27	μ'_n/μ'_p	−0.684 996 94(16)	2.4×10^{-7}	ILL-79	6.1.3
*B*28	δ_{Mu}	0(101) Hz	$[2.3 \times 10^{-8}]$	theory	6.2.1
*B*29.1	$\Delta\nu_{Mu}$	4 463 302.88(16) kHz	3.6×10^{-8}	LAMPF-82	6.2.2 (222)
*B*29.2	$\Delta\nu_{Mu}$	4 463 302 765(53) Hz	1.2×10^{-8}	LAMPF-99	6.2.2 (225)
*B*30	ν(58 MHz)	627 994.77(14) kHz	2.2×10^{-7}	LAMPF-82	6.2.2 (223)
*B*31	ν(72 MHz)	668 223 166(57) Hz	8.6×10^{-8}	LAMPF-99	8.2 (226)
*B*32.1[b]	Γ'_{p-90}(lo)	$2.675\,154\,05(30) \times 10^8$ s^{-1} T^{-1}	1.1×10^{-7}	NIST-89	8.2
*B*32.2[b]	Γ'_{p-90}(lo)	$2.675\,1530(18) \times 10^8$ s^{-1} T^{-1}	6.6×10^{-7}	NIM-95	8.2
*B*33[b]	Γ'_{h-90}(lo)	$2.037\,895\,37(37) \times 10^8$ s^{-1} T^{-1}	1.8×10^{-7}	KR/VN-98	8.2
*B*34.1[b]	Γ'_{p-90}(hi)	$2.675\,1525(43) \times 10^8$ s^{-1} T^{-1}	1.6×10^{-6}	NIM-95	8.2
*B*34.2[b]	Γ'_{p-90}(hi)	$2.675\,1518(27) \times 10^8$ s^{-1} T^{-1}	1.0×10^{-6}	NPL-79	8.2
*B*35.1[b]	R_K	25 812.808 31(62) Ω	2.4×10^{-8}	NIST-97	8.2
*B*35.2[b]	R_K	25 812.8071(11) Ω	4.4×10^{-8}	NMI-97	8.2
*B*35.3[b]	R_K	25 812.8092(14) Ω	5.4×10^{-8}	NPL-88	8.2
*B*35.4[b]	R_K	25 812.8084(34) Ω	1.3×10^{-7}	NIM-95	8.2
*B*35.5[b]	R_K	25 812.8081(14) Ω	5.3×10^{-8}	LNE-01	8.2
*B*36.1[b]	K_J	483 597.91(13) GHz V^{-1}	2.7×10^{-7}	NMI-89	8.2
*B*36.2[b]	K_J	483 597.96(15) GHz V^{-1}	3.1×10^{-7}	PTB-91	8.2
*B*37.1[c]	$K_J^2 R_K$	$6.036\,7625(12) \times 10^{33}$ J^{-1}s^{-1}	2.0×10^{-7}	NPL-90	8.2
*B*37.2[c]	$K_J^2 R_K$	$6.036\,761\,85(53) \times 10^{33}$ J^{-1} s^{-1}	8.7×10^{-8}	NIST-98	8.2
*B*37.3[c]	$K_J^2 R_K$	$6.036\,761\,85(22) \times 10^{33}$ J^{-1} s^{-1}	3.6×10^{-8}	NIST-07	8.2
*B*37.4[c]	$K_J^2 R_K$	$6.036\,7597(12) \times 10^{33}$ J^{-1} s^{-1}	2.0×10^{-7}	NPL-12	8.2.1 (245)
*B*37.5[b]	$K_J^2 R_K$	$6.036\,7617(18) \times 10^{33}$ J^{-1} s^{-1}	2.9×10^{-7}	METAS-11	8.2.2 (247)
*B*38[b]	$\mathcal{F}_{90}$	96 485.39(13) C mol^{-1}	1.3×10^{-6}	NIST-80	8.2
*B*39	d_{220}(MO*)	192 015.5508(42) fm	2.2×10^{-8}	INRIM-08	9.1 (250)
*B*40	d_{220}(W04)	192 015.5702(29) fm	1.5×10^{-8}	INRIM-09	9.1 (251)
*B*41.1	d_{220}(W4.2a)	192 015.563(12) fm	6.2×10^{-8}	PTB-81	9.1 (249)
*B*41.2	d_{220}(W4.2a)	192 015.5691(29) fm	1.5×10^{-8}	INRIM-09	9.1 (252)
*B*42	$1 - d_{220}(N)/d_{220}(W17)$	$7(22) \times 10^{-9}$		NIST-97	9.2

TABLE 20. Summary of principal input data for the determination of the 2010 recommended values of the fundamental constants (R_∞ and G excepted).—Continued

Item No.	Input datum	Value	Relative standard uncertainty[a] u_r	Identification	Sec. and Eq.
*B*43	$1-d_{220}(\mathrm{W17})/d_{220}(\mathrm{ILL})$	$-8(22)\times10^{-9}$		NIST-99	9.2
*B*44	$1-d_{220}(\mathrm{MO}^*)/d_{220}(\mathrm{ILL})$	$86(27)\times10^{-9}$		NIST-99	9.2
*B*45	$1-d_{220}(\mathrm{NR3})/d_{220}(\mathrm{ILL})$	$33(22)\times10^{-9}$		NIST-99	9.2
*B*46	$d_{220}(\mathrm{NR3})/d_{220}(\mathrm{W04})-1$	$-11(21)\times10^{-9}$		NIST-06	9.2
*B*47	$d_{220}(\mathrm{NR4})/d_{220}(\mathrm{W04})-1$	$25(21)\times10^{-9}$		NIST-06	9.2
*B*48	$d_{220}(\mathrm{W17})/d_{220}(\mathrm{W04})-1$	$11(21)\times10^{-9}$		NIST-06	9.2
*B*49	$d_{220}(\mathrm{W4.2a})/d_{220}(\mathrm{W04})-1$	$-1(21)\times10^{-9}$		PTB-98	9.2
*B*50	$d_{220}(\mathrm{W17})/d_{220}(\mathrm{W04})-1$	$22(22)\times10^{-9}$		PTB-98	9.2
*B*51	$d_{220}(\mathrm{MO}^*4)/d_{220}(\mathrm{W04})-1$	$-103(28)\times10^{-9}$		PTB-98	9.2
*B*52	$d_{220}(\mathrm{NR3})/d_{220}(\mathrm{W04})-1$	$-23(21)\times10^{-9}$		PTB-98	9.2
*B*53	$d_{220}/d_{220}(\mathrm{W04})-1$	$10(11)\times10^{-9}$		PTB-03	9.2
*B*54[c]	N_A	$6.022\,140\,82(18)\times10^{23}$ mol^{-1}	3.0×10^{-8}	IAC-11	9.6 (268)
*B*55	$\lambda_{meas}/d_{220}(\mathrm{ILL})$	0.002 904 302 46(50)	1.7×10^{-7}	NIST-99	9.3 (253)
*B*56[b]	$h/m(^{133}\mathrm{Cs})$	$3.002\,369\,432(46)\times10^{-9}$ m^2 s^{-1}	1.5×10^{-8}	StanfU-02	7.1 (235)
*B*57	$h/m(^{87}\mathrm{Rb})$	$4.591\,359\,2729(57)\times10^{-9}$ m^2 s^{-1}	1.2×10^{-9}	LKB-11	7.2 (237)
*B*58.1	R	8.314 504(70) J mol^{-1} K^{-1}	8.4×10^{-6}	NPL-79	10.1.1
*B*58.2	R	8.314 471(15) J mol^{-1} K^{-1}	1.8×10^{-6}	NIST-88	10.1.1
*B*58.3	R	8.314 467(22) J mol^{-1} K^{-1}	2.7×10^{-6}	LNE-09	10.1.2
*B*58.4	R	8.314 468(26) J mol^{-1} K^{-1}	3.1×10^{-6}	NPL-10	10.1.3
*B*58.5	R	8.314 412(63) J mol^{-1} K^{-1}	7.5×10^{-6}	INRIM-10	10.1.4
*B*58.6	R	8.314 456(10) J mol^{-1} K^{-1}	1.2×10^{-6}	LNE-11	10.1.2
*B*59[b]	k	$1.380\,653(13)\times10^{-23}$ J K^{-1}	9.1×10^{-6}	NIST-07	10.2.1
*B*60[b]	k/h	$2.083\,666(25)\times10^{10}$ Hz K^{-1}	1.2×10^{-6}	NIST-11	10.2.2
*B*61	$\lambda(\mathrm{CuK}\alpha_1)/d_{220}(\mathrm{W4.2a})$	0.802 327 11(24)	3.0×10^{-7}	FSUJ/PTB-91	9.4 (258)
*B*62	$\lambda(\mathrm{WK}\alpha_1)/d_{220}(\mathrm{N})$	0.108 852 175(98)	9.0×10^{-7}	NIST-79	9.4 (259)
*B*63	$\lambda(\mathrm{MoK}\alpha_1)/d_{220}(\mathrm{N})$	0.369 406 04(19)	5.3×10^{-7}	NIST-73	9.4 (260)
*B*64	$\lambda(\mathrm{CuK}\alpha_1)/d_{220}(\mathrm{N})$	0.802 328 04(77)	9.6×10^{-7}	NIST-73	9.4 (261)

[a]The values in brackets are relative to the quantities a_e, $g_{e^-}(^{12}C^{5+})$, $g_{e^-}(^{16}O^{7+})$, or $\Delta\nu_{Mu}$ as appropriate.
[b]Datum not included in the final least-squares adjustment that provides the recommended values of the constants.
[c]Datum included in the final least-squares adjustment with an expanded uncertainty.

example, Mills *et al.* (2011). All of these values are in general agreement, with none of the 28 differences exceeding $2u_{diff}$. However, some of the input data from which they are calculated have uncertainties so large that they will not be included in the final adjustment.

Finally, in Table 28 and Fig. 5 we compare four values of $A_r(e)$ calculated from different input data as indicated. They are in agreement, with all six differences less than $2u_{diff}$. Further, since the four uncertainties are comparable, all four of the source data are included in the final adjustment.

13.2. Multivariate analysis of data

Our multivariate analysis of the data employs a well-known least-squares method that takes correlations among the input data into account. Used in the three previous adjustments, it is described in Appendix E of CODATA-98 and references cited therein. We recall from that appendix that a least-squares adjustment is characterized by the number of input data N, number of variables or adjusted constants M, degrees of freedom $\nu = N - M$, measure χ^2, probability $p(\chi^2|\nu)$ of obtaining an observed value of χ^2 that large or larger for the given value of ν, Birge ratio $R_B = \sqrt{\chi^2/\nu}$, and normalized residual of the ith input datum $r_i = (x_i - \langle x_i \rangle)/u_i$, where x_i is the input datum, $\langle x_i \rangle$ its adjusted value, and u_i its standard uncertainty.

The observational equations for the input data are given in Tables 31, 33, and 35. These equations are written in terms of a particular independent subset of constants (broadly interpreted) called, as already noted, adjusted constants. These are the variables (or unknowns) of the adjustment. The least-squares calculation yields values of the adjusted constants that predict values of the input data through their observational equations that best agree with the data themselves in the least-squares sense. The adjusted constants used in the 2010 calculations are given in Tables 30, 32, and 34.

The symbol $\doteq$ in an observational equation indicates that an input datum of the type on the left-hand side is ideally given by the expression on the right-hand side containing adjusted constants. But because the equation is one of an overdetermined set that relates a datum to adjusted constants, the two sides are not necessarily equal. The best estimate of the value of an input datum is its observational equation evaluated with the least-squares adjusted values of the adjusted constants on which its observational equation depends. For some input data such as δ_e and R, the observational equation is simply $\delta_e \doteq \delta_e$ and $R \doteq R$.

TABLE 21. Non-negligible correlation coefficients $r(x_i, x_j)$ of the input data in Table 20. For simplicity, the two items of data to which a particular correlation coefficient corresponds are identified by their item numbers in Table 20.

$r(B1, B2.1) = 0.073$	$r(B39, B40) = 0.023$	$r(B43, B45) = 0.516$	$r(B47, B48) = 0.509$
$r(B2.2, B7) = 0.127$	$r(B39, B41.2) = 0.023$	$r(B43, B46) = 0.065$	$r(B49, B50) = 0.469$
$r(B2.2, B8) = 0.089$	$r(B39, B54) = -0.026$	$r(B43, B47) = 0.065$	$r(B49, B51) = 0.372$
$r(B5, B6) = 0.876$	$r(B40, B41.2) = 0.027$	$r(B43, B48) = -0.367$	$r(B49, B52) = 0.502$
$r(B7, B8) = 0.181$	$r(B40, B54) = -0.029$	$r(B44, B45) = 0.421$	$r(B50, B51) = 0.347$
$r(B15, B16) = 0.994$	$r(B41.2, B54) = -0.029$	$r(B44, B46) = 0.053$	$r(B50, B52) = 0.469$
$r(B17, B18) = 0.082$	$r(B42, B43) = -0.288$	$r(B44, B47) = 0.053$	$r(B51, B52) = 0.372$
$r(B29.1, B30) = 0.227$	$r(B42, B44) = 0.096$	$r(B44, B48) = 0.053$	$r(B58.3, B58.4) = 0.002$
$r(B29.2, B31) = 0.195$	$r(B42, B45) = 0.117$	$r(B45, B46) = -0.367$	$r(B58.3, B58.5) = 0.001$
$r(B32.2, B34.1) = -0.014$	$r(B42, B46) = 0.066$	$r(B45, B47) = 0.065$	$r(B58.3, B58.6) = 0.032$
$r(B36.1, B58.2) = 0.068$	$r(B42, B47) = 0.066$	$r(B45, B48) = 0.065$	$r(B58.4, B58.6) = 0.012$
$r(B37.1, B37.4) = 0.003$	$r(B42, B48) = 0.504$	$r(B46, B47) = 0.509$	
$r(B37.2, B37.3) = 0.140$	$r(B43, B44) = 0.421$	$r(B46, B48) = 0.509$	

TABLE 22. Summary of principal input data for the determination of the relative atomic mass of the electron from antiprotonic helium transitions. The numbers in parentheses $(n, l : n', l')$ denote the transition $(n, l) \rightarrow (n', l')$.

Item No.	Input datum	Value	Relative standard uncertainty[a] u_r	Identification[b]	Sec.
$C1$	$\delta_{\bar{p}^4He^+}(32, 31 : 31, 30)$	0.00(82) MHz	$[7.3 \times 10^{-10}]$	JINR-06	4.2.1
$C2$	$\delta_{\bar{p}^4He^+}(35, 33 : 34, 32)$	0.0(1.0) MHz	$[1.3 \times 10^{-9}]$	JINR-06	4.2.1
$C3$	$\delta_{\bar{p}^4He^+}(36, 34 : 35, 33)$	0.0(1.1) MHz	$[1.6 \times 10^{-9}]$	JINR-06	4.2.1
$C4$	$\delta_{\bar{p}^4He^+}(37, 34 : 36, 33)$	0.0(1.1) MHz	$[1.8 \times 10^{-9}]$	JINR-06	4.2.1
$C5$	$\delta_{\bar{p}^4He^+}(39, 35 : 38, 34)$	0.0(1.2) MHz	$[2.3 \times 10^{-9}]$	JINR-06	4.2.1
$C6$	$\delta_{\bar{p}^4He^+}(40, 35 : 39, 34)$	0.0(1.3) MHz	$[2.9 \times 10^{-9}]$	JINR-06	4.2.1
$C7$	$\delta_{\bar{p}^4He^+}(37, 35 : 38, 34)$	0.0(1.8) MHz	$[4.5 \times 10^{-9}]$	JINR-06	4.2.1
$C8$	$\delta_{\bar{p}^4He^+}(33, 32 : 31, 30)$	0.0(1.6) MHz	$[7.6 \times 10^{-10}]$	JINR-10	4.2.1
$C9$	$\delta_{\bar{p}^4He^+}(36, 34 : 34, 32)$	0.0(2.1) MHz	$[1.4 \times 10^{-9}]$	JINR-10	4.2.1
$C10$	$\delta_{\bar{p}^3He^+}(32, 31 : 31, 30)$	0.00(91) MHz	$[8.7 \times 10^{-10}]$	JINR-06	4.2.1
$C11$	$\delta_{\bar{p}^3He^+}(34, 32 : 33, 31)$	0.0(1.1) MHz	$[1.4 \times 10^{-9}]$	JINR-06	4.2.1
$C12$	$\delta_{\bar{p}^3He^+}(36, 33 : 35, 32)$	0.0(1.2) MHz	$[1.8 \times 10^{-9}]$	JINR-06	4.2.1
$C13$	$\delta_{\bar{p}^3He^+}(38, 34 : 37, 33)$	0.0(1.1) MHz	$[2.3 \times 10^{-9}]$	JINR-06	4.2.1
$C14$	$\delta_{\bar{p}^3He^+}(36, 34 : 37, 33)$	0.0(1.8) MHz	$[4.4 \times 10^{-9}]$	JINR-06	4.2.1
$C15$	$\delta_{\bar{p}^3He^+}(35, 33 : 33, 31)$	0.0(2.2) MHz	$[1.4 \times 10^{-9}]$	JINR-10	4.2.1
$C16$	$\nu_{\bar{p}^4He^+}(32, 31 : 31, 30)$	1 132 609 209(15) MHz	1.4×10^{-8}	CERN-06	4.2.2
$C17$	$\nu_{\bar{p}^4He^+}(35, 33 : 34, 32)$	804 633 059.0(8.2) MHz	1.0×10^{-8}	CERN-06	4.2.2
$C18$	$\nu_{\bar{p}^4He^+}(36, 34 : 35, 33)$	717 474 004(10) MHz	1.4×10^{-8}	CERN-06	4.2.2
$C19$	$\nu_{\bar{p}^4He^+}(37, 34 : 36, 33)$	636 878 139.4(7.7) MHz	1.2×10^{-8}	CERN-06	4.2.2
$C20$	$\nu_{\bar{p}^4He^+}(39, 35 : 38, 34)$	501 948 751.6(4.4) MHz	8.8×10^{-9}	CERN-06	4.2.2
$C21$	$\nu_{\bar{p}^4He^+}(40, 35 : 39, 34)$	445 608 557.6(6.3) MHz	1.4×10^{-8}	CERN-06	4.2.2
$C22$	$\nu_{\bar{p}^4He^+}(37, 35 : 38, 34)$	412 885 132.2(3.9) MHz	9.4×10^{-9}	CERN-06	4.2.2
$C23$	$\nu_{\bar{p}^4He^+}(33, 32 : 31, 30)$	2 145 054 858.2(5.1) MHz	2.4×10^{-9}	CERN-10	4.2.2
$C24$	$\nu_{\bar{p}^4He^+}(36, 34 : 34, 32)$	1 522 107 061.8(3.5) MHz	2.3×10^{-9}	CERN-10	4.2.2
$C25$	$\nu_{\bar{p}^3He^+}(32, 31 : 31, 30)$	1 043 128 608(13) MHz	1.3×10^{-8}	CERN-06	4.2.2
$C26$	$\nu_{\bar{p}^3He^+}(34, 32 : 33, 31)$	822 809 190(12) MHz	1.5×10^{-8}	CERN-06	4.2.2
$C27$	$\nu_{\bar{p}^3He^+}(36, 33 : 35, 32)$	646 180 434(12) MHz	1.9×10^{-8}	CERN-06	4.2.2
$C28$	$\nu_{\bar{p}^3He^+}(38, 34 : 37, 33)$	505 222 295.7(8.2) MHz	1.6×10^{-8}	CERN-06	4.2.2
$C29$	$\nu_{\bar{p}^3He^+}(36, 34 : 37, 33)$	414 147 507.8(4.0) MHz	9.7×10^{-9}	CERN-06	4.2.2
$C30$	$\nu_{\bar{p}^3He^+}(35, 33 : 33, 31)$	1 553 643 099.6(7.1) MHz	4.6×10^{-9}	CERN-10	4.2.2

[a]The values in brackets are relative to the corresponding transition frequency.
[b]JINR: Joint Institute for Nuclear Research, Dubna, Russian Federation; CERN: European Organization for Nuclear Research, Geneva, Switzerland.

TABLE 23. Non-negligible correlation coefficients $r(x_i, x_j)$ of the input data in Table 22. For simplicity, the two items of data to which a particular correlation coefficient corresponds are identified by their item numbers in Table 22.

$r(C1, C2) = 0.929$	$r(C4, C10) = 0.959$	$r(C9, C14) = -0.976$	$r(C18, C27) = 0.141$
$r(C1, C3) = 0.936$	$r(C4, C11) = 0.949$	$r(C9, C15) = 0.986$	$r(C18, C28) = 0.106$
$r(C1, C4) = 0.936$	$r(C4, C12) = 0.907$	$r(C10, C11) = 0.978$	$r(C18, C29) = 0.217$
$r(C1, C5) = 0.912$	$r(C4, C13) = 0.931$	$r(C10, C12) = 0.934$	$r(C19, C20) = 0.268$
$r(C1, C6) = 0.758$	$r(C4, C14) = -0.952$	$r(C10, C13) = 0.959$	$r(C19, C21) = 0.193$
$r(C1, C7) = -0.947$	$r(C4, C15) = 0.961$	$r(C10, C14) = -0.980$	$r(C19, C22) = 0.302$
$r(C1, C8) = 0.954$	$r(C5, C6) = 0.734$	$r(C10, C15) = 0.990$	$r(C19, C25) = 0.172$
$r(C1, C9) = 0.960$	$r(C5, C7) = -0.917$	$r(C11, C12) = 0.925$	$r(C19, C26) = 0.190$
$r(C1, C10) = 0.964$	$r(C5, C8) = 0.924$	$r(C11, C13) = 0.949$	$r(C19, C27) = 0.189$
$r(C1, C11) = 0.954$	$r(C5, C9) = 0.930$	$r(C11, C14) = -0.970$	$r(C19, C28) = 0.144$
$r(C1, C12) = 0.912$	$r(C5, C10) = 0.934$	$r(C11, C15) = 0.980$	$r(C19, C29) = 0.294$
$r(C1, C13) = 0.936$	$r(C5, C11) = 0.925$	$r(C12, C13) = 0.907$	$r(C20, C21) = 0.210$
$r(C1, C14) = -0.957$	$r(C5, C12) = 0.883$	$r(C12, C14) = -0.927$	$r(C20, C22) = 0.295$
$r(C1, C15) = 0.966$	$r(C5, C13) = 0.907$	$r(C12, C15) = 0.936$	$r(C20, C25) = 0.152$
$r(C2, C3) = 0.924$	$r(C5, C14) = -0.927$	$r(C13, C14) = -0.952$	$r(C20, C26) = 0.167$
$r(C2, C4) = 0.924$	$r(C5, C15) = 0.936$	$r(C13, C15) = 0.961$	$r(C20, C27) = 0.169$
$r(C2, C5) = 0.900$	$r(C6, C7) = -0.762$	$r(C14, C15) = -0.982$	$r(C20, C28) = 0.141$
$r(C2, C6) = 0.748$	$r(C6, C8) = 0.767$	$r(C16, C17) = 0.210$	$r(C20, C29) = 0.287$
$r(C2, C7) = -0.935$	$r(C6, C9) = 0.773$	$r(C16, C18) = 0.167$	$r(C21, C22) = 0.235$
$r(C2, C8) = 0.941$	$r(C6, C10) = 0.776$	$r(C16, C19) = 0.224$	$r(C21, C25) = 0.107$
$r(C2, C9) = 0.948$	$r(C6, C11) = 0.768$	$r(C16, C20) = 0.197$	$r(C21, C26) = 0.118$
$r(C2, C10) = 0.952$	$r(C6, C12) = 0.734$	$r(C16, C21) = 0.138$	$r(C21, C27) = 0.122$
$r(C2, C11) = 0.942$	$r(C6, C13) = 0.753$	$r(C16, C22) = 0.222$	$r(C21, C28) = 0.112$
$r(C2, C12) = 0.900$	$r(C6, C14) = -0.770$	$r(C16, C25) = 0.129$	$r(C21, C29) = 0.229$
$r(C2, C13) = 0.924$	$r(C6, C15) = 0.778$	$r(C16, C26) = 0.142$	$r(C22, C25) = 0.170$
$r(C2, C14) = -0.945$	$r(C7, C8) = -0.959$	$r(C16, C27) = 0.141$	$r(C22, C26) = 0.188$
$r(C2, C15) = 0.954$	$r(C7, C9) = -0.966$	$r(C16, C28) = 0.106$	$r(C22, C27) = 0.191$
$r(C3, C4) = 0.931$	$r(C7, C10) = -0.970$	$r(C16, C29) = 0.216$	$r(C22, C28) = 0.158$
$r(C3, C5) = 0.907$	$r(C7, C11) = -0.960$	$r(C17, C18) = 0.209$	$r(C22, C29) = 0.324$
$r(C3, C6) = 0.753$	$r(C7, C12) = -0.917$	$r(C17, C19) = 0.280$	$r(C23, C24) = 0.155$
$r(C3, C7) = -0.942$	$r(C7, C13) = -0.942$	$r(C17, C20) = 0.247$	$r(C23, C30) = 0.104$
$r(C3, C8) = 0.948$	$r(C7, C14) = 0.963$	$r(C17, C21) = 0.174$	$r(C24, C30) = 0.167$
$r(C3, C9) = 0.955$	$r(C7, C15) = -0.972$	$r(C17, C22) = 0.278$	$r(C25, C26) = 0.109$
$r(C3, C10) = 0.959$	$r(C8, C9) = 0.973$	$r(C17, C25) = 0.161$	$r(C25, C27) = 0.108$
$r(C3, C11) = 0.949$	$r(C8, C10) = 0.977$	$r(C17, C26) = 0.178$	$r(C25, C28) = 0.081$
$r(C3, C12) = 0.907$	$r(C8, C11) = 0.967$	$r(C17, C27) = 0.177$	$r(C25, C29) = 0.166$
$r(C3, C13) = 0.931$	$r(C8, C12) = 0.924$	$r(C17, C28) = 0.132$	$r(C26, C27) = 0.120$
$r(C3, C14) = -0.952$	$r(C8, C13) = 0.948$	$r(C17, C29) = 0.271$	$r(C26, C28) = 0.090$
$r(C3, C15) = 0.961$	$r(C8, C14) = -0.969$	$r(C18, C19) = 0.223$	$r(C26, C29) = 0.184$
$r(C4, C5) = 0.907$	$r(C8, C15) = 0.979$	$r(C18, C20) = 0.198$	$r(C27, C28) = 0.091$
$r(C4, C6) = 0.753$	$r(C9, C10) = 0.984$	$r(C18, C21) = 0.140$	$r(C27, C29) = 0.186$
$r(C4, C7) = -0.942$	$r(C9, C11) = 0.974$	$r(C18, C22) = 0.223$	$r(C28, C29) = 0.154$
$r(C4, C8) = 0.948$	$r(C9, C12) = 0.930$	$r(C18, C25) = 0.128$	
$r(C4, C9) = 0.955$	$r(C9, C13) = 0.955$	$r(C18, C26) = 0.142$	

The binding energies $E_b(X)/m_u c^2$ in the observational equations of Table 33 are treated as fixed quantities with negligible uncertainties, as are the bound-state g-factor ratios. The frequency f_p is not an adjusted constant but is included in the equation for data items $B30$ and $B31$ to indicate that they are functions of f_p. Finally, the observational equations for items $B30$ and $B31$, which are based on Eqs. (228)–(230) of Sec. 6.2.2, include the function $a_e(\alpha, \delta_e)$, as well as the theoretical expression for input data of type $B29$, $\Delta\nu_{Mu}$. The latter expression is discussed in Sec. 6.2.1 and is a function of R_∞, α, m_e/m_μ, and a_μ.

The self-sensitivity coefficient S_c for an input datum is a measure of the influence of a particular item of data on its corresponding adjusted value. As in previous adjustments, in general, for an input datum to be included in the final adjustment on which the 2010 recommended values are based, its value of S_c must be greater than 0.01, or 1%, which means that its uncertainty must be no more than about a factor of 10 larger than the uncertainty of the adjusted value of that quantity; see Sec. I.D of CODATA-98 for the justification of this 1% cutoff. However, the exclusion of a datum is not followed if, for example, a datum with $S_c < 0.01$ is part of a group of data obtained in a given experiment, or series of experiments, where most of the other data have self-sensitivity coefficients greater than 0.01. It is also not followed for G, because in this case there is substantial disagreement of some of the data with the smallest uncertainties and hence relatively greater significance of the data with larger uncertainties.

In summary, there is one major discrepancy among the data discussed so far: the disagreement of the NIST-07 watt balance value of $K_J^2 R_K$ and the IAC-11 enriched ^{28}Si XRCD value of N_A, items $B37.3$ and $B54$ of Table 20.

TABLE 24. Summary of values of G used to determine the 2010 recommended value (see also Table 17, Sec. 11).

Item No.	Value[a] (10^{-11} m^3 kg^{-1} s^{-2})	Relative standard uncertainty u_r	Identification
$G1$	6.672 48(43)	6.4×10^{-5}	NIST-82
$G2$	6.672 9(5)	7.5×10^{-5}	TR&D-96
$G3$	6.673 98(70)	1.0×10^{-4}	LANL-97
$G4$	6.674 255(92)	1.4×10^{-5}	UWash-00
$G5$	6.675 59(27)	4.0×10^{-5}	BIPM-01
$G6$	6.674 22(98)	1.5×10^{-4}	UWup-02
$G7$	6.673 87(27)	4.0×10^{-5}	MSL-03
$G8$	6.672 28(87)	1.3×10^{-4}	HUST-05
$G9$	6.674 25(12)	1.9×10^{-5}	UZur-06
$G10$	6.673 49(18)	2.7×10^{-5}	HUST-09
$G11$	6.672 34(14)	2.1×10^{-5}	JILA-10

[a]Correlation coefficients: $r(G1, G3) = 0.351$; $r(G8, G10) = 0.234$.

13.2.1. Data related to the Newtonian constant of gravitation G

Our least-squares analysis of the input data begins with the 11 values of G in Table 24, which are graphically compared in Fig. 6. (Because the G data are independent of all other data, they can be treated separately.) As discussed in Secs. 11.1.2 and 11.2.1, there are two correlation coefficients associated with these data: $r(G1, G3) = 0.351$ and $r(G8, G10) = 0.234$. It is clear from both the table and figure that the data are highly inconsistent. Of the 55 differences among the 11 values, the three largest, $11.4u_{\rm diff}$, $10.7u_{\rm diff}$, and $10.2u_{\rm diff}$, are between JILA-10 and three others: UWash-00, BIPM-01, and UZur-06, respectively. Further, eight range from $4u_{\rm diff}$ to $7u_{\rm diff}$. The weighted mean of the 11 values has a relative standard uncertainty of 8.6×10^{-6}. For this calculation, with $\nu = 10$, we have $\chi^2 = 209.6$, $p(209.6|10) \approx 0$, and $R_{\rm B} = 4.58$. Five data have normalized residuals $|r_i| > 2.0$: JILA-10, BIPM-01, UWash-00, NIST-82, and UZur-06; their respective values are -10.8, 6.4, 4.4, -3.2 and 3.2.

Repeating the calculation using only the six values of G with relative uncertainties $\leq 4.0 \times 10^{-5}$, namely, UWash-00, BIPM-01, MSL-03, UZur-06, HUST-09, and JILA-10, has little impact: the value of G increases by the fractional amount 5.0×10^{-6} and the relative uncertainty increases to 8.8×10^{-6}; for this calculation $\nu = 5$, $\chi^2 = 191.4$, $p(191.4|5) \approx 0$, and $R_{\rm B} = 6.19$; the values of r_i are 4.0, 6.3, -0.05, 3.0, -2.2, and -11.0, respectively.

Taking into account the historic difficulty in measuring G and the fact that all 11 values of G have no apparent issue besides the disagreement among them, the Task Group decided to take as the 2010 recommended value the weighted mean of the 11 values in Table 24 after each of their uncertainties is multiplied by the factor 14. This yields

$$G = 6.673\,84(80) \times 10^{-11}\ \text{m}^3\,\text{kg}^{-1}\,\text{s}^{-2} \quad [1.2 \times 10^{-4}]. \tag{284}$$

The largest normalized residual, that of JILA-10, is now -0.77, and the largest difference between values of G, that between JILA-10 and UWash-00, is $0.82u_{\rm diff}$. For the calculation yielding the recommended value, $\nu = 10$, $\chi^2 = 1.07$, $p(1.07|10) = 1.00$, and $R_{\rm B} = 0.33$. In view of the significant scatter of the measured values of G, the factor of 14 was chosen so that the smallest and largest values would differ from the recommended value by about twice its uncertainty; see Fig. 6. The 2010 recommended value represents a fractional decrease from the 2006 value of 0.66×10^{-4} and an increase in uncertainty of 20%.

13.2.2. Data related to all other constants

Tables 36–38 summarize 12 least-squares analyses, discussed in the following paragraphs, of the input data and correlation coefficients in Tables 18–23. Because the adjusted value of R_∞ is essentially the same for all five adjustments summarized in Table 36 and equal to that of adjustment 3 of Table 38, the values are not listed in Table 36. (Note that adjustment 3 in Tables 36 and 38 is the same adjustment.)

Adjustment 1: The initial adjustment includes all of the input data, three of which have normalized residuals whose absolute magnitudes are problematically greater than 2; see Table 37. They are the 2007 NIST watt-balance result for $K_{\rm J}^2 R_{\rm K}$, the 2011 IAC enriched silicon XRCD result for $N_{\rm A}$, and the 1989 NIST result for $\Gamma'_{\rm p-90}$(lo). All other input data have values of $|r_i|$ less than 2, except those for two antiprotonic ^{3}He transitions, data items $C25$ and $C27$ in Table 22, for which $r_{25} = 2.12$ and $r_{27} = 2.10$. However, the fact that their normalized residuals are somewhat greater than 2 is not a major concern, because their self-sensitivity coefficients $S_{\rm c}$ are considerably less than 0.01. In this regard, we see from Table 37 that two of the three inconsistent data have values of $S_{\rm c}$ considerably larger than 0.01; the exception is $\Gamma'_{\rm p-90}$(lo) with $S_{\rm c} = 0.0096$, which is rounded to 0.010 in the table.

Adjustment 2: The difference in the IAC-11 and NIST-07 values of h (see the first two lines of Table 26) is $3.8u_{\rm diff}$, where as before $u_{\rm diff}$ is the standard uncertainty of the difference. To reduce the difference between these two highly credible results to an acceptable level, that is, to $2u_{\rm diff}$ or slightly below, the Task Group decided that the uncertainties used in the adjustment for these data would be those in Table 20 multiplied by a factor of 2. It was also decided to apply the same factor to the uncertainties of all the data that contribute in a significant way to the determination of h, so that the relative weights of this set of data are unchanged. [Recall that if the difference between two values of the same quantity is $au_{\rm diff}$ and the uncertainty of each is increased by a factor b, the difference is reduced to $(a/b)u_{\rm diff}$.] Thus, adjustment 2 differs from adjustment 1 in that the uncertainties of data items $B36.1$, $B36.2$, $B37.1$ to $B37.5$, and $B54$ in Table 20, which are the two values of $K_{\rm J}$, the five values of $K_{\rm J}^2 R_{\rm K}$, and the value of $N_{\rm A}$, are increased by a factor of 2. [Although items $B34.1$, $B34.2$, and $B38$, the two values of $\Gamma'_{\rm p-90}$(hi) and $\mathcal{F}_{90}$, also contribute to the determination of h, their contribution is small and no multiplicative factor is applied.]

From Tables 36 and 37 we see that the values of α and h from adjustment 2 are very nearly the same as from adjustment 1,

TABLE 25. Inferred values of the fine-structure constant α in order of increasing standard uncertainty obtained from the indicated experimental data in Table 20.

Primary source	Item No.	Identification	Sec. and Eq.	α^{-1}	Relative standard uncertainty u_r
a_e	*B*13.2	HarvU-08	5.1.3 (128)	137.035 999 084(51)	3.7×10^{-10}
$h/m(^{87}\mathrm{Rb})$	*B*57	LKB-11	7.2	137.035 999 045(90)	6.6×10^{-10}
a_e	*B*11	UWash-87	5.1.3 (127)	137.035 998 19(50)	3.7×10^{-9}
$h/m(^{133}\mathrm{Cs})$	*B*56	StanfU-02	7.1	137.036 0000(11)	7.7×10^{-9}
R_K	*B*35.1	NIST-97	8.2	137.036 0037(33)	2.4×10^{-8}
$\Gamma'_{p-90}(\mathrm{lo})$	*B*32.1	NIST-89	8.2	137.035 9879(51)	3.7×10^{-8}
R_K	*B*35.2	NMI-97	8.2	137.035 9973(61)	4.4×10^{-8}
R_K	*B*35.5	LNE-01	8.2	137.036 0023(73)	5.3×10^{-8}
R_K	*B*35.3	NPL-88	8.2	137.036 0083(73)	5.4×10^{-8}
$\Delta\nu_{Mu}$	*B*29.1, *B*29.2	LAMPF	6.2.2 (233)	137.036 0018(80)	5.8×10^{-8}
$\Gamma'_{h-90}(\mathrm{lo})$	*B*33	KR/VN-98	8.2	137.035 9852(82)	6.0×10^{-8}
R_K	*B*35.4	NIM-95	8.2	137.036 004(18)	1.3×10^{-7}
$\Gamma'_{p-90}(\mathrm{lo})$	*B*32.2	NIM-95	8.2	137.036 006(30)	2.2×10^{-7}
ν_H, ν_D			4.1.1.13 (88)	137.036 003(41)	3.0×10^{-7}

that $|r_i|$ for both *B*37.3 and *B*54 have been reduced to below 1.4, and that the residual for $\Gamma'_{p-90}(\mathrm{lo})$ is unchanged.

Adjustment 3: Adjustment 3 is the adjustment on which the 2010 CODATA recommended values are based, and as such it is referred to as the "final adjustment." It differs from adjustment 2 in that, following the prescription described above, 18 input data with values of S_c less than 0.01 are deleted. These are data items *B*13.1, *B*32.1 to *B*36.2, *B*37.5, *B*38, *B*56, *B*59, and *B*60 in Table 20. (The range in values of S_c for the deleted data is 0.0001 to 0.0097, and no datum with a value of $S_c > 0.01$ was "converted" to a value with $S_c < 0.01$ due to the multiplicative factor.) Further, because $h/m(^{133}\mathrm{Cs})$, item *B*56, is deleted as an input datum due to its low weight, the two values of $A_r(^{133}\mathrm{Cs})$, items *B*10.1 and 10.2, which are not relevant to any other input datum, are also deleted and $A_r(^{133}\mathrm{Cs})$ is omitted as an adjusted constant. This brings the total number of omitted data items to 20. Table 36 shows that deleting them has virtually no impact on the values of α and h and Birge ratio R_B. The data for the final adjustment are quite consistent, as demonstrated by the value of χ^2: $p(58.1|67) = 0.77$.

Adjustments 4 and 5: The purpose of these adjustments is to test the robustness of the 2010 recommended values of α and h by omitting the most accurate data relevant to these constants. Adjustment 4 differs from adjustment 2 in that the four data that provide values of α with the smallest uncertainties are deleted, namely, items *B*13.1, *B*13.2, *B*56 and *B*57, the two values of a_e and the values of $h/m(^{133}\mathrm{Cs})$ and $h/m(^{87}\mathrm{Rb})$; see the first four entries of Table 25. [For the same reason as in adjustment 3, in adjustment 4 the two values of $A_r(^{133}\mathrm{Cs})$ are

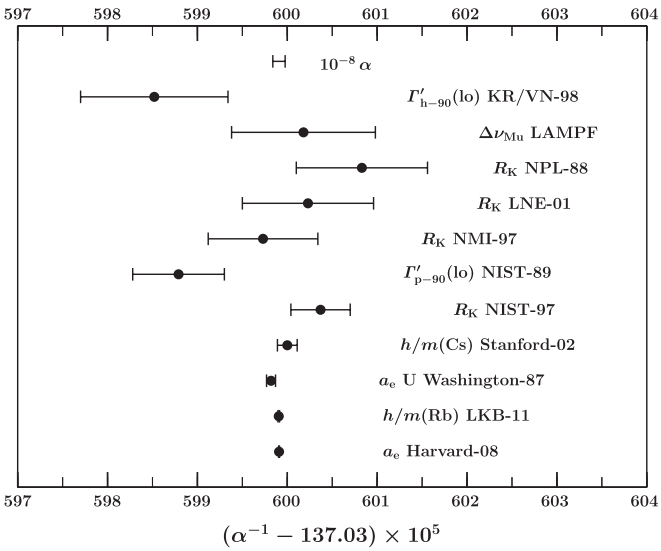

FIG. 1. Values of the fine-structure constant α with $u_r < 10^{-7}$ implied by the input data in Table 20, in order of decreasing uncertainty from top to bottom (see Table 25).

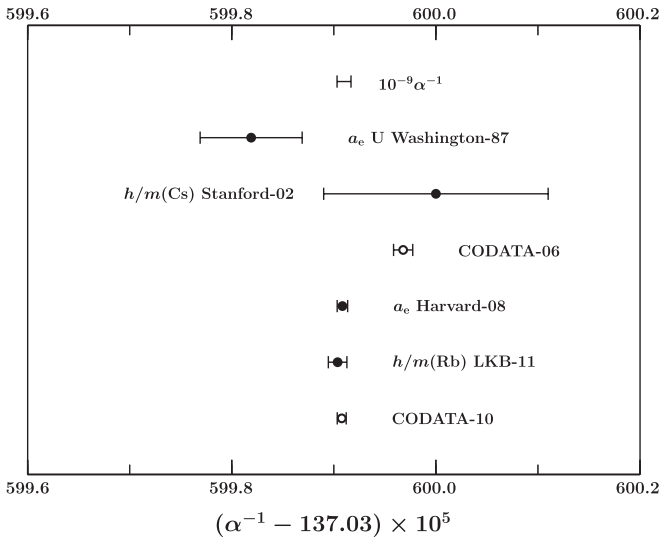

FIG. 2. Values of the fine-structure constant α with $u_r < 10^{-8}$ implied by the input data in Table 20 and the 2006 and 2010 CODATA recommended values in chronological order from top to bottom (see Table 25).

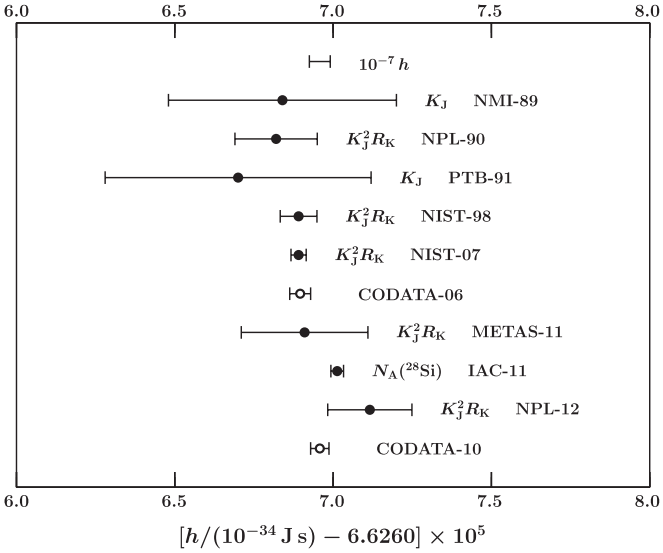

FIG. 3. Values of the Planck constant h with $u_r < 10^{-6}$ implied by the input data in Table 20 and the 2006 and 2010 CODATA recommended values in chronological order from top to bottom (see Table 26).

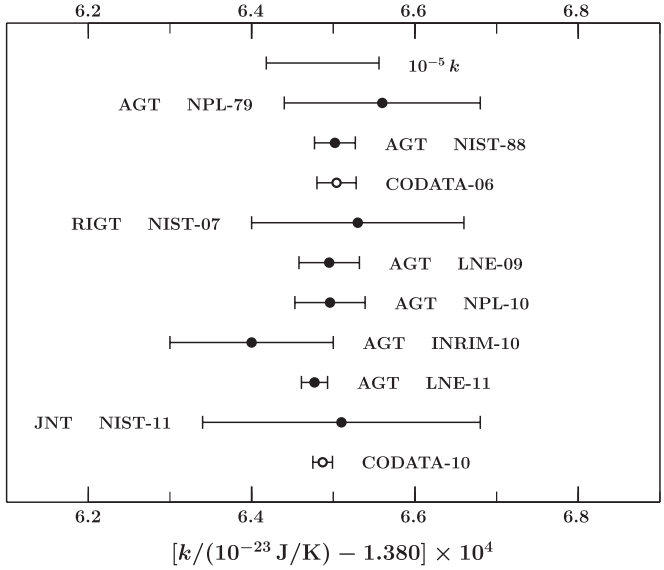

FIG. 4. Values of the Boltzmann constant k implied by the input data in Table 20 and the 2006 and 2010 CODATA recommended values in chronological order from top to bottom (see Table 27). AGT: acoustic gas thermometry; RIGT: refractive index gas thermometry; JNT: Johnson noise thermometry.

also deleted as input data and $A_r(^{133}Cs)$ is omitted as an adjusted constant; the same applies to $A_r(^{87}Rb)$.] Adjustment 5 differs from adjustment 1 in that the three data that provide values of h with the smallest uncertainties are deleted, namely, items $B37.2$, $B37.3$, and $B54$, the two NIST values of $K_J^2R_K$ and the IAC value of N_A; see the first three entries of Table 26. Also deleted are the data with $S_c < 0.01$ that contribute in a minimal way to the determination of α and are deleted in the final adjustment. Table 36 shows that the value of α from the less accurate α-related data used in adjustment 4, and the value of h from the less accurate h-related data used in adjustment 5 agree with the corresponding recommended values from adjustment 3. This agreement provides a consistency check on the 2010 recommended values.

Adjustments 6 to 12: The aim of the seven adjustments summarized in Table 38 is to investigate the data that determine the recommended values of R_∞, r_p, and r_d. Results from adjustment 3, the final adjustment, are included in the table for reference purposes. We begin with a discussion of adjustments 6–10, which are derived from adjustment 3 by deleting selected input data. We then discuss adjustments 11 and 12, which examine the impact of the value of the proton rms charge radius derived from the measurement of the Lamb shift in muonic hydrogen discussed in Sec. 4.1.3.2 and given in Eq. (97). Note that the value of R_∞ depends only weakly on the data in Tables 20 and 22.

In adjustment 6, the electron-scattering values of r_p and r_d, data items $A49.1$, $A49.2$, and $A50$ in Table 18, are not included. Thus, the values of these two quantities from adjustment 6 are based solely on H and D spectroscopic data. It is evident from a comparison of the results of this adjustment and adjustment 3 that the scattering values of the radii play a smaller role than the spectroscopic data in determining the 2010 recommended values of R_∞, r_p, and r_d.

Adjustment 7 is based on only hydrogen data, including the two scattering values of r_p but not the difference between the $1S_{1/2}-2S_{1/2}$ transition frequencies in H and D, item $A48$ in Table 18, hereafter referred to as the isotope shift. Adjustment 8 differs from adjustment 7 in that the two scattering values of r_p are deleted. Adjustments 9 and 10 are similar to 7 and 8 but are based on only deuterium data; that is, adjustment 9 includes the scattering value of r_d but not the isotope shift, while for adjustment 10 the scattering value is deleted. The results of these four adjustments show the dominant role of the hydrogen data and the importance of the isotope shift in determining the recommended value of r_d. Further, the four values of R_∞ from these adjustments agree with the 2010 recommended value, and the two values of r_p and of r_d also agree with their respective recommended values: the largest difference from the recommended value for the eight results is $1.4u_{diff}$.

Adjustment 11 differs from adjustment 3 in that it includes the muonic hydrogen value $r_p = 0.841\,69(66)$ fm, and adjustment 12 differs from adjustment 11 in that the three scattering values of the nuclear radii are deleted. Because the muonic hydrogen value is significantly smaller and has a significantly smaller uncertainty than the purely spectroscopic value of adjustment 6 and the two scattering values, it has a major impact on the results of adjustments 11 and 12, as can be seen from Table 38: for both adjustments the value of R_∞ shifts down by over 6 standard deviations and its uncertainty is reduced by a factor of 4.6. Moreover, and not surprisingly, the values of r_p and of r_d from both adjustments are significantly smaller than the recommended values and have significantly

TABLE 26. Inferred values of the Planck constant h in order of increasing standard uncertainty obtained from the indicated experimental data in Table 20.

Primary source	Item No.	Identification	Sec. and Eq.	$h/(\mathrm{J\,s})$	Relative standard uncertainty u_r
$N_A(^{28}Si)$	*B*54	IAC-11	9.6	$6.626\,070\,09(20) \times 10^{-34}$	3.0×10^{-8}
$K_J^2 R_K$	*B*37.3	NIST-07	8.2	$6.626\,068\,91(24) \times 10^{-34}$	3.6×10^{-8}
$K_J^2 R_K$	*B*37.2	NIST-98	8.2	$6.626\,068\,91(58) \times 10^{-34}$	8.7×10^{-8}
$K_J^2 R_K$	*B*37.1	NPL-90	8.2	$6.626\,0682(13) \times 10^{-34}$	2.0×10^{-7}
$K_J^2 R_K$	*B*37.4	NPL-12	8.2.1 (244)	$6.626\,0712(13) \times 10^{-34}$	2.0×10^{-7}
$K_J^2 R_K$	*B*37.5	METAS-11	8.2.2 (246)	$6.626\,0691(20) \times 10^{-34}$	2.9×10^{-7}
K_J	*B*36.1	NMI-89	8.2	$6.626\,0684(36) \times 10^{-34}$	5.4×10^{-7}
K_J	*B*36.2	PTB-91	8.2	$6.626\,0670(42) \times 10^{-34}$	6.3×10^{-7}
$\Gamma'_{p-90}(\mathrm{hi})$	*B*34.2	NPL-79	8.2	$6.626\,0730(67) \times 10^{-34}$	1.0×10^{-6}
$\mathcal{F}_{90}$	*B*38	NIST-80	8.2	$6.626\,0657(88) \times 10^{-34}$	1.3×10^{-6}
$\Gamma'_{p-90}(\mathrm{hi})$	*B*34.1	NIM-95	8.2	$6.626\,071(11) \times 10^{-34}$	1.6×10^{-6}

smaller uncertainties. The inconsistencies between the muonic hydrogen result for r_p and the spectroscopic and scattering results is demonstrated by the large value and low probability of χ^2 for adjustment 11; $p(104.9|68) = 0.0027$.

The impact of the muonic hydrogen value of r_p can also be seen by examining for adjustments 3, 11, and 12 the normalized residuals and self-sensitivity coefficients of the principal experimental data that determine R_∞, namely, items *A*26–*A*50 of Table 18. In brief, $|r_i|$ for these data in the final adjustment range from near 0 to 1.24 for item *A*50, the r_d scattering result, with the vast majority being less than 1. For the three greater than 1, $|r_i|$ is 1.03, 1.08, and 1.04. The value of S_c is 1.00 for items *A*26 and *A*48, the hydrogen $1S_{1/2}$–$2S_{1/2}$ transition frequency and the H-D isotope shift; and 0.42 for item *A*49.2, which is the more accurate of the two scattering values of r_p. Most others are a few percent, although some values of S_c are near 0. The situation is markedly different for adjustment 12. First, $|r_i|$ for item *A*30, the hydrogen transition frequency involving the $8D_{5/2}$ state, is 3.06 compared to 0.87 in adjustment 3; and items *A*41, *A*42, and *A*43, deuterium transitions involving the $8S_{1/2}$, $8D_{3/2}$, and $8D_{5/2}$ states, are now 2.5, 2.4, and 3.0, respectively, compared to 0.40, 0.17, and 0.68. Further, ten other transitions have residuals in the range 1.02 to 1.76. As a result, with this proton radius, the predictions of the theory for hydrogen and deuterium transition frequencies are not generally consistent with the experiments. Equally noteworthy is the fact that although S_c for items *A*26 and *A*48 remain equal to 1.00, for all other transition frequencies S_c is less than 0.01, which means that they play an inconsequential role in determining R_∞. The results for adjustment 11, which includes the scattering values of the nuclear radii as well as the muonic hydrogen value, are similar.

In view of the impact of the latter value on the internal consistency of the R_∞ data and its disagreement with the spectroscopic and scattering values, the Task Group decided that it was premature to include it as an input datum in the 2010 CODATA adjustment; it was deemed more prudent to wait to see if further research can resolve the discrepancy; see Sec. 4.1.3.2 for additional discussion.

13.2.3. Test of the Josephson and quantum-Hall-effect relations

As in CODATA-02 and CODATA-06, the exactness of the relations $K_J = 2e/h$ and $R_K = h/e^2$ is investigated by writing

$$K_J = \frac{2e}{h}(1+\epsilon_J) = \left(\frac{8\alpha}{\mu_0 ch}\right)^{1/2}(1+\epsilon_J), \tag{285}$$

$$R_K = \frac{h}{e^2}(1+\epsilon_K) = \frac{\mu_0 c}{2\alpha}(1+\epsilon_K), \tag{286}$$

where ϵ_J and ϵ_K are unknown correction factors taken to be additional adjusted constants. Replacing the relations $K_J = 2e/h$ and $R_K = h/e^2$ in the analysis leading to the observational equations in Table 33 with the generalizations in Eqs. (285) and (286) leads to the modified observational equations given in Table 39.

Although the NIST value of k/h, item *B*60, was obtained using the Josephson and quantum Hall effects, it is not included in the tests of the relations $K_J = 2e/h$ and $R_K = h/e^2$, because of its large uncertainty.

The results of seven different adjustments are summarized in Table 29. An entry of 0 in the ϵ_K column means that it is assumed that $R_K = h/e^2$ in the corresponding adjustment; similarly, an entry of 0 in the ϵ_J column means that it is assumed that $K_J = 2e/h$ in the corresponding adjustment. The following comments apply to the adjustments of Table 29.

Adjustment (i) uses all of the data and thus differs from adjustment 1 of Table 36 discussed in the previous section only in that the assumption $K_J = 2e/h$ and $R_K = h/e^2$ is relaxed. For this adjustment, $\nu = 86$, $\chi^2 = 78.1$, and $R_B = 1.02$. The normalized residuals r_i for the three inconsistent data items in

TABLE 27. Inferred values of the Boltzmann constant k in order of increasing standard uncertainty obtained from the indicated experimental data in Table 20.

Primary source	Item No.	Identification	Sec.	$k/(\mathrm{J\,K^{-1}})$	Relative standard uncertainty u_r
R	$B58.6$	LNE-11	10.1.2	$1.380\,6477(17) \times 10^{-23}$	1.2×10^{-6}
R	$B58.2$	NIST-88	10.1.1	$1.380\,6503(25) \times 10^{-23}$	1.8×10^{-6}
R	$B58.3$	LNE-09	10.1.2	$1.380\,6495(37) \times 10^{-23}$	2.7×10^{-6}
R	$B58.4$	NPL-10	10.1.3	$1.380\,6496(43) \times 10^{-23}$	3.1×10^{-6}
R	$B58.5$	INRIM-10	10.1.4	$1.380\,640(10) \times 10^{-23}$	7.5×10^{-6}
R	$B58.1$	NPL-79	10.1.1	$1.380\,656(12) \times 10^{-23}$	8.4×10^{-6}
k	$B59$	NIST-07	10.2.1	$1.380\,653(13) \times 10^{-23}$	9.1×10^{-6}
k/h	$B60$	NIST-11	10.2.2	$1.380\,652(17) \times 10^{-23}$	1.2×10^{-5}

TABLE 28. Inferred values of the electron relative atomic mass $A_r(e)$ in order of increasing standard uncertainty obtained from the indicated experimental data in Tables 20 and 22.

Primary source	Item No.	Identification	Sec. and Eq.	$A_r(e)$	Relative standard uncertainty u_r
$f_s(C)/f_c(C)$	$B17$	GSI-02	5.3.2 (188)	0.000 548 579 909 32(29)	5.2×10^{-10}
$f_s(O)/f_c(O)$	$B18$	GSI-04	5.3.2 (189)	0.000 548 579 909 57(42)	7.6×10^{-10}
$\Delta\nu_{pHe^+}$	$C16-C30$	CERN−06/10	4.2.3 (102)	0.000 548 579 909 14(75)	1.4×10^{-9}
$A_r(e)$	$B11$	UWash-95	3.4 (20)	0.000 548 579 9111(12)	2.1×10^{-9}

Table 37, the companion table to Table 36, are 0.75, −0.56, and 2.88. Examination of Table 29 shows that ϵ_K is consistent with 0 within 1.2 times its uncertainty of 1.8×10^{-8}, while ϵ_J is consistent with 0 within 2.4 times its uncertainty of 2.4×10^{-8}.

It is important to recognize that any conclusions that can be drawn from the values of ϵ_K and ϵ_J of adjustment (i) must be tempered, because not all of the individual values of ϵ_K and ϵ_J that contribute to their determination are consistent. This is demonstrated by adjustments (ii)–(vii) and Figs. 7 and 8. [Because of their comparatively small uncertainties, it is possible in these adjustments to take the 2010 recommended values for the constants a_e, α, R_∞, and $A_r(e)$, which appear in the observational equations of Table 39, and assume that they are exactly known.]

Adjustments (ii) and (iii) focus on ϵ_K: ϵ_J is set equal to 0 and values of ϵ_K are obtained from data whose observational equations are independent of h. These data are the five values of R_K, items $B35.1-B35.5$; and the three low-field gyromagnetic ratios, items $B32.1$, $B32.2$, and $B33$. We see from Table 29 that the two values of ϵ_K resulting from the two

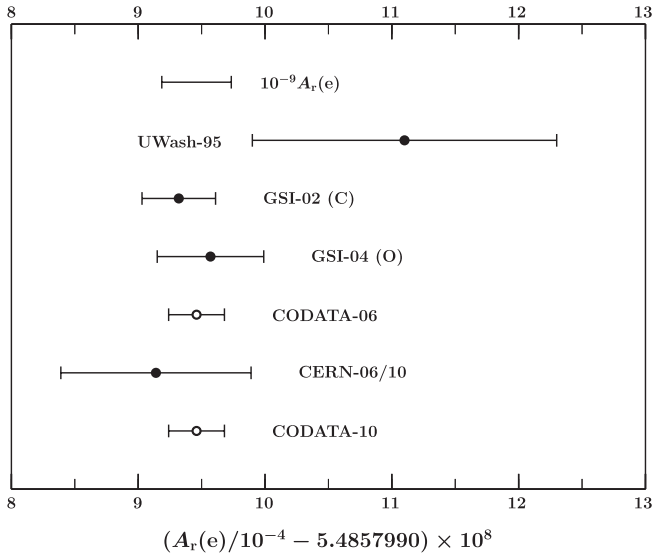

FIG. 5. Values of the electron relative atomic mass $A_r(e)$ implied by the input data in Tables 20 and 22 and the 2006 and 2010 CODATA recommended values in chronological order from top to bottom (see Table 28).

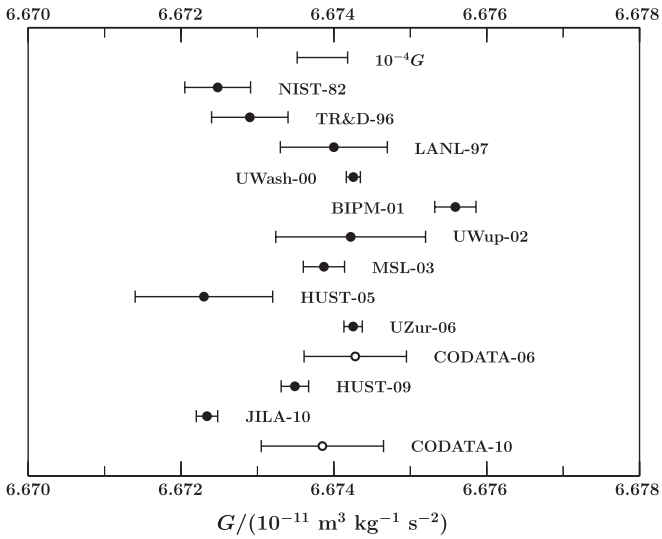

FIG. 6. Values of the Newtonian constant of gravitation G in Table 24 and the 2006 and 2010 CODATA recommended values in chronological order from top to bottom.

TABLE 29. Summary of the results of several least-squares adjustments to investigate the relations $K_J = (2e/h)(1+\epsilon_J)$ and $R_K = (h/e^2)(1+\epsilon_K)$. See the text for an explanation and discussion of each adjustment, but in brief, adjustment (i) uses all the data, (ii) assumes $K_J = 2e/h$ (that is, $\epsilon_J = 0$) and obtains ϵ_K from the five measured values of R_K, (iii) is based on the same assumption and obtains ϵ_K from the two values of the proton gyromagnetic ratio and one value of the helion gyromagnetic ratio, (iv) is (iii) but assumes $R_K = h/e^2$ (that is, $\epsilon_K = 0$) and obtains ϵ_J in place of ϵ_K, (v)–(vii) are based on the same assumption and obtain ϵ_J from all the measured values given in Table 20 for the quantities indicated.

Adjustment	Data included[a]	$10^8\epsilon_K$	$10^8\epsilon_J$
(i)	All	2.2(1.8)	5.7(2.4)
(ii)	R_K	2.9(1.8)	0
(iii)	$\Gamma'_{p,h-90}$(lo)	−25.4(9.3)	0
(iv)	$\Gamma'_{p,h-90}$(lo)	0	−25.4(9.3)
(v)	Γ'_{p-90}(hi), K_J, $K_J^2R_K$, $\mathcal{F}_{90}$	0	23.7(72.0)
(vi)	Γ'_{p-90}(hi), K_J, $K_J^2R_K$, $\mathcal{F}_{90}$, N_A	0	8.6(2.2)
(vii)	Γ'_{p-90}(hi), [K_J], [$K_J^2R_K$], $\mathcal{F}_{90}$, [N_A]	0	8.6(4.4)

[a]The data items in brackets have their uncertainties expanded by a factor of 2.

adjustments not only have opposite signs but their difference is $3.0u_{diff}$. Figure 7 compares the combined value of ϵ_K obtained from the five values of R_K with the five individual values, while Fig. 8 does the same for the results obtained from the three gyromagnetic ratios.

Adjustments (iv)–(vii) focus on ϵ_J: ϵ_K is set equal to 0 and values of ϵ_J are, with the exception of adjustment (iv), obtained from data whose observational equations are dependent on h. Examination of Table 29 shows that although the values of ϵ_J from adjustments (iv) and (v) are of opposite sign, their difference of 49.1×10^{-8} is less than the 73.0×10^{-8} uncertainty of the difference. However, the difference between the values of ϵ_J from adjustments (iv) and (vi) is $3.6u_{diff}$, and is $3.3u_{diff}$ even for the value of ϵ_J from adjustment (vii), in which

TABLE 30. The 28 adjusted constants (variables) used in the least-squares multivariate analysis of the Rydberg-constant data given in Table 18. These adjusted constants appear as arguments of the functions on the right-hand side of the observational equations of Table 31.

Adjusted constant	Symbol
Rydberg constant	R_∞
Bound-state proton rms charge radius	r_p
Bound-state deuteron rms charge radius	r_d
Additive correction to $E_H(1S_{1/2})/h$	$\delta_H(1S_{1/2})$
Additive correction to $E_H(2S_{1/2})/h$	$\delta_H(2S_{1/2})$
Additive correction to $E_H(3S_{1/2})/h$	$\delta_H(3S_{1/2})$
Additive correction to $E_H(4S_{1/2})/h$	$\delta_H(4S_{1/2})$
Additive correction to $E_H(6S_{1/2})/h$	$\delta_H(6S_{1/2})$
Additive correction to $E_H(8S_{1/2})/h$	$\delta_H(8S_{1/2})$
Additive correction to $E_H(2P_{1/2})/h$	$\delta_H(2P_{1/2})$
Additive correction to $E_H(4P_{1/2})/h$	$\delta_H(4P_{1/2})$
Additive correction to $E_H(2P_{3/2})/h$	$\delta_H(2P_{3/2})$
Additive correction to $E_H(4P_{3/2})/h$	$\delta_H(4P_{3/2})$
Additive correction to $E_H(8D_{3/2})/h$	$\delta_H(8D_{3/2})$
Additive correction to $E_H(12D_{3/2})/h$	$\delta_H(12D_{3/2})$
Additive correction to $E_H(4D_{5/2})/h$	$\delta_H(4D_{5/2})$
Additive correction to $E_H(6D_{5/2})/h$	$\delta_H(6D_{5/2})$
Additive correction to $E_H(8D_{5/2})/h$	$\delta_H(8D_{5/2})$
Additive correction to $E_H(12D_{5/2})/h$	$\delta_H(12D_{5/2})$
Additive correction to $E_D(1S_{1/2})/h$	$\delta_D(1S_{1/2})$
Additive correction to $E_D(2S_{1/2})/h$	$\delta_D(2S_{1/2})$
Additive correction to $E_D(4S_{1/2})/h$	$\delta_D(4S_{1/2})$
Additive correction to $E_D(8S_{1/2})/h$	$\delta_D(8S_{1/2})$
Additive correction to $E_D(8D_{3/2})/h$	$\delta_D(8D_{3/2})$
Additive correction to $E_D(12D_{3/2})/h$	$\delta_D(12D_{3/2})$
Additive correction to $E_D(4D_{5/2})/h$	$\delta_D(4D_{5/2})$
Additive correction to $E_D(8D_{5/2})/h$	$\delta_D(8D_{5/2})$
Additive correction to $E_D(12D_{5/2})/h$	$\delta_D(12D_{5/2})$

TABLE 31. Observational equations that express the input data related to R_∞ in Table 18 as functions of the adjusted constants in Table 30. The numbers in the first column correspond to the numbers in the first column of Table 18. Energy levels of hydrogenic atoms are discussed in Sec. 4.1. As pointed out at the beginning of that section, $E_X(nL_j)/h$ is in fact proportional to cR_∞ and independent of h, hence h is not an adjusted constant in these equations. See Sec. 13.2 for an explanation of the symbol $\doteq$.

Type of input datum	Observational equation
*A*1–*A*16	$\delta_H(nL_j) \doteq \delta_H(nL_j)$
*A*17–*A*25	$\delta_D(nL_j) \doteq \delta_D(nL_j)$
*A*26–*A*31, *A*38, *A*39	$\nu_H(n_1L_{1j_1} - n_2L_{2j_2}) \doteq [E_H(n_2L_{2j_2}; R_\infty, \alpha, A_r(e), A_r(p), r_p, \delta_H(n_2L_{2j_2})) - E_H(n_1L_{1j_1}; R_\infty, \alpha, A_r(e), A_r(p), r_p, \delta_H(n_1L_{1j_1}))]/h$
*A*32–*A*37	$\nu_H(n_1L_{1j_1} - n_2L_{2j_2}) - \frac{1}{4}\nu_H(n_3L_{3j_3} - n_4L_{4j_4}) \doteq \{E_H(n_2L_{2j_2}; R_\infty, \alpha, A_r(e), A_r(p), r_p, \delta_H(n_2L_{2j_2})) - E_H(n_1L_{1j_1}; R_\infty, \alpha, A_r(e), A_r(p), r_p, \delta_H(n_1L_{1j_1})) - \frac{1}{4}[E_H(n_4L_{4j_4}; R_\infty, \alpha, A_r(e), A_r(p), r_p, \delta_H(n_4L_{4j_4})) - E_H(n_3L_{3j_3}; R_\infty, \alpha, A_r(e), A_r(p), r_p, \delta_H(n_3L_{3j_3}))]\}/h$
*A*40–*A*44	$\nu_D(n_1L_{1j_1} - n_2L_{2j_2}) \doteq [E_D(n_2L_{2j_2}; R_\infty, \alpha, A_r(e), A_r(d), r_d, \delta_D(n_2L_{2j_2})) - E_D(n_1L_{1j_1}; R_\infty, \alpha, A_r(e), A_r(d), r_d, \delta_D(n_1L_{1j_1}))]/h$
*A*45, *A*46	$\nu_D(n_1L_{1j_1} - n_2L_{2j_2}) - \frac{1}{4}\nu_D(n_3L_{3j_3} - n_4L_{4j_4}) \doteq \{E_D(n_2L_{2j_2}; R_\infty, \alpha, A_r(e), A_r(d), r_d, \delta_D(n_2L_{2j_2})) - E_D(n_1L_{1j_1}; R_\infty, \alpha, A_r(e), A_r(d), r_d, \delta_D(n_1L_{1j_1})) - \frac{1}{4}[E_D(n_4L_{4j_4}; R_\infty, \alpha, A_r(e), A_r(d), r_d, \delta_D(n_4L_{4j_4})) - E_D(n_3L_{3j_3}; R_\infty, \alpha, A_r(e), A_r(d), r_d, \delta_D(n_3L_{3j_3}))]\}/h$
*A*47	$\nu_D(1S_{1/2} - 2S_{1/2}) - \nu_H(1S_{1/2} - 2S_{1/2}) \doteq \{E_D(2S_{1/2}; R_\infty, \alpha, A_r(e), A_r(d), r_d, \delta_D(2S_{1/2})) - E_D(1S_{1/2}; R_\infty, \alpha, A_r(e), A_r(d), r_d, \delta_D(1S_{1/2})) - [E_H(2S_{1/2}; R_\infty, \alpha, A_r(e), A_r(p), r_p, \delta_H(2S_{1/2})) - E_H(1S_{1/2}; R_\infty, \alpha, A_r(e), A_r(p), r_p, \delta_H(1S_{1/2}))]\}/h$
*A*48	$r_p \doteq r_p$
*A*49	$r_d \doteq r_d$

TABLE 32. The 39 adjusted constants (variables) used in the least-squares multivariate analysis of the input data in Table 20. These adjusted constants appear as arguments of the functions on the right-hand side of the observational equations of Table 33.

Adjusted constant	Symbol
Electron relative atomic mass	$A_r(e)$
Proton relative atomic mass	$A_r(p)$
Neutron relative atomic mass	$A_r(n)$
Deuteron relative atomic mass	$A_r(d)$
Triton relative atomic mass	$A_r(t)$
Helion relative atomic mass	$A_r(h)$
Alpha particle relative atomic mass	$A_r(\alpha)$
$^{16}O^{7+}$ relative atomic mass	$A_r(^{16}O^{7+})$
^{87}Rb relative atomic mass	$A_r(^{87}Rb)$
^{133}Cs relative atomic mass	$A_r(^{133}Cs)$
Average vibrational excitation energy	$A_r(E_{av})$
Fine-structure constant	α
Additive correction to a_e(th)	δ_e
Muon magnetic-moment anomaly	a_μ
Additive correction to g_C(th)	δ_C
Additive correction to g_O(th)	δ_O
Electron-proton magnetic-moment ratio	μ_{e^-}/μ_p
Deuteron-electron magnetic-moment ratio	μ_d/μ_{e^-}
Triton-proton magnetic-moment ratio	μ_t/μ_p
Shielding difference of d and p in HD	σ_{dp}
Shielding difference of t and p in HT	σ_{tp}
Electron to shielded proton magnetic-moment ratio	μ_{e^-}/μ'_p
Shielded helion to shielded proton magnetic-moment ratio	μ'_h/μ'_p
Neutron to shielded proton magnetic-moment ratio	μ_n/μ'_p
Electron-muon mass ratio	m_e/m_μ
Additive correction to $\Delta\nu_{Mu}$(th)	δ_{Mu}
Planck constant	h
Molar gas constant	R
Copper $K\alpha_1$ x unit	xu(CuKα_1)
Molybdenum $K\alpha_1$ x unit	xu(MoKα_1)
Ångstrom star	Å*
d_{220} of Si crystal ILL	d_{220}(ILL)
d_{220} of Si crystal N	d_{220}(N)
d_{220} of Si crystal WASO 17	d_{220}(W17)
d_{220} of Si crystal WASO 04	d_{220}(W04)
d_{220} of Si crystal WASO 4.2a	d_{220}(W4.2a)
d_{220} of Si crystal MO*	d_{220}(MO*)
d_{220} of Si crystal NR3	d_{220}(NR3)
d_{220} of Si crystal NR4	d_{220}(NR4)
d_{220} of an ideal Si crystal	d_{220}

the uncertainties of the most accurate data have been increased by the factor 2. (The multiplicative factor 2 is that used in adjustment 2 and the final adjustment; see Tables 36 and 37, and their associated text.) On the other hand, we see that the value of ϵ_J from adjustment (vi) is consistent with 0 only to within 3.9 times its uncertainty, but that this is reduced to 2.0 for the value of ϵ_J from adjustment (vii) which uses expanded uncertainties.

The results of the adjustments discussed above reflect the disagreement of the NIST-07 watt-balance value for $K_J^2R_K$, and to a lesser extent that of the similar NIST-98 value, items $B37.3$ and $B37.2$, with the IAC-11 enriched silicon value of N_A, item $B54$; and the disagreement of the NIST-89 result for Γ'_{p-90}(lo), and to a lesser extent the KR/VN-98 result for Γ'_{h-90}(lo), items $B32.1$ and $B33$, with the highly accurate values of α. If adjustment (i) is repeated with these five data deleted, we find $\epsilon_K = 2.8(1.8) \times 10^{-8}$ and $\epsilon_J = 15(49) \times 10^{-8}$. These values can be interpreted as confirming that ϵ_K is consistent with 0 to within 1.6 times its uncertainty of 1.8×10^{-8} and that ϵ_J is consistent with 0 well within its uncertainty of 49×10^{-8}.

We conclude this section by briefly discussing recent efforts to close the metrology triangle. Although there are variants, the basic idea is to use a single electron tunneling (SET) device that generates a quantized current $I = ef$ when an alternating voltage of frequency f is applied to it, where as usual e is the elementary charge. The current I is then compared to a current derived from Josephson and quantum-Hall-effect devices. In view of quantization of charge in units of e and conservation of charge, the equality of the currents shows that $K_JR_Ke = 2$, as expected, within the uncertainty of the measurements (Keller, 2008; Keller *et al.*, 2008; Feltin and Piquemal, 2009). Although there is no indication from the results reported to date that this relation is not valid, the uncertainties of the results are at best at the 1 to 2 parts in 10^6 level (Keller, Zimmerman, and Eichenberger, 2007; Keller *et al.*, 2008; Feltin *et al.*, 2011; Camarota *et al.*, 2012).

14. The 2010 CODATA Recommended Values

14.1. Calculational details

The 168 input data and their correlation coefficients initially considered for inclusion in the 2010 CODATA adjustment of the values of the constants are given in Tables 18–23. The 2010 recommended values are based on adjustment 3, called the final adjustment, summarized in Tables 36–38 and discussed in the associated text. Adjustment 3 omits 20 of the 168 initially considered input data, namely, items $B10.1$, $B10.2$, $B13.1$, $B32.1-B36.2$, $B37.5$, $B38$, $B56$, $B59$, and $B60$, because of their low weight (self-sensitivity coefficient $S_c < 0.01$). However, because the observational equation for $h/m(^{133}Cs)$, item $B56$, depends on $A_r(^{133}Cs)$ but item $B56$ is deleted because of its low weight, the two values of $A_r(^{133}Cs)$, items $B10.1$ and $B10.2$, are also deleted and $A_r(^{133}Cs)$ itself is deleted as an adjusted constant. Further, the initial uncertainties of five input data, items $B37.1-B37.4$ and $B54$, are multiplied by the factor 2, with the result that the absolute values of the normalized residuals $|r_i|$ of the five data are less than 1.4 and their disagreement is reduced to an acceptable level.

Each input datum in this final adjustment has a self-sensitivity coefficient S_c greater than 0.01, or is a subset of the data of an experiment or series of experiments that provide an input datum or input data with $S_c > 0.01$. Not counting such input data with $S_c < 0.01$, the seven data with $|r_i| > 1.2$ are $A50$,

TABLE 33. Observational equations that express the input data in Table 20 as functions of the adjusted constants in Table 32. The numbers in the first column correspond to the numbers in the first column of Table 20. For simplicity, the lengthier functions are not explicitly given. See Sec. 13.2 for an explanation of the symbol $\doteq$.

Type of input datum	Observational equation	Sec.
*B*1	$A_r(^1\mathrm{H}) \doteq A_r(\mathrm{p}) + A_r(\mathrm{e}) - E_b(^1\mathrm{H})/m_u c^2$	3.2
*B*2	$A_r(^2\mathrm{H}) \doteq A_r(\mathrm{d}) + A_r(\mathrm{e}) - E_b(^2\mathrm{H})/m_u c^2$	3.2
*B*3	$A_r(E_{av}) \doteq A_r(E_{av})$	3.3
*B*4	$\dfrac{f_c(\mathrm{H}_2^{+*})}{f_c(\mathrm{d})} \doteq \dfrac{A_r(\mathrm{d})}{2A_r(\mathrm{p}) + A_r(\mathrm{e}) - [2E_I(\mathrm{H}) + E_B(\mathrm{H}_2) - E_I(\mathrm{H}_2) - E_{av}]/m_u c^2}$	3.3
*B*5	$\dfrac{f_c(\mathrm{t})}{f_c(\mathrm{H}_2^{+*})} \doteq \dfrac{2A_r(\mathrm{p}) + A_r(\mathrm{e}) - [2E_I(\mathrm{H}) + E_B(\mathrm{H}_2) - E_I(\mathrm{H}_2) - E_{av}]/m_u c^2}{A_r(\mathrm{t})}$	3.3
*B*6	$\dfrac{f_c(^3\mathrm{He}^+)}{f_c(\mathrm{H}_2^{+*})} \doteq \dfrac{2A_r(\mathrm{p}) + A_r(\mathrm{e}) - [2E_I(\mathrm{H}) + E_B(\mathrm{H}_2) - E_I(\mathrm{H}_2) - E_{av}]/m_u c^2}{A_r(\mathrm{h}) + A_r(\mathrm{e}) - E_I(^3\mathrm{He}^+)/m_u c^2}$	3.3
*B*7	$A_r(^4\mathrm{He}) \doteq A_r(\alpha) + 2A_r(\mathrm{e}) - E_b(^4\mathrm{He})/m_u c^2$	3.2
*B*8	$A_r(^{16}\mathrm{O}) \doteq A_r(^{16}\mathrm{O}^{7+}) + 7A_r(\mathrm{e}) - [E_b(^{16}\mathrm{O}) - E_b(^{16}\mathrm{O}^{7+})]/m_u c^2$	3.2
*B*9	$A_r(^{87}\mathrm{Rb}) \doteq A_r(^{87}\mathrm{Rb})$	
*B*10	$A_r(^{133}\mathrm{Cs}) \doteq A_r(^{133}\mathrm{Cs})$	
*B*11	$A_r(\mathrm{e}) \doteq A_r(\mathrm{e})$	
*B*12	$\delta_e \doteq \delta_e$	
*B*13	$a_e \doteq a_e(\alpha, \delta_e)$	5.1.1
*B*14	$\bar{R} \doteq -\dfrac{a_\mu}{1 + a_e(\alpha, \delta_e)} \dfrac{m_e}{m_\mu} \dfrac{\mu_{e^-}}{\mu_p}$	5.2.2
*B*15	$\delta_C \doteq \delta_C$	
*B*16	$\delta_O \doteq \delta_O$	
*B*17	$\dfrac{f_s(^{12}\mathrm{C}^{5+})}{f_c(^{12}\mathrm{C}^{5+})} \doteq -\dfrac{g_C(\alpha, \delta_C)}{10A_r(\mathrm{e})} \left[12 - 5A_r(\mathrm{e}) + \dfrac{E_b(^{12}\mathrm{C}) - E_b(^{12}\mathrm{C}^{5+})}{m_u c^2}\right]$	5.3.2
*B*18	$\dfrac{f_s(^{16}\mathrm{O}^{7+})}{f_c(^{16}\mathrm{O}^{7+})} \doteq -\dfrac{g_O(\alpha, \delta_O)}{14A_r(\mathrm{e})} A_r(^{16}\mathrm{O}^{7+})$	5.3.2
*B*19	$\dfrac{\mu_{e^-}(\mathrm{H})}{\mu_p(\mathrm{H})} \doteq \dfrac{g_{e^-}(\mathrm{H})}{g_{e^-}} \left(\dfrac{g_p(\mathrm{H})}{g_p}\right)^{-1} \dfrac{\mu_{e^-}}{\mu_p}$	
*B*20	$\dfrac{\mu_d(\mathrm{D})}{\mu_{e^-}(\mathrm{D})} \doteq \dfrac{g_d(\mathrm{D})}{g_d} \left(\dfrac{g_{e^-}(\mathrm{D})}{g_{e^-}}\right)^{-1} \dfrac{\mu_d}{\mu_{e^-}}$	
*B*21	$\dfrac{\mu_p(\mathrm{HD})}{\mu_d(\mathrm{HD})} \doteq [1 + \sigma_{dp}] \dfrac{\mu_p}{\mu_{e^-}} \dfrac{\mu_{e^-}}{\mu_d}$	
*B*22	$\sigma_{dp} \doteq \sigma_{dp}$	
*B*23	$\dfrac{\mu_t(\mathrm{HT})}{\mu_p(\mathrm{HT})} \doteq [1 - \sigma_{tp}] \dfrac{\mu_t}{\mu_p}$	
*B*24	$\sigma_{tp} \doteq \sigma_{tp}$	
*B*25	$\dfrac{\mu_{e^-}(\mathrm{H})}{\mu'_p} \doteq \dfrac{g_{e^-}(\mathrm{H})}{g_{e^-}} \dfrac{\mu_{e^-}}{\mu'_p}$	
*B*26	$\dfrac{\mu'_h}{\mu'_p} \doteq \dfrac{\mu'_h}{\mu'_p}$	
*B*27	$\dfrac{\mu_n}{\mu'_p} \doteq \dfrac{\mu_n}{\mu'_p}$	
*B*28	$\delta_{Mu} \doteq \delta_{Mu}$	
*B*29	$\Delta\nu_{Mu} \doteq \Delta\nu_{Mu}\left(R_\infty, \alpha, \dfrac{m_e}{m_\mu}, \delta_{Mu}\right)$	6.2.1
*B*30, *B*31	$\nu(f_p) \doteq \nu\left(f_p; R_\infty, \alpha, \dfrac{m_e}{m_\mu}, \dfrac{\mu_{e^-}}{\mu_p}, \delta_e, \delta_{Mu}\right)$	6.2.2
*B*32	$\Gamma'_{p-90}(\mathrm{lo}) \doteq -\dfrac{K_{J-90} R_{K-90} [1 + a_e(\alpha, \delta_e)] \alpha^3}{2\mu_0 R_\infty} \left(\dfrac{\mu_{e^-}}{\mu'_p}\right)^{-1}$	

TABLE 33. Observational equations that express the input data in Table 20 as functions of the adjusted constants in Table 32. The numbers in the first column correspond to the numbers in the first column of Table 20. For simplicity, the lengthier functions are not explicitly given. See Sec. 13.2 for an explanation of the symbol ≐.—Continued

Type of input datum	Observational equation	Sec.
*B*33	$\Gamma'_{\mathrm{h-90}}(\mathrm{lo}) \doteq \dfrac{K_{\mathrm{J-90}}R_{\mathrm{K-90}}[1+a_{\mathrm{e}}(\alpha,\delta_{\mathrm{e}})]\alpha^3}{2\mu_0 R_\infty}\left(\dfrac{\mu_{\mathrm{e}^-}}{\mu'_{\mathrm{p}}}\right)^{-1}\dfrac{\mu'_{\mathrm{h}}}{\mu'_{\mathrm{p}}}$	
*B*34	$\Gamma'_{\mathrm{p-90}}(\mathrm{hi}) \doteq -\dfrac{c[1+a_{\mathrm{e}}(\alpha,\delta_{\mathrm{e}})]\alpha^2}{K_{\mathrm{J-90}}R_{\mathrm{K-90}}R_\infty h}\left(\dfrac{\mu_{\mathrm{e}^-}}{\mu'_{\mathrm{p}}}\right)^{-1}$	
*B*35	$R_{\mathrm{K}} \doteq \dfrac{\mu_0 c}{2\alpha}$	
*B*36	$K_{\mathrm{J}} \doteq \left(\dfrac{8\alpha}{\mu_0 c h}\right)^{1/2}$	
*B*37	$K_{\mathrm{J}}^2 R_{\mathrm{K}} \doteq \dfrac{4}{h}$	
*B*38	$\mathcal{F}_{90} \doteq \dfrac{cM_{\mathrm{u}}A_{\mathrm{r}}(\mathrm{e})\alpha^2}{K_{\mathrm{J-90}}R_{\mathrm{K-90}}R_\infty h}$	
*B*39–*B*41	$d_{220}(X) \doteq d_{220}(X)$	
*B*42–*B*53	$\dfrac{d_{220}(X)}{d_{220}(Y)} - 1 \doteq \dfrac{d_{220}(X)}{d_{220}(Y)} - 1$	
*B*54	$N_{\mathrm{A}} \doteq \dfrac{cM_{\mathrm{u}}A_{\mathrm{r}}(\mathrm{e})\alpha^2}{2R_\infty h}$	
*B*55	$\dfrac{\lambda_{\mathrm{meas}}}{d_{220}(\mathrm{ILL})} \doteq \dfrac{\alpha^2 A_{\mathrm{r}}(\mathrm{e})}{R_\infty d_{220}(\mathrm{ILL})}\dfrac{A_{\mathrm{r}}(\mathrm{n})+A_{\mathrm{r}}(\mathrm{p})}{[A_{\mathrm{r}}(\mathrm{n})+A_{\mathrm{r}}(\mathrm{p})]^2 - A_{\mathrm{r}}^2(\mathrm{d})}$	9.3
*B*56, *B*57	$\dfrac{h}{m(X)} \doteq \dfrac{A_{\mathrm{r}}(\mathrm{e})}{A_{\mathrm{r}}(X)}\dfrac{c\alpha^2}{2R_\infty}$	7.1
*B*58	$R \doteq R$	
*B*59	$k \doteq \dfrac{2R_\infty hR}{cM_{\mathrm{u}}A_{\mathrm{r}}(\mathrm{e})\alpha^2}$	
*B*60	$\dfrac{k}{h} \doteq \dfrac{2R_\infty R}{cM_{\mathrm{u}}A_{\mathrm{r}}(\mathrm{e})\alpha^2}$	
*B*61, *B*64	$\dfrac{\lambda(\mathrm{CuK}\alpha_1)}{d_{220}(X)} \doteq \dfrac{1\,537.400\,\mathrm{xu}(\mathrm{CuK}\alpha_1)}{d_{220}(X)}$	9.4
*B*62	$\dfrac{\lambda(\mathrm{WK}\alpha_1)}{d_{220}(\mathrm{N})} \doteq \dfrac{0.209\,010\,0\ \text{Å}^*}{d_{220}(\mathrm{N})}$	9.4
*B*63	$\dfrac{\lambda(\mathrm{MoK}\alpha_1)}{d_{220}(\mathrm{N})} \doteq \dfrac{707.831\,\mathrm{xu}(\mathrm{MoK}\alpha_1)}{d_{220}(\mathrm{N})}$	9.4

*B*11, *B*37.3, *B*54, *C*19, *C*21, and *C*28; their values of r_i are −1.24, 1.43, 1.39, −1.31, −1.60, −1.83, and 1.76, respectively.

As discussed in Sec. 13.2.1, the 2010 recommended value of *G* is the weighted mean of the 11 measured values in Table 24 after the uncertainty of each is multiplied by the factor 14. Although these data can be treated separately because they are independent of all of the other data, they could have been included with the other data. For example, if the 11 values of *G* with expanded uncertainties are added to the 148 input data of adjustment 3, *G* is taken as an additional adjusted constant so that these 11 values can be included in a new adjustment using the observational equation $G \doteq G$, and the so-modified adjustment 3 is repeated, then we find for this "grand final adjustment" that $N = 160$,

TABLE 34. The 15 adjusted constants relevant to the antiprotonic helium data given in Table 22. These adjusted constants appear as arguments of the theoretical expressions on the right-hand side of the observational equations of Table 35.

Transition	Adjusted constant
$\bar{p}^4He^+: (32,31) \rightarrow (31,30)$	$\delta_{\bar{p}^4He^+}(32,31:31,30)$
$\bar{p}^4He^+: (35,33) \rightarrow (34,32)$	$\delta_{\bar{p}^4He^+}(35,33:34,32)$
$\bar{p}^4He^+: (36,34) \rightarrow (35,33)$	$\delta_{\bar{p}^4He^+}(36,34:35,33)$
$\bar{p}^4He^+: (37,34) \rightarrow (36,33)$	$\delta_{\bar{p}^4He^+}(37,34:36,33)$
$\bar{p}^4He^+: (39,35) \rightarrow (38,34)$	$\delta_{\bar{p}^4He^+}(39,35:38,34)$
$\bar{p}^4He^+: (40,35) \rightarrow (39,34)$	$\delta_{\bar{p}^4He^+}(40,35:39,34)$
$\bar{p}^4He^+: (37,35) \rightarrow (38,34)$	$\delta_{\bar{p}^4He^+}(37,35:38,34)$
$\bar{p}^4He^+: (33,32) \rightarrow (31,30)$	$\delta_{\bar{p}^4He^+}(33,32:31,30)$
$\bar{p}^4He^+: (36,34) \rightarrow (34,32)$	$\delta_{\bar{p}^4He^+}(36,34:34,32)$
$\bar{p}^3He^+: (32,31) \rightarrow (31,30)$	$\delta_{\bar{p}^3He^+}(32,31:31,30)$
$\bar{p}^3He^+: (34,32) \rightarrow (33,31)$	$\delta_{\bar{p}^3He^+}(34,32:33,31)$
$\bar{p}^3He^+: (36,33) \rightarrow (35,32)$	$\delta_{\bar{p}^3He^+}(36,33:35,32)$
$\bar{p}^3He^+: (38,34) \rightarrow (37,33)$	$\delta_{\bar{p}^3He^+}(38,34:37,33)$
$\bar{p}^3He^+: (36,34) \rightarrow (37,33)$	$\delta_{\bar{p}^3He^+}(36,34:37,33)$
$\bar{p}^3He^+: (35,33) \rightarrow (33,31)$	$\delta_{\bar{p}^3He^+}(35,33:33,31)$

$M = 83$, $\nu = 77$, $\chi^2 = 59.1$, $p(59.1|77) = 0.94$, and $R_B = 0.88$. Of course, the resulting values of the adjusted constants, and of the normalized residuals and self-sensitivity coefficients of the input data, are exactly the same as those from adjustment 3 and the weighted mean of the 11 measured values of G with expanded uncertainties.

In any event, the 2010 recommended values are calculated from the set of best estimated values, in the least-squares sense, of 82 adjusted constants, including G, and their variances and covariances, together with (i) those constants that have exact values such as μ_0 and c; and (ii) the values of m_τ, G_F, and $\sin^2\theta_W$ given in Sec. 12 of this report; see Sec. V.B of CODATA-98 for details.

14.2. Tables of values

Tables 40–47 give the 2010 CODATA recommended values of the basic constants and conversion factors of physics and chemistry and related quantities. Although very similar in form and content to their 2006 counterparts, several new recommended values have been included in the 2010 tables and a few have been deleted. The values of the four new constants, $m_n - m_p$ in kg and u, and $(m_n - m_p)c^2$ in J and MeV, are given in Table 41 under the heading "Neutron, n"; and the values of the four new constants μ_h, μ_h/μ_B, μ_h/μ_N, and g_h are given in the same table under the heading "Helion, h." The three constants deleted, μ_t/μ_e, μ_t/μ_p, and μ_t/μ_n, were in the 2006 version of Table 41 under the heading "Triton, t." It was decided that these constants were of limited interest and the values can be calculated from other constants in the table.

The values of the four new helion-related constants are calculated from the adjusted constant μ'_h/μ'_p and the theoretically predicted shielding correction $\sigma_h = 59.967\,43(10) \times 10^{-6}$ due to Rudziński, Puchalski, and Pachucki (2009) using the relation $\mu'_h = \mu_h(1 - \sigma_h)$; see Sec. 6.1.2.

Table 40 is a highly abbreviated list of the values of the constants and conversion factors most commonly used. Table 41 is a much more extensive list of values categorized as follows: UNIVERSAL; ELECTROMAGNETIC; ATOMIC AND NUCLEAR; and PHYSICOCHEMICAL. The ATOMIC AND NUCLEAR category is subdivided into 11 subcategories: General; Electroweak; Electron, e^-; Muon, μ^-; Tau, τ^-; Proton, p; Neutron, n; Deuteron, d; Triton, t; Helion, h; and Alpha particle, α. Table 42 gives the variances, covariances, and correlation coefficients of a selected group of constants. (Use of the covariance matrix is discussed in Appendix E of CODATA-98.) Table 43 gives the

TABLE 35. Observational equations that express the input data related to antiprotonic helium in Table 22 as functions of adjusted constants in Tables 32 and 34. The numbers in the first column correspond to the numbers in the first column of Table 22. Definitions of the symbols and values of the parameters in these equations are given in Sec. 4.2. See Sec. 13.2 for an explanation of the symbol $\doteq$.

Type of input datum	Observational equation
$C1-C9$	$\delta_{\bar{p}^4He^+}(n,l:n',l') \doteq \delta_{\bar{p}^4He^+}(n,l:n',l')$
$C10-C15$	$\delta_{\bar{p}^3He^+}(n,l:n',l') \doteq \delta_{\bar{p}^3He^+}(n,l:n',l')$
$C16-C24$	$\Delta\nu_{\bar{p}^4He^+}(n,l:n',l') \doteq \Delta\nu^{(0)}_{\bar{p}^4He^+}(n,l:n',l') + a_{\bar{p}^4He^+}(n,l:n',l')\left[\left(\frac{A_r(e)}{A_r(p)}\right)^{(0)}\left(\frac{A_r(p)}{A_r(e)}\right) - 1\right]$
	$+ b_{\bar{p}^4He^+}(n,l:n',l')\left[\left(\frac{A_r(e)}{A_r(\alpha)}\right)^{(0)}\left(\frac{A_r(\alpha)}{A_r(e)}\right) - 1\right] + \delta_{\bar{p}^4He^+}(n,l:n',l')$
$C25-C30$	$\Delta\nu_{\bar{p}^3He^+}(n,l:n',l') \doteq \Delta\nu^{(0)}_{\bar{p}^3He^+}(n,l:n',l') + a_{\bar{p}^3He^+}(n,l:n',l')\left[\left(\frac{A_r(e)}{A_r(p)}\right)^{(0)}\left(\frac{A_r(p)}{A_r(e)}\right) - 1\right]$
	$+ b_{\bar{p}^3He^+}(n,l:n',l')\left[\left(\frac{A_r(e)}{A_r(h)}\right)^{(0)}\left(\frac{A_r(h)}{A_r(e)}\right) - 1\right] + \delta_{\bar{p}^3He^+}(n,l:n',l')$

TABLE 36. Summary of the results of some of the least-squares adjustments used to analyze the input data given in Tables 18–23. The values of α and h are those obtained in the adjustment, N is the number of input data, M is the number of adjusted constants, $\nu = N - M$ is the degrees of freedom, and $R_B = \sqrt{\chi^2/\nu}$ is the Birge ratio. See the text for an explanation and discussion of each adjustment, but in brief, adjustment 1 is all the data; 2 is the same as 1 except with the uncertainties of the key data that determine h multiplied by 2; 3 is 2 with the low-weight input data deleted and is the adjustment on which the 2010 recommended values are based; 4 is 2 with the input data that provide the most accurate values of alpha deleted; and 5 is 1 with the input data that provide the most accurate values of h deleted as well as low-weight data for α.

Adj.	N	M	ν	χ^2	R_B	α^{-1}	$u_r(\alpha^{-1})$	h/(J s)	$u_r(h)$
1	169	83	86	89.3	1.02	137.035 999 075(44)	3.2×10^{-10}	$6.626\,069\,58(15) \times 10^{-34}$	2.2×10^{-8}
2	169	83	86	75.7	0.94	137.035 999 073(44)	3.2×10^{-10}	$6.626\,069\,57(29) \times 10^{-34}$	4.4×10^{-8}
3	149	82	67	58.1	0.93	137.035 999 074(44)	3.2×10^{-10}	$6.626\,069\,57(29) \times 10^{-34}$	4.4×10^{-8}
4	161	81	80	69.4	0.93	137.036 0005(20)	1.4×10^{-8}	$6.626\,069\,50(31) \times 10^{-34}$	4.7×10^{-8}
5	154	82	72	57.2	0.89	137.035 999 074(44)	3.2×10^{-10}	$6.626\,069\,48(80) \times 10^{-34}$	1.2×10^{-7}

TABLE 37. Normalized residuals r_i and self-sensitivity coefficients S_c that result from the five least-squares adjustments summarized in Table 36 for the three input data with the largest absolute values of r_i in adjustment 1. S_c is a measure of how the least-squares estimated value of a given type of input datum depends on a particular measured or calculated value of that type of datum; see Appendix E of CODATA-98. See the text for an explanation and discussion of each adjustment; brief explanations are given in the caption to Table 36.

			Adj. 1		Adj. 2		Adj. 3		Adj. 4		Adj. 5	
Item No.	Input quantity	Identification	r_i	S_c	r_i	S_c	r_i	S_c	r_i	S_c	r_i	S_c
*B*37.3	$K_J^2 R_K$	NIST-07	2.83	0.367	1.39	0.367	1.39	0.371	1.23	0.413	Deleted	
*B*54	N_A	IAC-11	−2.57	0.555	−1.32	0.539	−1.31	0.546	−1.16	0.587	Deleted	
*B*32.1	Γ'_{p-90}(lo)	NIST-89	2.19	0.010	2.19	0.010	Deleted		2.46	0.158	Deleted	

TABLE 38. Summary of the results of some of the least-squares adjustments used to analyze the input data related to R_∞. The values of R_∞, r_p, and r_d are those obtained in the indicated adjustment, N is the number of input data, M is the number of adjusted constants, $\nu = N - M$ is the degrees of freedom, and $R_B = \sqrt{\chi^2/\nu}$ is the Birge ratio. See the text for an explanation and discussion of each adjustment. In brief, adjustment 6 is 3 but the scattering data for the nuclear radii are omitted; 7 is 3, but with only the hydrogen data included (no isotope shift); 8 is 7 with the r_p data deleted; 9 and 10 are similar to 7 and 8, but for the deuterium data; 11 is 3 with the muonic Lamb-shift value of r_p included; and 12 is 11, but without the scattering values of r_p and r_d.

Adj.	N	M	ν	χ^2	R_B	R_∞ (m^{-1})	$u_r(R_\infty)$	r_p (fm)	r_d (fm)
3	149	82	67	58.1	0.93	10 973 731.568 539(55)	5.0×10^{-12}	0.8775(51)	2.1424(21)
6	146	82	64	55.5	0.93	10 973 731.568 521(82)	7.4×10^{-12}	0.8758(77)	2.1417(31)
7	131	72	59	53.4	0.95	10 973 731.568 561(60)	5.5×10^{-12}	0.8796(56)	
8	129	72	57	52.5	0.96	10 973 731.568 528(94)	8.6×10^{-12}	0.8764(89)	
9	114	65	49	46.9	0.98	10 973 731.568 37(13)	1.1×10^{-11}		2.1288(93)
10	113	65	48	46.8	0.99	10 973 731.568 28(30)	2.7×10^{-11}		2.121(25)
11	150	82	68	104.9	1.24	10 973 731.568 175(12)	1.1×10^{-12}	0.842 25(65)	2.128 24(28)
12	147	82	65	74.3	1.07	10 973 731.568 171(12)	1.1×10^{-12}	0.841 93(66)	2.128 11(28)

TABLE 39. Generalized observational equations that express input data $B32-B38$ in Table 20 as functions of the adjusted constants in Tables 30 and 32 with the additional adjusted constants ϵ_J and ϵ_K as given in Eqs. (285) and (286). The numbers in the first column correspond to the numbers in the first column of Table 20. For simplicity, the lengthier functions are not explicitly given. See Sec. 13.2 for an explanation of the symbol $\doteq$.

Type of input datum	Generalized observational equation
$B32^*$	$\Gamma'_{p-90}(\text{lo}) \doteq -\dfrac{K_{J-90}R_{K-90}[1+a_e(\alpha,\delta_e)]\alpha^3}{2\mu_0 R_\infty(1+\epsilon_J)(1+\epsilon_K)}\left(\dfrac{\mu_{e^-}}{\mu'_p}\right)^{-1}$
$B33^*$	$\Gamma'_{h-90}(\text{lo}) \doteq \dfrac{K_{J-90}R_{K-90}[1+a_e(\alpha,\delta_e)]\alpha^3}{2\mu_0 R_\infty(1+\epsilon_J)(1+\epsilon_K)}\left(\dfrac{\mu_{e^-}}{\mu'_p}\right)^{-1}\dfrac{\mu'_h}{\mu'_p}$
$B34^*$	$\Gamma'_{p-90}(\text{hi}) \doteq -\dfrac{c[1+a_e(\alpha,\delta_e)]\alpha^2}{K_{J-90}R_{K-90}R_\infty h}(1+\epsilon_J)(1+\epsilon_K)\left(\dfrac{\mu_{e^-}}{\mu'_p}\right)^{-1}$
$B35^*$	$R_K \doteq \dfrac{\mu_0 c}{2\alpha}(1+\epsilon_K)$
$B36^*$	$K_J \doteq \left(\dfrac{8\alpha}{\mu_0 ch}\right)^{1/2}(1+\epsilon_J)$
$B37^*$	$K_J^2 R_K \doteq \dfrac{4}{h}(1+\epsilon_J)^2(1+\epsilon_K)$
$B38^*$	$\mathcal{F}_{90} \doteq \dfrac{cM_u A_r(e)\alpha^2}{K_{J-90}R_{K-90}R_\infty h}(1+\epsilon_J)(1+\epsilon_K)$

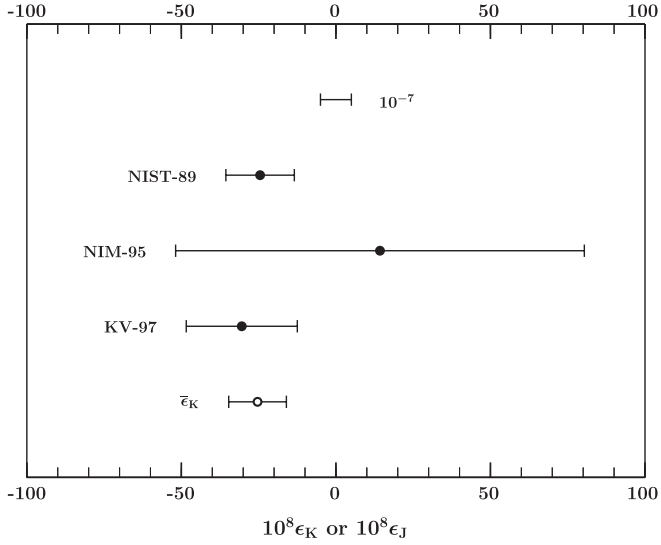

FIG. 8. Comparison of the three individual values of ϵ_K obtained from the three low-field gyromagnetic ratios, data items $B32.1$, $B32.2$, and $B33$, and the combined value (open circle) from adjustment (iii) given in Table 29. The applicable observational equations in Table 39 are $B32^*$ and $B33^*$. Because of the form of these equations, the value of ϵ_K when $\epsilon_J = 0$ is identical to the value of ϵ_J when $\epsilon_K = 0$, hence the label at the bottom of the figure.

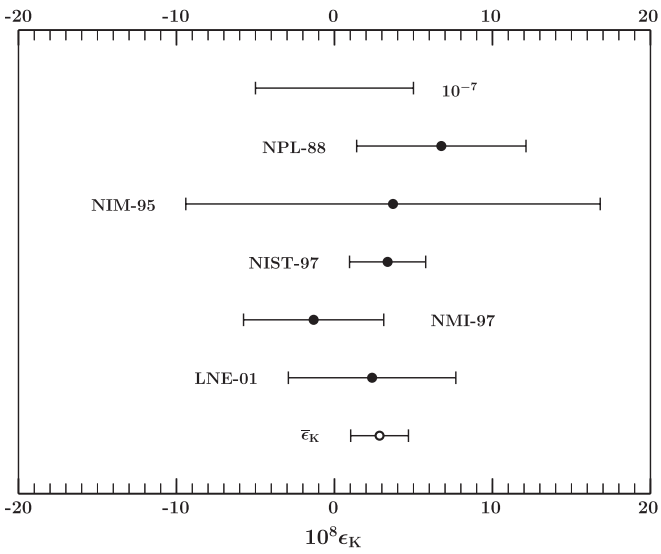

FIG. 7. Comparison of the five individual values of ϵ_K obtained from the five values of R_K, data items $B35.1-B35.5$, and the combined value (open circle) from adjustment (ii) given in Table 29. The applicable observational equation in Table 39 is $B35^*$.

internationally adopted values of various quantities; Table 44 lists the values of a number of x-ray related quantities; Table 45 lists the values of various non-SI units; and Tables 46 and 47 give the values of various energy equivalents.

All of the values given in Tables 40–47 are available on the Web pages of the Fundamental Constants Data Center of the NIST Physical Measurement Laboratory at physics.nist.gov/constants. This electronic version of the 2010 CODATA recommended values of the constants also includes a much more extensive correlation coefficient matrix. In fact, the correlation coefficient of any two constants listed in the tables is accessible on the Web site, as well as the automatic conversion of the value of an energy-related quantity expressed in one unit to the corresponding value expressed in another unit (in essence, an automated version of Tables 46 and 47).

15. Summary and Conclusion

The focus of this section is (i) comparison of the 2010 and 2006 recommended values of the constants and identification of those new results that have contributed most to the changes in the 2006 values; (ii) presentation of several conclusions that can be drawn from the 2010 recommended values and the input data on which they are based; and (iii) identification of new experimental and theoretical work that can advance our knowledge of the values of the constants.

Topic (iii) is of special importance in light of the adoption by the 24th General Conference on Weights and Measures

TABLE 40. An abbreviated list of the CODATA recommended values of the fundamental constants of physics and chemistry based on the 2010 adjustment.

Quantity	Symbol	Numerical value	Unit	Relative std. uncert. u_r
Speed of light in vacuum	c, c_0	299 792 458	$m\,s^{-1}$	Exact
Magnetic constant	μ_0	$4\pi \times 10^{-7}$	$N\,A^{-2}$	
		$= 12.566\,370\,614\ldots \times 10^{-7}$	$N\,A^{-2}$	Exact
Electric constant $1/\mu_0 c^2$	ϵ_0	$8.854\,187\,817\ldots \times 10^{-12}$	$F\,m^{-1}$	Exact
Newtonian constant of gravitation	G	$6.673\,84(80) \times 10^{-11}$	$m^3\,kg^{-1}\,s^{-2}$	1.2×10^{-4}
Planck constant	h	$6.626\,069\,57(29) \times 10^{-34}$	J s	4.4×10^{-8}
$h/2\pi$	$\hbar$	$1.054\,571\,726(47) \times 10^{-34}$	J s	4.4×10^{-8}
Elementary charge	e	$1.602\,176\,565(35) \times 10^{-19}$	C	2.2×10^{-8}
Magnetic flux quantum $h/2e$	Φ_0	$2.067\,833\,758(46) \times 10^{-15}$	Wb	2.2×10^{-8}
Conductance quantum $2e^2/h$	G_0	$7.748\,091\,7346(25) \times 10^{-5}$	S	3.2×10^{-10}
Electron mass	m_e	$9.109\,382\,91(40) \times 10^{-31}$	kg	4.4×10^{-8}
Proton mass	m_p	$1.672\,621\,777(74) \times 10^{-27}$	kg	4.4×10^{-8}
Proton-electron mass ratio	m_p/m_e	1836.152 672 45(75)		4.1×10^{-10}
Fine-structure constant $e^2/4\pi\epsilon_0\hbar c$	α	$7.297\,352\,5698(24) \times 10^{-3}$		3.2×10^{-10}
inverse fine-structure constant	α^{-1}	137.035 999 074(44)		3.2×10^{-10}
Rydberg constant $\alpha^2 m_e c/2h$	R_∞	10 973 731.568 539(55)	m^{-1}	5.0×10^{-12}
Avogadro constant	N_A, L	$6.022\,141\,29(27) \times 10^{23}$	mol^{-1}	4.4×10^{-8}
Faraday constant $N_A e$	F	96 485.3365(21)	$C\,mol^{-1}$	2.2×10^{-8}
Molar gas constant	R	8.314 4621(75)	$J\,mol^{-1}\,K^{-1}$	9.1×10^{-7}
Boltzmann constant R/N_A	k	$1.380\,6488(13) \times 10^{-23}$	$J\,K^{-1}$	9.1×10^{-7}
Stefan-Boltzmann constant $(\pi^2/60)k^4/\hbar^3 c^2$	σ	$5.670\,373(21) \times 10^{-8}$	$W\,m^{-2}\,K^{-4}$	3.6×10^{-6}
		Non-SI units accepted for use with the SI		
Electron volt (e/C) J	eV	$1.602\,176\,565(35) \times 10^{-19}$	J	2.2×10^{-8}
(Unified) atomic mass unit $\frac{1}{12}m(^{12}C)$	u	$1.660\,538\,921(73) \times 10^{-27}$	kg	4.4×10^{-8}

(CGPM) at its meeting in Paris in October 2011 of Resolution 1 entitled "On the possible future revision of the International System of Units, the SI," available on the BIPM Web site at bipm.org/utils/common/pdf/24_CGPM_Resolutions.pdf.

In brief, this resolution notes the intention of the CIPM to propose, possibly to the 25th CGPM in 2014, a revision of the SI. The "new SI," as it is called to distinguish it from the current SI, will be the system of units in which seven reference constants, including the Planck constant h, elementary charge e, Boltzmann constant k, and Avogadro constant N_A, have exact assigned values. Resolution 1 also looks to CODATA to provide the necessary values of these four constants for the new definition. Details of the proposed new SI may be found in Mills *et al.* (2011) and the references cited therein; see also Mohr and Newell (2010) and Taylor (2011).

15.1. Comparison of 2010 and 2006 CODATA recommended values

Table 48 compares the 2010 and 2006 recommended values of a representative group of constants. The fact that the values of many constants are obtained from expressions proportional to the fine-structure constant α, Planck constant h, or molar gas constant R raised to various powers leads to the regularities observed in the numbers in columns 2 to 4. For example, the first six quantities are obtained from expressions proportional to α^a, where $|a| = 1$, 2, 3, or 6. The next 15 quantities, h through the magnetic moment of the proton μ_p, are calculated from expressions containing the factor h^a, where $|a| = 1$ or $1/2$. And the five quantities R through the Stefan-Boltzmann constant σ are proportional to R^a, where $|a| = 1$ or 4.

Further comments on some of the entries in Table 48 are as follows.

(i) The large shift in the 2006 recommended value of α is mainly due to the discovery and correction of an error in the numerically calculated value of the eighth-order coefficient $A_1^{(8)}$ in the theoretical expression for a_e; see Sec. 5.1.1. Its reduction in uncertainty is due to two new results. The first is the 2008 improved value of a_e obtained at Harvard University with a relative standard uncertainty of 2.4×10^{-10} compared to the 6.6×10^{-10} uncertainty of the earlier Harvard result used in the 2006 adjustment. The second result is the 2011 improved LKB atom-recoil value of $h/m(^{87}Rb)$ with an uncertainty of 1.2×10^{-9} compared to the 1.3×10^{-8} uncertainty of the earlier LKB result used in 2006. The much reduced uncertainty of g_e is also due to the improved value of α.

(ii) The change in the 2006 recommended value of h is due to the 2011 IAC result for N_A with a relative standard uncertainty

TABLE 41. The CODATA recommended values of the fundamental constants of physics and chemistry based on the 2010 adjustment.

Quantity	Symbol	Numerical value	Unit	Relative std. uncert. u_r
		UNIVERSAL		
Speed of light in vacuum	c, c_0	299 792 458	$m\,s^{-1}$	Exact
Magnetic constant	μ_0	$4\pi \times 10^{-7}$	$N\,A^{-2}$	
		$= 12.566\,370\,614\ldots \times 10^{-7}$	$N\,A^{-2}$	Exact
Electric constant $1/\mu_0 c^2$	ϵ_0	$8.854\,187\,817\ldots \times 10^{-12}$	$F\,m^{-1}$	Exact
Characteristic impedance of vacuum $\mu_0 c$	Z_0	376.730 313 461…	Ω	Exact
Newtonian constant of gravitation	G	$6.673\,84(80) \times 10^{-11}$	$m^3\,kg^{-1}\,s^{-2}$	1.2×10^{-4}
	$G/\hbar c$	$6.708\,37(80) \times 10^{-39}$	$(GeV/c^2)^{-2}$	1.2×10^{-4}
Planck constant	h	$6.626\,069\,57(29) \times 10^{-34}$	J s	4.4×10^{-8}
		$4.135\,667\,516(91) \times 10^{-15}$	eV s	2.2×10^{-8}
$h/2\pi$	$\hbar$	$1.054\,571\,726(47) \times 10^{-34}$	J s	4.4×10^{-8}
		$6.582\,119\,28(15) \times 10^{-16}$	eV s	2.2×10^{-8}
	$\hbar c$	197.326 9718(44)	MeV fm	2.2×10^{-8}
Planck mass $(\hbar c/G)^{1/2}$	m_P	$2.176\,51(13) \times 10^{-8}$	kg	6.0×10^{-5}
energy equivalent	$m_P c^2$	$1.220\,932(73) \times 10^{19}$	GeV	6.0×10^{-5}
Planck temperature $(\hbar c^5/G)^{1/2}/k$	T_P	$1.416\,833(85) \times 10^{32}$	K	6.0×10^{-5}
Planck length $\hbar/m_P c = (\hbar G/c^3)^{1/2}$	l_P	$1.616\,199(97) \times 10^{-35}$	m	6.0×10^{-5}
Planck time $l_P/c = (\hbar G/c^5)^{1/2}$	t_P	$5.391\,06(32) \times 10^{-44}$	s	6.0×10^{-5}
		ELECTROMAGNETIC		
Elementary charge	e	$1.602\,176\,565(35) \times 10^{-19}$	C	2.2×10^{-8}
	e/h	$2.417\,989\,348(53) \times 10^{14}$	$A\,J^{-1}$	2.2×10^{-8}
Magnetic flux quantum $h/2e$	Φ_0	$2.067\,833\,758(46) \times 10^{-15}$	Wb	2.2×10^{-8}
Conductance quantum $2e^2/h$	G_0	$7.748\,091\,7346(25) \times 10^{-5}$	S	3.2×10^{-10}
inverse of conductance quantum	G_0^{-1}	12 906.403 7217(42)	Ω	3.2×10^{-10}
Josephson constant[a] $2e/h$	K_J	$483\,597.870(11) \times 10^9$	$Hz\,V^{-1}$	2.2×10^{-8}
von Klitzing constant[b] $h/e^2 = \mu_0 c/2\alpha$	R_K	25 812.807 4434(84)	Ω	3.2×10^{-10}
Bohr magneton $e\hbar/2m_e$	μ_B	$927.400\,968(20) \times 10^{-26}$	$J\,T^{-1}$	2.2×10^{-8}
		$5.788\,381\,8066(38) \times 10^{-5}$	$eV\,T^{-1}$	6.5×10^{-10}
	μ_B/h	$13.996\,245\,55(31) \times 10^9$	$Hz\,T^{-1}$	2.2×10^{-8}
	μ_B/hc	46.686 4498(10)	$m^{-1}\,T^{-1}$	2.2×10^{-8}
	μ_B/k	0.671 713 88(61)	$K\,T^{-1}$	9.1×10^{-7}
Nuclear magneton $e\hbar/2m_p$	μ_N	$5.050\,783\,53(11) \times 10^{-27}$	$J\,T^{-1}$	2.2×10^{-8}
		$3.152\,451\,2605(22) \times 10^{-8}$	$eV\,T^{-1}$	7.1×10^{-10}
	μ_N/h	7.622 593 57(17)	$MHz\,T^{-1}$	2.2×10^{-8}
	μ_N/hc	$2.542\,623\,527(56) \times 10^{-2}$	$m^{-1}\,T^{-1}$	2.2×10^{-8}
	μ_N/k	$3.658\,2682(33) \times 10^{-4}$	$K\,T^{-1}$	9.1×10^{-7}
		ATOMIC AND NUCLEAR		
		General		
Fine-structure constant $e^2/4\pi\epsilon_0\hbar c$	α	$7.297\,352\,5698(24) \times 10^{-3}$		3.2×10^{-10}
inverse fine-structure constant	α^{-1}	137.035 999 074(44)		3.2×10^{-10}
Rydberg constant $\alpha^2 m_e c/2h$	R_∞	10 973 731.568 539(55)	m^{-1}	5.0×10^{-12}
	$R_\infty c$	$3.289\,841\,960\,364(17) \times 10^{15}$	Hz	5.0×10^{-12}
	$R_\infty hc$	$2.179\,872\,171(96) \times 10^{-18}$	J	4.4×10^{-8}
		13.605 692 53(30)	eV	2.2×10^{-8}
Bohr radius $\alpha/4\pi R_\infty = 4\pi\epsilon_0\hbar^2/m_e e^2$	a_0	$0.529\,177\,210\,92(17) \times 10^{-10}$	m	3.2×10^{-10}
Hartree energy $e^2/4\pi\epsilon_0 a_0 = 2R_\infty hc = \alpha^2 m_e c^2$	E_h	$4.359\,744\,34(19) \times 10^{-18}$	J	4.4×10^{-8}
		27.211 385 05(60)	eV	2.2×10^{-8}
Quantum of circulation	$h/2m_e$	$3.636\,947\,5520(24) \times 10^{-4}$	$m^2\,s^{-1}$	6.5×10^{-10}
	h/m_e	$7.273\,895\,1040(47) \times 10^{-4}$	$m^2\ s^{-1}$	6.5×10^{-10}
		Electroweak		
Fermi coupling constant[c]	$G_F/(\hbar c)^3$	$1.166\,364(5) \times 10^{-5}$	GeV^{-2}	4.3×10^{-6}
Weak mixing angle[d] θ_W (on-shell scheme)				
$\sin^2\theta_W = s_W^2 \equiv 1 - (m_W/m_Z)^2$	$\sin^2\theta_W$	0.2223(21)		9.5×10^{-3}
		Electron, e^-		
Electron mass	m_e	$9.109\,382\,91(40) \times 10^{-31}$	kg	4.4×10^{-8}
		$5.485\,799\,0946(22) \times 10^{-4}$	u	4.0×10^{-10}
energy equivalent	$m_e c^2$	$8.187\,105\,06(36) \times 10^{-14}$	J	4.4×10^{-8}
		0.510 998 928(11)	MeV	2.2×10^{-8}

TABLE 41. The CODATA recommended values of the fundamental constants of physics and chemistry based on the 2010 adjustment.—Continued

Quantity	Symbol	Numerical value	Unit	Relative std. uncert. u_r
Electron-muon mass ratio	m_e/m_μ	$4.836\,331\,66(12) \times 10^{-3}$		2.5×10^{-8}
Electron-tau mass ratio	m_e/m_τ	$2.875\,92(26) \times 10^{-4}$		9.0×10^{-5}
Electron-proton mass ratio	m_e/m_p	$5.446\,170\,2178(22) \times 10^{-4}$		4.1×10^{-10}
Electron-neutron mass ratio	m_e/m_n	$5.438\,673\,4461(32) \times 10^{-4}$		5.8×10^{-10}
Electron-deuteron mass ratio	m_e/m_d	$2.724\,437\,1095(11) \times 10^{-4}$		4.0×10^{-10}
Electron-triton mass ratio	m_e/m_t	$1.819\,200\,0653(17) \times 10^{-4}$		9.1×10^{-10}
Electron-helion mass ratio	m_e/m_h	$1.819\,543\,0761(17) \times 10^{-4}$		9.2×10^{-10}
Electron to alpha particle mass ratio	m_e/m_α	$1.370\,933\,555\,78(55) \times 10^{-4}$		4.0×10^{-10}
Electron charge-to-mass quotient	$-e/m_e$	$-1.758\,820\,088(39) \times 10^{11}$	$C\,kg^{-1}$	2.2×10^{-8}
Electron molar mass $N_A m_e$	$M(e)$, M_e	$5.485\,799\,0946(22) \times 10^{-7}$	$kg\,mol^{-1}$	4.0×10^{-10}
Compton wavelength $h/m_e c$	λ_C	$2.426\,310\,2389(16) \times 10^{-12}$	m	6.5×10^{-10}
$\lambda_C/2\pi = \alpha a_0 = \alpha^2/4\pi R_\infty$	$\lambda\!\!\!^{-}_C$	$386.159\,268\,00(25) \times 10^{-15}$	m	6.5×10^{-10}
Classical electron radius $\alpha^2 a_0$	r_e	$2.817\,940\,3267(27) \times 10^{-15}$	m	9.7×10^{-10}
Thomson cross section $(8\pi/3)r_e^2$	σ_e	$0.665\,245\,8734(13) \times 10^{-28}$	m^2	1.9×10^{-9}
Electron magnetic moment	μ_e	$-928.476\,430(21) \times 10^{-26}$	$J\,T^{-1}$	2.2×10^{-8}
to Bohr magneton ratio	μ_e/μ_B	$-1.001\,159\,652\,180\,76(27)$		2.6×10^{-13}
to nuclear magneton ratio	μ_e/μ_N	$-1838.281\,970\,90(75)$		4.1×10^{-10}
Electron magnetic-moment anomaly $\lvert\mu_e\rvert/\mu_B - 1$	a_e	$1.159\,652\,180\,76(27) \times 10^{-3}$		2.3×10^{-10}
Electron g-factor $-2(1 + a_e)$	g_e	$-2.002\,319\,304\,361\,53(53)$		2.6×10^{-13}
Electron-muon magnetic-moment ratio	μ_e/μ_μ	206.766 9896(52)		2.5×10^{-8}
Electron-proton magnetic-moment ratio	μ_e/μ_p	−658.210 6848(54)		8.1×10^{-9}
Electron to shielded proton magnetic-moment ratio (H_2O, sphere, 25 °C)	μ_e/μ'_p	−658.227 5971(72)		1.1×10^{-8}
Electron-neutron magnetic-moment ratio	μ_e/μ_n	960.920 50(23)		2.4×10^{-7}
Electron-deuteron magnetic-moment ratio	μ_e/μ_d	−2143.923 498(18)		8.4×10^{-9}
Electron to shielded helion magnetic-moment ratio (gas, sphere, 25 °C)	μ_e/μ'_h	864.058 257(10)		1.2×10^{-8}
Electron gyromagnetic ratio $2\lvert\mu_e\rvert/\hbar$	γ_e	$1.760\,859\,708(39) \times 10^{11}$	$s^{-1}\,T^{-1}$	2.2×10^{-8}
	$\gamma_e/2\pi$	28 024.952 66(62)	$MHz\,T^{-1}$	2.2×10^{-8}
		Muon, μ^-		
Muon mass	m_μ	$1.883\,531\,475(96) \times 10^{-28}$	kg	5.1×10^{-8}
		0.113 428 9267(29)	u	2.5×10^{-8}
energy equivalent	$m_\mu c^2$	$1.692\,833\,667(86) \times 10^{-11}$	J	5.1×10^{-8}
		105.658 3715(35)	MeV	3.4×10^{-8}
Muon-electron mass ratio	m_μ/m_e	206.768 2843(52)		2.5×10^{-8}
Muon-tau mass ratio	m_μ/m_τ	$5.946\,49(54) \times 10^{-2}$		9.0×10^{-5}
Muon-proton mass ratio	m_μ/m_p	0.112 609 5272(28)		2.5×10^{-8}
Muon-neutron mass ratio	m_μ/m_n	0.112 454 5177(28)		2.5×10^{-8}
Muon molar mass $N_A m_\mu$	$M(\mu)$, M_μ	$0.113\,428\,9267(29) \times 10^{-3}$	$kg\,mol^{-1}$	2.5×10^{-8}
Muon Compton wavelength $h/m_\mu c$	$\lambda_{C,\mu}$	$11.734\,441\,03(30) \times 10^{-15}$	m	2.5×10^{-8}
$\lambda_{C,\mu}/2\pi$	$\lambda\!\!\!^{-}_{C,\mu}$	$1.867\,594\,294(47) \times 10^{-15}$	m	2.5×10^{-8}
Muon magnetic moment	μ_μ	$-4.490\,448\,07(15) \times 10^{-26}$	$J\,T^{-1}$	3.4×10^{-8}
to Bohr magneton ratio	μ_μ/μ_B	$-4.841\,970\,44(12) \times 10^{-3}$		2.5×10^{-8}
to nuclear magneton ratio	μ_μ/μ_N	−8.890 596 97(22)		2.5×10^{-8}
Muon magnetic-moment anomaly $\lvert\mu_\mu\rvert/(e\hbar/2m_\mu) - 1$	a_μ	$1.165\,920\,91(63) \times 10^{-3}$		5.4×10^{-7}
Muon g-factor $-2(1 + a_\mu)$	g_μ	$-2.002\,331\,8418(13)$		6.3×10^{-10}
Muon-proton magnetic-moment ratio	μ_μ/μ_p	−3.183 345 107(84)		2.6×10^{-8}
		Tau, τ^-		
Tau mass[e]	m_τ	$3.167\,47(29) \times 10^{-27}$	kg	9.0×10^{-5}
		1.907 49(17)	u	9.0×10^{-5}
energy equivalent	$m_\tau c^2$	$2.846\,78(26) \times 10^{-10}$	J	9.0×10^{-5}
		1776.82(16)	MeV	9.0×10^{-5}
Tau-electron mass ratio	m_τ/m_e	3477.15(31)		9.0×10^{-5}
Tau-muon mass ratio	m_τ/m_μ	16.8167(15)		9.0×10^{-5}
Tau-proton mass ratio	m_τ/m_p	1.893 72(17)		9.0×10^{-5}
Tau-neutron mass ratio	m_τ/m_n	1.891 11(17)		9.0×10^{-5}
Tau molar mass $N_A m_\tau$	$M(\tau)$, M_τ	$1.907\,49(17) \times 10^{-3}$	$kg\,mol^{-1}$	9.0×10^{-5}
Tau Compton wavelength $h/m_\tau c$	$\lambda_{C,\tau}$	$0.697\,787(63) \times 10^{-15}$	m	9.0×10^{-5}

TABLE 41. The CODATA recommended values of the fundamental constants of physics and chemistry based on the 2010 adjustment.—Continued

Quantity	Symbol	Numerical value	Unit	Relative std. uncert. u_r
$\lambda_{C,\tau}/2\pi$	$\lambda\!\!\!^{-}_{C,\tau}$	$0.111\,056(10) \times 10^{-15}$	m	9.0×10^{-5}
		Proton, p		
Proton mass	m_p	$1.672\,621\,777(74) \times 10^{-27}$	kg	4.4×10^{-8}
		1.007 276 466 812(90)	u	8.9×10^{-11}
energy equivalent	$m_p c^2$	$1.503\,277\,484(66) \times 10^{-10}$	J	4.4×10^{-8}
		938.272 046(21)	MeV	2.2×10^{-8}
Proton-electron mass ratio	m_p/m_e	1836.152 672 45(75)		4.1×10^{-10}
Proton-muon mass ratio	m_p/m_μ	8.880 243 31(22)		2.5×10^{-8}
Proton-tau mass ratio	m_p/m_τ	0.528 063(48)		9.0×10^{-5}
Proton-neutron mass ratio	m_p/m_n	0.998 623 478 26(45)		4.5×10^{-10}
Proton charge-to-mass quotient	e/m_p	$9.578\,833\,58(21) \times 10^{7}$	C kg^{-1}	2.2×10^{-8}
Proton molar mass $N_A m_p$	$M(p), M_p$	$1.007\,276\,466\,812(90) \times 10^{-3}$	kg mol^{-1}	8.9×10^{-11}
Proton Compton wavelength $h/m_p c$	$\lambda_{C,p}$	$1.321\,409\,856\,23(94) \times 10^{-15}$	m	7.1×10^{-10}
$\lambda_{C,p}/2\pi$	$\lambda\!\!\!^{-}_{C,p}$	$0.210\,308\,910\,47(15) \times 10^{-15}$	m	7.1×10^{-10}
Proton rms charge radius	r_p	$0.8775(51) \times 10^{-15}$	m	5.9×10^{-3}
Proton magnetic moment	μ_p	$1.410\,606\,743(33) \times 10^{-26}$	J T^{-1}	2.4×10^{-8}
to Bohr magneton ratio	μ_p/μ_B	$1.521\,032\,210(12) \times 10^{-3}$		8.1×10^{-9}
to nuclear magneton ratio	μ_p/μ_N	2.792 847 356(23)		8.2×10^{-9}
Proton g-factor $2\mu_p/\mu_N$	g_p	5.585 694 713(46)		8.2×10^{-9}
Proton-neutron magnetic-moment ratio	μ_p/μ_n	−1.459 898 06(34)		2.4×10^{-7}
Shielded proton magnetic moment (H_2O, sphere, 25 °C)	μ'_p	$1.410\,570\,499(35) \times 10^{-26}$	J T^{-1}	2.5×10^{-8}
to Bohr magneton ratio	μ'_p/μ_B	$1.520\,993\,128(17) \times 10^{-3}$		1.1×10^{-8}
to nuclear magneton ratio	μ'_p/μ_N	2.792 775 598(30)		1.1×10^{-8}
Proton magnetic shielding correction $1 - \mu'_p/\mu_p$ (H_2O, sphere, 25 °C)	σ'_p	$25.694(14) \times 10^{-6}$		5.3×10^{-4}
Proton gyromagnetic ratio $2\mu_p/\hbar$	γ_p	$2.675\,222\,005(63) \times 10^{8}$	s^{-1} T^{-1}	2.4×10^{-8}
	$\gamma_p/2\pi$	42.577 4806(10)	MHz T^{-1}	2.4×10^{-8}
Shielded proton gyromagnetic ratio $2\mu'_p/\hbar$ (H_2O, sphere, 25 °C)	γ'_p	$2.675\,153\,268(66) \times 10^{8}$	s^{-1} T^{-1}	2.5×10^{-8}
	$\gamma'_p/2\pi$	42.576 3866(10)	MHz T^{-1}	2.5×10^{-8}
		Neutron, n		
Neutron mass	m_n	$1.674\,927\,351(74) \times 10^{-27}$	kg	4.4×10^{-8}
		1.008 664 916 00(43)	u	4.2×10^{-10}
energy equivalent	$m_n c^2$	$1.505\,349\,631(66) \times 10^{-10}$	J	4.4×10^{-8}
		939.565 379(21)	MeV	2.2×10^{-8}
Neutron-electron mass ratio	m_n/m_e	1838.683 6605(11)		5.8×10^{-10}
Neutron-muon mass ratio	m_n/m_μ	8.892 484 00(22)		2.5×10^{-8}
Neutron-tau mass ratio	m_n/m_τ	0.528 790(48)		9.0×10^{-5}
Neutron-proton mass ratio	m_n/m_p	1.001 378 419 17(45)		4.5×10^{-10}
Neutron-proton mass difference	$m_n - m_p$	$2.305\,573\,92(76) \times 10^{-30}$	kg	3.3×10^{-7}
		0.001 388 449 19(45)	u	3.3×10^{-7}
energy equivalent	$(m_n - m_p)c^2$	$2.072\,146\,50(68) \times 10^{-13}$	J	3.3×10^{-7}
		1.293 332 17(42)	MeV	3.3×10^{-7}
Neutron molar mass $N_A m_n$	$M(n), M_n$	$1.008\,664\,916\,00(43) \times 10^{-3}$	kg mol^{-1}	4.2×10^{-10}
Neutron Compton wavelength $h/m_n c$	$\lambda_{C,n}$	$1.319\,590\,9068(11) \times 10^{-15}$	m	8.2×10^{-10}
$\lambda_{C,n}/2\pi$	$\lambda\!\!\!^{-}_{C,n}$	$0.210\,019\,415\,68(17) \times 10^{-15}$	m	8.2×10^{-10}
Neutron magnetic moment	μ_n	$-0.966\,236\,47(23) \times 10^{-26}$	J T^{-1}	2.4×10^{-7}
to Bohr magneton ratio	μ_n/μ_B	$-1.041\,875\,63(25) \times 10^{-3}$		2.4×10^{-7}
to nuclear magneton ratio	μ_n/μ_N	−1.913 042 72(45)		2.4×10^{-7}
Neutron g-factor $2\mu_n/\mu_N$	g_n	−3.826 085 45(90)		2.4×10^{-7}
Neutron-electron magnetic-moment ratio	μ_n/μ_e	$1.040\,668\,82(25) \times 10^{-3}$		2.4×10^{-7}
Neutron-proton magnetic-moment ratio	μ_n/μ_p	−0.684 979 34(16)		2.4×10^{-7}
Neutron to shielded proton magnetic-moment ratio (H_2O, sphere, 25 °C)	μ_n/μ'_p	−0.684 996 94(16)		2.4×10^{-7}
Neutron gyromagnetic ratio $2\lvert\mu_n\rvert/\hbar$	γ_n	$1.832\,471\,79(43) \times 10^{8}$	s^{-1} T^{-1}	2.4×10^{-7}
	$\gamma_n/2\pi$	29.164 6943(69)	MHz T^{-1}	2.4×10^{-7}

TABLE 41. The CODATA recommended values of the fundamental constants of physics and chemistry based on the 2010 adjustment.—Continued

Quantity	Symbol	Numerical value	Unit	Relative std. uncert. u_r
		Deuteron, d		
Deuteron mass	m_d	$3.343\,583\,48(15) \times 10^{-27}$	kg	4.4×10^{-8}
		2.013 553 212 712(77)	u	3.8×10^{-11}
energy equivalent	$m_d c^2$	$3.005\,062\,97(13) \times 10^{-10}$	J	4.4×10^{-8}
		1875.612 859(41)	MeV	2.2×10^{-8}
Deuteron-electron mass ratio	m_d/m_e	3670.482 9652(15)		4.0×10^{-10}
Deuteron-proton mass ratio	m_d/m_p	1.999 007 500 97(18)		9.2×10^{-11}
Deuteron molar mass $N_A m_d$	$M(d), M_d$	$2.013\,553\,212\,712(77) \times 10^{-3}$	kg mol^{-1}	3.8×10^{-11}
Deuteron rms charge radius	r_d	$2.1424(21) \times 10^{-15}$	m	9.8×10^{-4}
Deuteron magnetic moment	μ_d	$0.433\,073\,489(10) \times 10^{-26}$	J T^{-1}	2.4×10^{-8}
to Bohr magneton ratio	μ_d/μ_B	$0.466\,975\,4556(39) \times 10^{-3}$		8.4×10^{-9}
to nuclear magneton ratio	μ_d/μ_N	0.857 438 2308(72)		8.4×10^{-9}
Deuteron g-factor μ_d/μ_N	g_d	0.857 438 2308(72)		8.4×10^{-9}
Deuteron-electron magnetic-moment ratio	μ_d/μ_e	$-4.664\,345\,537(39) \times 10^{-4}$		8.4×10^{-9}
Deuteron-proton magnetic-moment ratio	μ_d/μ_p	0.307 012 2070(24)		7.7×10^{-9}
Deuteron-neutron magnetic-moment ratio	μ_d/μ_n	−0.448 206 52(11)		2.4×10^{-7}
		Triton, t		
Triton mass	m_t	$5.007\,356\,30(22) \times 10^{-27}$	kg	4.4×10^{-8}
		3.015 500 7134(25)	u	8.2×10^{-10}
energy equivalent	$m_t c^2$	$4.500\,387\,41(20) \times 10^{-10}$	J	4.4×10^{-8}
		2808.921 005(62)	MeV	2.2×10^{-8}
Triton-electron mass ratio	m_t/m_e	5496.921 5267(50)		9.1×10^{-10}
Triton-proton mass ratio	m_t/m_p	2.993 717 0308(25)		8.2×10^{-10}
Triton molar mass $N_A m_t$	$M(t), M_t$	$3.015\,500\,7134(25) \times 10^{-3}$	kg mol^{-1}	8.2×10^{-10}
Triton magnetic moment	μ_t	$1.504\,609\,447(38) \times 10^{-26}$	J T^{-1}	2.6×10^{-8}
to Bohr magneton ratio	μ_t/μ_B	$1.622\,393\,657(21) \times 10^{-3}$		1.3×10^{-8}
to nuclear magneton ratio	μ_t/μ_N	2.978 962 448(38)		1.3×10^{-8}
Triton g-factor $2\mu_t/\mu_N$	g_t	5.957 924 896(76)		1.3×10^{-8}
		Helion, h		
Helion mass	m_h	$5.006\,412\,34(22) \times 10^{-27}$	kg	4.4×10^{-8}
		3.014 932 2468(25)	u	8.3×10^{-10}
energy equivalent	$m_h c^2$	$4.499\,539\,02(20) \times 10^{-10}$	J	4.4×10^{-8}
		2808.391 482(62)	MeV	2.2×10^{-8}
Helion-electron mass ratio	m_h/m_e	5495.885 2754(50)		9.2×10^{-10}
Helion-proton mass ratio	m_h/m_p	2.993 152 6707(25)		8.2×10^{-10}
Helion molar mass $N_A m_h$	$M(h), M_h$	$3.014\,932\,2468(25) \times 10^{-3}$	kg mol^{-1}	8.3×10^{-10}
Helion magnetic moment	μ_h	$-1.074\,617\,486(27) \times 10^{-26}$	J T^{-1}	2.5×10^{-8}
to Bohr magneton ratio	μ_h/μ_B	$-1.158\,740\,958(14) \times 10^{-3}$		1.2×10^{-8}
to nuclear magneton ratio	μ_h/μ_N	−2.127 625 306(25)		1.2×10^{-8}
Helion g-factor $2\mu_h/\mu_N$	g_h	−4.255 250 613(50)		1.2×10^{-8}
Shielded helion magnetic moment (gas, sphere, 25 °C)	μ'_h	$-1.074\,553\,044(27) \times 10^{-26}$	J T^{-1}	2.5×10^{-8}
to Bohr magneton ratio	μ'_h/μ_B	$-1.158\,671\,471(14) \times 10^{-3}$		1.2×10^{-8}
to nuclear magneton ratio	μ'_h/μ_N	−2.127 497 718(25)		1.2×10^{-8}
Shielded helion to proton magnetic-moment ratio (gas, sphere, 25 °C)	μ'_h/μ_p	−0.761 766 558(11)		1.4×10^{-8}
Shielded helion to shielded proton magnetic-moment ratio (gas/H_2O, spheres, 25 °C)	μ'_h/μ'_p	−0.761 786 1313(33)		4.3×10^{-9}
Shielded helion gyromagnetic ratio $2\lvert\mu'_h\rvert/\hbar$ (gas, sphere, 25 °C)	γ'_h	$2.037\,894\,659(51) \times 10^{8}$	s^{-1} T^{-1}	2.5×10^{-8}
	$\gamma'_h/2\pi$	32.434 100 84(81)	MHz T^{-1}	2.5×10^{-8}
		Alpha particle, α		
Alpha particle mass	m_α	$6.644\,656\,75(29) \times 10^{-27}$	kg	4.4×10^{-8}
		4.001 506 179 125(62)	u	1.5×10^{-11}
energy equivalent	$m_\alpha c^2$	$5.971\,919\,67(26) \times 10^{-10}$	J	4.4×10^{-8}
		3727.379 240(82)	MeV	2.2×10^{-8}
Alpha particle to electron mass ratio	m_α/m_e	7294.299 5361(29)		4.0×10^{-10}

TABLE 41. The CODATA recommended values of the fundamental constants of physics and chemistry based on the 2010 adjustment.—Continued

Quantity	Symbol	Numerical value	Unit	Relative std. uncert. u_r
Alpha particle to proton mass ratio	m_α/m_p	3.972 599 689 33(36)		9.0×10^{-11}
Alpha particle molar mass $N_A m_\alpha$	$M(\alpha)$, M_α	$4.001\,506\,179\,125(62) \times 10^{-3}$	kg mol^{-1}	1.5×10^{-11}
		PHYSICOCHEMICAL		
Avogadro constant	N_A, L	$6.022\,141\,29(27) \times 10^{23}$	mol^{-1}	4.4×10^{-8}
Atomic mass constant $m_u = \frac{1}{12}m(^{12}C) = 1$ u	m_u	$1.660\,538\,921(73) \times 10^{-27}$	kg	4.4×10^{-8}
energy equivalent	$m_u c^2$	$1.492\,417\,954(66) \times 10^{-10}$	J	4.4×10^{-8}
		931.494 061(21)	MeV	2.2×10^{-8}
Faraday constant[f] $N_A e$	F	96 485.3365(21)	C mol^{-1}	2.2×10^{-8}
Molar Planck constant	$N_A h$	$3.990\,312\,7176(28) \times 10^{-10}$	J s mol^{-1}	7.0×10^{-10}
	$N_A hc$	0.119 626 565 779(84)	J m mol^{-1}	7.0×10^{-10}
Molar gas constant	R	8.314 4621(75)	J mol^{-1} K^{-1}	9.1×10^{-7}
Boltzmann constant R/N_A	k	$1.380\,6488(13) \times 10^{-23}$	J K^{-1}	9.1×10^{-7}
		$8.617\,3324(78) \times 10^{-5}$	eV K^{-1}	9.1×10^{-7}
	k/h	$2.083\,6618(19) \times 10^{10}$	Hz K^{-1}	9.1×10^{-7}
	k/hc	69.503 476(63)	m^{-1} K^{-1}	9.1×10^{-7}
Molar volume of ideal gas RT/p				
$T = 273.15$ K, $p = 100$ kPa	V_m	$22.710\,953(21) \times 10^{-3}$	m^3 mol^{-1}	9.1×10^{-7}
Loschmidt constant N_A/V_m	n_0	$2.651\,6462(24) \times 10^{25}$	m^{-3}	9.1×10^{-7}
Molar volume of ideal gas RT/p				
$T = 273.15$ K, $p = 101.325$ kPa	V_m	$22.413\,968(20) \times 10^{-3}$	m^3 mol^{-1}	9.1×10^{-7}
Loschmidt constant N_A/V_m	n_0	$2.686\,7805(24) \times 10^{25}$	m^{-3}	9.1×10^{-7}
Sackur-Tetrode (absolute entropy) constant[g]				
$\frac{5}{2} + \ln[(2\pi m_u kT_1/h^2)^{3/2} kT_1/p_0]$				
$T_1 = 1$ K, $p_0 = 100$ kPa	S_0/R	−1.151 7078(23)		2.0×10^{-6}
$T_1 = 1$ K, $p_0 = 101.325$ kPa		−1.164 8708(23)		1.9×10^{-6}
Stefan-Boltzmann constant $(\pi^2/60)k^4/\hbar^3 c^2$	σ	$5.670\,373(21) \times 10^{-8}$	W m^{-2} K^{-4}	3.6×10^{-6}
First radiation constant $2\pi hc^2$	c_1	$3.741\,771\,53(17) \times 10^{-16}$	W m^2	4.4×10^{-8}
First radiation constant for spectral radiance $2hc^2$	c_{1L}	$1.191\,042\,869(53) \times 10^{-16}$	W m^2 sr^{-1}	4.4×10^{-8}
Second radiation constant hc/k	c_2	$1.438\,7770(13) \times 10^{-2}$	m K	9.1×10^{-7}
Wien displacement law constants				
$b = \lambda_{max} T = c_2/4.965\,114\,231\ldots$	b	$2.897\,7721(26) \times 10^{-3}$	m K	9.1×10^{-7}
$b' = \nu_{max}/T = 2.821\,439\,372\ldots c/c_2$	b'	$5.878\,9254(53) \times 10^{10}$	Hz K^{-1}	9.1×10^{-7}

[a]See Table 43 for the conventional value adopted internationally for realizing representations of the volt using the Josephson effect.
[b]See Table 43 for the conventional value adopted internationally for realizing representations of the ohm using the quantum Hall effect.
[c]Value recommended by the Particle Data Group (Nakamura *et al.*, 2010).
[d]Based on the ratio of the masses of the W and Z bosons m_W/m_Z recommended by the Particle Data Group (Nakamura *et al.*, 2010). The value for $\sin^2\theta_W$ they recommend, which is based on a particular variant of the modified minimal subtraction ($\overline{MS}$) scheme, is $\sin^2\hat{\theta}_W(M_Z) = 0.231\,16(13)$.
[e]This and all other values involving m_τ are based on the value of $m_\tau c^2$ in MeV recommended by the Particle Data Group (Nakamura *et al.*, 2010).
[f]The numerical value of F to be used in coulometric chemical measurements is 96 485.3321(43) [4.4×10^{-8}] when the relevant current is measured in terms of representations of the volt and ohm based on the Josephson and quantum Hall effects and the internationally adopted conventional values of the Josephson and von Klitzing constants K_{J-90} and R_{K-90} given in Table 43.
[g]The entropy of an ideal monatomic gas of relative atomic mass A_r is given by $S = S_0 + \frac{3}{2}R\ln A_r - R\ln(p/p_0) + \frac{5}{2}R\ln(T/\mathrm{K})$.

TABLE 42. The variances, covariances, and correlation coefficients of the values of a selected group of constants based on the 2010 CODATA adjustment. The numbers in bold above the main diagonal are 10^{16} times the numerical values of the relative covariances; the numbers in bold on the main diagonal are 10^{16} times the numerical values of the relative variances; and the numbers in italics below the main diagonal are the correlation coefficients.[a]

	α	h	e	m_e	N_A	m_e/m_μ	F
α	**0.0010**	**0.0010**	**0.0010**	**−0.0011**	**0.0009**	**−0.0021**	**0.0019**
h	*0.0072*	**19.4939**	**9.7475**	**19.4918**	**−19.4912**	**−0.0020**	**−9.7437**
e	*0.0145*	*1.0000*	**4.8742**	**9.7454**	**−9.7452**	**−0.0020**	**−4.8709**
m_e	*−0.0075*	*0.9999*	*0.9998*	**19.4940**	**−19.4929**	**0.0021**	**−9.7475**
N_A	*0.0060*	*−0.9999*	*−0.9997*	*−1.0000*	**19.4934**	**−0.0017**	**9.7483**
m_e/m_μ	*−0.0251*	*−0.0002*	*−0.0004*	*0.0002*	*−0.0002*	**6.3872**	**−0.0037**
F	*0.0265*	*−0.9993*	*−0.9990*	*−0.9997*	*0.9997*	*−0.0007*	**4.8774**

[a]The relative covariance is $u_r(x_i, x_j) = u(x_i, x_j)/(x_i x_j)$, where $u(x_i, x_j)$ is the covariance of x_i and x_j; the relative variance is $u_r^2(x_i) = u_r(x_i, x_i)$: and the correlation coefficient is $r(x_i, x_j) = u(x_i, x_j)/[u(x_i)u(x_j)]$.

TABLE 43. Internationally adopted values of various quantities.

Quantity	Symbol	Numerical value	Unit	Relative std. uncert. u_r
Relative atomic mass[a] of ^{12}C	$A_r(^{12}C)$	12		Exact
Molar mass constant	M_u	1×10^{-3}	kg mol^{-1}	Exact
Molar mass[b] of ^{12}C	$M(^{12}C)$	12×10^{-3}	kg mol^{-1}	Exact
Conventional value of Josephson constant[c]	K_{J-90}	483 597.9	GHz V^{-1}	Exact
Conventional value of von Klitzing constant[d]	R_{K-90}	25 812.807	Ω	Exact
Standard-state pressure		100	kPa	Exact
Standard atmosphere		101.325	kPa	Exact

[a]The relative atomic mass $A_r(X)$ of particle X with mass $m(X)$ is defined by $A_r(X) = m(X)/m_u$, where $m_u = m(^{12}C)/12 = M_u/N_A = 1$ u is the atomic mass constant, M_u is the molar mass constant, N_A is the Avogadro constant, and u is the unified atomic mass unit. Thus the mass of particle X is $m(X) = A_r(X)$ u and the molar mass of X is $M(X) = A_r(X)M_u$.
[b]Value fixed by the SI definition of the mole.
[c]This is the value adopted internationally for realizing representations of the volt using the Josephson effect.
[d]This is the value adopted internationally for realizing representations of the ohm using the quantum Hall effect.

TABLE 44. Values of some x-ray-related quantities based on the 2010 CODATA adjustment of the values of the constants.

Quantity	Symbol	Numerical value	Unit	Relative std. uncert. u_r
Cu x unit: $\lambda(CuK\alpha_1)/1\,537.400$	xu(CuKα_1)	$1.002\,076\,97(28) \times 10^{-13}$	m	2.8×10^{-7}
Mo x unit: $\lambda(MoK\alpha_1)/707.831$	xu(MoKα_1)	$1.002\,099\,52(53) \times 10^{-13}$	m	5.3×10^{-7}
Ångstrom star: $\lambda(WK\alpha_1)/0.209\,010\,0$	Å*	$1.000\,014\,95(90) \times 10^{-10}$	m	9.0×10^{-7}
Lattice parameter[a] of Si (in vacuum, 22.5 °C)	a	$543.102\,0504(89) \times 10^{-12}$	m	1.6×10^{-8}
{220} lattice spacing of Si $a/\sqrt{8}$ (in vacuum, 22.5 °C)	d_{220}	$192.015\,5714(32) \times 10^{-12}$	m	1.6×10^{-8}
Molar volume of Si $M(Si)/\rho(Si) = N_A a^3/8$ (in vacuum, 22.5 °C)	$V_m(Si)$	$12.058\,833\,01(80) \times 10^{-6}$	m^3 mol^{-1}	6.6×10^{-8}

[a]This is the lattice parameter (unit cell edge length) of an ideal single crystal of naturally occurring Si free of impurities and imperfections, and is deduced from measurements on extremely pure and nearly perfect single crystals of Si by correcting for the effects of impurities.

TABLE 45. The values in SI units of some non-SI units based on the 2010 CODATA adjustment of the values of the constants.

Quantity	Symbol	Numerical value	Unit	Relative std. uncert. u_r
		Non-SI units accepted for use with the SI		
Electron volt: (e/C) J	eV	$1.602\,176\,565(35) \times 10^{-19}$	J	2.2×10^{-8}
(Unified) atomic mass unit: $\frac{1}{12}m(^{12}C)$	u	$1.660\,538\,921(73) \times 10^{-27}$	kg	4.4×10^{-8}
		Natural units (n.u.)		
n.u. of velocity	c, c_0	299 792 458	m s^{-1}	Exact
n.u. of action: $h/2\pi$	$\hbar$	$1.054\,571\,726(47) \times 10^{-34}$	J s	4.4×10^{-8}
		$6.582\,119\,28(15) \times 10^{-16}$	eV s	2.2×10^{-8}
	$\hbar c$	197.326 9718(44)	MeV fm	2.2×10^{-8}
n.u. of mass	m_e	$9.109\,382\,91(40) \times 10^{-31}$	kg	4.4×10^{-8}
n.u. of energy	$m_e c^2$	$8.187\,105\,06(36) \times 10^{-14}$	J	4.4×10^{-8}
		0.510 998 928(11)	MeV	2.2×10^{-8}
n.u. of momentum	$m_e c$	$2.730\,924\,29(12) \times 10^{-22}$	kg m s^{-1}	4.4×10^{-8}
		0.510 998 928(11)	MeV/c	2.2×10^{-8}
n.u. of length: $\hbar/m_e c$	$\lambda\!\!\!^{-}_C$	$386.159\,268\,00(25) \times 10^{-15}$	m	6.5×10^{-10}
n.u. of time	$\hbar/m_e c^2$	$1.288\,088\,668\,33(83) \times 10^{-21}$	s	6.5×10^{-10}
		Atomic units (a.u.)		
a.u. of charge	e	$1.602\,176\,565(35) \times 10^{-19}$	C	2.2×10^{-8}
a.u. of mass	m_e	$9.109\,382\,91(40) \times 10^{-31}$	kg	4.4×10^{-8}
a.u. of action: $h/2\pi$	$\hbar$	$1.054\,571\,726(47) \times 10^{-34}$	J s	4.4×10^{-8}
a.u. of length: Bohr radius (bohr) $\alpha/4\pi R_\infty$	a_0	$0.529\,177\,210\,92(17) \times 10^{-10}$	m	3.2×10^{-10}
a.u. of energy: Hartree energy (hartree) $e^2/4\pi\epsilon_0 a_0 = 2R_\infty hc = \alpha^2 m_e c^2$	E_h	$4.359\,744\,34(19) \times 10^{-18}$	J	4.4×10^{-8}
a.u. of time	$\hbar/E_h$	$2.418\,884\,326\,502(12) \times 10^{-17}$	s	5.0×10^{-12}

TABLE 45. The values in SI units of some non-SI units based on the 2010 CODATA adjustment of the values of the constants.—Continued

Quantity	Symbol	Numerical value	Unit	Relative std. uncert. u_r
a.u. of force	E_h/a_0	$8.238\,722\,78(36) \times 10^{-8}$	N	4.4×10^{-8}
a.u. of velocity: αc	$a_0 E_h/\hbar$	$2.187\,691\,263\,79(71) \times 10^{6}$	$m\,s^{-1}$	3.2×10^{-10}
a.u. of momentum	$\hbar/a_0$	$1.992\,851\,740(88) \times 10^{-24}$	$kg\,m\,s^{-1}$	4.4×10^{-8}
a.u. of current	$eE_h/\hbar$	$6.623\,617\,95(15) \times 10^{-3}$	A	2.2×10^{-8}
a.u. of charge density	e/a_0^3	$1.081\,202\,338(24) \times 10^{12}$	$C\,m^{-3}$	2.2×10^{-8}
a.u. of electric potential	E_h/e	27.211 385 05(60)	V	2.2×10^{-8}
a.u. of electric field	E_h/ea_0	$5.142\,206\,52(11) \times 10^{11}$	$V\,m^{-1}$	2.2×10^{-8}
a.u. of electric field gradient	E_h/ea_0^2	$9.717\,362\,00(21) \times 10^{21}$	$V\,m^{-2}$	2.2×10^{-8}
a.u. of electric dipole moment	ea_0	$8.478\,353\,26(19) \times 10^{-30}$	C m	2.2×10^{-8}
a.u. of electric quadrupole moment	ea_0^2	$4.486\,551\,331(99) \times 10^{-40}$	$C\,m^2$	2.2×10^{-8}
a.u. of electric polarizability	$e^2a_0^2/E_h$	$1.648\,777\,2754(16) \times 10^{-41}$	$C^2\,m^2\,J^{-1}$	9.7×10^{-10}
a.u. of 1st hyperpolarizability	$e^3a_0^3/E_h^2$	$3.206\,361\,449(71) \times 10^{-53}$	$C^3\,m^3\,J^{-2}$	2.2×10^{-8}
a.u. of 2nd hyperpolarizability	$e^4a_0^4/E_h^3$	$6.235\,380\,54(28) \times 10^{-65}$	$C^4\,m^4\,J^{-3}$	4.4×10^{-8}
a.u. of magnetic flux density	$\hbar/ea_0^2$	$2.350\,517\,464(52) \times 10^{5}$	T	2.2×10^{-8}
a.u. of magnetic dipole moment: $2\mu_B$	$\hbar e/m_e$	$1.854\,801\,936(41) \times 10^{-23}$	$J\,T^{-1}$	2.2×10^{-8}
a.u. of magnetizability	$e^2a_0^2/m_e$	$7.891\,036\,607(13) \times 10^{-29}$	$J\,T^{-2}$	1.6×10^{-9}
a.u. of permittivity: $10^7/c^2$	e^2/a_0E_h	$1.112\,650\,056\ldots \times 10^{-10}$	$F\,m^{-1}$	Exact

of 3.0×10^{-8} obtained using ^{28}Si enriched single crystals. It provides a value of h with the same uncertainty, which is smaller than the 3.6×10^{-8} uncertainty of the value of h from the 2007 NIST watt-balance measurement of $K_J^2R_K$; the latter played the dominant role in determining the 2006 recommended value. The two differ by about 18 parts in 10^8, resulting in a shift of the 2006 recommended value by nearly twice its uncertainty. In the 2006 adjustment inconsistencies among some of the electrical and silicon crystal data (all involving natural silicon) led the Task Group to increase the uncertainties of these data by the multiplicative factor 1.5 to reduce the inconsistencies to an acceptable level. In the 2010 adjustment, inconsistencies among the data that determine h are reduced to an acceptable level by using a multiplicative factor of 2. Consequently the uncertainties of the 2006 and 2010 recommended values of h do not differ significantly.

(iii) The 2006 recommended value of the molar gas constant R was determined by the 1988 NIST speed-of-sound result with a relative standard uncertainty of 1.8×10^{-6}, and to a much lesser extent the 1979 NPL speed-of-sound result with an uncertainty of 8.4×10^{-6} obtained with a rather different type of apparatus. The six new data of potential interest related to R that became available during the four years between the 2006 and 2010 adjustments have uncertainties ranging from 1.2×10^{-6} to 12×10^{-6} and agree with each other as well as with the NIST and NPL values. Further, the self-sensitivity coefficients of four of the six were sufficiently large for them to be included in the 2010 final adjustment, and they are responsible for the small shift in the 2006 recommended value and the reduction of its uncertainty by nearly a factor of 2.

(iv) Other constants in Table 48 whose changes are worth noting are the Rydberg constant R_∞, proton relative atomic mass $A_r(p)$, and {220} natural Si lattice spacing d_{220}. The reduction in uncertainty of R_∞ is due to improvements in the theory of H and D energy levels and the 2010 LKB result for the $1S_{1/2}-3S_{1/2}$ transition frequency in hydrogen with a relative standard uncertainty of 4.4×10^{-12}. For $A_r(p)$, the reduction in uncertainty is due to the 2008 Stockholm University (SMILETRAP) result for the ratio of the cyclotron frequency of the excited hydrogen molecular ion to that of the deuteron, $f_c(H_2^{+*})/f_c(d)$, with a relative uncertainty of 1.7×10^{-10}. The changes in d_{220} arise from the omission of the 1999 PTB result for $h/m_n d_{220}$(W04), the 2004 NMIJ result for d_{220}(NR3), the 2007 INRIM results for d_{220}(W4.2a), and d_{220}(MO*), and the inclusion of the new 2008 INRIM result for d_{220}(MO*) as well as the new 2009 INRIM results for d_{220}(W04) and d_{220}(W4.2a).

15.2. Some implications of the 2010 CODATA recommended values and adjustment for metrology and physics

Conventional electric units. The adoption of the conventional values $K_{J-90} = 483\,597.9$ GHz/V and $R_{K-90} = 25\,812.807\ \Omega$ for the Josephson and von Klitzing constants in 1990 can be viewed as establishing conventional, practical units of voltage and resistance, V_{90} and Ω_{90}, given by $V_{90} = (K_{J-90}/K_J)$ V and $\Omega_{90} = (R_K/R_{K-90})\ \Omega$. Other conventional electric units follow from V_{90} and Ω_{90}, for example, $A_{90} = V_{90}/\Omega_{90}$, $C_{90} = A_{90}$ s, $W_{90} = A_{90}V_{90}$, $F_{90} = C_{90}/V_{90}$, and $H_{90} = \Omega_{90}$ s, which are the conventional, practical units of current, charge, power, capacitance, and inductance, respectively (Taylor and Mohr, 2001). For the relations between K_J and K_{J-90}, and R_K and R_{K-90}, the 2010 adjustment gives

$$K_J = K_{J-90}[1 - 6.3(2.2) \times 10^{-8}], \qquad (287)$$

TABLE 46. The values of some energy equivalents derived from the relations $E = mc^2 = hc/\lambda = h\nu = kT$, and based on the 2010 CODATA adjustment of the values of the constants; 1 eV = (e/C) J, 1 u = $m_u = \frac{1}{12}m(^{12}\mathrm{C}) = 10^{-3}$ kg mol$^{-1}/N_A$, and $E_h = 2R_\infty hc = \alpha^2 m_e c^2$ is the Hartree energy (hartree).

	Relevant unit			
	J	kg	m^{-1}	Hz
J	(1 J) = 1 J	$(1\ \mathrm{J})/c^2 = 1.112\,650\,056\ldots \times 10^{-17}$ kg	$(1\ \mathrm{J})/hc = 5.034\,117\,01(22) \times 10^{24}\ \mathrm{m}^{-1}$	$(1\ \mathrm{J})/h = 1.509\,190\,311(67) \times 10^{33}$ Hz
kg	$(1\ \mathrm{kg})c^2 = 8.987\,551\,787\ldots \times 10^{16}$ J	(1 kg) = 1 kg	$(1\ \mathrm{kg})c/h = 4.524\,438\,73(20) \times 10^{41}\ \mathrm{m}^{-1}$	$(1\ \mathrm{kg})c^2/h = 1.356\,392\,608(60) \times 10^{50}$ Hz
m^{-1}	$(1\ \mathrm{m}^{-1})hc = 1.986\,445\,684(88) \times 10^{-25}$ J	$(1\ \mathrm{m}^{-1})h/c = 2.210\,218\,902(98) \times 10^{-42}$ kg	$(1\ \mathrm{m}^{-1}) = 1\ \mathrm{m}^{-1}$	$(1\ \mathrm{m}^{-1})c = 299\,792\,458$ Hz
Hz	$(1\ \mathrm{Hz})h = 6.626\,069\,57(29) \times 10^{-34}$ J	$(1\ \mathrm{Hz})h/c^2 = 7.372\,496\,68(33) \times 10^{-51}$ kg	$(1\ \mathrm{Hz})/c = 3.335\,640\,951\ldots \times 10^{-9}\ \mathrm{m}^{-1}$	(1 Hz) = 1 Hz
K	$(1\ \mathrm{K})k = 1.380\,6488(13) \times 10^{-23}$ J	$(1\ \mathrm{K})k/c^2 = 1.536\,1790(14) \times 10^{-40}$ kg	$(1\ \mathrm{K})k/hc = 69.503\,476(63)\ \mathrm{m}^{-1}$	$(1\ \mathrm{K})k/h = 2.083\,6618(19) \times 10^{10}$ Hz
eV	$(1\ \mathrm{eV}) = 1.602\,176\,565(35) \times 10^{-19}$ J	$(1\ \mathrm{eV})/c^2 = 1.782\,661\,845(39) \times 10^{-36}$ kg	$(1\ \mathrm{eV})/hc = 8.065\,544\,29(18) \times 10^{5}\ \mathrm{m}^{-1}$	$(1\ \mathrm{eV})/h = 2.417\,989\,348(53) \times 10^{14}$ Hz
u	$(1\ \mathrm{u})c^2 = 1.492\,417\,954(66) \times 10^{-10}$ J	(1 u) = $1.660\,538\,921(73) \times 10^{-27}$ kg	$(1\ \mathrm{u})c/h = 7.513\,006\,6042(53) \times 10^{14}\ \mathrm{m}^{-1}$	$(1\ \mathrm{u})c^2/h = 2.252\,342\,7168(16) \times 10^{23}$ Hz
E_h	$(1\ E_h) = 4.359\,744\,34(19) \times 10^{-18}$ J	$(1\ E_h)/c^2 = 4.850\,869\,79(21) \times 10^{-35}$ kg	$(1\ E_h)/hc = 2.194\,746\,313\,708(11) \times 10^{7}\ \mathrm{m}^{-1}$	$(1\ \mathrm{E_h})/h = 6.579\,683\,920\,729(33) \times 10^{15}$ Hz

TABLE 47. The values of some energy equivalents derived from the relations $E = mc^2 = hc/\lambda = h\nu = kT$, and based on the 2010 CODATA adjustment of the values of the constants; 1 eV = (e/C) J, 1 u = $m_u = \frac{1}{12}m(^{12}\mathrm{C}) = 10^{-3}$ kg mol$^{-1}/N_A$, and $E_h = 2R_\infty hc = \alpha^2 m_e c^2$ is the Hartree energy (hartree).

	Relevant unit			
	K	eV	u	E_h
J	$(1\ \mathrm{J})/k = 7.242\,9716(66) \times 10^{22}$ K	$(1\ \mathrm{J}) = 6.241\,509\,34(14) \times 10^{18}$ eV	$(1\ \mathrm{J})/c^2 = 6.700\,535\,85(30) \times 10^{9}$ u	$(1\ \mathrm{J}) = 2.293\,712\,48(10) \times 10^{17}\ E_h$
kg	$(1\ \mathrm{kg})c^2/k = 6.509\,6582(59) \times 10^{39}$ K	$(1\ \mathrm{kg})c^2 = 5.609\,588\,85(12) \times 10^{35}$ eV	(1 kg) = $6.022\,141\,29(27) \times 10^{26}$ u	$(1\ \mathrm{kg})c^2 = 2.061\,485\,968(91) \times 10^{34}\ E_h$
m^{-1}	$(1\ \mathrm{m}^{-1})hc/k = 1.438\,7770(13) \times 10^{-2}$ K	$(1\ \mathrm{m}^{-1})hc = 1.239\,841\,930(27) \times 10^{-6}$ eV	$(1\ \mathrm{m}^{-1})h/c = 1.331\,025\,051\,20(94) \times 10^{-15}$ u	$(1\ \mathrm{m}^{-1})hc = 4.556\,335\,252\,755(23) \times 10^{-8}\ E_h$
Hz	$(1\ \mathrm{Hz})h/k = 4.799\,2434(44) \times 10^{-11}$ K	$(1\ \mathrm{Hz})h = 4.135\,667\,516(91) \times 10^{-15}$ eV	$(1\ \mathrm{Hz})h/c^2 = 4.439\,821\,6689(31) \times 10^{-24}$ u	$(1\ \mathrm{Hz})h = 1.519\,829\,846\,0045(76) \times 10^{-16}\ E_h$
K	(1 K) = 1 K	$(1\ \mathrm{K})k = 8.617\,3324(78) \times 10^{-5}$ eV	$(1\ \mathrm{K})k/c^2 = 9.251\,0868(84) \times 10^{-14}$ u	$(1\ \mathrm{K})k = 3.166\,8114(29) \times 10^{-6}\ E_h$
eV	$(1\ \mathrm{eV})/k = 1.160\,4519(11) \times 10^{4}$ K	(1 eV) = 1 eV	$(1\ \mathrm{eV})/c^2 = 1.073\,544\,150(24) \times 10^{-9}$ u	$(1\ \mathrm{eV}) = 3.674\,932\,379(81) \times 10^{-2}\ E_h$
u	$(1\ \mathrm{u})c^2/k = 1.080\,954\,08(98) \times 10^{13}$ K	$(1\ \mathrm{u})c^2 = 931.494\,061(21) \times 10^{6}$ eV	(1 u) = 1 u	$(1\ \mathrm{u})c^2 = 3.423\,177\,6845(24) \times 10^{7}\ E_h$
E_h	$(1\ E_h)/k = 3.157\,7504(29) \times 10^{5}$ K	$(1\ E_h) = 27.211\,385\,05(60)$ eV	$(1\ E_h)/c^2 = 2.921\,262\,3246(21) \times 10^{-8}$ u	$(1\ E_h) = 1\ E_h$

TABLE 48. Comparison of the 2010 and 2006 CODATA adjustments of the values of the constants by the comparison of the corresponding recommended values of a representative group of constants. Here D_r is the 2010 value minus the 2006 value divided by the standard uncertainty u of the 2006 value (i.e., D_r is the change in the value of the constant from 2006 to 2010 relative to its 2006 standard uncertainty).

Quantity	2010 rel. std. uncert. u_r	Ratio 2006 u_r to 2010 u_r	D_r
α	3.2×10^{-10}	2.1	6.5
R_K	3.2×10^{-10}	2.1	−6.5
a_0	3.2×10^{-10}	2.1	6.5
λ_C	6.5×10^{-10}	2.1	6.5
r_e	9.7×10^{-10}	2.1	6.5
σ_e	1.9×10^{-9}	2.1	6.5
h	4.4×10^{-8}	1.1	1.9
m_e	4.4×10^{-8}	1.1	1.7
m_h	4.4×10^{-8}	1.1	1.7
m_α	4.4×10^{-8}	1.1	1.7
N_A	4.4×10^{-8}	1.1	−1.7
E_h	4.4×10^{-8}	1.1	1.9
c_1	4.4×10^{-8}	1.1	1.9
e	2.2×10^{-8}	1.1	1.9
K_J	2.2×10^{-8}	1.1	−1.8
F	2.2×10^{-8}	1.1	−1.4
γ'_p	2.5×10^{-8}	1.1	−1.3
μ_B	2.2×10^{-8}	1.1	2.3
μ_N	2.2×10^{-8}	1.1	2.3
μ_e	2.2×10^{-8}	1.1	−2.3
μ_p	2.4×10^{-8}	1.1	2.2
R	9.1×10^{-7}	1.9	−0.7
k	9.1×10^{-7}	1.9	−0.7
V_m	9.1×10^{-7}	1.9	−0.7
c_2	9.1×10^{-7}	1.9	0.7
σ	3.6×10^{-6}	1.9	−0.7
G	1.2×10^{-4}	0.8	−0.7
R_∞	5.0×10^{-12}	1.3	0.2
m_e/m_p	4.1×10^{-10}	1.1	0.0
m_e/m_μ	2.5×10^{-8}	1.0	−0.4
$A_r(e)$	4.0×10^{-10}	1.1	0.1
$A_r(p)$	8.9×10^{-11}	1.2	0.4
$A_r(n)$	4.2×10^{-10}	1.0	0.1
$A_r(d)$	3.8×10^{-11}	1.0	−0.2
$A_r(t)$	8.2×10^{-10}	1.0	0.0
$A_r(h)$	8.3×10^{-10}	1.0	−0.2
$A_r(\alpha)$	1.5×10^{-11}	1.0	0.0
d_{220}	1.6×10^{-8}	1.6	−1.0
g_e	2.6×10^{-13}	2.8	0.5
g_μ	6.3×10^{-10}	1.0	−0.3
μ_p/μ_B	8.1×10^{-9}	1.0	0.0
μ_p/μ_N	8.2×10^{-9}	1.0	0.0
μ_n/μ_N	2.4×10^{-7}	1.0	0.0
μ_d/μ_N	8.4×10^{-9}	1.0	0.0
μ_e/μ_p	8.1×10^{-9}	1.0	0.0
μ_n/μ_p	2.4×10^{-7}	1.0	0.0
μ_d/μ_p	7.7×10^{-9}	1.0	0.0

$$R_K = R_{K-90}[1 + 1.718(32) \times 10^{-8}], \tag{288}$$

which lead to

$$V_{90} = [1 + 6.3(2.2) \times 10^{-8}]\ \text{V}, \tag{289}$$

$$\Omega_{90} = [1 + 1.718(32) \times 10^{-8}]\ \Omega, \tag{290}$$

$$A_{90} = [1 + 4.6(2.2) \times 10^{-8}]\ \text{A}, \tag{291}$$

$$C_{90} = [1 + 4.6(2.2) \times 10^{-8}]\ \text{C}, \tag{292}$$

$$W_{90} = [1 + 10.8(4.4) \times 10^{-8}]\ \text{W}, \tag{293}$$

$$F_{90} = [1 - 1.718(32) \times 10^{-8}]\ \text{F}, \tag{294}$$

$$H_{90} = [1 + 1.718(32) \times 10^{-8}]\ \text{H}. \tag{295}$$

Equations (289) and (290) show that V_{90} exceeds V and Ω_{90} exceeds Ω by the fractional amounts $6.3(2.2) \times 10^{-8}$ and $1.718(32) \times 10^{-8}$, respectively. This means that measured voltages and resistances traceable to the Josephson effect and K_{J-90} and the quantum Hall effect and R_{K-90}, respectively, are too small relative to the SI by these same fractional amounts. However, these differences are well within the 40×10^{-8} uncertainty assigned to V_{90}/V and the 10×10^{-8} uncertainty assigned to Ω_{90}/Ω by the Consultative Committee for Electricity and Magnetism (CCEM) of the CIPM (Quinn, 1989, 2001).

Josephson and quantum Hall effects. Although there is extensive theoretical and experimental evidence for the exactness of the Josephson and quantum-Hall-effect relations $K_J = 2e/h$ and $R_K = h/e^2$, and some of the input data available for the 2010 adjustment provide additional supportive evidence for these expressions, some other data are not supportive. This dichotomy reflects the rather significant inconsistencies among a few key data, particularly the highly accurate IAC enriched silicon XRCD result for N_A, and the comparably accurate NIST watt-balance result for $K_J^2 R_K$, and will only be fully resolved when the inconsistencies are reconciled.

The new SI. Implementation of the new SI requires that the four reference constants h, e, k, and N_A must be known with sufficiently small uncertainties to meet current and future measurement needs. However, of equal if not greater importance, the causes of any inconsistencies among the data that provide their values must be understood. Although the key data that provide the 2010 recommended value of k would appear to be close to meeting both requirements, this is not the case for h, e, and N_A, which are in fact interrelated. We have

$$N_A h = \frac{c A_r(e) M_u \alpha^2}{2R_\infty}, \tag{296}$$

$$e = \left(\frac{2\alpha h}{\mu_0 c}\right)^{1/2}. \tag{297}$$

Since the combined relative standard uncertainty of the 2010 recommended values of the constants on the right-hand side of Eq. (296) is only 7.0×10^{-10}, a measurement of h with

a given relative uncertainty, even as small as 5×10^{-9}, determines N_A with essentially the same relative uncertainty. Further, since the recommended value of α has a relative uncertainty of only 3.2×10^{-10}, based on Eq. (297) the relative uncertainty of e will be half that of h or N_A. For these reasons, the 2010 recommended values of h and N_A have the same 4.4×10^{-8} relative uncertainty, and the uncertainty of the recommended value of e is 2.2×10^{-8}. However, these uncertainties are twice as large as they would have been if there were no disagreement between the watt-balance values of h and the enriched silicon XRCD value of N_A. This disagreement led to an increase in the uncertainties of the relevant data by a factor of 2. More specifically, if the data had been consistent the uncertainties of the recommended values of h and N_A would be 2.2×10^{-8} and 1.1×10^{-8} for e. Because these should be sufficiently small for the new SI to be implemented, the significance of the disagreement and the importance of measurements of h and N_A are apparent.

Proton radius. The proton rms charge radius r_p determined from the Lamb shift in muonic hydrogen disagrees significantly with values determined from H and D transition frequencies as well as from electron-proton scattering experiments. Although the uncertainty of the muonic hydrogen value is significantly smaller than the uncertainties of these other values, its negative impact on the internal consistency of the theoretically predicted and experimentally measured frequencies, as well as on the value of the Rydberg constant, was deemed so severe that the only recourse was not to include it in the final least-squares adjustment on which the 2010 recommended values are based.

Muon magnetic-moment anomaly. Despite extensive new theoretical work, the long-standing significant difference between the theoretically predicted, standard-model value of a_μ and the experimentally determined value remains unresolved. Because the difference is from 3.3 to possibly 4.5 times the standard uncertainty of the difference, depending on the way the all-important hadronic contribution to the theoretical expression for a_μ is evaluated, the theory was not incorporated in the 2010 adjustment. The recommended values of a_μ and those of other constants that depend on it are, therefore, based on experiment.

Electron magnetic-moment anomaly, fine-structure constant, and QED. The most accurate value of the fine-structure constant α currently available from a single experiment has a relative standard uncertainty of 3.7×10^{-10}; it is obtained by equating the QED theoretical expression for the electron magnetic-moment anomaly a_e and the most accurate experimental value of a_e, obtained from measurements on a single electron in a Penning trap. This value of α is in excellent agreement with a competitive experimental value with an uncertainty of 6.6×10^{-10}. Because the latter is obtained from the atom-recoil determination of the quotient $h/m(^{87}\mathrm{Rb})$ using atom-interferometry and is only weakly dependent on QED theory, the agreement provides one of the most significant confirmations of quantum electrodynamics.

Newtonian constant of gravitation. The situation regarding measurements of G continues to be problematic and has become more so in the past four years. Two new results with comparatively small uncertainties have become available for the 2010 adjustment, leading to an increase in the scatter among the now 11 values of G. This has resulted in a 20% increase in the uncertainty of the 2010 recommended value compared to that of its 2006 predecessor. Clearly, there is a continuing problem for the determination of this important, but poorly known, fundamental constant; the uncertainty of the 2010 recommended value is now 120 parts in 10^6.

15.3. Suggestions for future work

For evaluation of the fundamental constants, it is desirable not only to have multiple results with competitive uncertainties for a given quantity, but also to have one or more results obtained by a different method. If the term "redundant" is used to describe such an ideal set of data, there is usually only limited redundancy among the key data available for any given CODATA adjustment.

With this in mind, based on the preceding discussion, our suggestions are as follows:

(i) Resolution of the disagreement between the most accurate watt-balance result for $K_J^2 R_K$ and the XRCD result for N_A. Approaches to solving this problem might include new measurements of $K_J^2 R_K$ using watt balances of different design (or their equivalent) with uncertainties at the 2 to 3 parts in 10^8 level, a thorough review by the researchers involved of their existing measurements of this quantity, tests of the exactness of the relations $K_J = 2e/h$ and $R_K = h/e^2$, independent measurements of the isotopic composition of the enriched silicon crystals and their d_{220} lattice spacing used in the determination of N_A (these are the two principal quantities for which only one measurement exists), and a thorough review by the researchers involved of the many corrections required to obtain N_A from the principal quantities measured.

(ii) Measurements of k (and related quantities such as k/h) with uncertainties at the 1 to 3 parts in 10^6 level using the techniques of dielectric gas thermometry, refractive index gas thermometry, noise thermometry, and Doppler broadening. These methods are very different from acoustic gas thermometry, which is the dominant method used to date.

(iii) Resolution of the discrepancy between the muonic hydrogen inferred value of r_p and the spectroscopic value from H and D transition frequencies. Work underway on frequency measurements in hydrogen as well as the analysis of μ^-p and μ^-d data and possible measurements in μ^-h and $\mu^-\alpha$ should provide additional useful information. Independent evaluations of electron-scattering data to determine r_p are encouraged as well as verification of the theory of H, D, and muonic hydrogen-like energy levels.

(iv) Independent calculation of the eighth- and tenth-order coefficients in the QED expression for a_e, in order to increase confidence in the value of α from a_e.
(v) Resolution of the disagreement between the theoretical expression for a_μ and its experimental value. This discrepancy along with the discrepancy between theory and experiment in muonic hydrogen are two important problems in muon-related physics.
(vi) Determinations of G with an uncertainty of 1 part in 10^5 using new and innovative approaches that might resolve the disagreements among the measurements made within the past three decades.

List of Symbols and Abbreviations

AMDC	Atomic Mass Data Center, Centre de Spectrométrie Nucléaire et de Spectrométrie de Masse, Orsay, France
$A_r(X)$	Relative atomic mass of X: $A_r(X) = m(X)/m_u$
A_{90}	Conventional unit of electric current: $A_{90} = V_{90}/\Omega_{90}$
Å*	Ångström star: $\lambda(\mathrm{WK}\alpha_1) = 0.209\ 010\ 0$ Å*
a_e	Electron magnetic-moment anomaly: $a_e = (\lvert g_e\rvert - 2)/2$
a_μ	Muon magnetic-moment anomaly: $a_\mu = (\lvert g_\mu\rvert - 2)/2$
BIPM	International Bureau of Weights and Measures, Sèvres, France
BNL	Brookhaven National Laboratory, Upton, New York, USA
CERN	European Organization for Nuclear Research, Geneva, Switzerland
CIPM	International Committee for Weights and Measures
CODATA	Committee on Data for Science and Technology of the International Council for Science
CPT	Combined charge conjugation, parity inversion, and time reversal
c	Speed of light in vacuum
d	Deuteron (nucleus of deuterium D, or ^{2}H)
d_{220}	{220} lattice spacing of an ideal crystal of naturally occurring silicon
$d_{220}(X)$	{220} lattice spacing of crystal X of naturally occurring silicon
E_b	Binding energy
e	Symbol for either member of the electron-positron pair; when necessary, e^- or e^+ is used to indicate the electron or positron
e	Elementary charge: absolute value of the charge of the electron
F	Faraday constant: $F = N_A e$
FSU	Florida State University, Tallahassee, Florida, USA
FSUJ	Friedrich-Schiller University, Jena, Germany
$\mathcal{F}_{90}$	$\mathcal{F}_{90} = (F/A_{90})$ A
G	Newtonian constant of gravitation
g	Local acceleration of free fall
g_d	Deuteron g-factor: $g_d = \mu_d/\mu_N$
g_e	Electron g-factor: $g_e = 2\mu_e/\mu_B$
g_p	Proton g-factor: $g_p = 2\mu_p/\mu_N$
g'_p	Shielded proton g-factor: $g'_p = 2\mu'_p/\mu_N$
g_t	Triton g-factor: $g_t = 2\mu_t/\mu_N$
$g_X(Y)$	g-factor of particle X in the ground (1S) state of hydrogenic atom Y
g_μ	Muon g-factor: $g_\mu = 2\mu_\mu/(e\hbar/2m_\mu)$
GSI	Gesellschaft für Schweironenforschung, Darmstadt, Germany
HD	HD molecule (bound state of hydrogen and deuterium atoms)
HT	HT molecule (bound state of hydrogen and tritium atoms)
h	Helion (nucleus of ^{3}He)
h	Planck constant; $\hbar = h/2\pi$
HarvU	Harvard University, Cambridge, Massachusetts, USA
IAC	International Avogadro Coordination
ILL	Institut Max von Laue-Paul Langevin, Grenoble, France
INRIM	Istituto Nazionale di Ricerca Metrologica, Torino, Italy
IRMM	Institute for Reference Materials and Measurements, Geel, Belgium
JILA	Joint institute of University of Colorado and NIST, Boulder, Colorado, USA
JINR	Joint institute for Nuclear Research, Dubna, Russian Federation
KRISS	Korea Research Institute of Standards and Science, Taedok Science Town, Republic of Korea
KR/VN	KRISS-VNIIM collaboration
K_J	Josephson constant: $K_J = 2e/h$
K_{J-90}	Conventional value of the Josephson constant K_J: $K_{J-90} = 483\,597.9$ GHz V^{-1}
k	Boltzmann constant: $k = R/N_A$
LAMPF	Clinton P. Anderson Meson Physics Facility at Los Alamos National Laboratory, Los Alamos, New Mexico, USA
LKB	Laboratoire Kastler-Brossel, Paris, France
LK/SY	LKB and SYRTE collaboration
LNE	Laboratoire national de métrologie et d'essais, Trappes, France
METAS	Federal Office of Metrology, Bern-Wabern, Switzerland
MIT	Massachusetts Institute of Technology, Cambridge, Massachusetts, USA
MPQ	Max-Planck-Institut für Quantenoptik, Garching, Germany
$M(X)$	Molar mass of X: $M(X) = A_r(X)M_u$
Mu	Muonium (μ^+e^- atom)
M_u	Molar mass constant: $M_u = 10^{-3}$ kg mol^{-1}
m_u	Unified atomic mass constant: $m_u = m(^{12}\mathrm{C})/12$

m_X, $m(X)$	Mass of X (for the electron e, proton p, and other elementary particles, the first symbol is used, i.e., m_e, m_p, etc.)
N_A	Avogadro constant
NIM	National Institute of Metrology, Beijing, People's Republic of China
NIST	National Institute of Standards and Technology, Gaithersburg, Maryland and Boulder, Colorado, USA
NMI	National Metrology Institute, Lindfield, Australia
NMIJ	National Metrology Institute of Japan, Tsukuba, Japan
NPL	National Physical Laboratory, Teddington, UK
n	Neutron
PTB	Physikalisch-Technische Bundesanstalt, Braunschweig and Berlin, Germany
p	Proton
$\bar{p}^A He^+$	Antiprotonic helium ($^AHe^+ + \bar{p}$ atom, $A = 3$ or 4)
QED	Quantum electrodynamics
$p(\chi^2\|\nu)$	Probability that an observed value of chi square for ν degrees of freedom would exceed χ^2
R	Molar gas constant
$\bar{R}$	Ratio of muon anomaly difference frequency to free proton NMR frequency
R_B	Birge ratio: $R_B = (\chi^2/\nu)^{1/2}$
r_d	Bound-state rms charge radius of the deuteron
R_K	von Klitzing constant: $R_K = h/e^2$
R_{K-90}	Conventional value of the von Klitzing constant R_K: $R_{K-90} = 25\,812.807\ \Omega$
r_p	Bound-state rms charge radius of the proton
R_∞	Rydberg constant: $R_\infty = m_e c\alpha^2/2h$
$r(x_i, x_j)$	Correlation coefficient of estimated values x_i and x_j: $r(x_i, x_j) = u(x_i, x_j)/[u(x_i)u(x_j)]$
S_c	Self-sensitivity coefficient
SI	Système international d'unités (International System of Units)
StanfU	Stanford University, Stanford, California, USA
SU	Stockholm University, Stockholm, Sweden
StPtrsb	St. Petersburg, Russian Federation
SYRTE	Systèmes de référence Temps Espace, Paris, France
T	Thermodynamic temperature
Type A	Uncertainty evaluation by the statistical analysis of series of observations
Type B	Uncertainty evaluation by means other than the statistical analysis of series of observations
t_{90}	Celsius temperature on the International Temperature Scale of 1990 (ITS-90)
t	Triton (nucleus of tritium T, or ^3H)
USus	University of Sussex, Sussex, UK
UWash	University of Washington, Seattle, Washington, USA
u	Unified atomic mass unit (also called the dalton, Da): $1\ u = m_u = m(^{12}C)/12$
u_{diff}	Standard uncertainty of difference between two values (σ sometimes used in place of u_{diff})
$u(x_i)$	Standard uncertainty (i.e., estimated standard deviation) of an estimated value x_i of a quantity X_i (also simply u)
$u_r(x_i)$	Relative standard uncertainty of an estimated value x_i of a quantity X_i: $u_r(x_i) = u(x_i)/\|x_i\|$, $x_i \neq 0$ (also simply u_r)
$u(x_i, x_j)$	Covariance of estimated values x_i and x_j
$u_r(x_i, x_j)$	Relative covariance of estimated values x_i and x_j : $u_r(x_i, x_j) = u(x_i, x_j)/(x_i x_j)$
$V_m(Si)$	Molar volume of naturally occurring silicon
VNIIM	D. I. Mendeleyev All-Russian Research Institute for Metrology, St. Petersburg, Russian Federation
V_{90}	Conventional unit of voltage based on the Josephson effect and K_{J-90}: $V_{90} = (K_{J-90}/K_J)\ V$
W_{90}	Conventional unit of power: $W_{90} = V_{90}^2/\Omega_{90}$
XRCD	X ray crystal density method for determining N_A
XROI	Combined x-ray and optical interferometer
xu($CuK\alpha_1$)	Cu x unit: $\lambda(CuK\alpha_1) = 1537.400\ xu(CuK\alpha_1)$
xu($MoK\alpha_1$)	Mo x unit: $\lambda(MoK\alpha_1) = 707.831\ xu(MoK\alpha_1)$
$x(X)$	Amount-of-substance fraction of X
YaleU	Yale University, New Haven, Connecticut, USA
α	Fine-structure constant: $\alpha = e^2/4\pi\epsilon_0\hbar c \approx 1/137$
α	Alpha particle (nucleus of ^4He)
$\Gamma'_{X-90}(lo)$	$\Gamma'_{X-90}(lo) = (\gamma'_X A_{90})\ A^{-1}$, X = p or h
$\Gamma'_{p-90}(hi)$	$\Gamma'_{p-90}(hi) = (\gamma'_p/A_{90})\ A$
γ_p	Proton gyromagnetic ratio: $\gamma_p = 2\mu_p/\hbar$
γ'_p	Shielded proton gyromagnetic ratio: $\gamma'_p = 2\mu'_p/\hbar$
γ'_h	Shielded helion gyromagnetic ratio: $\gamma'_h = 2\|\mu'_h\|/\hbar$
$\Delta\nu_{Mu}$	Muonium ground-state hyperfine splitting
δ_e	Additive correction to the theoretical expression for the electron magnetic-moment anomaly a_e
δ_{Mu}	Additive correction to the theoretical expression for the ground-state hyperfine splitting of muonium $\Delta\nu_{Mu}$
$\delta_{\bar{p}He}$	Additive correction to the theoretical expression for a particular transition frequency of antiprotonic helium
$\delta_X(nL_j)$	Additive correction to the theoretical expression for an energy level of either hydrogen H or deuterium D with quantum numbers n, L, and j
ϵ_0	Electric constant: $\epsilon_0 = 1/\mu_0 c^2$
$\doteq$	Symbol used to relate an input datum to its observational equation

$\lambda(X\mathrm{K}\alpha_1)$	Wavelength of $\mathrm{K}\alpha_1$ x-ray line of element X
λ_{meas}	Measured wavelength of the 2.2 MeV capture γ ray emitted in the reaction $\mathrm{n} + \mathrm{p} \rightarrow \mathrm{d} + \gamma$
μ	Symbol for either member of the muon-antimuon pair; when necessary, μ^- or μ^+ is used to indicate the negative muon or positive muon
μ_{B}	Bohr magneton: $\mu_{\mathrm{B}} = e\hbar/2m_{\mathrm{e}}$
μ_{N}	Nuclear magneton: $\mu_{\mathrm{N}} = e\hbar/2m_{\mathrm{p}}$
$\mu_X(Y)$	Magnetic moment of particle X in atom or molecule Y
μ_0	Magnetic constant: $\mu_0 = 4\pi \times 10^{-7}\ \mathrm{N/A^2}$
μ_X, μ'_X	Magnetic moment, or shielded magnetic moment, of particle X
ν	Degrees of freedom of a particular adjustment
$\nu(f_{\mathrm{p}})$	Difference between muonium hyperfine splitting Zeeman transition frequencies ν_{34} and ν_{12} at a magnetic flux density B corresponding to the free proton NMR frequency f_{p}
σ	Stefan-Boltzmann constant: $\sigma = 2\pi^5 k^4/15h^3c^2$
τ	Symbol for either member of the tau-antitau pair; when necessary, τ^- or τ^+ is used to indicate the negative tau or positive tau
χ^2	The statistic chi square
Ω_{90}	Conventional unit of resistance based on the quantum Hall effect and $R_{\mathrm{K-90}}$: $\Omega_{90} = (R_{\mathrm{K}}/R_{\mathrm{K-90}})\ \Omega$

Acknowledgments

We gratefully acknowledge the help of our many colleagues throughout the world who provided the CODATA Task Group on Fundamental Constants with results prior to formal publication and for promptly and patiently answering our many questions about their work. We wish to thank Barry M. Wood, the current chair of the Task Group, as well as our fellow Task Group members, for their invaluable guidance and suggestions during the course of the 2010 adjustment effort.

16. References

C. Adamuscin, S. Dubnicka, and A. Z. Dubnickova, Prog. Part. Nucl. Phys. **67**, 479 (2012).
J. Alnis, A. Matveev, N. Kolachevsky, T. Udem, and T. W. Hänsch, Phys. Rev. A **77**, 053809 (2008).
AMDC, amdc.in2p3.fr/masstables/Ame2003/a0p4sqza.cov03 (2003).
AMDC, amdc.in2p3.fr (2006).
B. Andreas *et al.*, Metrologia **48**, S1 (2011a).
B. Andreas *et al.*, Phys. Rev. Lett. **106**, 030801 (2011b).
I. Angeli, At. Data Nucl. Data Tables **87**, 185 (2004).
T. Aoyama, M. Hayakawa, T. Kinoshita, and M. Nio, Phys. Rev. Lett. **99**, 110406 (2007).
T. Aoyama, M. Hayakawa, T. Kinoshita, and M. Nio, Phys. Rev. D **77**, 053012 (2008).
T. Aoyama, M. Hayakawa, T. Kinoshita, and M. Nio, Phys. Rev. D **84**, 053003 (2011).
T. R. Armstrong and M. P. Fitzgerald, Phys. Rev. Lett. **91**, 201101 (2003).
O. Arnoult, F. Nez, L. Julien, and F. Biraben, Eur. Phys. J. D **60**, 243 (2010).
J. Arrington, Phys. Rev. Lett. **107**, 119101 (2011).
J. Arrington, W. Melnitchouk, and J. A. Tjon, Phys. Rev. C **76**, 035205 (2007).
G. Audi, A. H. Wapstra, and C. Thibault, Nucl. Phys. A **729**, 337 (2003).
C. H. Bagley, Ph.D. thesis (University of Colorado, Boulder, CO, 1996).
C. H. Bagley (private communication) (2010).
C. H. Bagley and G. G. Luther, Phys. Rev. Lett. **78**, 3047 (1997).
P. A. Baikov, and D. J. Broadhurst, in *New Computing Techniques in Physics Research IV. International Workshop on Software Engineering, Artificial Intelligence, and Expert Systems for High Energy and Nuclear Physics*, edited by B. Denby and D. Perret-Gallix (World Scientific, Singapore, 1995), pp. 167–172.
W. A. Barker and F. N. Glover, Phys. Rev. **99**, 317 (1955).
P. Becker (private communication) (2011).
P. Becker, K. Dorenwendt, G. Ebeling, R. Lauer, W. Lucas, R. Probst, H.-J. Rademacher, G. Reim, P. Seyfried, and H. Siegert, Phys. Rev. Lett. **46**, 1540 (1981).
W. Beer, A. L. Eichenberger, B. Jeanneret, B. Jeckelmann, A. R. Pourzand, P. Richard, and J. P. Schwarz, IEEE Trans. Instrum. Meas. **52**, 626 (2003).
W. Beer, A. L. Eichenberger, B. Jeanneret, B. Jeckelmann, P. Richard, H. Schneiter, A. R. Pourzand, A. Courteville, and R. Dändliker, IEEE Trans. Instrum. Meas. **50**, 583 (2001).
W. Beer, B. Jeanneret, B. Jeckelmann, P. Richard, A. Courteville, Y. Salvadé, and R. Dändliker, IEEE Trans. Instrum. Meas. **48**, 192 (1999).
T. Beier, Phys. Rep. **339**, 79 (2000).
T. Beier, H. Häffner, N. Hermanspahn, S. G. Karshenboim, H.-J. Kluge, W. Quint, S. Stahl, J. Verdú, and G. Werth, Phys. Rev. Lett. **88**, 011603, (2001).
T. Beier, I. Lindgren, H. Persson, S. Salomonson, P. Sunnergren, H. Häffner, and N. Hermanspahn, Phys. Rev. A **62**, 032510 (2000).
M. Benayoun, P. David, L. DelBuono, and F. Jegerlehner, Eur. Phys. J. C **72**, 1848 (2012).
G. W. Bennett *et al.*, Phys. Rev. D **73**, 072003 (2006).
S. P. Benz, A. Pollarolo, J. Qu, H. Rogalla, C. Urano, W. L. Tew, P. D. Dresselhaus, and D. R. White, Metrologia **48**, 142 (2011).
I. Bergström, C. Carlberg, T. Fritioff, G. Douysset, J. Schönfelder, and R. Schuch, Nucl. Instrum. Methods Phys. Res., Sect. A **487**, 618 (2002).
D. J. Berkeland, E. A. Hinds, and M. G. Boshier, Phys. Rev. Lett. **75**, 2470 (1995).
J. Bernauer (private communication) (2010).
J. C. Bernauer *et al.*, Phys. Rev. Lett. **105**, 242001 (2010).
J. C. Bernauer *et al.*, Phys. Rev. Lett. **107**, 119102 (2011).
H. Bettin (private communication) (2011).
BIPM, *International System of Units (SI)* (Bureau international des poids et mesures, Sèvres, France, 2006), 8th ed.
F. Biraben (private communication) (2011).
J. S. Borbely, M. C. George, L. D. Lombardi, M. Weel, D. W. Fitzakerley, and E. A. Hessels, Phys. Rev. A **79**, 060503 (2009).
E. Borie, Ann. Phys. (N.Y.) **327**, 733 (2012).
L. A. Borisoglebsky and E. E. Trofimenko, Phys. Lett. **81B**, 175 (1979).
R. Bouchendira, P. Cladé, S. Guellati-Khélifa, F. Nez, and F. Biraben, Phys. Rev. Lett. **106**, 080801 (2011).
S. Bourzeix, B. de Beauvoir, F. Nez, M. D. Plimmer, F. de Tomasi, L. Julien, F. Biraben, and D. N. Stacey, Phys. Rev. Lett. **76**, 384 (1996).
V. E. Bower and R. S. Davis, J. Res. Natl. Bur. Stand. **85**, 175 (1980).
G. Breit, Nature (London) **122**, 649 (1928).
G. Breit and I. I. Rabi, Phys. Rev. **38**, 2082 (1931).
M. Cadoret, E. de Mirandes, P. Cladé, S. Guellati-Khélifa, C. Schwob, F. Nez, L. Julien, and F. Biraben, Phys. Rev. Lett. **101**, 230801 (2008a).
M. Cadoret, E. De Mirandes, P. Cladé, F. Nez, L. Julien, F. Biraben, and S. Guellati-Khélifa, Eur. Phys. J. Special Topics **172**, 121 (2009).
M. Cadoret, E. d. Mirandes, P. Cladé, S. Guellati-Khélifa, C. Schwob, F. Nez, L. Julien, and F. Biraben, Eur. Phys. J. Special Topics **163**, 101 (2008b).
M. Cadoret, E. d. Mirandés, P. Cladé, S. Guellati-Khélifa, F. Nez, and F. Biraben, C.R. Physique **12**, 379 (2011).
B. Camarota, H. Scherer, M. W. Keller, S. V. Lotkhov, G.-D. Willenberg, and F. J. Ahlers, Metrologia **49**, 8 (2012).

J. Castillega, D. Livingston, A. Sanders, and D. Shiner, Phys. Rev. Lett. **84**, 4321 (2000).
G. Cavagnero, H. Fujimoto, G. Mana, E. Massa, K. Nakayama, and G. Zosi, Metrologia **41**, 56 (2004);**41**, 445(E) (2004).
T. Chiba, Prog. Theor. Phys. **126**, 993 (2011).
P. Cladé, E. de Mirandes, M. Cadoret, S. Guellati-Khélifa, C. Schwob, F. Nez, L. Julien, and F. Biraben, Phys. Rev. A **74**, 052109 (2006).
P. Cladé, T. Plisson, S. Guellati-Khélifa, F. Nez, and F. Biraben, Eur. Phys. J. D **59**, 349 (2010).
F. E. Close and H. Osborn, Phys. Lett. **34B**, 400 (1971).
W. K. Clothier, G. J. Sloggett, H. Bairnsfather, M. F. Currey, and D. J. Benjamin, Metrologia **26**, 9 (1989).
E. R. Cohen and B. N. Taylor, J. Phys. Chem. Ref. Data **2**, 663 (1973).
E. R. Cohen and B. N. Taylor, Rev. Mod. Phys. **59**, 1121 (1987).
A. R. Colclough, T. J. Quinn, and T. R. D. Chandler, Proc. R. Soc. A **368**, 125 (1979).
A. Czarnecki, U. D. Jentschura, and K. Pachucki, Phys. Rev. Lett. **95**, 180404 (2005).
A. Czarnecki, B. Krause, and W. J. Marciano, Phys. Rev. Lett. **76**, 3267 (1996).
A. Czarnecki, W. J. Marciano, and A. Vainshtein, Phys. Rev. D **67**, 073006 (2003); **73**, 119901(E) (2006).
A. Czarnecki and K. Melnikov, Phys. Rev. Lett. **87**, 013001 (2001).
A. Czarnecki, K. Melnikov, and A. Yelkhovsky, Phys. Rev. A **63**, 012509 (2000).
M. Davier and A. Höcker, Phys. Lett. B **435**, 427 (1998).
M. Davier, A. Hoecker, B. Malaescu, and Z. Zhang, Eur. Phys. J. C **71**, 1515 (2011).
B. de Beauvoir, F. Nez, L. Julien, B. Cagnac, F. Biraben, D. Touahri, L. Hilico, O. Acef, A. Clairon, and J. J. Zondy, Phys. Rev. Lett. **78**, 440 (1997).
M. de Podesta (private communication) (2011).
M. de Podesta, E. F. May, J. B. Mehl, L. Pitre, R. M. Gavioso, G. Benedetto, P. A. Giuliano Albo, D. Truong, and D. Flack, Metrologia **47**, 588, (2010).
M. Dowling, J. Mondéjar, J. H. Piclum, and A. Czarnecki, Phys. Rev. A **81**, 022509 (2010).
G. W. F. Drake and R. A. Swainson, Phys. Rev. A **41**, 1243 (1990).
A. Eichenberger, H. Baumann, B. Jeanneret, B. Jeckelmann, P. Richard, and W. Beer, Metrologia **48**, 133 (2011).
A. Eichenberger, G. Genevès, and P. Gournay, Eur. Phys. J. Special Topics **172**, 363 (2009).
S. I. Eidelman, S. G. Karshenboim, and V. A. Shelyuto, Can. J. Phys. **80**, 1297 (2002).
M. I. Eides, Phys. Rev. A **53**, 2953 (1996).
M. I. Eides (private communication) (2002).
M. I. Eides and H. Grotch, Phys. Rev. A **52**, 3360 (1995a).
M. I. Eides and H. Grotch, Phys. Rev. A **52**, 1757 (1995b).
M. I. Eides and H. Grotch, Ann. Phys. (N.Y.) **260**, 191 (1997a).
M. I. Eides and H. Grotch, Phys. Rev. A **56**, R2507 (1997b).
M. I. Eides and H. Grotch, Phys. Rev. A **55**, 3351 (1997c).
M. I. Eides, H. Grotch, and V. A. Shelyuto, Phys. Rev. A **55**, 2447 (1997).
M. I. Eides, H. Grotch, and V. A. Shelyuto, Phys. Rev. A **63**, 052509 (2001a).
M. I. Eides, H. Grotch, and V. A. Shelyuto, Phys. Rep. **342**, 63 (2001b).
M. I. Eides, H. Grotch, and V. A. Shelyuto, *Theory of Light Hydrogenic Bound States*, Springer Tracts in Modern Physics (Springer, Berlin, 2007), p. 222.
M. I. Eides and T. J. S. Martin, Phys. Rev. Lett. **105**, 100402 (2010).
M. I. Eides and T. J. S. Martin, Can. J. Phys. **89**, 117 (2011).
M. I. Eides and V. A. Shelyuto, Phys. Rev. A **52**, 954 (1995).
M. I. Eides and V. A. Shelyuto, Phys. Rev. A **70**, 022506 (2004).
M. I. Eides and V. A. Shelyuto, Can. J. Phys. **85**, 509 (2007).
M. I. Eides and V. A. Shelyuto, Phys. Rev. D **80**, 053008 (2009a).
M. I. Eides and V. A. Shelyuto, Phys. Rev. Lett. **103**, 133003 (2009b).
M. I. Eides and V. A. Shelyuto, J. Exp. Theor. Phys. **110**, 17 (2010).
A. S. Elkhovskiĭ, Zh. Eksp. Teor. Fiz. **110**, 431 [JETP **83**, 230 (1996)].
G. W. Erickson, J. Phys. Chem. Ref. Data **6**, 831 (1977).
G. W. Erickson and D. R. Yennie, Ann. Phys. (N.Y.) **35**, 271, (1965).
D. L. Farnham, R. S. Van Dyck, Jr., and P. B. Schwinberg, Phys. Rev. Lett. **75**, 3598 (1995).
R. Faustov, Phys. Lett. **33B**, 422 (1970).
B. Fellmuth, J. Fischer, C. Gaiser, O. Jusko, T. Priruenrom, W. Sabuga, and T. Zandt, Metrologia **48**, 382 (2011).
N. Feltin and F. Piquemal, Eur. Phys. J. Special Topics **172**, 267, (2009).
N. Feltin, B. Steck, L. DeVoille, S. Sassine, B. Chenaud, W. Poirier, F. Schopfer, G. Sprengler, S. Djordjevic, O. Seron, and F. Piquemal, Revue Française de Métrologie **2011-1**, 3 (2011).
L. Ferroglio, G. Mana, and E. Massa, Opt. Express **16**, 16877 (2008).
M. Fischer *et al.*, Phys. Rev. Lett. **92**, 230802 (2004).
J. L. Flowers, B. W. Petley, and M. G. Richards, Metrologia **30**, 75 (1993).
J. L. Friar, Z. Phys. A **292**, 1 (1979a); **303**, 84(E) (1981).
J. L. Friar, Ann. Phys. (N.Y.) **122**, 151 (1979b).
J. L. Friar, J. Martorell, and D. W. L. Sprung, Phys. Rev. A **59**, 4061 (1999).
J. L. Friar and G. L. Payne, Phys. Rev. C **56**, 619 (1997a).
J. L. Friar and G. L. Payne, Phys. Rev. A **56**, 5173 (1997b).
K. Fujii (private communication) (2010).
K. Fujii *et al.*, IEEE Trans. Instrum. Meas. **54**, 854 (2005).
T. Funck and V. Sienknecht, IEEE Trans. Instrum. Meas. **40**, 158 (1991).
G. Gabrielse, Int. J. Mass Spectrom. **251**, 273 (2006).
G. Gabrielse, in *Lepton Dipole Moments*, Advanced Series on Directions in High Energy Physics, edited by B. L. Roberts and W. J. Marciano (World Scientific, Singapore, 2010), Vol. 20, Chap. 5, pp. 157–194.
C. Gaiser and B. Fellmuth, Metrologia **49**, L4 (2012).
R. Gavioso (private communication) (2011).
R. Gavioso, M. de Podesta, and L. Pitre, (2011) (private communication).
R. M. Gavioso, G. Benedetto, P. A. Giuliano Albo, D. Madonna Ripa, A. Merlone, C. Guianvarc'h, F. Moro, and R. Cuccaro, Metrologia **47**, 387 (2010).
M. C. George, L. D. Lombardi, and E. A. Hessels, Phys. Rev. Lett. **87**, 173002 (2001).
S. George, K. Blaum, F. Herfurth, A. Herlert, M. Kretzschmar, S. Nagy, S. Schwarz, L. Schweikhard, and C. Yazidjian, Int. J. Mass Spectrom. **264**, 110 (2007).
G. Giusfredi, P. C. Pastor, P. D. Natale, D. Mazzotti, C. D. Mauro, L. Fallani, G. Hagel, V. Krachmalnicoff, and M. Inguscio, Can. J. Phys. **83**, 301 (2005).
C. Glattli, C.R. Physique **12**, 319 (2011).
D. A. Glazov and V. M. Shabaev, Phys. Lett. A **297**, 408 (2002).
M. O. Goerbig, C. R. Physique **12**, 369 (2011).
E. A. Golosov, A. S. Elkhovskiĭ, A. I. Mil'shteĭn, and I. B. Khriplovich, Zh. Eksp. Teor. Fiz. **107**, 393 [JETP **80**, 208 (1995)].
G. L. Greene, N. F. Ramsey, W. Mampe, J. M. Pendlebury, K. Smith, W. B. Dress, P. D. Miller, and P. Perrin, Phys. Rev. D **20**, 2139 (1979).
G. L. Greene, N. F. Ramsey, W. Mampe, J. M. Pendlebury, K. Smith, W. D. Dress, P. D. Miller, and P. Perrin, Phys. Lett. **71B**, 297 (1977).
H. Grotch, Phys. Rev. Lett. **24**, 39 (1970).
J. H. Gundlach and S. M. Merkowitz, Phys. Rev. Lett. **85**, 2869 (2000).
J. H. Gundlach and S. M. Merkowitz, (2002) (private communication).
H. Häffner, T. Beier, S. Djekić, N. Hermanspahn, H.-J. Kluge, W. Quint, S. Stahl, J. Verdú, T. Valenzuela, and G. Werth, Eur. Phys. J. D **22**, 163 (2003).
K. Hagiwara, R. Liao, A. D. Martin, D. Nomura, and T. Teubner, J. Phys. G **38**, 085003 (2011).
E. W. Hagley and F. M. Pipkin, Phys. Rev. Lett. **72**, 1172 (1994).
D. Hanneke, S. Fogwell, and G. Gabrielse, Phys. Rev. Lett. **100**, 120801 (2008).
D. Hanneke, S. Fogwell Hoogerheide, and G. Gabrielse, Phys. Rev. A **83**, 052122 (2011).
A. Hartland, R. G. Jones, and D. J. Legg, Document No. CCE/88-9 submitted to the 18th meeting of the Comité Consultatif d'Électricité of the CIPM, (1988).
J. Härtwig, S. Grosswig, P. Becker, and D. Windisch, Phys. Status Solidi A **125**, 79 (1991).
R. S. Hayano, Proc. Jpn. Acad., Ser. B **86**, 1 (2010).
M. Hori (private communication) (2006).
M. Hori (private communication) (2010).
M. Hori, Can. J. Phys. **89**, 1 (2011).
M. Hori and V. I. Korobov, Phys. Rev. A **81**, 062508 (2010).
M. Hori, A. Sótér, D. Barna, A. Dax, R. Hayano, S. Friedreich, B. Juhász, T. Pask, E. Widmann, D. Horváth, L. Venturelli, and N. Zurlo, Nature (London) **475**, 484 (2011).

M. Hori *et al.*, Phys. Rev. Lett. **96**, 243401 (2006).
Z.-K. Hu, J.-Q. Guo, and J. Luo, Phys. Rev. D **71**, 127505 (2005).
A. Huber, T. Udem, B. Gross, J. Reichert, M. Kourogi, K. Pachucki, M. Weitz, and T. W. Hänsch, Phys. Rev. Lett. **80**, 468 (1998).
D. J. Hylton, Phys. Rev. A **32**, 1303 (1985).
V. G. Ivanov, S. G. Karshenboim, and R. N. Lee, Phys. Rev. A **79**, 012512 (2009).
T. J. B. M. Janssen, N. E. Fletcher, R. Goebel, J. M. Willaims, A. Tzalenchuk, R. Yakimova, S. Kubatkin, S. Lara-Avila, and V. I. Falko, New J. Phys. **13**, 093026 (2011).
T. J. B. M. Janssen, J. M. Williams, N. E. Fletcher, R. Goebel, A. Tzalenchuk, R. Yakimova, S. Lara-Avila, S. Kubatkin, and V. I. Fal'ko, Metrologia **49**, 294 (2012).
A. Jeffery, R. E. Elmquist, J. Q. Shields, L. H. Lee, M. E. Cage, S. H. Shields, and R. F. Dziuba, Metrologia **35**, 83 (1998).
A.-M. Jeffery, R. E. Elmquist, L. H. Lee, J. Q. Shields, and R. F. Dziuba, IEEE Trans. Instrum. Meas. **46**, 264 (1997).
F. Jegerlehner and A. Nyffeler, Phys. Rep. **477**, 1 (2009).
F. Jegerlehner and R. Szafron, Eur. Phys. J. C **71**, 1632 (2011).
U. Jentschura and K. Pachucki, Phys. Rev. A **54**, 1853 (1996).
U. D. Jentschura, J. Phys. A **36**, L229 (2003).
U. D. Jentschura, Phys. Rev. A **70**, 052108 (2004).
U. D. Jentschura, Phys. Rev. A **74**, 062517 (2006).
U. D. Jentschura, Phys. Rev. A **79**, 044501 (2009).
U. D. Jentschura (private communication) (2011a).
U. D. Jentschura, Ann. Phys. (N.Y.) **326**, 500 (2011b).
U. D. Jentschura, Ann. Phys. (N.Y.) **326**, 516 (2011c).
U. D. Jentschura, A. Czarnecki, and K. Pachucki, Phys. Rev. A **72**, 062102 (2005).
U. D. Jentschura, A. Czarnecki, K. Pachucki, and V. A. Yerokhin, Int. J. Mass Spectrom. **251**, 102 (2006).
U. D. Jentschura, J. Evers, C. H. Keitel, and K. Pachucki, New J. Phys. **4**, 49 (2002).
U. D. Jentschura, A. Matveev, C. G. Parthey, J. Alnis, R. Pohl, T. Udem, N. Kolachevsky, and T. W. Hänsch, Phys. Rev. A **83**, 042505 (2011).
U. D. Jentschura and P. J. Mohr, Phys. Rev. A **69**, 064103 (2004).
U. D. Jentschura and P. J. Mohr, Phys. Rev. A **72**, 014103 (2005).
U. D. Jentschura, P. J. Mohr, and G. Soff, Phys. Rev. Lett. **82**, 53 (1999).
U. D. Jentschura, P. J. Mohr, and G. Soff, Phys. Rev. A **63**, 042512 (2001).
U. D. Jentschura and I. Nándori, Phys. Rev. A **66**, 022114 (2002).
U. D. Jentschura, M. Puchalski, and P. J. Mohr, Phys. Rev. A **84**, 064102 (2011).
U. D. Jentschura and V. A. Yerokhin, Phys. Rev. A **81**, 012503 (2010).
U. D. Jentschura, S. Kotochigova, E. O. Le Bigot, and P. J. Mohr, (2005), NIST Technical Note 1469, physics.nist.gov/hdel.
Z. Jiang *et al.*, Metrologia **48**, 246 (2011).
O. V. Karagioz, and V. P. Izmailov, Izmeritel'naya Tekhnika **39**, 3 [Meas. Tech. **39**, 979 (1996)].
S. G. Karshenboim, J. Phys. B **28**, L77 (1995).
S. G. Karshenboim, J. Phys. B **29**, L29 (1996).
S. G. Karshenboim, Z. Phys. D **39**, 109 (1997).
S. G. Karshenboim, Phys. Lett. A **266**, 380 (2000).
S. G. Karshenboim and V. G. Ivanov, Can. J. Phys. **80**, 1305 (2002).
S. G. Karshenboim, V. G. Ivanov, Y. I. Neronov, B. P. Nikolaev, and Y. N. Tolparov, Can. J. Phys. **83**, 405 (2005).
S. G. Karshenboim, V. G. Ivanov, and V. M. Shabaev, Can. J. Phys. **79**, 81 (2001a).
S. G. Karshenboim, V. G. Ivanov, and V. M. Shabaev, Zh. Eksp. Teor. Fiz. **120**, 546 [JETP **93**, 477 (2001)].
S. G. Karshenboim and A. I. Milstein, Phys. Lett. B **549**, 321 (2002).
S. G. Karshenboim, V. A. Shelyuto, and A. I. Vainshtein, Phys. Rev. D **78**, 065036 (2008).
S. G. Karshenboĭm, Zh. Eksp. Teor. Fiz. **103**, 1105 [JETP **76**, 541 (1993)].
M. W. Keller, Metrologia **45**, 102 (2008).
M. W. Keller, F. Piquemal, N. Feltin, B. Steck, and L. Devoille, Metrologia **45**, 330 (2008).
M. W. Keller, N. M. Zimmerman, and A. L. Eichenberger, Metrologia **44**, 505 (2007).
E. G. Kessler, Jr., M. S. Dewey, R. D. Deslattes, A. Henins, H. G. Börner, M. Jentschel, C. Doll, and H. Lehmann, Phys. Lett. A **255**, 221 (1999).
I. B. Khriplovich and R. A. Sen'kov, Phys. Lett. A **249** 474 (1998).
I. B. Khriplovich and R. A. Sen'kov, Phys. Lett. B **481**, 447 (2000).
B. P. Kibble, in *Atomic Masses and Fundamental Constants 5*, edited by J. H. Sanders, and A. H. Wapstra (Plenum Press, New York, 1975), pp. 545–551.
B. P. Kibble and G. J. Hunt, Metrologia **15**, 5 (1979).
B. P. Kibble, I. A. Robinson, and J. H. Belliss, Metrologia **27**, 173 (1990).
T. Kinoshita, in *Lepton Dipole Moments*, Advanced Series on Directions in High Energy Physics, edited by B. L. Roberts and W. J. Marciano (World Scientific, Singapore, 2010), Vol. 20, Chap. 3, pp. 69–117.
T. Kinoshita and M. Nio, Phys. Rev. D **73**, 013003 (2006).
T. Kinoshita, B. Nizic, and Y. Okamoto, Phys. Rev. D **41**, 593 (1990).
U. Kleinevoß, Bestimmung der Newtonschen Gravitationskonstanten G, Ph. D. thesis (University of Wuppertal, 2002).
U. Kleinvoß, H. Meyer, H. Piel, and S. Hartmann (private communication) (to be published) (2002).
D. Kleppner (private communication) (1997).
N. Kolachevsky, M. Fischer, S. G. Karshenboim, and T. W. Hänsch, Phys. Rev. Lett. **92**, 033003 (2004).
N. Kolachevsky, A. Matveev, J. Alnis, C. G. Parthey, S. G. Karshenboim, and T. W. Hänsch, Phys. Rev. Lett. **102**, 213002 (2009).
V. I. Korobov (private communication) (2006).
V. I. Korobov, Phys. Rev. A **77**, 042506 (2008).
V. I. Korobov (private communication) (2010).
S. Kotochigova (private communication) (2006).
S. Kotochigova and P. J. Mohr, (2006) (private communication).
S. Kotochigova, P. J. Mohr, and B. N. Taylor, Can. J. Phys. **80**, 1373 (2002).
T. Kramer, C. Kreisbeck, V. Krueckl, E. J. Heller, R. E. Parrott, and C.-T. Liang, Phys. Rev. B **81**, 081410 (2010).
B. Krause, Phys. Lett. B **390**, 392 (1997).
E. Krüger, W. Nistler, and W. Weirauch, Metrologia **36**, 147 (1999).
K. Kuroda, Phys. Rev. Lett. **75**, 2796 (1995).
K. Kuroda, Meas. Sci. Technol. **10**, 435 (1999).
G. Łach, B. Jeziorski, and K. Szalewicz, Phys. Rev. Lett. **92**, 233001 (2004).
S. Laporta, Phys. Lett. B **523**, 95 (2001).
S. Laporta, Int. J. Mod. Phys. A **23**, 5007 (2008).
S. Laporta, P. Mastrolia, and E. Remiddi, Nucl. Phys. **B688**, 165 (2004).
S. Laporta and E. Remiddi, Phys. Lett. B **379**, 283 (1996).
R. N. Lee, A. I. Milstein, I. S. Terekhov, and S. G. Karshenboim, Phys. Rev. A **71**, 052501 (2005).
C. Lemarchand, M. Triki, B. Darquié, C. J. Bordé, C. Chardonnet, and C. Daussy, New J. Phys. **13**, 073028 (2011).
S. Li, B. Han, Z. Li, and J. Lan, Measurement **45**, 1 (2012).
R. Liu *et al.*, Acta Metrol. Sin. **16**, 161 (1995).
W. Liu *et al.*, Phys. Rev. Lett. **82**, 711 (1999).
A. Louchet-Chauvet, S. Merlet, Q. Bodart, A. Landragin, F. Pereira Dos Santos, H. Baumann, G. D'Agostino, and C. Origlia, IEEE Trans. Instrum. Meas. **60**, 2527 (2011).
S. R. Lundeen and F. M. Pipkin, Metrologia **22**, 9 (1986).
J. Luo (private communication) (2010).
J. Luo (private communication) (2011).
J. Luo, Q. Liu, L.-C. Tu, C.-G. Shao, L.-X. Liu, S.-Q. Yang, Q. Li, and Y.-T. Zhang, Phys. Rev. Lett. **102**, 240801 (2009).
G. Luther (private communication) (1986).
G. Luther (private communication) (2010).
G. G. Luther and W. R. Towler, Phys. Rev. Lett. **48**, 121 (1982).
G. Mana (private communication) (2011).
A. V. Manohar and I. W. Stewart, Phys. Rev. Lett. **85**, 2248 (2000).
F. G. Mariam, High Precision Measurement of the Muonium Ground State Hyperfine Interval and the Muon Magnetic Moment, Ph.D. thesis (Yale University, 1981).
F. G. Mariam *et al.*, Phys. Rev. Lett. **49**, 993 (1982).
A. P. Martynenko, Yad. Fiz. **69**, 1344 [Phys. At. Nucl. **69**, 1309 (2006)].
E. Massa, G. Mana, L. Ferroglio, E. G. Kessler, D. Schiel, and S. Zakel, Metrologia **48**, S44 (2011).
E. Massa, G. Mana, and U. Kuetgens, Metrologia **46**, 249 (2009).
E. Massa, G. Mana, U. Kuetgens, and L. Ferroglio, New J. Phys. **11**, 053013 (2009).
E. Massa, G. Mana, U. Kuetgens, and L. Ferroglio, Metrologia **48**, S37 (2011).
E. Massa and A. Nicolaus, Metrologia **48**, (2011).
P. Mastrolia and E. Remiddi, in *The Hydrogen Atom: Precision Physics of Simple Atomic Systems*, edited by S. G. Karshenboim, F. S. Pavone, G. F. Bassani, M. Inguscio, and T. W. Hänsch (Springer, Berlin, 2001), pp. 776–783.

S. Matsumura, N. Kanda, T. Tomaru, H. Ishizuka, and K. Kuroda, Phys. Lett. A **244**, 4 (1998).
K. Melnikov and T. van Ritbergen, Phys. Rev. Lett. **84**, 1673 (2000).
K. Melnikov and A. Yelkhovsky, Phys. Lett. B **458**, 143 (1999).
S. Merlet, Q. Bodart, N. Malossi, A. Landragin, F. Pereira Dos Santos, O. Gitlein, and L. Timmen, Metrologia **47**, L9 (2010).
I. M. Mills, P. J. Mohr, T. J. Quinn, B. N. Taylor, and E. R. Williams, Phil. Trans. R. Soc. A **369**, 3907 (2011).
A. I. Milstein, O. P. Sushkov, and I. S. Terekhov, Phys. Rev. Lett. **89**, 283003 (2002).
A. I. Milstein, O. P. Sushkov, and I. S. Terekhov, Phys. Rev. A **67**, 062111 (2003a).
A. I. Milstein, O. P. Sushkov, and I. S. Terekhov, Phys. Rev. A **67**, 062103 (2003b).
A. I. Milstein, O. P. Sushkov, and I. S. Terekhov, Phys. Rev. A **69**, 022114 (2004).
P. J. Mohr, in *Beam-Foil Spectroscopy*, edited by I. A. Sellin, and D. J. Pegg (Plenum Press, New York, 1975), pp. 89–96.
P. J. Mohr, Phys. Rev. A **26**, 2338 (1982).
P. J. Mohr, At. Data Nucl. Data Tables **29**, 453 (1983).
P. J. Mohr and D. B. Newell, Am. J. Phys. **78**, 338 (2010).
P. J. Mohr and B. N. Taylor, Rev. Mod. Phys. **72**, 351 (2000).
P. J. Mohr and B. N. Taylor, Rev. Mod. Phys. **77**, 1 (2005).
P. J. Mohr, B. N. Taylor, and D. B. Newell, Rev. Mod. Phys. **80**, 633 (2008).
M. R. Moldover, C.R. Physique **10**, 815 (2009).
M. R. Moldover, J. P. M. Trusler, T. J. Edwards, J. B. Mehl, and R. S. Davis, J. Res. Natl. Bur. Stand. **93**, 85 (1988).
J. Mondéjar, J. H. Piclum, and A. Czarnecki, Phys. Rev. A **81**, 062511 (2010).
B. J. Mount, M. Redshaw, and E. G. Myers, Phys. Rev. A **82**, 042513 (2010).
S. Nagy, T. Fritioff, M. Björkhage, I. Bergström, and R. Schuch, Europhys. Lett. **74**, 404 (2006).
K. Nakamura *et al.*, J. Phys. G **37**, 075021 (2010).
Y. I. Neronov and V. S. Aleksandrov, Pis'ma Zh. Eksp. Teor. Fiz. **94**, 452 [JETP Lett. **94**, 418 (2011)].
Y. I. Neronov and S. G. Karshenboim, Phys. Lett. A **318**, 126 (2003).
D. Nevado and A. Pineda, Phys. Rev. C **77**, 035202 (2008).
G. Newton, D. A. Andrews, and P. J. Unsworth, Phil. Trans. R. Soc. A **290**, 373 (1979).
B. Odom, D. Hanneke, B. D'Urso, and G. Gabrielse, Phys. Rev. Lett. **97**, 030801 (2006).
F. W. J. Olver, D. W. Lozier, R. F. Boisvert, and C. W. Clark, *NIST Handbook of Mathematical Functions* (National Institute of Standards and Technology and Cambridge University Press, Gaithersburg and Cambridge, 2010).
K. Pachucki, Phys. Rev. A **48**, 2609 (1993a).
K. Pachucki, Phys. Rev. A **48**, 120 (1993b).
K. Pachucki, Phys. Rev. Lett. **72**, 3154 (1994).
K. Pachucki, Phys. Rev. A **52**, 1079 (1995).
K. Pachucki, Phys. Rev. A **63**, 042503 (2001).
K. Pachucki, Phys. Rev. Lett. **97**, 013002 (2006).
K. Pachucki, Phys. Rev. A **78**, 012504 (2008).
K. Pachucki, A. Czarnecki, U. D. Jentschura, and V. A. Yerokhin, Phys. Rev. A **72**, 022108 (2005).
K. Pachucki and H. Grotch, Phys. Rev. A **51**, 1854 (1995).
K. Pachucki and U. D. Jentschura, Phys. Rev. Lett. **91**, 113005 (2003).
K. Pachucki, U. D. Jentschura, and V. A. Yerokhin, Phys. Rev. Lett. **93**, 150401 (2004); **94**, 229902(E) (2005).
K. Pachucki and S. G. Karshenboim, J. Phys. B **28**, L221 (1995).
K. Pachucki and S. G. Karshenboim, Phys. Rev. A **60**, 2792 (1999).
K. Pachucki and J. Sapirstein, in *Lepton Dipole Moments*, edited by B. L. Roberts and W. J. Marciano, Advanced Series on Directions in High Energy Physics, Vol 20 (World Scientific, Singapore, 2010), Chap. 7, pp. 219–272.
K. Pachucki and V. A. Yerokhin, Phys. Rev. A **79**, 062516 (2009); **81**, 039903(E) (2010).
K. Pachucki and V. A. Yerokhin, Can. J. Phys. **89**, 95 (2011a).
K. Pachucki and V. A. Yerokhin, J. Phys. Conf. Ser. **264**, 012007 (2011b).
K. Pachucki and V. A. Yerokhin, Phys. Rev. Lett. **104**, 070403 (2010).
P. G. Park, C. H. Choi, C. S. Kim, V. Y. Shifrin, and V. N. Khorev, J. Korean Phys. Soc. **34**, 327 (1999).
H. V. Parks and J. E. Faller, Phys. Rev. Lett. **105**, 110801 (2010).
C. G. Parthey *et al.*, Phys. Rev. Lett. **107**, 203001 (2011).
C. G. Parthey, A. Matveev, J. Alnis, R. Pohl, T. Udem, U. D. Jentschura, N. Kolachevsky, and T. W. Hänsch, Phys. Rev. Lett. **104**, 233001 (2010).
A. A. Penin, Phys. Rev. B **79**, 113303 (2009); **81**, 089902(E) (2010).
N. M. R. Peres, Rev. Mod. Phys. **82**, 2673 (2010).
B. W. Petley and R. W. Donaldson, Metrologia **20**, 81 (1984).
W. D. Phillips, W. E. Cooke, and D. Kleppner, Metrologia **13**, 179 (1977).
W. D. Phillips, D. Kleppner, and F. G. Walther, (1984) (private communication).
L. Pitre (private communication) (2011).
L. Pitre, C. Guianvarc'h, F. Sparasci, A. Guillou, D. Truong, Y. Hermier, and M. E. Himbert, C. R. Physique **10**, 835 (2009).
L. Pitre, F. Sparasci, D. Truong, A. Guillou, L. Risegari, and M. E. Himbert, Int. J. Thermophys. **32**, 1825 (2011).
R. Pohl *et al.*, Nature (London) **466**, 213 (2010).
R. Pohl *et al.*, J. Phys. Conf. Ser. **264**, 012008 (2011).
J. Prades, E. de Rafael, and A. Vainshtein, in *Lepton Dipole Moments*, edited by B. L. Roberts and W. J. Marciano, Advanced Series on Directions in High Energy Physics, Vol. 20 (World Scientific, Singapore, 2010), Chap. 9, pp. 303–317.
M. Puchalski, U. D. Jentschura, and P. J. Mohr, Phys. Rev. A **83**, 042508 (2011).
T. J. Quinn, Metrologia **26**, 69 (1989).
T. J. Quinn, Metrologia **38**, 89 (2001).
T. J. Quinn, C. C. Speake, S. J. Richman, R. S. Davis, and A. Picard, Phys. Rev. Lett. **87**, 111101 (2001).
S. Rainville *et al.*, Nature (London) **438**, 1096 (2005).
N. F. Ramsey, in *Quantum Electrodynamics*, edited by T. Kinoshita (World Scientific, Singapore, 1990), Chap. 13, pp. 673–695.
M. Redshaw, J. McDaniel, and E. G. Myers, Phys. Rev. Lett. **100**, 093002 (2008).
B. L. Roberts (private communication) (2009).
I. A. Robinson, Metrologia **49**, 113 (2012).
I. A. Robinson and B. P. Kibble, Metrologia **44**, 427 (2007).
G. Ron *et al.*, Phys. Rev. C **84**, 055204 (2011).
A. Rudziński, M. Puchalski, and K. Pachucki, J. Chem. Phys. **130**, 244102 (2009).
J. Sapirstein, J. Phys. B **43**, 074015 (2010).
J. R. Sapirstein, E. A. Terray, and D. R. Yennie, Phys. Rev. D **29**, 2290 (1984).
J. R. Sapirstein and D. R. Yennie, in *Quantum Electrodynamics*, edited by T. Kinoshita (World Scientific, Singapore, 1990), Chap. 12, pp 560–672.
S. Schlamminger, E. Holzschuh, W. Kündig, F. Nolting, R. E. Pixley, J. Schurr, and U. Straumann, Phys. Rev. D **74**, 082001 (2006).
J. W. Schmidt, R. M. Gavioso, E. F. May, and M. R. Moldover, Phys. Rev. Lett. **98**, 254504 (2007).
C. Schwob, L. Jozefowski, B. de Beauvoir, L. Hilico, F. Nez, L. Julien, F. Biraben, O. Acef, and A. Clairon, Phys. Rev. Lett. **82**, 4960 (1999); **86**, 4193(E) (2001).
V. M. Shabaev, A. N. Artemyev, T. Beier, and G. Soff, J. Phys. B **31**, L337 (1998).
V. Y. Shifrin, V. N. Khorev, P. G. Park, C. H. Choi, and C. S. Kim, Izmeritel'naya Tekhnika **1998**, 68 (1998).
V. Y. Shifrin, P. G. Park, V. N. Khorev, C. H. Choi, and C. S. Kim, IEEE Trans. Instrum. Meas. **47**, 638 (1998).
V. Y. Shifrin, P. G. Park, V. N. Khorev, C. H. Choi, and S. Lee, IEEE Trans. Instrum. Meas. **48**, 196 (1999).
D. L. Shiner and R. Dixson, IEEE Trans. Instrum. Meas. **44**, 518, (1995).
I. Sick, Phys. Lett. B **576**, 62 (2003).
I. Sick, Can. J. Phys. **85**, 409 (2007).
I. Sick, in *Precision Physics of Simple Atoms and Molecules*, edited by S. G. Karshenboim, Lect. Notes Phys. (Springer, Berlin, Heidelberg, 2008), Vol. 745, pp 57–77.
I. Sick, Few-Body Syst. **50**, 367 (2011).
I. Sick, Prog. Part. Nucl. Phys. **67**, 473 (2012).
V. Sienknecht and T. Funck, IEEE Trans. Instrum. Meas. **34**, 195 (1985).
V. Sienknecht and T. Funck, Metrologia **22**, 209 (1986).
G. W. Small, B. W. Ricketts, P. C. Coogan, B. J. Pritchard, and M. M. R. Sovierzoski, Metrologia **34**, 241 (1997).

M. Smiciklas and D. Shiner, Phys. Rev. Lett. **105**, 123001 (2010).
A. Solders, I. Bergström, S. Nagy, M. Suhonen, and R. Schuch, Phys. Rev. A **78**, 012514 (2008).
R. L. Steiner, E. R. Williams, R. Liu, and D. B. Newell, IEEE Trans. Instrum. Meas. **56**, 592 (2007).
M. Stock, Phil. Trans. R. Soc. A **369**, 3936 (2011).
D. Stöckinger, in *Lepton Dipole Moments*, edited by B. L. Roberts and W. J. Marciano, Advanced Series on Directions in High Energy Physics, Vol 20 (World Scientific, Singapore, 2010), Chap. 12, pp. 393–438.
S. Sturm, A. Wagner, B. Schabinger, J. Zatorski, Z. Harman, W. Quint, G. Werth, C. H. Keitel, and K. Blaum, Phys. Rev. Lett. **107**, 023002 (2011).
M. Suhonen, I. Bergström, T. Fritioff, S. Nagy, A. Solders, and R. Schuch, JINST **2**, P06003 (2007).
G. Sutton, R. Underwood, L. Pitre, M. de Podesta, and S. Valkiers, Int. J. Thermophys. **31**, 1310 (2010).
B. N. Taylor, J. Res. Natl. Inst. Stand. Technol. **116**, 797 (2011).
B. N. Taylor and P. J. Mohr, IEEE Trans. Instrum. Meas. **50**, 563 (2001).
M. Tomaselli, T. Kühl, W. Nörtershäuser, S. Borneis, A. Dax, D. Marx, H. Wang, and S. Fritzsche, Phys. Rev. A **65**, 022502 (2002).
G. Trapon, O. Thévenot, J. C. Lacueille, and W. Poirier, Metrologia **40**, 159 (2003).
G. Trapon, O. Thévenot, J.-C. Lacueille, W. Poirier, H. Fhima, and G. Genevès, IEEE Trans. Instrum. Meas. **50**, 572 (2001).
L.-C. Tu, Q. Li, Q.-L. Wang, C.-G. Shao, S.-Q. Yang, L.-X. Liu, Q. Liu, and J. Luo, Phys. Rev. D **82**, 022001 (2010).
J.-P. Uzan, Living Rev. Relativity **14**, 1 (2011) [http://www.livingreviews.org/lrr-2011-2].
S. Valkiers, G. Mana, K. Fujii, and P. Becker, Metrologia **48**, S26 (2011).
S. Valkiers, D. Vendelbo, M. Berglund, and M. de Podesta, Int. J. Mass Spectrom. **291**, 41 (2010).
R. S. Van Dyck, Jr. (2010) (private communication).
R. S. Van Dyck, Jr., D. B. Pinegar, S. V. Liew, and S. L. Zafonte, Int. J. Mass Spectrom. **251**, 231 (2006).
R. S. Van Dyck, Jr., P. B. Schwinberg, and H. G. Dehmelt, Phys. Rev. Lett. **59**, 26 (1987).
J. Verdú (2006) (private communication).
J. Verdú, S. Djekić, S. Stahl, T. Valenzuela, M. Vogel, G. Werth, T. Beier, H.-J. Kluge, and W. Quint, Phys. Rev. Lett. **92**, 093002 (2004).
A. H. Wapstra, G. Audi, and C. Thibault, Nucl. Phys. **A729**, 129 (2003).
J. Weis and K. von Klitzing, Phil. Trans. R. Soc. A **369**, 3954 (2011).
M. Weitz, A. Huber, F. Schmidt-Kaler, D. Leibfried, W. Vassen, C. Zimmermann, K. Pachucki, T. W. Hänsch, L. Julien, and F. Biraben, Phys. Rev. A **52**, 2664 (1995).
G. Werth (2003) (private communication).
E. H. Wichmann and N. M. Kroll, Phys. Rev. **101**, 843 (1956).
A. Wicht, J. M. Hensley, E. Sarajlic, and S. Chu, Phys. Scr. **T102**, 82 (2002).
E. R. Williams, G. R. Jones, Jr., S. Ye, R. Liu, H. Sasaki, P. T. Olsen, W. D. Phillips, and H. P. Layer, IEEE Trans. Instrum. Meas. **38**, 233, (1989).
E. R. Williams, R. L. Steiner, D. B. Newell, and P. T. Olsen, Phys. Rev. Lett. **81**, 2404 (1998).
P. F. Winkler, D. Kleppner, T. Myint, and F. G. Walther, Phys. Rev. A **5**, 83 (1972).
B. M. Wood and S. Solve, Metrologia **46**, R13 (2009).
B. J. Wundt and U. D. Jentschura, Phys. Lett. B **659**, 571 (2008).
V. A. Yerokhin, Phys. Rev. A **62**, 012508 (2000).
V. A. Yerokhin, Eur. Phys. J. D **58**, 57 (2010).
V. A. Yerokhin, A. N. Artemyev, V. M. Shabaev, and G. Plunien, Phys. Rev. A **72**, 052510 (2005).
V. A. Yerokhin, P. Indelicato, and V. M. Shabaev, Phys. Rev. Lett. **89**, 143001 (2002).
V. A. Yerokhin, P. Indelicato, and V. M. Shabaev, Phys. Rev. Lett. **91**, 073001 (2003).
V. A. Yerokhin, P. Indelicato, and V. M. Shabaev, Phys. Rev. A **71**, 040101 (2005a).
V. A. Yerokhin, P. Indelicato, and V. M. Shabaev, Zh. Eksp. Teor. Fiz. **128**, 322 [JETP **101**, 280 (2005)].
V. A. Yerokhin, P. Indelicato, and V. M. Shabaev, Can. J. Phys. **85**, 521 (2007).
V. A. Yerokhin, P. Indelicato, and V. M. Shabaev, Phys. Rev. A **77**, 062510 (2008).
V. A. Yerokhin and U. D. Jentschura, Phys. Rev. Lett. **100**, 163001 (2008).
V. A. Yerokhin and U. D. Jentschura, Phys. Rev. A **81**, 012502, (2010).
V. A. Yerokhin, Phys. Rev. A **83**, 012507 (2011).
H. Yi, T. Li, X. Wang, F. Zhang, W. Huo, and W. Yi, Metrologia **49**, 62 (2012).
T. Zelevinsky, D. Farkas, and G. Gabrielse, Phys. Rev. Lett. **95**, 203001 (2005).
Z. Zhan *et al.*, Phys. Lett. B **705**, 59 (2011).
J. T. Zhang, (2011) (private communication).
J. T. Zhang, H. Lin, X. J. Feng, J. P. Sun, K. A. Gillis, M. R. Moldover, and Y. Y. Duan, Int. J. Thermophys. **32**, 1297 (2011).
Z. Zhang, X. Wang, D. Wang, X. Li, Q. He, and Y. Ruan, Acta Metrol. Sin. **16**, 1 (1995).